

## **INFORMATION TO USERS**

This manuscript has been reproduced from the microfilm master. UMI films the text directly from the original or copy submitted. Thus, some thesis and dissertation copies are in typewriter face, while others may be from any type of computer printer.

**The quality of this reproduction is dependent upon the quality of the copy submitted. Broken or indistinct print, colored or poor quality illustrations and photographs, print bleedthrough, substandard margins, and improper alignment can adversely affect reproduction.**

In the unlikely event that the author did not send UMI a complete manuscript and there are missing pages, these will be noted. Also, if unauthorized copyright material had to be removed, a note will indicate the deletion.

Oversize materials (e.g., maps, drawings, charts) are reproduced by sectioning the original, beginning at the upper left-hand corner and continuing from left to right in equal sections with small overlaps.

Photographs included in the original manuscript have been reproduced xerographically in this copy. Higher quality 6" x 9" black and white photographic prints are available for any photographs or illustrations appearing in this copy for an additional charge. Contact UMI directly to order.

**Bell & Howell Information and Learning  
300 North Zeeb Road, Ann Arbor, MI 48106-1346 USA**

**UMI<sup>®</sup>**  
800-521-0600



UNIVERSITY OF ALBERTA

**ICHTHOLOGY AND PALAEOENVIRONMENT OF THE LOWER  
TRIASSIC MONTNEY FORMATION, KAYBOB AND KAYBOB  
SOUTH FIELDS AREA, WEST-CENTRAL ALBERTA**

By

DEMIAN J. C. ROBBINS



A thesis submitted to the Faculty of Graduate Studies and Research in partial  
fulfillment of the requirements for the degree of Master of Science

Department of Earth and Atmospheric Science

Edmonton, Alberta

Fall, 1999



National Library  
of Canada

Acquisitions and  
Bibliographic Services

395 Wellington Street  
Ottawa ON K1A 0N4  
Canada

Bibliothèque nationale  
du Canada

Acquisitions et  
services bibliographiques

395, rue Wellington  
Ottawa ON K1A 0N4  
Canada

*Your file Votre référence*

*Our file Notre référence*

The author has granted a non-exclusive licence allowing the National Library of Canada to reproduce, loan, distribute or sell copies of this thesis in microform, paper or electronic formats.

The author retains ownership of the copyright in this thesis. Neither the thesis nor substantial extracts from it may be printed or otherwise reproduced without the author's permission.

L'auteur a accordé une licence non exclusive permettant à la Bibliothèque nationale du Canada de reproduire, prêter, distribuer ou vendre des copies de cette thèse sous la forme de microfiche/film, de reproduction sur papier ou sur format électronique.

L'auteur conserve la propriété du droit d'auteur qui protège cette thèse. Ni la thèse ni des extraits substantiels de celle-ci ne doivent être imprimés ou autrement reproduits sans son autorisation.

0-612-47088-1

Canada

**University of Alberta**

**Library Release Form**

**Name of Author:** DEMIAN J. C. ROBBINS

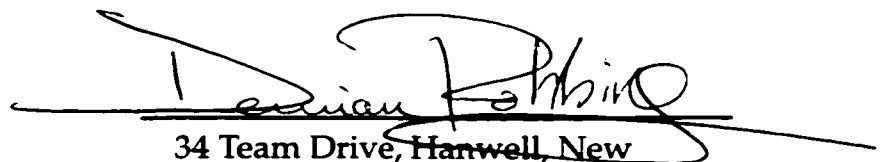
**Title of Thesis:** ICHNOLOGY AND PALAEOENVIRONMENT OF THE LOWER TRIASSIC MONTNEY FORMATION, KAYBOB AND KAYBOB SOUTH FIELDS AREA, WEST-CENTRAL ALBERTA

**Degree:** Master of Science

**Year this Degree Granted:** 1999

Permission is hereby granted to the University of Alberta Library to reproduce single copies of this thesis and to lend or sell such copies for private, scholarly or scientific research purposes only.

The author reserves all other publication and other rights in association with the copyright in the thesis, and except as herein before provided, neither the thesis nor any substantial portion thereof may be printed or otherwise reproduced in any material form whatever without the author's prior written permission.

  
34 Team Drive, Hanwell, New  
Brunswick, Canada, E3E 2H2


Date: 30 September, 1999

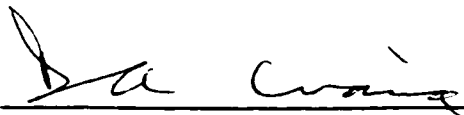
**University of Alberta**

**Faculty of Graduate Studies and Research**

The undersigned certify that they have read, and recommend to the Faculty of Graduate Studies and Research for acceptance, a thesis entitled ICHNOLOGY AND PALAEOENVIRONMENT OF THE LOWER TRIASSIC MONTNEY FORMATION, KAYBOB AND KAYBOB SOUTH FIELDS AREA, WEST-CENTRAL ALBERTA submitted by DEMIAN JAMES CORNELIS ROBBINS in partial fulfillment of the requirements for the degree of MASTER OF SCIENCE.

  
\_\_\_\_\_  
Dr. S. G. Pemberton

  
\_\_\_\_\_  
Dr. J. F. Lerbekmo

  
\_\_\_\_\_  
Dr. D. A. Craig - External Examiner

DATE: 24 September 1999

**This thesis is dedicated to three people:**

**Firstly to my parents, Chris Robbins and Marijke Hurkens.  
I can't imagine asking for better people to call Mom and Dad.**

**Secondly, to my grandmother Wilhelmina Hurkens,  
who passed away after this thesis study began.  
No one could have shown greater strength in the face of adversity.**

## ABSTRACT

Thirty-nine core and more than 300 well logs examined from the Lower Montney Formation around the Kaybob and Kaybob South hydrocarbon fields exhibited fifteen facies grouped into three facies associations, two siliciclastic and one bioclastic. Clastic Association One (CA1) comprised three gradationally interbedded facies of interlaminated very fine sand and silt that exhibit a distinct tidal and seasonal influence on sedimentation. It was characterized by an impoverished, but locally abundant, assemblage of 5 major and 6 rare ichnogenera, predominated by *Lingulichnus*. Locally intercalated or overlying CA1 is Clastic Association Two (CA2), comprised of 5 facies indicative of episodic deposition and penecontemporaneous alteration of sediments. The Bioclastic Association, which has a locally erosive and discordant morphology, comprises 5 facies dominated by coarse shell fragments and minor intercalated clastics. Two additional facies of limited distribution were not assigned to a facies association.

CA1 is interpreted as the deposits of a tidally influenced, seasonally active delta front. Ichnofossils of this association exhibit characteristics consistent with a sheltered, salinity- and oxygen-stressed environment. CA2 beds occurring within CA1 represent a mix of autocyclic and allocyclic perturbations of ambient, stressed deltaic setting. Thicker accumulations of CA2 that overlie CA1, and locally exhibit lateral equivalence with the Bioclastic Association, represent a barrier-bar-tidal inlet system.

Internal stratigraphy of the Montney in this area is difficult to decipher. However, two locally mappable units were identified. Both exhibit a channel-constrained morphology. A lower, sandy channel within CA1 represents a possible distributary mouth. Sinuous, elongate isopach thicks in the Bioclastic Association represent tidal inlet channels.



## Acknowledgements

At the most formal level I would like to thank my supervisory committee: my supervisor Dr. S. George Pemberton and Doctors J. Lerbekmo and D. Craig. They gave a fair and (dare I say it?) friendly treatment to a relative unknown. I would also like to thank Dr. Pemberton and the National Sciences and Engineering Research Council (NSERC Operating Grant No. A0816) for funding this project.

I must first and foremost thank my supervisor George Pemberton. He had the patience and generosity to see past a rocky start and carry through to a happy ending. Without his tolerance and support this thesis could not have happened and I would not be the scientist that I am (or hope I can be). If I can live up to half the example George has set for me, I'll be an endlessly happy man.

I would also like to thank Dr. Ron K. Pickerill, my mentor and Bachelor's supervisor at the University of New Brunswick, who showed me that there was a whole field with endless possibilities called Ichnology, and with that probably shaped the rest of my career. What can be said about a person who can redirect 17 years of obsessive fixation on dinosaurs into a field that focuses on worm tunnels, bug tracks and invertebrate droppings... and feel like it was the best choice that could ever have been made? All that comes to my mind is a fervent and honest "Thank *you!*"

This thesis could also never have been achieved without the constant and active support of my parents. They started it all with a firm finger pointing to the library when a 4-year old drove them mad with questions about dinosaurs, and never thought to send me in another direction when that expanded to include all things geological as the years went by. They never once tired of encouraging me when things seemed grim or insurmountable. Thanks are also due to them also for giving me a solid boot to the backside (metaphorically speaking, of course!) when I needed it, which was more often than I, or anyone else, could ever have wanted. The dedication says it all.

Thanks awfully to all the guys I've had the honour to work with in the Ichnology Research Group at the University of Alberta. They tolerated a guy that at times probably seemed like a semi-recluse, and they offered uncountable insights into both geology and life in general: Sue Gordichuk (George's tireless secretary, who does more for us all, in the background, than we may ever know), Murray Gingras, Arjun Keswani, Yaojun Han and Jason Lavigne (both of whom I followed here from UNB), John-Paul Zonneveld (another rocky start that turned out well in the end), Errin Kimball, Ian Armitage, Chad Harris, Glenn Schmidt, Steve Hubbard,

Jason Frank, Tom Saunders, Jeff Reinprecht and Eric Hanson. I would particularly like to thank Errin, Ian and Chad for their helpful comments on my thesis when things were down to the wire and deadlines loomed threateningly.

Special thanks are owed to Murray and Arjun. Murray was a good friend from the start, taking me on a fishing trip within a week of my arrival in Alberta. Not once did he fail to give a pat on the back, a reassuring thumbs-up, or blunt assessment when it was needed. His insights and comments on both the ideas and drafts of the thesis as they evolved were invaluable. He never grudged me (as far as I can tell!) a share of his time, his cache of alcohol, a little cash if it was needed, or his opinions, about which he is far too modest. Arjun was a solid friend as soon as we got to know each other, and someone who could be counted upon to erase preconceptions or offer a whole new perspective on a problem. He has always been willing to spend a couple of hours thrashing out a philosophical issue, staring down a thin-section, or just chatting about the time of day.

I would also like to thank those people who helped make my sojourn in Edmonton an enjoyable experience. First, I must thank Theresa and the rest of George's family for all the wonderful barbecues and dinners. Nobody I know puts up a better and more generous spread for a bunch of starving graduate students: shrimp rings for people who would be happy with hot dogs. Bless them. I would also like to thank my various roommates from the past four years, particularly Nick Spyksma, Al and Madeleine Namit, Murray Gingras, Val Slowiak, and John Day and David Catonio. They all put a roof over my head, put up with my company, and accepted my (at times) spotty income (truly have I learned the meaning of "feast or famine"!).

I cannot imagine that two pages have even begun to cover all the thanks, large and small, due to those that made the last four years both possible and enjoyable. To all those whom I may have managed to miss, I offer my apologies and thanks for both their help and their understanding.

# TABLE OF CONTENTS

	PAGES
<b>CHAPTER 1</b>	
<b>INTRODUCTION</b> .....	1
<b>Introductory Remarks</b> .....	1
<b>General Stratigraphy</b> .....	1
<b>Study Area</b> .....	3
<b>Database and Methods</b> .....	5
<b>CHAPTER 2</b>	
<b>GENERAL INFORMATION AND PREVIOUS WORK</b> .....	8
<b>Part 1. Regional stratigraphy, tectonics, and palaeoenvironment</b> .....	8
<b>Regional stratigraphy and historical perspective</b> .....	8
Peace River region and northeastern British Columbia .....	8
Southern and central Foothills, Alberta .....	10
Peace River and Alberta Interior Plains subsurface .....	11
<b>Tectonic Framework</b> .....	13
<b>Palaeoclimatological setting</b> .....	15
<b>Global anoxia in the lowermost Triassic</b> .....	16
<b>Part 2. Kaybob and Kaybob South Fields study area</b> .....	16
Stratigraphy and previous work - Kaybob and Kaybob South areas .....	16
Local stratigraphy - Kaybob and Kaybob South Field areas .....	17
<b>Part 3. Lingulidae: palaeoecology and environmental significance</b> .....	18
Introductory remarks .....	18
Lingulidae: general palaeontology .....	22
Lingulids: biological and ethological parameters .....	22
Lingulids: environmental parameters .....	27
Lingulids: taphonomy .....	29
Lingulid ecology: summary .....	31
<b>CHAPTER 3</b>	
<b>FACIES, FACIES ASSOCIATIONS, ICHNOLOGY</b>	
<b>AND SEDIMENTOLOGY</b> .....	32
<b>Introduction</b> .....	32

<b>Facies Descriptions .....</b>	<b>32</b>
<b>CLASTIC FACIES ASSOCIATION ONE.....</b>	<b>35</b>
Facies A: Interlaminated, pyritiferous silt, sand and muddy silt .....	35
Facies B: Upward fining interlaminated and interbedded vfg sand and silt .....	42
Subfacies B1: Silt-dominated facies B.....	53
Subfacies B2: Sand-dominated facies B .....	58
Facies C: Upward coarsening, interlaminated sand and minor silt .....	74
<b>CLASTIC FACIES ASSOCIATION TWO .....</b>	<b>76</b>
Facies D: Convolute and chaotically laminated sand and silt. ....	77
Facies E: Massive, apparently structureless to diffusely laminated sand .....	84
Facies F: Texturally graded, well-sorted sand .....	87
Facies G: Homogenized to partially homogenized, pyritiferous silty sand. ....	90
Facies H: Very fine sand and pelletized silt .....	93
<b>BIOCLASTIC FACIES ASSOCIATION .....</b>	<b>96</b>
Facies I: 'Fine'-matrix coquina .....	97
Facies J: Coarse-matrix coquina.....	100
Facies K: Interbedded very fine sand and coquina. ....	101
Facies L: Interbedded silty sand and coquina .....	104
Facies M: Coquina with interbedded fractured and 'brecciating' silty sand .....	106
<b>ANOMALOUS OR UNCOMMON FACIES.....</b>	<b>111</b>
Facies N: 'Lam-scram' sand or sand and silt .....	111
Facies O: Upward-fining, interlaminated and interbedded silt and fg-mg sand .....	113
 <b>CHAPTER 4</b>	
<b>STRATIGRAPHIC RELATIONSHIPS AND</b>	
<b>PALAEOENVIRONMENT .....</b>	<b>115</b>

**Part 1. Internal stratigraphic relationships** ..... 115

**Part 2. Lateral relationship of CA2 lithologies  
and the Bioclastic Association.** ..... 122

    Evidence for lateral equivalence ..... 122

**Part 3. Palaeoenvironmental interpretation of  
the Kaybob/Kaybob South area** ..... 129

    Clastic Association One: review and comments ..... 129

    Clastic Association Two: review and comments ..... 130

    Bioclastic Association: review and comments ..... 130

    Ambient (CA1) palaeoenvironment: discussion ..... 131

    CA2 and the Bioclastic Association: interpretation ..... 133

    Summary and depositional history: Kaybob/Kaybob South area ..... 134

**CHAPTER 5**

**SUMMARY AND CONCLUSIONS** ..... 135

**Introductory remarks** ..... 135

**Sedimentology and Ichnology** ..... 135

**Internal Stratigraphy** ..... 136

**Palaeoenvironmental framework** ..... 136

**CONCLUSIONS** ..... 137

**REFERENCES** ..... 138

# LIST OF TABLES

PAGES

## CHAPTER 2

Table 2.1 Summary of Lingulid biological parameters .....30

## CHAPTER 3

Table 3.1 Summary table of facies described in this study .....33

# LIST OF FIGURES

PAGES

## CHAPTER 1

Fig. 1.1 Triassic stratigraphic correlation chart.....	2
Fig. 1.2 Montney Formation - Internal divisions. ....	4
Fig. 1.3 Location map of study area. ....	6

## CHAPTER 2

Fig. 2.1 Triassic total isopach and provenance. ....	14
Fig. 2.2 Characteristic well log responses. ....	19
Fig. 2.3 Montney Fm. – Permian and Jurassic contacts. ....	20
Fig. 2.4 Lingulid depth distribution and life expectancy. ....	24
Fig. 2.5 Lingulid burrowing behaviour. ....	26

## CHAPTER 3

Fig. 3.1 Facies A – bedding styles. ....	37
Fig. 3.2 Facies A – sedimentary structures. ....	38
Fig. 3.3 Facies A – ichnology and palaeontology.....	39
Fig. 3.4 Facies A – box shot. ....	40
Fig. 3.5 Facies B – bedding styles. ....	45
Fig. 3.6 Facies B – sedimentary structures. ....	46
Fig. 3.7 Facies B – Bioturbation. ....	47
Fig. 3.8 Facies B – vertical migration of burrows. ....	48
Fig. 3.9 Facies B – additional ichnology. ....	49
Fig. 3.10 Facies B – boxshot. ....	50
Fig. 3.11 Subfacies B1 – bedding styles. ....	54
Fig. 3.12 Subfacies B1 – sedimentary structures. ....	55
Fig. 3.13 Subfacies B1 – ichnofossils. ....	56
Fig. 3.14 Subfacies B2 – Box shot. ....	59
Fig. 3.15 Subfacies B2 – bedding styles. ....	61
Fig. 3.16 Subfacies B2 – sedimentary structures I. ....	62
Fig. 3.17. Subfacies B2 – sedimentary structures II. ....	63
Fig. 3.18 Subfacies B2 – Vertical migration and sedimentation rates. ....	64
Fig. 3.19 Subfacies B2 – Ichnofossils I. ....	66
Fig. 3.20 Subfacies B2 – Ichnofossils II. ....	68

Fig. 3.21 Subfacies B2 – Ichnofossils III. ....	70
Fig. 3.22 Subfacies B2 – indiscrete bioturbate textures. ....	72
Fig. 3.23 Facies C. ....	75
Fig. 3.24 Facies D – box shot. ....	78
Fig. 3.25 Facies D – sedimentary structures I. ....	79
Fig. 3.26 Facies D – sedimentary structures II. ....	81
Fig. 3.27 Facies E. ....	85
Fig. 3.28 Facies F. ....	88
Fig. 3.29 Facies G. ....	91
Fig. 3.30 Facies H. ....	94
Fig. 3.31 Facies I and Facies J. ....	98
Fig. 3.32 Facies K. ....	102
Fig. 3.33 Facies L. ....	105
Fig. 3.34 Facies M. ....	108
Fig. 3.35 Facies N. ....	112

#### CHAPTER 4

Fig. 4.1 Problems in Montney correlation: well 11-28-62-19w5. ....	116
Fig. 4.2 Problems in Montney correlation: well 4-36-64-19w5 ....	118
Fig. 4.3 Problems in Montney correlation: well 2-2-63-20w5 ....	120
Fig. 4.4 Core location map. ....	123
Fig. 4.5 Isopach map of the Bioclastic Association. ....	124
Fig. 4.6 Coquinal cross section. ....	126
Fig. 4.7 Depth to base of the sand unit. ....	127
Fig. 4.8 Channel sand section. ....	128



# CHAPTER 1: INTRODUCTION

## Introductory Remarks

This study was undertaken to develop a better understanding of the enigmatic, dolomitized fine sands and coquinas present along the subcrop edge of the Montney Formation. Interest in the Montney has grown only recently. Although a number of regional-scale reviews and studies of the formation have appeared in the literature since the beginning of the 1990s (Gibson and Edwards 1990, Edwards *et al.* 1994, Davies *et al.* 1997, Moslow and Davies 1997), there has been only one detailed local study (Mederos, 1995), centered on the Sturgeon Lake Field area.

The discovery of the Montney Turbidite Play in the 1980s, and its continuing development throughout the 1990s, has spurred an increase in the pace and volume of work regarding the Montney Formation. By 1995, it had become apparent that in a Formation as complex as the Montney, many smaller exploration opportunities had been overlooked.

With this in mind, it was decided that the enigmatic, complexly interbedded clastic and coquinal facies in the easternmost portions of the Montney would provide a valuable contribution to academics and explorationists alike.

## General Stratigraphy

The Montney Formation (Lower Triassic, Daiber Group) and its correlatives outcrop in the Foothills and Front Ranges of the Rocky Mountains, and are encountered in the subsurface of the Foothills and plains of northeastern British Columbia and west central Alberta. Throughout this region, there are a number of changes in nomenclature (Fig. 1.1). Outcropping Lower Triassic strata in northeastern British Columbia and the southernmost Yukon are termed the Toad and Grayling Formations. Outcrops observed in the southern Alberta Foothills and Rocky Mountains are referred to as the Vega and Phroso Siltstone Members of the Sulphur Mountain Formation (Spray River Group). It is only in the subsurface of Alberta and northeast British Columbia, particularly in the Peace River area, that the Montney Formation is encountered. However, because of its relevance to the oil industry, collectively referring to all of these equivalent strata as the Montney Formation in general discussions has become an accepted practice (*e.g.* Edwards *et*

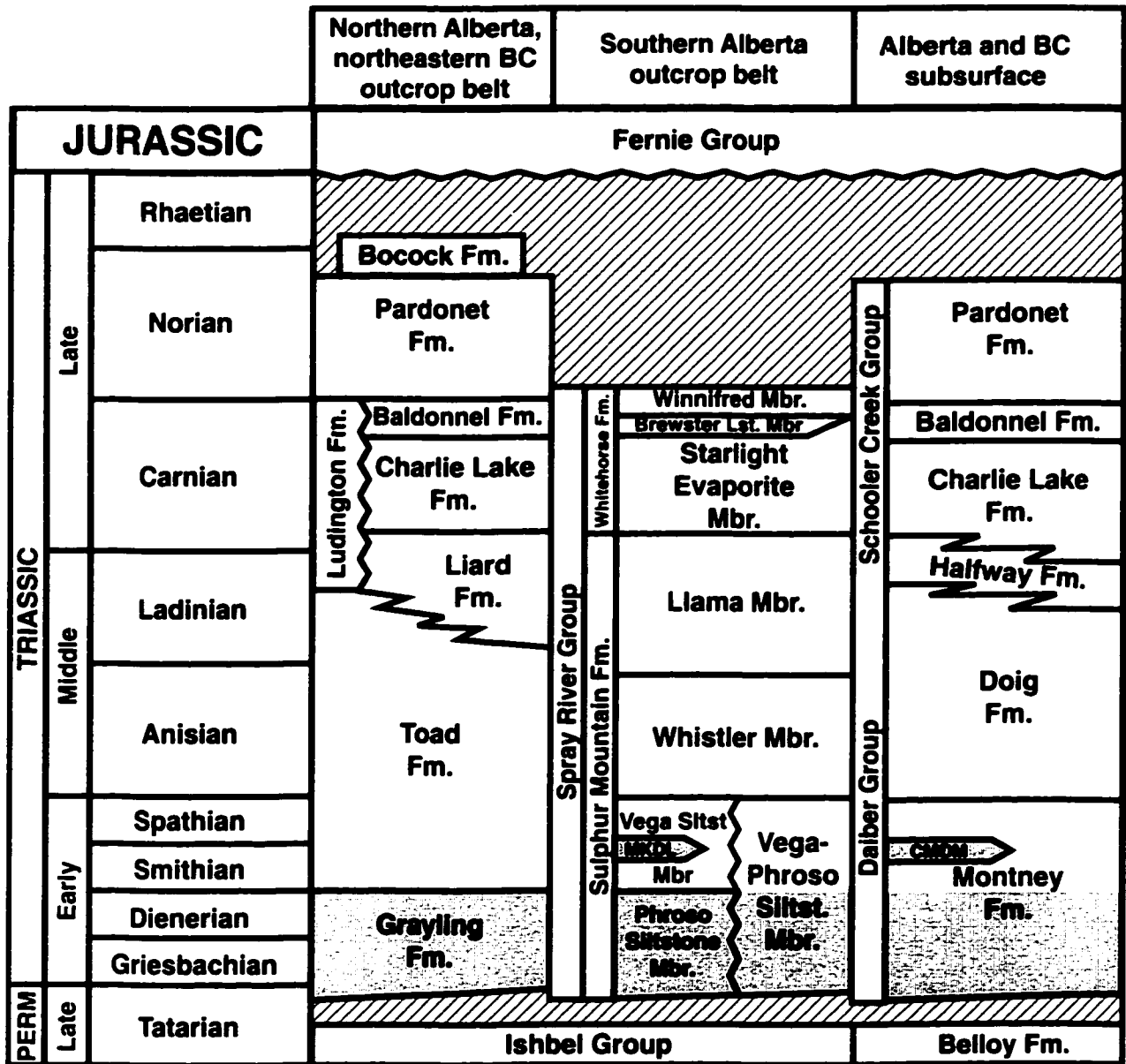


Fig. 1.1 Triassic stratigraphic correlation chart.

Triassic formations of the Alberta Basin (Western Canada Sedimentary Basin), northeastern BC and western Alberta. Modified from Gibson and Barclay (1989) and Davies (1997a). The units shaded in gray correlate to the strata examined in this study. Abbreviations used in chart: MKDL - Mackenzie Dolomite Lentil, CMDM - Coquinal Middle Dolomite Member.

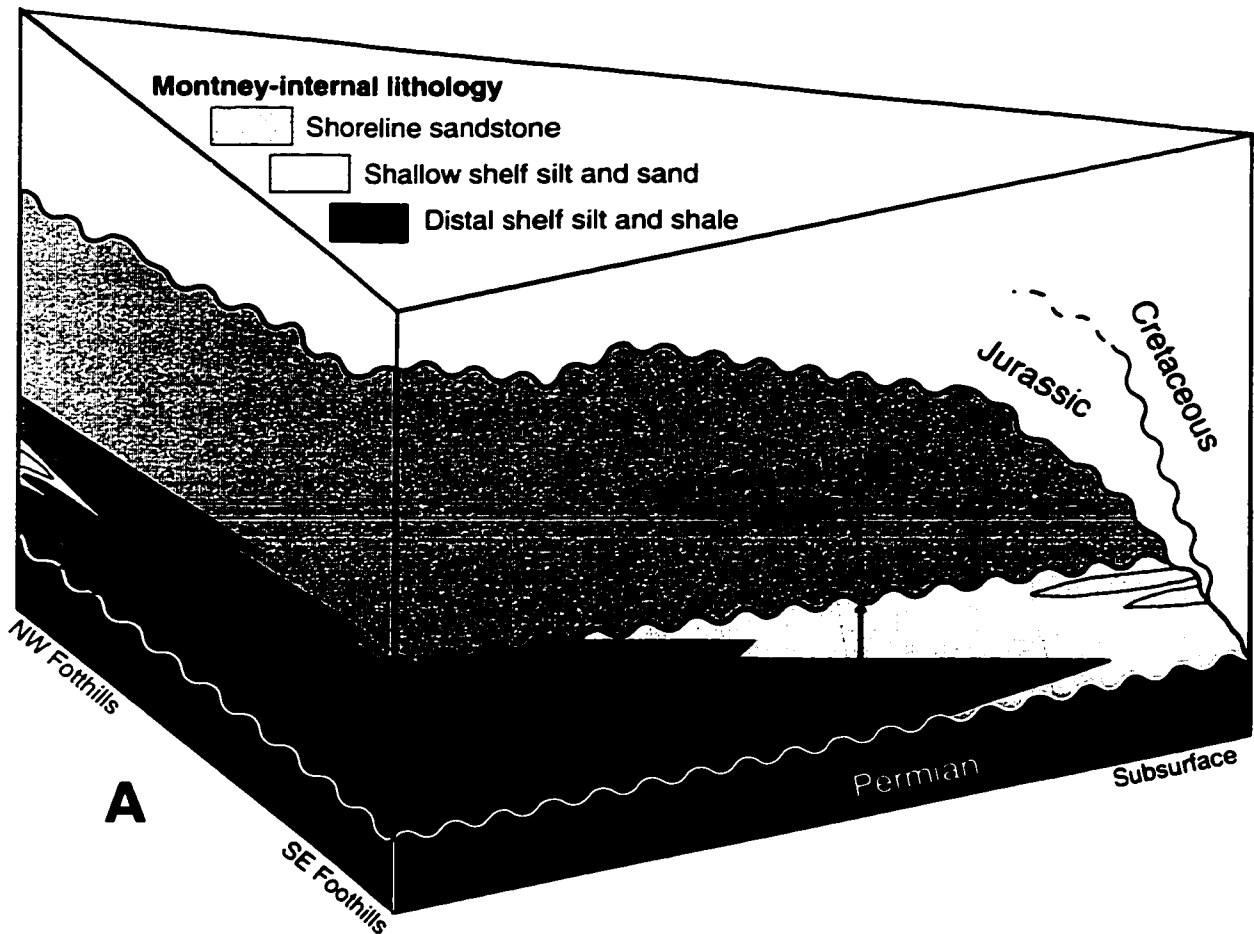
*al.* 1994, Podruski *et al.* 1988) that will be continued in this study.

The Montney Formation lies unconformably on the Permian chert and sands of the Belloy Formation over most of its extent. Exceptions include the southern Alberta Foothills, where it lies unconformably on the Ranger Canyon Formation of the Permian Ishbel Group, and the Liard sub-basin, where it lies unconformably on the Permian Kindle Group. Where they have not been removed by later Mesozoic erosion, phosphatic shales at the base of the Triassic Doig Formation conformably overlie the Montney. Elsewhere, primarily near the subcrop edge, the Montney is truncated and unconformably overlain by black organic shales of the Jurassic Nordegg Formation (Fernie Group). Where the Jurassic is removed by pre-Cretaceous erosion and incision lower Cretaceous strata of the Bluesky/Gething interval unconformably overlie the Montney.

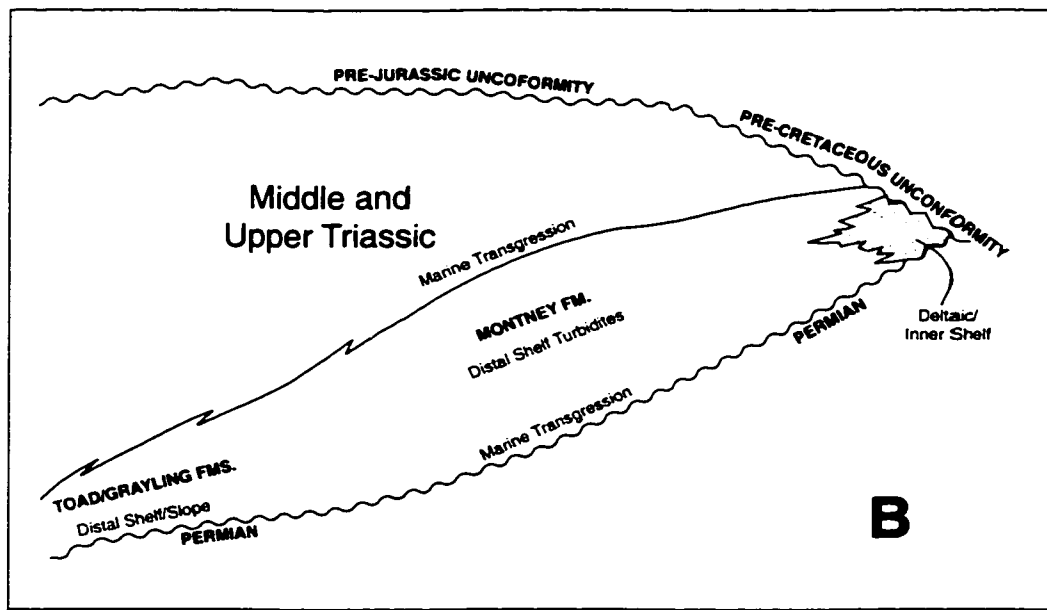
Internally the Montney is a particularly complex formation (Fig. 1.2.), and encompasses a very broad range of facies. In the westernmost subsurface and in the Rocky Mountains outcrop belt, the Montney includes deep shelf and slope environments; these are primarily represented by turbidite deposits hosted in dark mudstones and siltstones (Moslow & Davies 1994, 1997). Eastward and landward, the Montney grades through silts and fine sands of a mid-shelf character (Pelletier 1960, 1961; Gibson, 1968; Gibson & Barclay 1989), into progressively shallowing, increasingly sandy deposits characterized by hummocky cross-stratified tempestites (Gibson & Barclay 1989). At its easternmost extent, near the subcrop edge, the Montney is comprised of sand, silts, and coquinas of debated nature, but which the majority of workers consider deltaically influenced, shallow-shelf to nearshore deposits (*e.g.* Edwards *et al.* 1994, Gibson 1971b, Gibson & Barclay 1989). In effect, facies of the Montney Formation represent a near-completely preserved marine basin within a single lithostratigraphic unit.

### **Study Area**

With the goals of this project in mind, there were a number of important considerations to be taken into account when selecting the study area. Firstly, as in any subsurface study, it was necessary to identify an area with a substantial database in the form of cores and geophysical well logs. Secondly, in order to build a practical environmental model, the study needed to incorporate substantial occurrences of both the coquinal and clastic facies that characterize the Montney subcrop-edge



**A**



**B**

**Fig. 1.2 Montney Formation - Internal divisions.**

Two examples depicting the overall stratigraphic framework and internal palaeoenvironmental division of the Montney Formation. (A) modified from Gibson & Barclay 1989, (B) from Edwards *et al.* 1994.

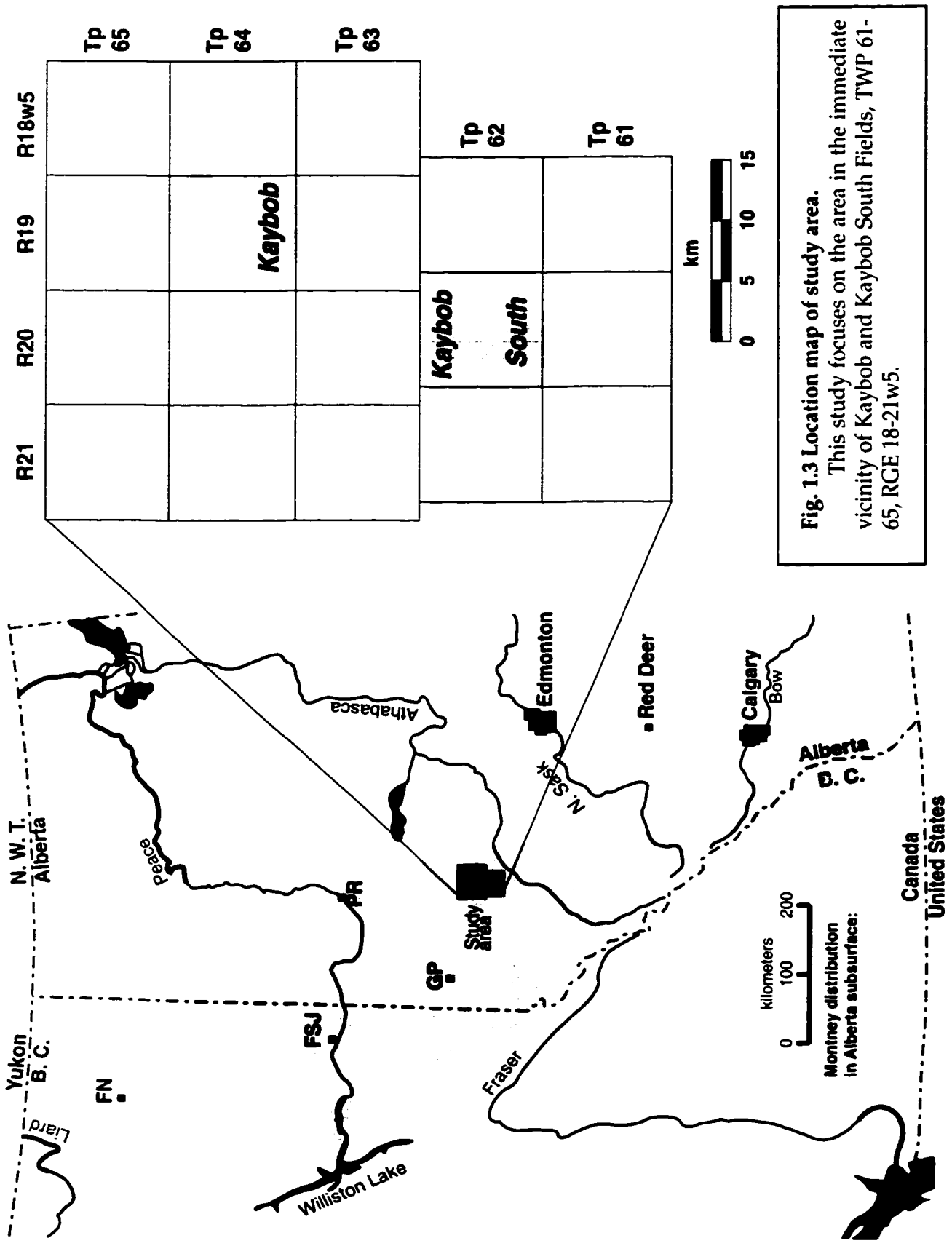
area. Finally, because the study was designed to assist hydrocarbon exploration and development efforts, the ideal study area would include both coquinal and clastic reservoirs producing from the Montney.

An appropriate area was identified in the vicinity of the Kaybob and Kaybob South fields near Fox Creek, Alberta, encompassing Townships 61-65, Ranges 18-21w5 (Fig. 1.3). In the northeast, the study area is approximately 16 km from the Montney subcrop edge. Kaybob South Field, discovered in 1961, is centered on TWP 62-20w5 and represents the second largest Triassic oil discovery in Western Canada (Podruski *et al.* 1988, Edwards *et al.* 1994). It is also the largest Montney development field (Podruski *et al.* 1988), producing hydrocarbons from a thick coquina lens. Immediately to the north, centered on TWP 64-19w5 is the older Kaybob Field, a development in the Devonian Swan Hills Formation, which has along its northeastern flank a number of oil and gas wells producing from Montney clastic facies. A number of smaller Devonian and Cretaceous fields in the area fill out the core and well-log database.

The Coquinal Middle Dolomite Member of Davies *et al.* (1997) reaches its thickest accumulation (approximately 35 m) in the study area, along the southeast margin of Kaybob South field (*op. cit.*). Finally, G. R. Davies (pers. comm., 1995) indicated there were a number of wells in the area with particularly abundant and well-preserved ichnofossils which would provide a useful basis for the ichnological aspect of the study.

### **Database and Methods**

Thirty-nine cores totaling 712 m were logged for sedimentological and ichnological characteristics. Of these, 13 were logged in detail with a resolution of approximately 2.5 cm, and the remaining 26 were logged based on facies interpreted from the detailed logs with a resolution of approximately 10 cm. Primary emphasis was placed on recording gross lithology, physical sedimentary structures, biogenic sedimentary structures, and grain size. Grain size was determined based on visual inspection and comparison with a Can-Strat grain size card. Several samples of typical facies were collected, sectioned, and examined under magnification in order to identify mineralogy and any microscopic-scale body and trace fossils that may have been present. Photographs were scanned into a computer and annotated digitally.



**Fig. 1.3 Location map of study area.**  
 This study focuses on the area in the immediate vicinity of Kaybob and Kaybob South Fields, TWP 61-65, RGE 18-21w5.

In addition to this core database, the gamma ray and sonic or porosity logs for 213 wells from the study area were examined in order to map significant bounding surfaces and time-stratigraphic units. As a practical consideration, the database was limited to a single well from each Legal Subdivision. Additionally, only wells that included a complete cross-section of the Montney, from the upper contact with the Jurassic Nordegg Formation to the lower contact with the Permian Belloy Formation, were used. Observations from cored wells were compared with their respective logs in order to correlate significant surfaces with the corresponding geophysical responses. These correlations were extended to adjacent wells, and the resulting data was then entered into Easy MCadContour© PPC for digital mapping and contouring.

## CHAPTER 2: GENERAL INFORMATION AND PREVIOUS WORK

### Part 1. Regional stratigraphy, tectonics, and palaeoenvironment

#### Regional stratigraphy and historical perspective

Early studies of the Lower Triassic Montney Formation and its equivalents can be divided into three regional spheres of interest. Each region developed a separate nomenclature and stratigraphy, all of which (Fig. 1.1) have remained in use. Concerted efforts to correlate units between these separate regions began in the 1950s and were largely completed by 1970.

In the north, studies were centered on outcrops in the Peace and Liard River valleys of northeastern British Columbia; this stratigraphy was later expanded to include a region extending from the southern Yukon to the northern Alberta Foothills of the Pine River area. In the south, studies centered on outcrop exposures in the immediate vicinity of Banff; this nomenclature was extended south to the Alberta-US border and north to the region between the Pine and Smoky rivers. In both of these regions, the earliest mention of Triassic material dates to the late nineteenth century (*e.g.* Selwyn 1877, McConnell 1887). The third region, which only began to receive attention in the 1950s with the onset of concerted oil exploration, comprises the subsurface Triassic of the Alberta and British Columbia plains.

What follows in this section is an abridged history of Lower Triassic study in Alberta and British Columbia; detailed reviews of earlier work may be found in McLearn and Kindle (1950) for the northern region, Hunt and Ratcliffe (1959) for the subsurface, and Gibson (1968) for the southern region. Excellent basin-wide reviews are found in Barss *et al.* (1964) and Edwards *et al.* (1994). Detailed biostratigraphy was outside the scope of this study, and consequently the history of biostratigraphic work is largely omitted below. However, reviews of Triassic ammonoid biostratigraphy may be found in Tozer (1967, 1994) and an updated conodont biostratigraphy has been published by Orchard and Tozer (1997).

#### Peace River region and northeastern British Columbia

Triassic rocks in the Peace River region were first reported by A. R. C. Selwyn (1877), from outcrop on the upper Peace River. Other early reports on Triassic outcrops include those of G. M. Dawson, from the Pine River valley (Dawson 1881) and from the Yukon border region (Dawson 1888); and R. G. McConnell (1891),



from the lower reaches of the Grand Canyon of the Liard River. None of these reports are detailed, and they primarily provide brief descriptions of lithology and fossils.

Between 1917 and 1942, both the Geological Survey of Canada and the British Columbia Department of Mines sponsored numerous expeditions into the Peace River region. The most prominent of Triassic workers during this period was F. H. McLearn of the Geological Survey, who concentrated on outcrop studies and fossil collections. His palaeontological work (*e.g.* McLearn 1939, 1945, 1946) constitutes the bulk of the regional Triassic biostratigraphic zonation.

The construction of the Alaska Highway in 1943 opened the way for concerted geological exploration. In the summer of that year, there were no fewer than seven geological exploration parties at work in the region (McLearn & Kindle, 1950). In 1944, E. D. Kindle formally designated the Lower Triassic Toad and Grayling Formations based on outcrop studies in the Liard River Basin (Kindle 1944, 1946). The first clear attempt at correlating Triassic units from the northern foothills with those of the southern foothills was made by McLearn (1945). He tentatively correlated the Grayling and the lowermost Sulphur Mountain Member (now Formation) of the Spray River Formation (now Group), based on the shared presence of the *Claraia stachei* fauna. McLearn and Kindle (1950) extended the Toad and Grayling nomenclature to cover most of the Lower Triassic outcrop belt from the Liard River south to the Peace River.

Between 1950 and 1960 there is a notable hiatus in publications on the Triassic outcrops in the region, possibly due to a concentration of research in the regional subsurface after the discovery of oil and gas around Fort St. John. Renewed study of the Peace River Triassic outcrop belt began with Pelletier (1960), who made detailed measurements of palaeocurrent directions in the Grayling and Toad Formations. Pelletier (*op. cit.*) determined that the Lower Triassic sediments were deposited along a northwest-southeast trending coastline, with a source to the northwest. Pelletier (1960, 1961) also first recognized the westward progradation of Lower Triassic lithofacies, and made the first palaeoenvironmental interpretations for the Grayling (deep shelf) and Toad (nearshore shelf) Formations. Pelletier (1963) then extended, with some reservations, McLearn and Kindle's (1950) Lower Triassic nomenclature further south, from the Peace River to the Pine Pass region. Finally, Gibson (1971a), after reexamining this region, confirmed the rationale regarding Pelletier's (1963) extension.

Subsequent examination of the Lower Triassic in the northern Foothills outcrop

belt has largely been confined to regional reviews and syntheses (e.g. Gibson & Barclay 1989, Edwards *et al.* 1994).

### **Southern and central Foothills, Alberta**

Studies of the Triassic in the central to southern Alberta Foothills centered on areas immediately adjacent to Banff, beginning with R. G. McConnell (1887) who described the Upper Banff Shales from outcrops in the Bow River valley. These were ascribed by McConnell (*op. cit.*) to the Carboniferous based on the substantial presence of carbonate lenses and cements and their location between his Carboniferous, Upper Banff Limestones (now the Rundle Group) and the sandstones of the Cretaceous.

In his study of Cascade Basin coals, D. B. Dowling (1907) recognized that McConnell's Upper Banff Shales probably belonged in the Permo-Triassic, despite a lack of relevant fossil data. Fossils later collected by H. W. Shimer (1911, according to Best 1958) induced him to place the Upper Banff Shales in the Permian. Finally, E. M. Kindle, in Lambe (1916), was able to provide conclusive fossil evidence, which placed the Upper Banff Shales firmly in the Triassic.

Study of the Triassic outside the immediate vicinity of Banff through the 1920s, 1930s and 1940s was sporadic and disorganized compared with the concerted work taking place during this period in the Peace River region. Numerous short reports summarized in Barss *et al.* (1964) examined fossils and lithology from some localities. The modern nomenclature and stratigraphy for this region began to take shape when E. M. Kindle (1924) proposed the Spray River Formation for the Triassic of the Banff and Jasper Parks region, designating a type section in the Spray River. P. S. Warren (1945), based on lithological and palaeontological work, subdivided the Spray River Formation into two units: the Lower Triassic Sulphur Mountain Member, described from the Sulphur Mountain gorge south of Banff, and the Middle to Upper Triassic Whitehorse Member, from the Whitehorse Creek valley near Cadomin, Alberta.

Concerted effort by individual workers and the Geological Survey of Canada to examine the Triassic of the southern Alberta Foothills began in the 1950s. Irish (1951), based on work north of Jasper National Park, first noted that the Whitehorse Member should probably be elevated to Formation status, but did not recommend a similar elevation of the Sulphur Mountain Member. Subsequent workers (e.g. Manko 1960, Mountjoy 1962) refer to both units as formations. However, a formal recommendation elevating the Sulphur Mountain and Whitehorse to Formations

and the Spray River to a Group, does not appear until Irish (1965).

Detailed study of the Triassic outcrops between the Peace River and the Alberta-United States border, sponsored by the Geological Survey of Canada, was undertaken by D. W. Gibson (*e.g.* 1965, 1968, 1971a, and many others; see Gibson, 1974). Gibson (1968) formalized, with modification, the informal Triassic subdivisions of Manko (1960), designating among others the Lower Triassic Phroso Siltstone and Vega Siltstone Members of the Sulphur Mountain Formation. Subsequent papers (summarized in Gibson 1974, 1975) by the same author extended this nomenclature south to the American border and north to the Peace River. Gibson (1968) also made the first clear attempt to determine the palaeoenvironment of the Vega and Phroso Siltstones, proposing a possibly 'anoxic' delta-front to shallow shelf environment for the Phroso, and a shallower, wave-influenced shelf for the overlying Vega Siltstone. Gibson (1974) formalized a third Lower Triassic unit, the MacKenzie Dolomite Lentil, which was first described in a publication by Best (1958, see also Barss *et al.* 1964) as the 'Middle Dolomite Unit'.

Similar to the Peace River Region, after the completion of Gibson's study (1975), most examinations of the Lower Triassic in the southern foothills has been relegated to regional discussions and reviews (*e.g.* Edwards *et al.* 1994).

### **Peace River and Alberta Interior Plains subsurface**

Although large-scale drilling and exploration programs were not the norm in this region until after 1950, a number of companies drilled exploratory wells in the 1920s and 1930s.

The earliest published discussion of the subsurface Triassic was completed by Best (1958) who included brief descriptions of several wells from the foothills between Hinton and Nordegg. This paper (Best, *op. cit.*) included a subsurface cross-section that highlighted, among other features, a prominent Middle Dolomite Unit occurring within the Sulphur Mountain Member of the Spray River Formation. Although discussion of regional Triassic stratigraphy is outside the scope of this thesis, it is curious that Gibson (1974) and Davies *et al.* (1997) failed to take note of Best's (1958) unit when erecting the 'Mackenzie Dolomite Lentil' and 'Coquinal Middle Dolomite Member', respectively.

The first major synthesis of the Triassic subsurface was that of Hunt and Ratcliffe (1959). In this paper, the Toad and Grayling Formations of Kindle (1944, 1946) were extended to include their subsurface correlatives, based on core and geophysical well log data from northeastern British Columbia and western Alberta.

Hunt and Ratcliffe (1959) is also the first publication to discuss the anomalous lithologies of the Grayling subcrop edge; these units had recently garnered interest with the 1958 discovery of oil in this interval at the Sturgeon Lake South Field.

Armitage (1962) rejected Hunt and Ratcliffe's (1959) extension of the Toad and Grayling Formations to the subsurface as the type sections since these units were located 300 miles to the northwest and no firm correlation between the regions existed. Based on subsurface work, Armitage (1962) went on to erect the Lower Triassic Daiber Group, which was divided into a lower Montney Formation and an upper Doig formation. A type section containing both units was designated in the Texaco NFA Buick Creek No. 7 well (6-26-87-21w6). However, this section was within the deep marine shelf mud and silt that comprise the bulk of the Montney Formation and has little in common with the lithologies of the eastern subcrop edge. The Montney, as described in this paper, was considered correlative in its lower portion with the Grayling, and in its upper portion with the lower Toad. A brief discussion depositional setting described the eastern Montney porous units as beach sands (Armitage 1962, p. 42).

Miall (1976) was the first worker to focus on the eastern Montney porous sands and coquinas, which had by this time proven to contain substantial hydrocarbon reserves following the development of the Sturgeon Lake Field and the 1961 discovery of the Kaybob South Field. Miall (*op. cit.*) discussed the presence of four 'porous members' within the Toad-Grayling Formation, and indicates a probable river-dominated deltaic depositional environment, based on the geometry of net porous pay isopach maps.

Following Miall's (1976) publication, there is a long hiatus in published studies of the Lower Triassic. Podruski *et al.* (1988) reexamined the eastern Montney conceptually, in a section evaluating the further hydrocarbon potential of the Montney coquinas and sands. Brief discussions of the Montney and its equivalents appeared in regional reviews such as Gibson and Barclay (1989) and Gibson and Edwards (1990). However, it was not until the mid-1990s when renewed interest in the Montney Formation, spurred by substantial gas discoveries in Montney turbidites, led to a new series of publications.

Davies (1994) was the first publication to discuss a possible sequence-stratigraphic internal division of the Montney Formation. Moslow and Davies (1994) discussed some aspects of Montney turbidites based on subsurface work as well as outcrop study from Vega and Phroso Siltstone exposures in Jasper National Park. The Canadian Society of Petroleum Geologists published a special volume in

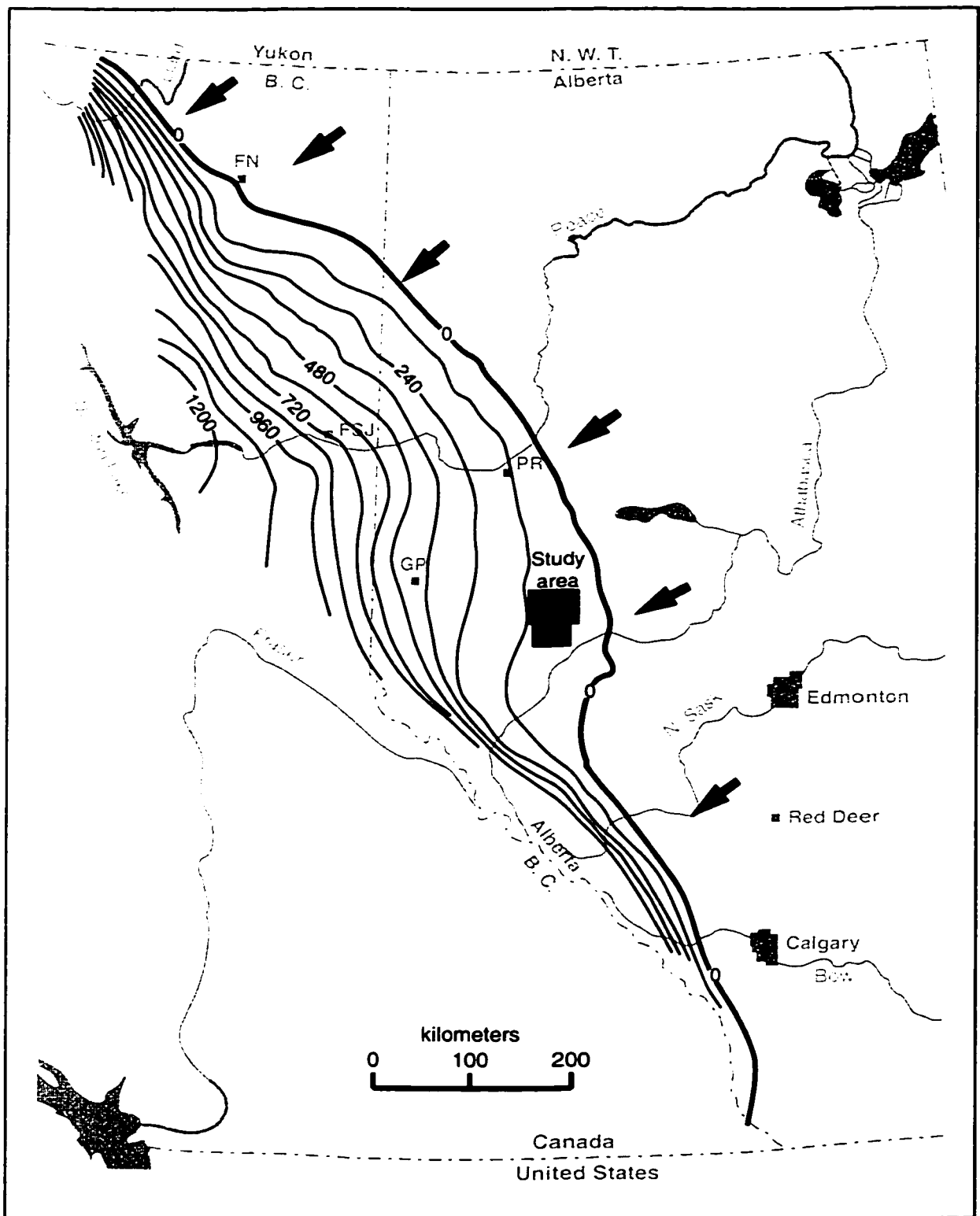
December 1997, focusing on the Triassic, and particularly the Montney Formation. In this volume, Davies *et al.* (1997) and Moslow and Davies (1997) published regional reports on the sedimentology of the Montney Formation, with emphasis on the turbidite hydrocarbon play. They also erected the 'Coquinal Middle Dolomite Member' for the thickest and most extensive unit of Montney subcrop-edge sand and coquina. In the same volume, Henderson (1997), and Paull *et al.* (1997) examined the conodont biostratigraphy of the basal Montney and MacKenzie Dolomite Lenticle, respectively. Of particular interest, Henderson (1997) indicates a probable latest Permian age for the lowermost Montney and its equivalents.

### **Tectonic Framework**

The Lower Triassic succession in western Alberta and northeastern British Columbia is contained within the Alberta Basin of the Western Canada Sedimentary Basin. The primary depocentre for the entire Triassic was located in the Peace River Embayment (Edwards *et al.* 1994), a prominent negative feature that persisted from the late Carboniferous through the Jurassic. According to published maps (*e.g.* Gibson & Barclay 1989, Edwards *et al.* 1994), in Lower Triassic time, the Peace River Embayment was a large, epicratonic basin that stretched from near Fort Nelson, BC to the vicinity of Edson, Alberta (Fig. 2.1). South of Edson, the preserved Triassic trends roughly parallel to the eastern margin of the Rocky Mountain Foothills and continues on into northwestern Montana and northern Idaho.

The provenance of Lower Triassic sediments is generally agreed to have been from low-lying, low relief Permian and Carboniferous rocks north and northeast of the basin (Pelletier 1960, 1963; Gibson & Barclay 1989) (Fig. 2.1). Progressive eastward truncation by pre-Jurassic and pre-Cretaceous erosion has removed the ancient Triassic shoreline. However, the eastern erosional edges of all the Lower to Middle Triassic formations are characterized by probable nearshore and shoreface facies, and thus are probably not far from the original eastern shoreline (Barss *et al.* 1964, Edwards *et al.* 1994).

There is a general lack of evidence for a western sedimentary source anywhere in the Triassic, as well as an apparent absence of terrane accretion until the Jurassic. This has led most workers (*e.g.* Gibson 1993, Edwards *et al.* 1994, Davies *et al.* 1997) to adopt as a working hypothesis, the existence of a passive continental margin in the Alberta Basin throughout Triassic time. However, reported occurrences of minor bentonite within the Montney (see for example Edwards *et al.* 1994, p. 259) has led nearly all workers to reserve final judgement. Complicating the issue, are recent



**Fig. 2.1 Triassic total isopach and provenance.**

Contour interval is 120 m. Large black arrows indicate provenance of Triassic terrigenous clastic sediments. Based on Gibson (1993). Map abbreviations: FN - Fort Nelson, FSJ - Fort St. John, GP - Grande Prairie, PR - Peace River.

computer-modeled palaeotectonic reconstructions, such as Smith *et al.* (1994) and Golonka *et al.* (1994) which depict substantial landmasses immediately offshore western North America in what is now central to coastal British Columbia. Furthermore, Wittenberg (1992) suggested nearby tectonism based on his study of the Doig-Halfway interval in the Middle Triassic. More recently, Zonneveld *et al.* (1997) and Zonneveld (1999) have indicated there is increasing evidence for tectonism and possibly nearby island arcs throughout Triassic time.

Three major Transgressive-Regressive cycles are recognized from the Triassic of the Western Canada Sedimentary Basin (Podruski *et al.* 1988), of which the Lower Triassic Montney Formation and equivalents comprise the first. What follows is a summary of Podruski *et al.* (1988), with some refinements by later workers (*e.g.* Gibson & Barclay 1989, Davies 1997a).

Rapid, eastward transgression of the lowermost Montney began in the latest Permian or earliest Triassic (Griesbachian) time. During late Griesbachian and throughout Dienerian time, sea level remained relatively stable, with minor basinward progradation of Lower Montney sediments. A sharp regression sometime after the end of the Dienerian led to the deposition of the Coquinal Middle Dolomite in nearshore areas and possibly the thick turbidite sequences found basinward. Renewed, slower transgression with brief regressive intervals and progradation produced the Upper Montney deposits which are most likely Smithian-Spathian or Spathian in age, depending on the timing of the Coquinal Middle Dolomite deposition.

### **Palaeoclimatological setting**

The thick redbed and evaporite deposits of the Middle Triassic Charlie Lake Formation, as well as palaeoclimatic reconstructions (Golonka *et al.* 1994, Smith *et al.* 1994) centering the Alberta Basin at a latitude of about 30°N have led most workers to interpret an arid-zone, desert to semi-desert climate for most of the Triassic Period. Gibson and Barclay (1989) speculate that the lack of redbeds and evaporites in the Lower Triassic might be indicative of more temperate conditions. However, Davies *et al.* (1997) reports that anhydrite cement, and quartz pseudomorphs after anhydrite, are relatively common in the Montney and suggests this is indicative of an arid setting.

Davies (1997a) discusses Triassic palaeoclimate in some detail, synthesizing material published by a variety of authors. In this paper (Davies, *op. cit.*), the Montney palaeoclimate is considered to be arid at least seasonally, with desert

conditions developed inland. Based on Golonka *et al.* (1994), a dominance of northeasterly winds in the summer, and onshore winds in the winter, is postulated. Fluvial transport of sediments is considered negligible (*contra* Gibson 1971a, Gibson & Barclay 1989, Edwards *et al.* 1994, and most other workers who invoke a notable deltaic influence in landward areas), with a seasonal fluvial deposition being restricted to coastal lagoons; primary sediment transportation is ascribed to the summer northeasterlies. Although occurrences of evaporitic deposits are absent in the Montney, coastal brine pans are invoked as a source for Montney anhydrite and early-diagenetic dolomite.

Although some of the conclusions of Davies (1997a) may need confirmation, and despite the reservations of Gibson and Barclay (1989), it seems to be a generally accepted consensus that an arid to semi-arid climate may be assigned to the period of Montney deposition. This is based primarily on the latitudinal position of the North American continent during the Lower Triassic and the definitely arid environment of the Middle Triassic Charlie Lake Formation.

### **Global anoxia in the lowermost Triassic**

Discussion of a major global anoxic event and its probable association with the Palaeozoic-Mesozoic mass extinction, in the latest Permian and earliest Triassic, has become prominent in the recent literature (*e.g.* Wignall & Hallam, 1993). This event likely has considerable relevance to the apparent lack of biological diversity in the lower Montney Formation, as well as the prominence of dysaerobic conditions in the Montney and its correlatives mentioned by numerous workers (*e.g.* Gibson 1968, Gibson & Barclay 1989, Davies 1997). It may also play a prominent role in the odd trace fossil assemblages observed throughout the Lower to Middle Triassic in western Canada.

## **Part 2. Kaybob and Kaybob South Fields study area**

### **Stratigraphy and previous work - Kaybob and Kaybob South areas**

There has been very little published work on the lower Montney Formation in the Kaybob area. This is surprising considering the significance of Kaybob South: it is the largest pool found to date in the Montney, and the second largest pool yet found in the Triassic of western Canada (Podruski *et al.* 1988, Edwards *et al.* 1994). In fact, with the exception of an unpublished Master's Thesis at the University of



Alberta focusing on the Sturgeon Lake Field (Mederos 1995; CSPG abstract, Mederos & Moslow 1996), all studies that include an examination of the eastern Montney are regional in scope.

Hunt and Ratcliffe (1959) mention the eastern Montney around the Sturgeon Lake Field, referring to the sands and coquinas as 'longitudinal bars' within a nearshore environment. Armitage (1962) did not amend this interpretation significantly, referring to the coarse units as beach bars. Metherell (1966) briefly discussed aspects of the Kaybob South Field such as discovery date, estimated reserves, and producing interval. Miall (1976), in his discussion of Montney porous units, briefly mentions the Kaybob South Field and places it in his 'Porous Member 2'. However, his net porous section isopach maps, which he uses to propose a river-dominated deltaic origin for the units, end immediately north of the Kaybob South area.

Basin-wide reviews of the Triassic such as Barss *et al.* (1964), Gibson (1993) and Edwards *et al.* (1994) all comment on the significance of the eastern Montney subcrop deposits. These make passing reference to palaeoenvironmental interpretations. Gibson and Barclay (1989), Gibson and Edwards (1990), and Gibson (1993) all broadly interpret the eastern Montney lithologies, including the Kaybob area, as a shallow shelf, possibly deltaically-influenced, based largely on Gibson's (1968, 1974) sedimentology and Gibson's (1971b, 1974) petrology.

The Triassic of the Peace River Embayment area in northeastern British Columbia and west central Alberta has received more comprehensive treatment in the literature. However, the usual southern limit on this region, in most studies, is placed immediately to the north of the Kaybob area (*e.g.* Gibson & Edwards 1990, Davies *et al.* 1997). Davies *et al.* (1997), although regional in nature, included descriptions of Montney facies from the eastern subcrop edge area, and incorporated some material from the vicinity of Kaybob South. They interpret the bulk of these facies to represent lower-to-upper shoreface deposits, with possible subtidal to intertidal sand flats. Based on palaeoclimatological work such as that of Golonka *et al.* (1994), they categorically reject any notable fluvial influence (*contra* Gibson and other workers), citing an arid climate and a lack of evidence for fluvial activity anywhere in the Triassic succession of Alberta.

### **Local stratigraphy - Kaybob and Kaybob South Field areas**

In the study area encompassed by this thesis (TWP 61-65, RGE 18-21w5) the Montney Formation dips gently to the southwest. Thickness, which increases

towards the west, ranges from a minimum of 52 feet (15.85 m) in the northeast at well 8-26-65-18w5, to a maximum of 314 feet (95.7 m) at well 6-31-64-21w5. The Coquinal Middle Dolomite Member of Davies *et al.* (1997) ranges from zero, to a maximum thickness of 114 feet (34.7 m) in well 13-7-62-19w5. All of the material in this area may be assigned to the Lower Montney Formation, as defined by Davies *et al.* (1997), and may be correlated with the Grayling Formation of northeastern British Columbia and the Phroso Siltstone Member (Sulphur Mountain Formation, Spray River Group) of central and southern Alberta.

Black, organic shales of the Lower Jurassic Nordegg Formation (Ferne Group) unconformably overlie the Montney Formation throughout the study area (Fig. 2.3 (A)). Although not present in all core, a thin conglomeratic pebble lag, rarely exceeding ~5 cm in thickness, is commonly observed immediately above the Montney-Nordegg contact (Fig. 2.3 (B)). The uppermost Montney locally exhibits a somewhat altered or weathered appearance (Fig. 2.3 (B)), extending 25-75 cm below the contact with the Jurassic.

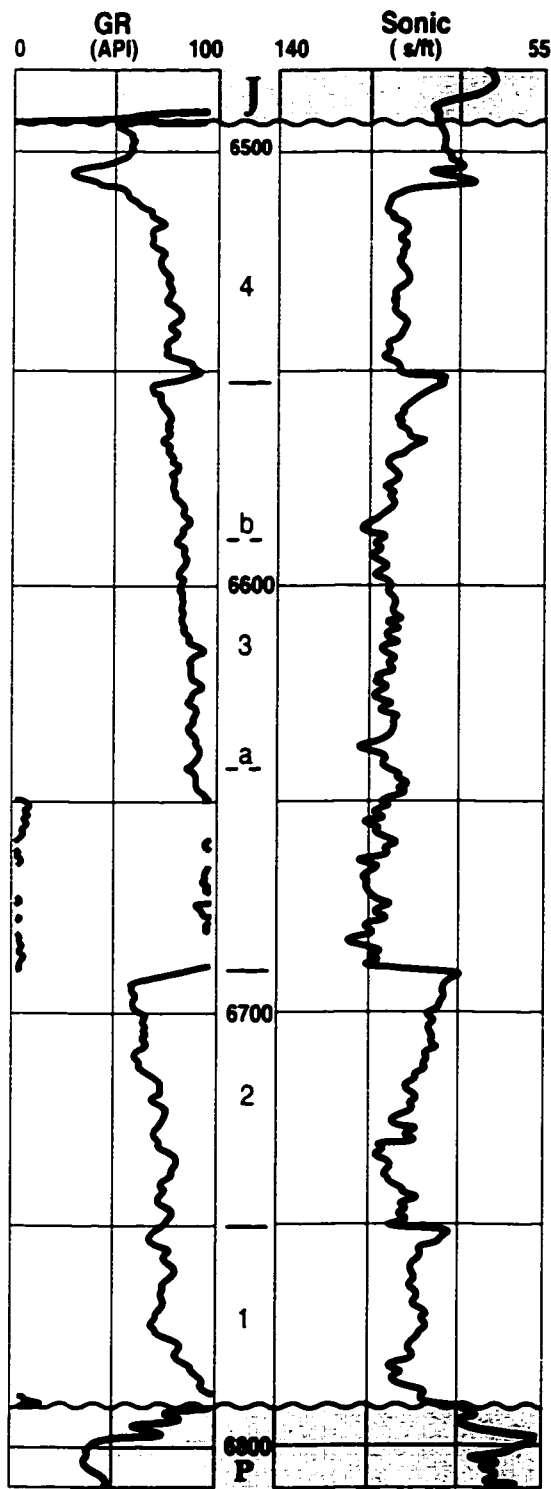
Mixed chert and sandstones of the Upper Permian Belloy Formation (Ishbel Group) underlie the Montney in the Kaybob-Kaybob South area. In the one core examined that crosses the Permian-Triassic contact (6-36-64-20w5) the contact is erosive, with an irregular surface and an immediately overlying 5 cm thick pebbly conglomerate lag (Fig. 2.3 (C)).

With the exception of the Coquinal Middle Dolomite Member, the internal stratigraphy of the Lower Montney is not defined in this area. Examination of typical geophysical logs (Fig. 2.2.) from the study area suggest the presence of at least 4, and probably more, coarsening upward 'units' within the clastic portion of the sediments.

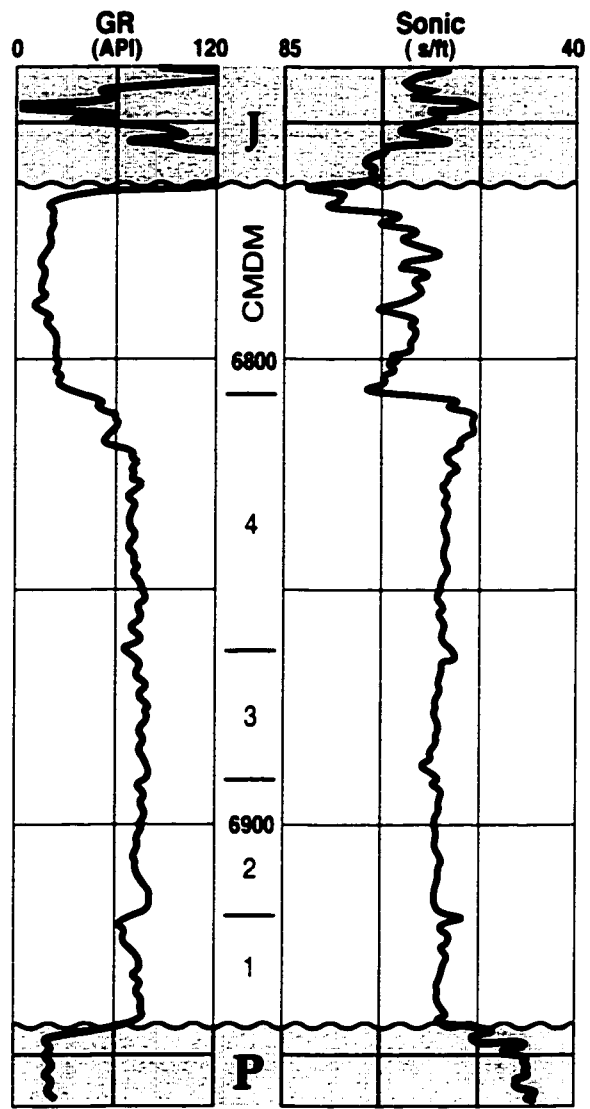
### **Part 3. Lingulidae: palaeoecology and environmental significance**

#### **Introductory remarks**

It will become readily apparent in subsequent chapters that the Lingulidae, and in particular the burrows (*Lingulichnus*) attributed to these organisms, are singularly important biotic constituents of the eastern Montney palaeoenvironment. Although no statistical count was undertaken in this study, it is probable that, excluding the cosmopolitan and ubiquitous *Planolites* and *Palaeophycus* ichnofossils, *Lingulichnus* represents 95% or more of the individual burrows observed in all the studied core. Dense, monospecific communities of *Lingulichnus* are commonly



**A** 16-33-63-21w5



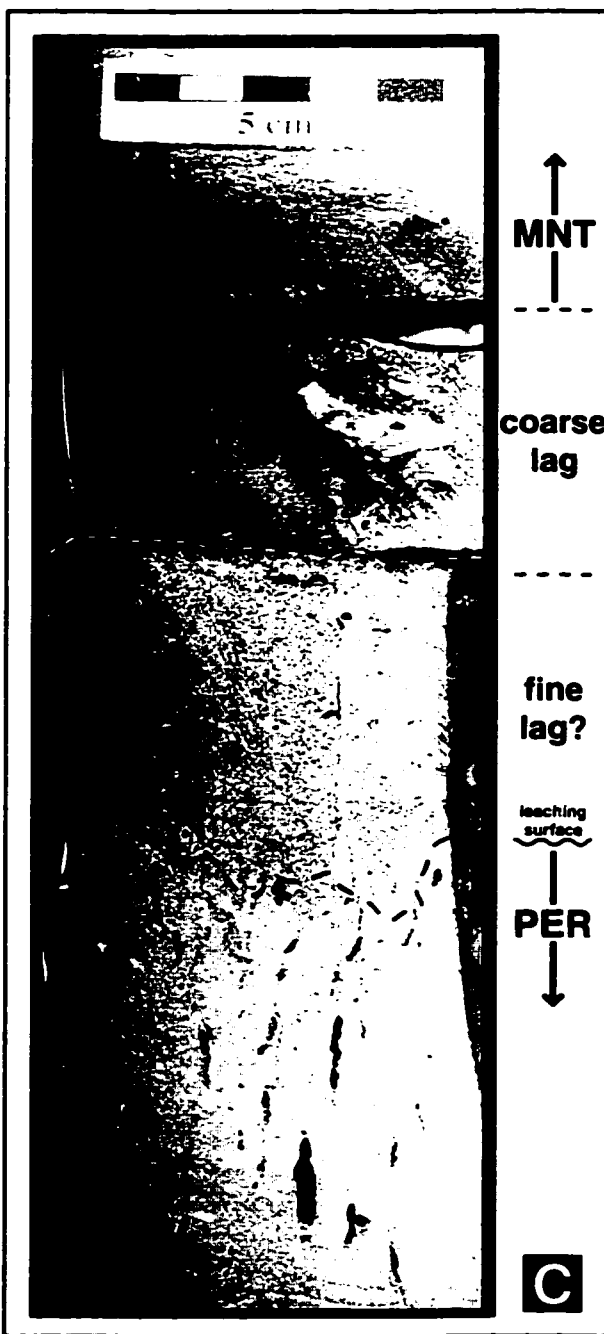
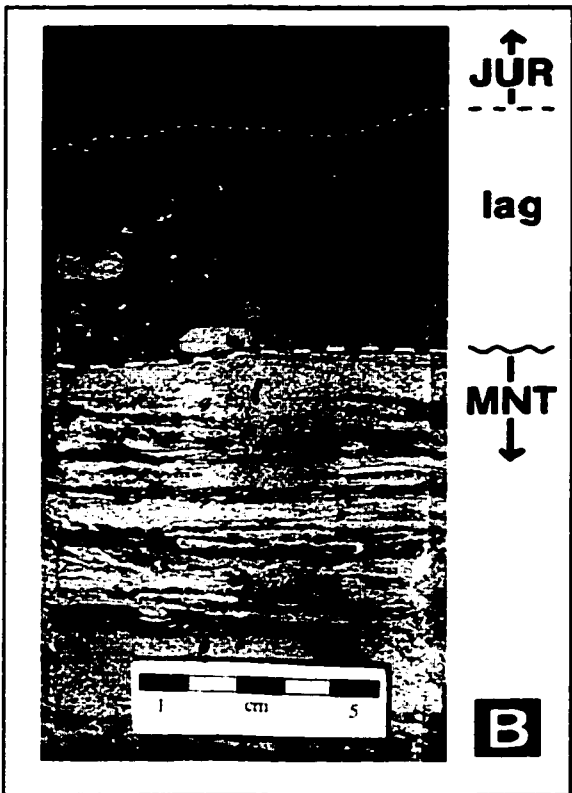
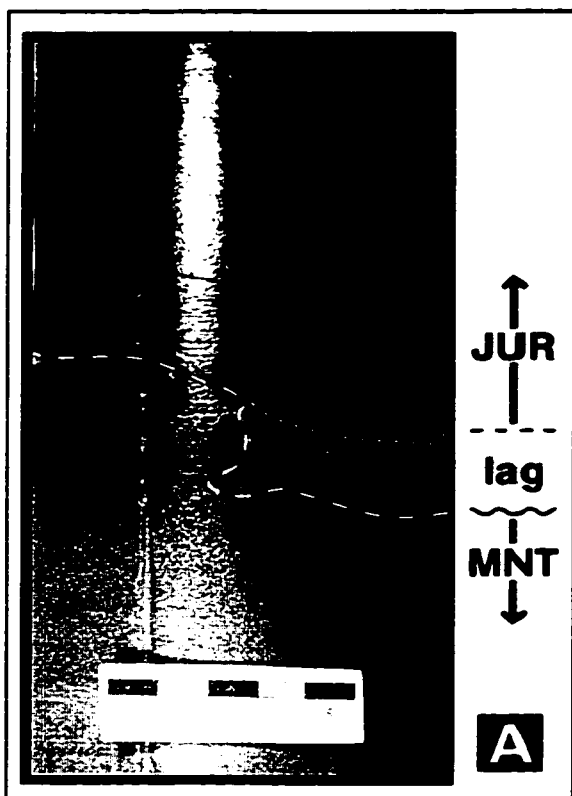
**B** 10-17-62-19w5

**Fig. 2.2 Characteristic well log responses.**

(A) Gamma ray and sonic logs through one of the thicker clastic successions, suggesting the presence of at least 4 coarsening upward units (1-4). Note that the combination of sonic and gamma ray suggest there may be as many as 6 units (defined by the two additional surfaces a-b, within unit 3). (B) Gamma ray and sonic logs through a well containing a thick coquinal unit. Here, too, the gamma ray log is somewhat equivocal, and the sonic log is important in demarcating possible surfaces. Both of these are older wells, with depths in feet.

**Fig. 2.3 Montney Fm. – Permian and Jurassic contacts.**

(A) Contact between the Montney Formation and the Jurassic Nordegg Fm. (Ferne Grp.), with the commonly developed lag deposit trapped in a small pocket eroded into the Montney. Note the homogenized appearance, interpreted as weathering from exposure before transgression of the Jurassic. From well 10-16-62-21w5, 7111' (2168 m). (B) More typical occurrence of the lag at the base of the Jurassic, ~5cm thick with relatively large clasts. From well 11-28-62-19w5, 6566' (2001 m). (C) Triassic-Permian contact. Note the leached appearance of the Permian chert bed, with vertical vug-like voids. It is overlain by fine silicified sand of equivocal age, interpreted as transgressive deposit associated with the Montney. It is possible, however, that it is in fact a Permian sandstone. A coarse lag is visible immediately below laminated sands of the lowermost Montney Formation. From well 6-36-64-20w5, ~6189' (1886 m).



observed, locally developing a pervasive fabric that destroys nearly all trace of physical sedimentary structures or preexisting burrows. Furthermore, the only body fossils observed in any siliciclastic facies of this study, aside from rare (pelecypod?) shell fragments at the bases of some sandstones, are the disarticulated valves of lingulid brachiopods, typically scattered on lamination and bedding surfaces.

The overwhelming predominance of lingulid brachiopods in the Montney palaeocommunity suggests that an understanding of lingulid ecology and biological parameters is essential to an increased understanding of the eastern Montney. The bulk of current knowledge regarding lingulid palaeoecology has been developed and summarized by C. C. Emig, J. C. Plaziat, and their coworkers (Emig 1986, 1997; Emig *et al.* 1978; Plaziat *et al.* 1978). The content of these papers and some additional contributions are reviewed and summarized in this section. Details specific to the occurrences and interpretation of lingulids and *Lingulichnus* in this study are covered in the individual facies descriptions and interpretations of the following chapter.

### **Lingulidae: general palaeontology**

Lingulid brachiopods comprise an order within Class Inarticulata of the Brachiopoda. The Lingulidae first appear in the early Cambrian (Rowell & Grant 1987) and have persisted into modern times. Although as many as 85 genera of Lingulides are known (Rowell & Grant, 1987), most are fossils dating from the early Palaeozoic. Only two modern lingulid genera exist, *Glottidia* and *Lingula*. According to Emig *et al.* (1978) and Emig (1997), *Glottidia* first appears in the early Tertiary, and only *Lingula* is known from Mesozoic rocks, including the earliest Triassic.

Lingulids are biological conservatives, and are recognized to have occupied the same ecological niche since their Cambrian evolutionary inception.

### **Lingulids: biological and ethological parameters**

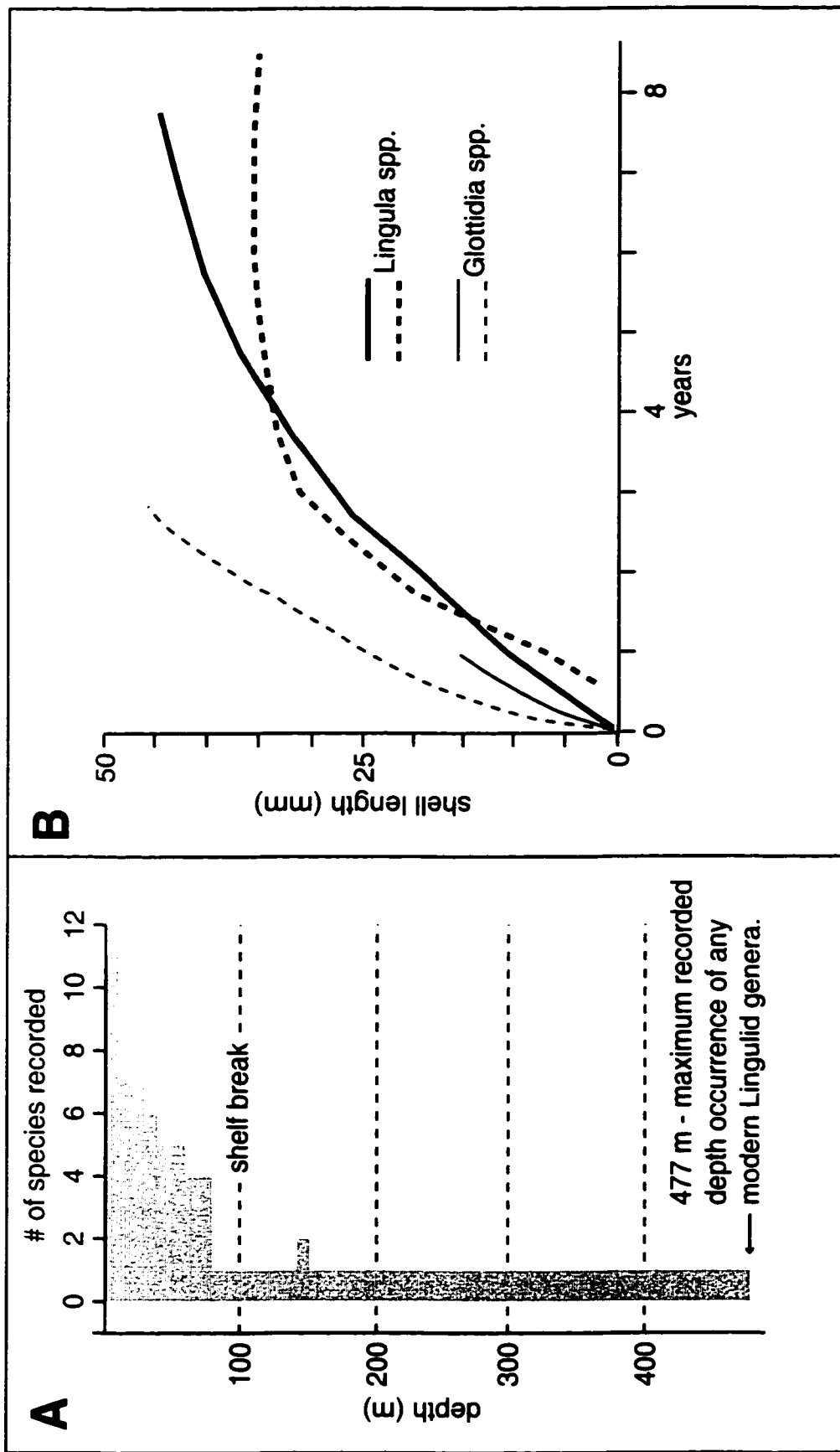
Fossil Lingulids are morphologically simple and provide few direct clues regarding their environmental parameters. Useful palaeoecological conclusions may sometimes be drawn from the sedimentary context of fossil specimens (*e.g.* Emig 1986, Ferguson 1963). However, most of what is known about lingulid behaviour and environmental preferences has been drawn from laboratory and field studies of modern specimens (*e.g.* Thayer & Steele-Petrovic 1975, Emig 1981, Hammond 1983, Savazzi 1991). Many of these authors are agreed on the biological conservatism of the Lingulidae and consider the inferences of these modern studies to be applicable to most fossil lingulids. According to Emig (1986, see references therein), the

preference of lingulids for the 'infralittoral' [shoreface to upper offshore transition] zone is well documented in the fossil record. Emig (1997) and Plaziat *et al.* (1978) categorically state that conclusions drawn from modern lingulids are applicable at least as far back as the early Triassic.

**Modern distribution:** Lingulid brachiopods are found in tropical to subtropical shallow marine environments throughout the world. The genus *Glottidia* is the dominant occupant of lingulid habitats in North and South America, whereas *Lingula* is the dominant occupant over the rest of the order's range. Locally, lingulids may be found in cool, temperate waters such as off the north coast of Japan (Yatsu 1902, Emig 1983). In all occurrences, the lingulids are predominantly inhabitants of shallow, subtidal environments; most species have also been recorded, locally, from the lower intertidal zone (Fig. 2.4 (A)). lingulid diversity rapidly diminishes seaward, with only one species commonly recorded beyond the shelf-slope break. The deepest recorded occurrence of a living lingulid is at 477 m (Fig. 2.4 (A)).

**Life cycle:** According to Emig (1997), experimental data on lingulid life span remains limited, but specimens of *Lingula* in laboratory growth rate experiments have lived as long as 10-12 years (Fig. 2.4 (B)). The largest species, both living and fossil, may attain an adult shell length of 4-5 cm (Rowell & Grant 1987). Lingulids have an unusually (for brachiopods) extended planktonic larval stage, which is of prime importance with respect to their global distribution and their capacity for rapid settlement and exploitation of newly available or relatively isolated habitats; an example of the latter is modern *Lingula* populations in Hawaii (Emig 1997). Details of lingulid ontogeny may be found in Rowell and Grant (1987, pp. 467-468). Once the larva settles on an acceptable substrate, it immediately begins construction of a burrow. Adult lingulids are completely sessile, and though capable of reburrowing if exhumed, they do not otherwise move any distance once the larval stage is completed.

**Burrow morphology:** modern lingulid burrows, and the trace fossil *Lingulichnus* Hakes 1976 which is attributed to lingulids, are composed of two main parts (Fig. 2.5 (A)). A modern, inhabited burrow has a broadly spatulate appearance, with an upper dwelling portion occupied by the producer and a lower pedicle portion which serves to anchor the organism to the substrate. The dwelling portion, commonly lined with a thin layer of mucus for stability, generally has a cross-section approximating the dorsoventral shape of the lingulid brachiopod. The lower portion is typically circular in cross-section, with the same diameter as the producer's pedicle; at the distal end the lower portion widens into a bulb to accommodate the anchoring



**Fig. 2.4 Lingulid depth distribution and life expectancy.**

(A) Recorded distribution of the 12 modern Lingulid species. Note that of the 12, 11 have been recorded from the intertidal zone, and that only one is typically found deeper than ~80 m. (B) Shell size vs. age chart for species of *Glottidia* and *Lingula*. Note that *Lingula* tends to grow quickly over the first 3-4 years, then slows significantly over the remainder. Emig (1997), emphasizes that the database for Lingulid life expectancy and growth rates is still very sparse, and that this graph is preliminary. Both (A) and (B) are from Emig (1997).

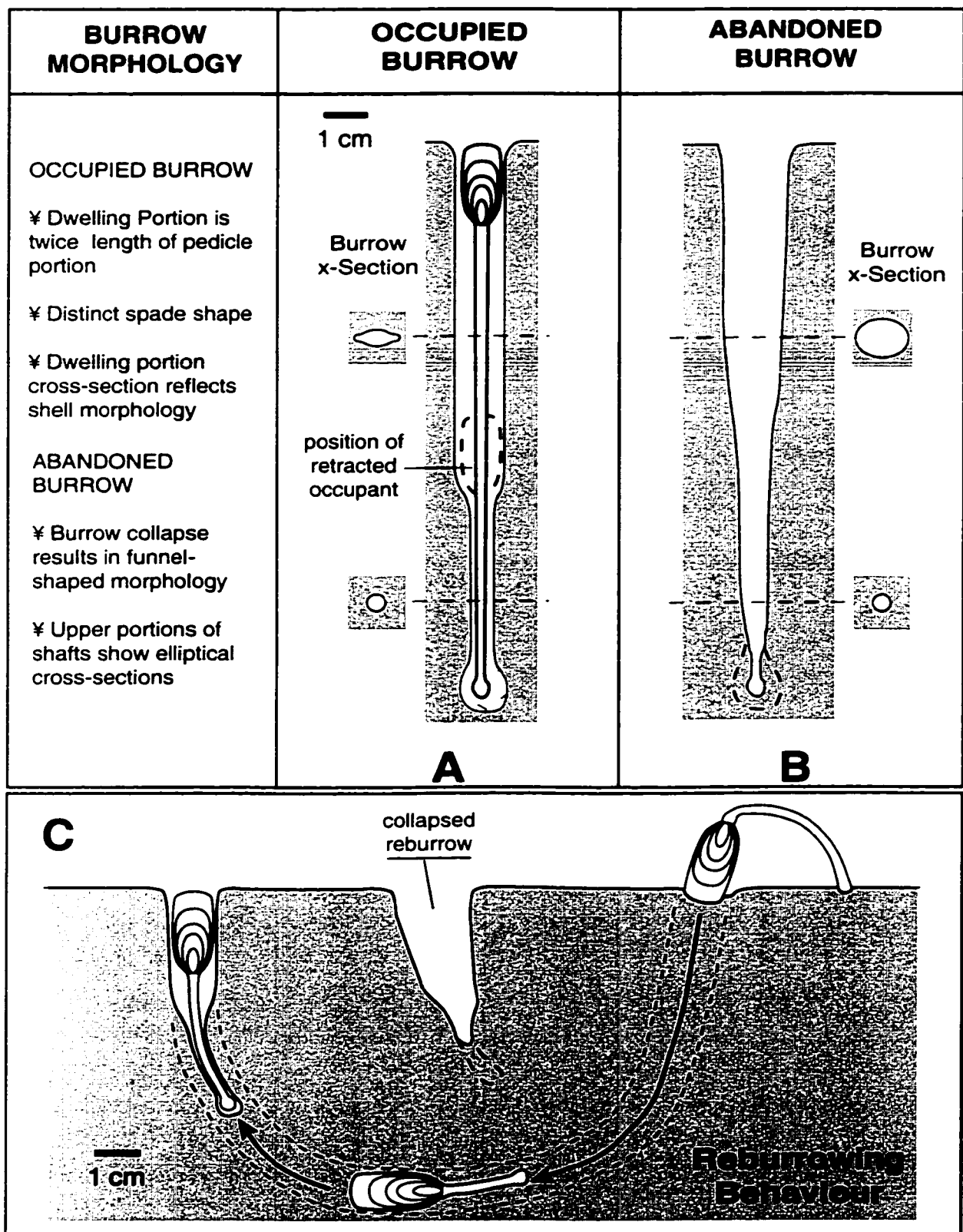


base of the pedicle (Fig. 2.5 (A)). In an abandoned burrow, collapse of the dwelling portion walls produces a funnel-like morphology, with a circular or oblong cross-section; the lower portion remains largely unchanged in appearance (Fig. 2.5 (B)). The dwelling portion of a complete burrow typically comprises two-thirds of the total burrow length, while the pedicle portion comprises the remaining third. Total length of the burrow, as a general rule, is approximately ten-times the length of the producer's shell (Thayer & Steele-Petrovic 1975, Emig 1982, 1997, Emig *et al.* 1978, Savazzi 1991).

In this study it became apparent that *Lingulichnus* is not the only ichnofossil attributable to lingulid brachiopods, depending on variations in preservation and the producing animal's behaviour. Where preserved in the absence of the dwelling portion, the pedicle portion resembles *Skolithos*. Slow upward adjustment of the burrow can produce *Teichichnus*-like structures. Rare, poorly preserved burrows may resemble *Conichnus* or *Monocraterion*.

**Reburrowing capacity:** lingulid burrows are normally constructed perpendicular to the sediment-water interface and then extended vertically as the animal grows and responds to sedimentation. In cases where the animal has had to reburrow into the sediment after exhumation, however, the burrow can adopt a curved appearance (Fig. 2.5 (C)). When an adult lingulid is required to reburrow, it does so by initially digging downwards with the pedicle trailing behind. After reaching sufficient depth, it turns to burrow horizontally, then vertically back to the surface, producing an overall U-shaped morphology. In cases where the surface is reached before both shell and pedicle are vertically aligned, the pedicle portion may remain distinctly oblique or curved, along the lower arc of the U-burrow. The burrowing process actively backfills the downward limb, which is rarely preserved or visible (Thayer & Steele-Petrovic 1975, Emig 1982, 1997, Emig *et al.* 1978, Savazzi 1991). Emig (1982, 1997) and Hammond (1983), among others, note that larger individuals, over ~2 cm, commonly fail to reburrow successfully and consequently do not survive exhumation.

**Sedimentation response:** as lingulids must be able to extend to the top of their burrows in order to feed, they are required to maintain a maximum depth relative to the sediment-water interface (*e.g.* Emig 1982, 1997, Hammond 1983). Slow erosion or deposition requiring minimal vertical adjustment is easily accomplished. However, rapid erosion generally results in exhumation of the organisms, and consequently death unless able to reburrow. lingulids are better equipped to respond to rapid deposition (Emig 1997). They are capable of quick upward migration,



**Fig. 2.5 Lingulid burrowing behaviour.**

(A) Occupied burrow. (B) Abandoned burrow after collapse. (C) Reburrowing behaviour. For additional details see text. All three diagrams are based on Emig (1997).

commonly accelerated relative to normal reburrowing (Emig, *op. cit.*). They may also extend their pedicle up to 20 times shell length in order to accommodate the upward translation (Emig 1983). Survivorship is reduced, however, if the newly deposited material is too coarse and the animals are consequently unable to stabilize the burrow extension, or if the new deposit is thicker than the maximum pedicle extension of 20 times shell length (Emig 1983, 1997).

### **Lingulids: environmental parameters.**

Lingulids have commonly been perceived as environmental generalists, a misconception reinforced by earlier publications regarding lingulids (*e.g.* Thayer & Steele-Petrovic 1975, Emig *et al.* 1978, Plaziat *et al.* 1978). Later experiments and observations (*e.g.* Emig 1983, Hammond 1983, Savazzi 1991) have revealed that the true adaptive advantage of lingulids is a short-term capacity to withstand extreme fluctuations in their environment. All modern lingulids are broadly tolerant, at least temporarily, to salinity and temperature variation, exposure and desiccation, and dysaerobia. All of these parameters fluctuate considerably in the preferred (sub-) tropical, subtidal-intertidal habitat of lingulids. Emig (1997) interprets this as an indication of a long-term adaptation of the lingulid order to this environment. The only factor for which lingulids have a narrow tolerance is substrate, and in particular, the grain-size parameter (Thayer & Steele-Petrovic 1975, Emig *et al.* 1978, Plaziat *et al.* 1978). Because of their broad tolerances, lingulids may be found in almost any shallow marine environmental context. However, in most such cases they occur only in small numbers, attributable to the fact that under normal marine conditions they are at a serious competitive disadvantage with pelecypods and other brachiopods (Emig 1997, and references therein). However, any monospecific, or nearly monospecific, assemblages, modern or ancient, dominated by lingulids or *Lingulichnus* are almost certainly restricted, shallow subtidal regimes and very likely reflect a fluvial-marine setting (Plaziat *et al.* 1978, Emig 1986, 1997).

**Substrate:** living lingulid brachiopods exclusively occupy soft substrates, necessary for the construction and maintenance of their burrows. They exhibit a marked preference for sediments in the fine, to very fine, sand size category (*i.e.* over 50% of grains 90-250  $\mu\text{m}$  in diameter) (Emig 1983, 1997). They are also common in fine and very fine sands with a clay matrix or a coarse sand component (Emig 1997). According to Emig (*op. cit.*), this falls into the fraction of sediments where saltation load is dominant. Where suspension (<60  $\mu\text{m}$ ) or traction load (220-600  $\mu\text{m}$ ) sediments predominate, lingulid populations fall off rapidly. Thayer and Steele-

Petrovic (1975), Emig *et al.* (1978), and other earlier publications attributed the fine (silt and smaller) grain size limitation to clogging of the lingulid filtration mechanism and consequent suffocation. However, Emig (1983) concluded the fine grain-size limitation was due to the inability of the animals to maintain their burrow walls in 'soupy', mud-rich substrates. Lack of burrow stability is also the primary limitation of lingulid populations in coarser sediments (Thayer & Steele Petrovic 1975, Emig 1983).

**Salinity:** contrary to common perception, lingulids are essentially stenohaline organisms, occupying only environments where salinity usually approximates normal marine conditions (35‰) (Hammond 1983, Emig 1997). However, they are capable of a strong osmotic response for short durations, able to withstand salinity as low as 17‰ and as high as 45‰ for several hours to a few days (Emig *et al.* 1978, Hammond 1983, Emig 1997). Despite the apparent preference of lingulids, particularly in the tropics, for deltaically influenced subtidal environments, none of the modern lingulid species appear to be specifically adapted to brackish conditions. Rather, they are among the limited number of organisms able to withstand the abrupt salinity fluctuations common in such environments, which, except during floods, typically remain near normal marine salinity (Emig 1983, 1997). Specifically, lingulids can survive hypersaline (>40‰) conditions and salinity below ~18‰ for a few days, and salinity below 10‰ for a few hours (Emig 1986).

**Temperature:** temperature does not appear to be a limiting factor within a lingulid population, although separate populations conditioned to a given temperature range can be exterminated when exposed to temperatures outside that range (Emig 1997). For example, the north Japanese lingulids examined in Emig (1983) commonly experience winter water temperatures as low as 1°C without ill effect; however, lingulids conditioned to tropical norms (18°C+) quickly die when exposed to water even as relatively warm as 15°C (Emig 1997). The maximum survival time for substantially sub-normal temperatures is 1-3 weeks (Emig 1986)

**Oxygenation:** Lingulids exhibit considerable tolerance with respect to short-term dysaerobic conditions in both the water column and the substrate (Hammen *et al.* 1962, Plaziat *et al.* 1978, Emig 1997). This characteristic is due to the presence of hemerythrin in the coelomic fluid of lingulid brachiopods which, unlike hemoglobin, is capable of stocking oxygen for an extended period (Hammen *et al.* 1962). However, it seems that this adaptation was not developed in direct response to dysaerobic water columns. Rather, it developed as response to temporary respiratory cessation (*e.g.* when subaerially exposed at low tides) (Emig 1997). A

resistance to diminished oxygen in the water column was a secondary benefit (Emig, *op. cit.*). Dysaerobic or stagnant conditions can be tolerated for several days to a few weeks depending on intensity, whereas anaerobic conditions can only be tolerated for a few hours at most (Emig 1986, 1997).

**Bathymetry:** as noted above, modern lingulids have been found living as deep as 477m below sea level (Emig 1997). Of the 12 living species of lingulid from both genera, 11 have been reported from the intertidal zone (Emig, *op. cit.*). However, they are most commonly found, in their greatest populations and densities, in the 'infralittoral zone' [shoreface to offshore transition], between 1-20m depth (Emig 1997).

### **Lingulids: taphonomy**

When a lingulid dies from natural (*i.e.* non-catastrophic) causes, its pedicle detaches. The animal is extruded from the burrow as decompositional gas produces a net buoyancy. The soft parts quickly decompose, and the soft, thin phosphatic shell is quickly comminuted (Emig 1983, 1990). In consequence, nothing except the burrow (sedimentary conditions permitting) is preserved. Lingulids and their burrows are only preserved in quantity under catastrophic conditions, and represent mass-death assemblages (Emig 1986).

The primary threat-response of lingulids is retraction to the base of the burrow (Paine 1970, Thayer & Steele-Petrovic 1975, Emig *et al.* 1978, Emig 1986, 1997). As a consequence, animals preserved *in-situ* within the burrow characterize many lingulid mass-death assemblages. According to Emig (1986, 1997), four events commonly result in this style of preservation (see also Table 2.1): hypersalinity, subaerial exposure, abrupt or prolonged temperature decrease, and deposition of mud. In all these cases, the lingulids are commonly able to survive short-term perturbations, but extended exposure to the condition in question results in partial or complete withdrawal and consequent *in-situ* preservation (Emig 1986, 1997). The second common preservation mode for lingulid mass-death events recognized by Emig (1986, 1997) is characterized by disseminated, disarticulated valves scattered over a bedding surface, or as a thin lens or bed. Three events may lead to this style (Table 2.1): abrupt or prolonged decrease in salinity, abrupt, thick, or prolonged coarse (2mm+ grain size) sedimentation, or exhumation by a storm. The natural response of the animals in the former two is to exit the burrow, resulting in scattered valves or a very thin bed; in the case of storms, the animals are commonly deposited en-masse as a shell bank, typically producing a lenticular deposit (Emig 1986).

STRESS	ORGANISM RESPONSE	SURVIVABILITY	TAPHONOMIC IMPLICATIONS (MASS MORTALITY ASSEMBLAGES)
Hypersalinity (>40‰)	Retraction into burrow (exploits buffering capacity of interstitial pore waters)	Hours to days	Death results in <i>in-situ</i> preservation
Reduced salinity (18‰-30‰)	Tolerant, no response	Months to indefinitely	Normal death, extrusion, and comminution
Low salinity (10‰-18‰)	Accelerate osmotic regulation; extrudes from burrow after prolonged exposure	Days	Preservation as disseminated valves or thin bed
Very low salinity (<10‰)	Osmotic regulation quickly fails; extrudes from burrow	Hours	Preservation as disseminated valves or thin bed.
Dysaerobia	No specialized response	Days to weeks	Normal death, extrusion, and comminution
Anoxia	No specialized response	Hours	Normal death, extrusion, and comminution
Emerston and/or desiccation	Retraction into burrow, rely on hemerythrin O <sub>2</sub> reserves	~3 days maximum	<i>In-situ</i> preservation
Rapid coarse (grains >2mm) deposition	Escape upward if new coarse bed thickness <20x shell length (maximum pedicle extension)	Hours if new deposit too thick or burrow cannot be maintained; indefinitely if it can	Preservation as disseminated shell bed if burrow unobtainable
Slow coarse deposition	No specialized response; extrusion if unable to maintain burrow	Indefinitely if able to maintain burrow; if not, hours to days	Preservation as disseminated shell bed
Fines ( <i>i.e.</i> ≤fine silt) deposition	Retraction into burrow if unable to maintain burrow opening in soupy sediment	Days to weeks	<i>In-situ</i> preservation
Exhumation	Reburrow if able	Hours to a day if unable to reburrow	Normal death and comminution unless exhumed by storm; in latter case, deposited as a shell bank (lenticular bed).

**Table 2.1 Summary table of lingulid biological parameters. Compiled from Emig (1986, 1997).**

### **Lingulid ecology: summary**

Lingulid brachiopods are biological and evolutionary conservatives that have maintained a sessile, infaunal mode of life since their appearance in the early Cambrian (Rowell & Grant 1987, Emig 1997). Modern species inhabit subtropical and tropical waters around the globe, with isolated populations extending into the temperate zones (Emig 1997). With respect to salinity, temperature, and oxygenation, lingulids are broadly tolerant of extreme, but short duration (days to weeks), fluctuations in their preferred normal marine conditions (Plaziat *et al.* 1978, Emig 1986, 1997). Consequently, modern species are particularly well adapted to shallow subtidal to intertidal environments, commonly with a notable fluvial influence; this has been the preferred niche of lingulids since at least the beginning of the Mesozoic (Plaziat *et al.* 1978, Emig 1997). They are not as numerous in less stressed settings, where they are at a competitive disadvantage with adaptively specialized pelecypod mollusks and articulate brachiopods (Emig 1997).

The burrow of modern lingulids, and the morphologically equivalent ichnofossil *Lingulichnus*, is a composite form consisting of an upper dwelling burrow and a lower pedicle portion. Lingulids show a marked preference for constructing their burrows in very fine to fine sandy substrates, and are sometimes capable of reburrowing if exhumed (Thayer & Steele-Petrovic 1975, Emig *et al.* 1978, Savazzi 1991, Emig 1983, 1997).

Mass assemblages of lingulid body fossils and/or *Lingulichnus* are not uncommon in the fossil record (*e.g.* Ferguson 1963, Emig *et al.* 1978, Emig 1997). Because lingulid shells are fragile, preservation of lingulid body fossils is uncommon except in mass-death assemblages associated with rapid deposition and an abrupt or prolonged perturbation of the lingulid habitat (Emig 1986, 1997). Monospecific, or nearly monospecific, mass occurrences of lingulids or *Lingulichnus* throughout the Phanerozoic, and particularly since the beginning of the Mesozoic, can almost certainly be interpreted as shallow marine, subtidal to intertidal, typically fluvially- or deltaically- influenced deposits (Plaziat *et al.* 1978, Emig 1986, 1997).

## CHAPTER 3: FACIES, FACIES ASSOCIATIONS, ICHNOLOGY AND SEDIMENTOLOGY.

### INTRODUCTION

The primary goal of this study is the interpretation of an environmental and genetic context for deposition of the eastern Montney Formation in and around the Kaybob/Kaybob South area. Comprehensive examination from both sedimentological and ichnological perspectives is essential to proper understanding of ancient depositional environments (*e.g.* Frey & Pemberton 1985, Pemberton *et al.* 1992a). Facies analysis, by grouping sediments displaying similar lithological and biological characteristics into recognizable units and then examining the interrelationship of these units, provided the best foundation from which to integrate results and develop a palaeoenvironmental framework.

In the study area, three Facies Associations, of which two are siliciclastic and one is bioclastic, may be identified. The two siliciclastic associations comprise the Lower Montney Formation of Davies *et al.* (1997), while the bioclastic (coquinal) association correlates with the Coquinal Middle Dolomite Member (Davies *et al.*, *op. cit.*) of the Montney Formation.

The genetic context of most facies observed in this study is in part dependent on stratigraphic relationships that are elaborated upon in Chapter 4. However, a brief description of genetic setting is included in the individual interpretation of each facies.

### FACIES DESCRIPTIONS

Sediments in the study area may be divided into 15 facies based primarily on sedimentology and lithology (Table 3.1). Grain size of siliciclastic material was identified in core by visual comparison with a Canstrat card. A number of thin sections were examined in order to confirm the observations and insure that cementation or diagenetic textures were not distorting original grain sizes. Bioclastic grain sizes were large enough to be measured with a ruler. Where possible, the size of bioclasts as measured on the sides of core segments were compared to grains on the top and bottom of core segments in order to ensure maximum dimensions were obtained.



FACIES	LITHOLOGY	SEDIMENTARY STRUCTURES	ICHTNOFOSSILS	BODY FOSSILS	ENVIRONMENT
A	Interlaminated vfg sand, coarse silt, and mud. Pyritiferous.	Lenticular, wavy-  el, low-angle   el to planar   el lam. Rare ripples. Poss. starved & climbing ripples. Prd silt drps.	Rare <i>Pl</i> , <i>Pa</i> , <i>Ch</i>	None observed	Dysacrobic Prodelta or offshore transition
B	Interlaminated fining-up vfg sand and coarse silt	L-am. graded beds. Wavy-  el, ripply lam. Flasers, ripple x-lam, hb x-lam, prd silt drps. Ptzd horiz.	Ab <i>Li</i> , Com <i>Pl</i> , <i>Pa</i> , <i>Te</i> , <i>Th</i> , rare <i>Di</i> , <i>Sk</i> . Very rare <i>Be</i> , <i>Ar</i> .	Disseminated valves of <i>Lingula</i>	Tide infl. lower delta front or lower shoreface, locally middle delta-front/shoreface
B1	Facies B 80%+ silt. Locally pyritiferous.	Wavy-  el, low-angle   el or planar   el lam. Prd silt drps. Rare ripples.	<i>Li</i> , <i>Pl</i> , <i>Pa</i>	Disseminated valves of <i>Lingula</i>	Tide infl. upper prodelta to lower delta front, or lower shoreface
B2	Facies B 60%+ sand.	Same as B	Same as B	None observed	Tide infl. lower to middle delta front, or middle-upper shoreface
C	Upward coarsening vfg sand and minor coarse silt	Abundant ptzd horiz. Rarely preserved ripply lam, flasers, ripple x-lam. Poss hb x-lam, reactiv. Surf.	Rarely preserved <i>Li</i> , <i>Th</i> , <i>Pl</i> , <i>Sk</i>	None observed	Tide infl. upper delta front or upper shoreface.
D	Convolute and chaotic silty sand	Synsedimentary deformation structures	None native, all relicts from precursor sed	None observed	Slumped and loaded beds, in any of above envs.

**Table 3.1.A. Summary table of facies described in this study.** Abbreviations: ||el = parallel. Prd silt drps = Paired silt drapes. Ab = Abundant, Comm = Common, Unc = uncommon. hb x-lam = herringbone (bidirectional) ripple cross-lamination, ptzd horiz = pelletized horizons. *Ar* = *Arenicolites*, *Be* =

*Bergaueria*, *Ch* = *Chondrites*, *Di* = *Diplocraterion*, *Fug* = escape traces (Fuguchia), *Li* = *Lingulichnus*, *Pa* = *Palaeophlyctus*, *Pl* = *Planolites*, *Sk* = *Skolithos*, *Te* =

*Teichichnus*, *Th* = *Thalassinoides*. vfg = very fine grained, fg = fine-grained, mg = medium grained, vcg = very coarse grained

E	Massive to finely lam vfg and fg sand	HCS, planar-  el, low angle   el lam. Rip-up clasts. Comm. Structureless app.	Normally absent. Rarely, Fug.	Comminuted calcitic shells	Storm deposits, shallow shelf or shoreface.
F	Texturally graded vfg sand	Rare, same as B.	Rare <i>Li</i> , Fug.	None observed	Waning storm beds or sed-grav flow deposits, within above envs.
G	Homogenized silty sand	None native, all relicts from precursor sed.	None native, all relicts from precursor beds	Normally none. Rarely, moulds of shells	Dewatered beds, within above envs.
H	Sand and pelletized silt	Ab. pelletization	Very rare <i>Te</i> , <i>Li</i> , <i>Pl</i>	None	Bioturbated or dewatered beds, any of above envs.
I	'fine'-matrixed coquina	Unc. Low-angle   el, rare conv. lam	None observed	Ab. comminuted pelecypod bioclasts, mainly <i>Claraia</i> .	Undifferentiated. (?tidal) channel-fill and storm deposits
J	'coarse'-matrix coquina	None observed	None observed	Same as I.	Channel lag
K	Interbedded patchy sand and coquina	High-angle lam. Local channel-fill x-bedding	None observed	Same as I	Tidal delta.
L	Interbedded sandy silt and coquina	Low-angle   el lam.	Very rare <i>Sk</i> , <i>Li</i> , <i>Pl</i>	Same as I.	Alternating storm-fairweather beds
M	Interbedded 'brecciating' sandy silt and coquina	Brecciation surfaces	None observed	Same as I	Beach, bar, or intertidal flat.
N	'Lam-scrum' sand and silt	HCS and planar-  el or low angle   el lam.	Thoroughly bioturbated layers, rare identifiable <i>Pa</i> , <i>Pl</i> , ? <i>Te</i> , ? <i>Li</i> , ? <i>Sk</i>	None observed	Amalgamated storm beds, shoreface to offshore transition.
O	Interlaminated fining-up mg-veg sand and silt	Same as B	<i>Li</i> , <i>Sk</i> , <i>Te</i> , <i>Pa</i> , <i>Pl</i>	None observed	Tide infl. delta front or upper shoreface.

**Table 3.1.B. Summary table of facies described in this study.** Abbreviations: ||el = parallel. Prd silt drps = Paired silt drapes. Ab = Abundant, Comm =

Common, Unc = uncommon. hb x-lam = herringbone (bidirectional) ripple cross-lamination, ptzd horiz = pelletized horizons. *Ar* = *Arenicolites*, *Be* =

*Bergaueria*, *Ch* = *Chondrites*, *Di* = *Diplocraterion*, Fug = escape traces (Fuguechnia), *Li* = *Lingulichnus*, *Pa* = *Palaeophycus*, *Pl* = *Planolites*, *Sk* = *Skolithos*, *Te* =

*Teichichnus*, *Th* = *Thalassinoides*. vfg = very fine grained, fg = fine-grained, mg = medium grained, vcg = very coarse grained

## CLASTIC FACIES ASSOCIATION ONE

Clastic Association One (CA1) consists of three major facies (A, B, and C). Facies B is further subdivided into two subfacies, B1 and B2, representative end-members of a depositional continuum. CA1 comprises the bulk of clastic sedimentation in the study area. All three facies tend to be interbedded and interfingered on a scale of several decimeters to a few tens of meters; however an overall coarsening upward trend is commonly observed. Interlaminated, pyritiferous silt and very fine sand (facies A) is typically overlain by interbedded, upward fining very fine sand and silt (facies B). Typically, subfacies B1 (strongly silt-dominated facies B) and B2 (strongly sand-dominated facies B) are complexly interdigitated, with an overall upward predominance of B2. Facies B, and in particular, subfacies B2 beds, is locally overlain by relatively thick-bedded, upward coarsening sand and minor silt (facies C). Thin beds of facies D and G (Clastic Association Two) are a common accessory component of CA1.

In all cases, CA1 consists of only coarse silt (~0.06-0.03 mm;  $\Phi 4$ - $\Phi 5$ ) and very fine sand (~0.1-0.06 mm;  $\Phi 3$ - $\Phi 4$ ). 'Finning' and 'coarsening' of sediment is generally defined by, respectively, a progressive increase or decrease in the quantity and thickness of discrete silt laminae (laminar grading, Reineck & Singh 1980). The only exception to these grain size parameters is facies A, which locally incorporates a small (<2%) 'mud' (*i.e.* fine silt to clay,  $<\Phi 5$ ) component.

Bioturbate textures within CA1 range from absent through pervasive. Facies A typically shows an absent to rare bioturbate texture, while facies C is abundantly to pervasively bioturbated. Facies B although commonly barren may exhibit any bioturbate texture, ranging from absent to abundant over as little as one meter of core. Ichnogenera observed in CA1 include all of those identified in the study area, comprising ?*Arenicolites*, ?*Bergaueria*, *Chondrites*, *Diplocraterion*, escape traces (*Fugichnia*), ?*Helminthopsis*, *Lingulichnus*, ?*Ophiomorpha*, *Palaeophycus*, *Planolites*, *Skolithos*, and *Thalassinoides*. Of these, only *Planolites*, *Palaeophycus*, and *Lingulichnus* were observed from nearly all cores.

### **Facies A: Interlaminated, pyritiferous silt, sand and muddy silt**

**Sedimentological characteristics:** facies A consists of thinly interlaminated silt and vfg (<0.1 mm) sand, with minor amounts (<2%) of 'muddy' silt. Sands are white to

light gray, locally light to medium brown, in colour. Silt is variably light to dark gray or gray-green. Muddy silt is typically dark grey.

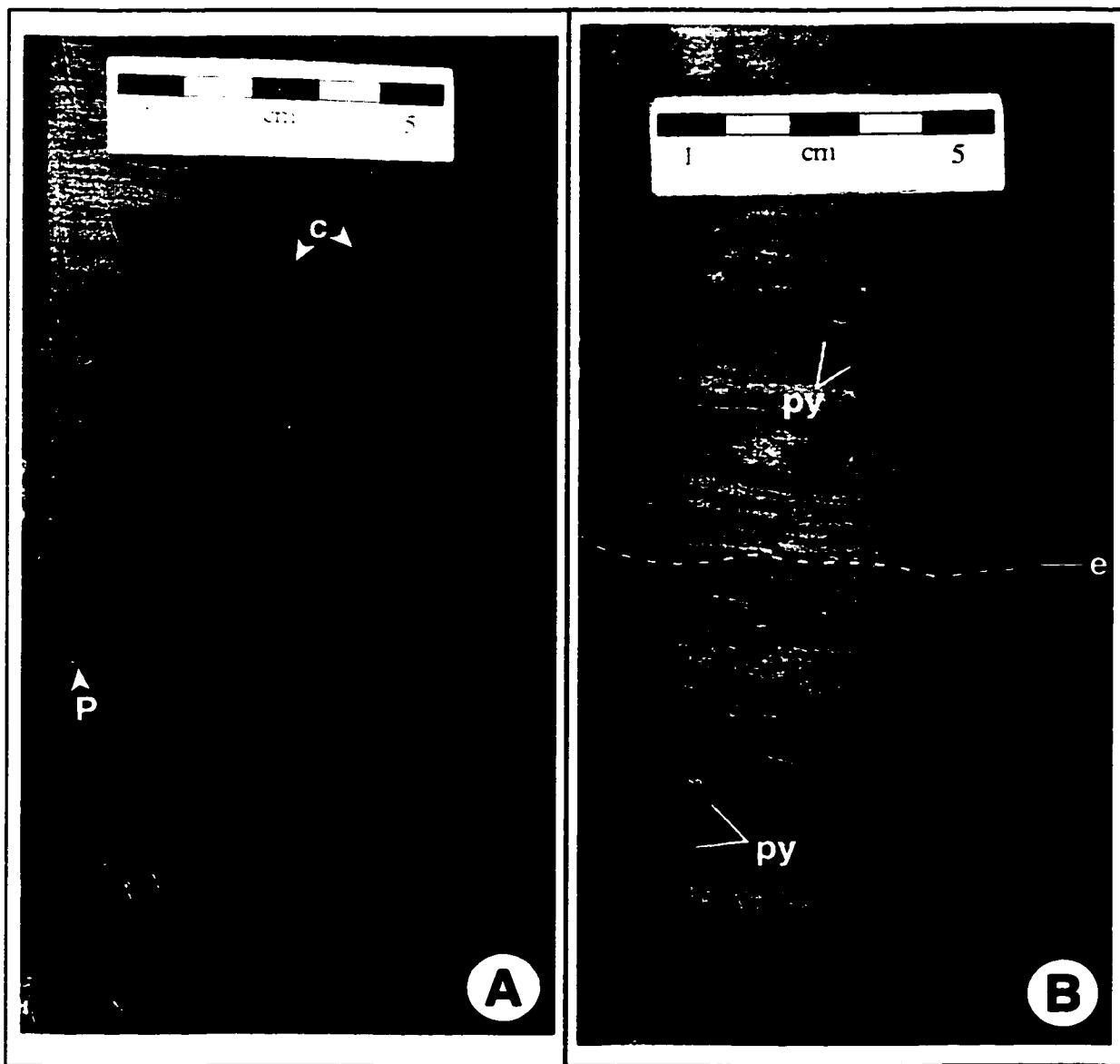
Silty layers are the dominant lithological component, typically comprising 50-80% of facies A volume. Where this facies grades towards facies B, sand content can exceed 50%, locally. The silt layers exhibit wavy parallel to low-angle parallel lamination and are generally continuous across core. Sandy laminae are dominantly lenticular (Figs. 3.1-3.3). Locally, thicker lenses of sand display internal textural variations or silt-highlighted structure suggestive of ripple foresets (Fig. 3.2 (B), 3.3 (B)). As the sand content in facies A grades towards 40-50%, individual lenses typically merge to form continuous wavy-parallel laminae. These commonly develop the light or medium brown coloration more typical of facies B and C. Sparsely distributed (<2% of facies A volume), thin muddy silt layers are typically continuous across core and exhibit wavy-parallel or irregular lamination.

Bedding is difficult to discern in facies A, which lacks discrete laminasets or prominent discontinuities. Minor erosive surfaces are observed to truncate underlying laminations locally (Fig. 3.1 (A)). Sedimentary structures other than those already mentioned are rare; they include starved ripples and possible climbing ripples (Figs. 3.1 (A), 3.3 (A)).

Pyrite is an important accessory of facies A (Figs. 3.1 (B), 3.2), occurring throughout as patchy, disseminated accumulations of small (<0.1 mm), irregular to subrounded crystals. Larger (up to 1 mm), possibly aggregated crystals are rare. Single horizons within silt layers, sand lenses, burrow fills, and burrow walls may all exhibit substantial pyritization. Pyrite mineralization almost completely replaces clastic material in some muddy silt layers. An unusual characteristic of facies A is 'graded' pyrite accumulations (Fig. 3.2 (B)). These are thin, irregular (usually <10 mm) zones where pyrite crystals show normal or (rarely) reverse grading defined by vertical variation in size and density of the individual pyrite masses.

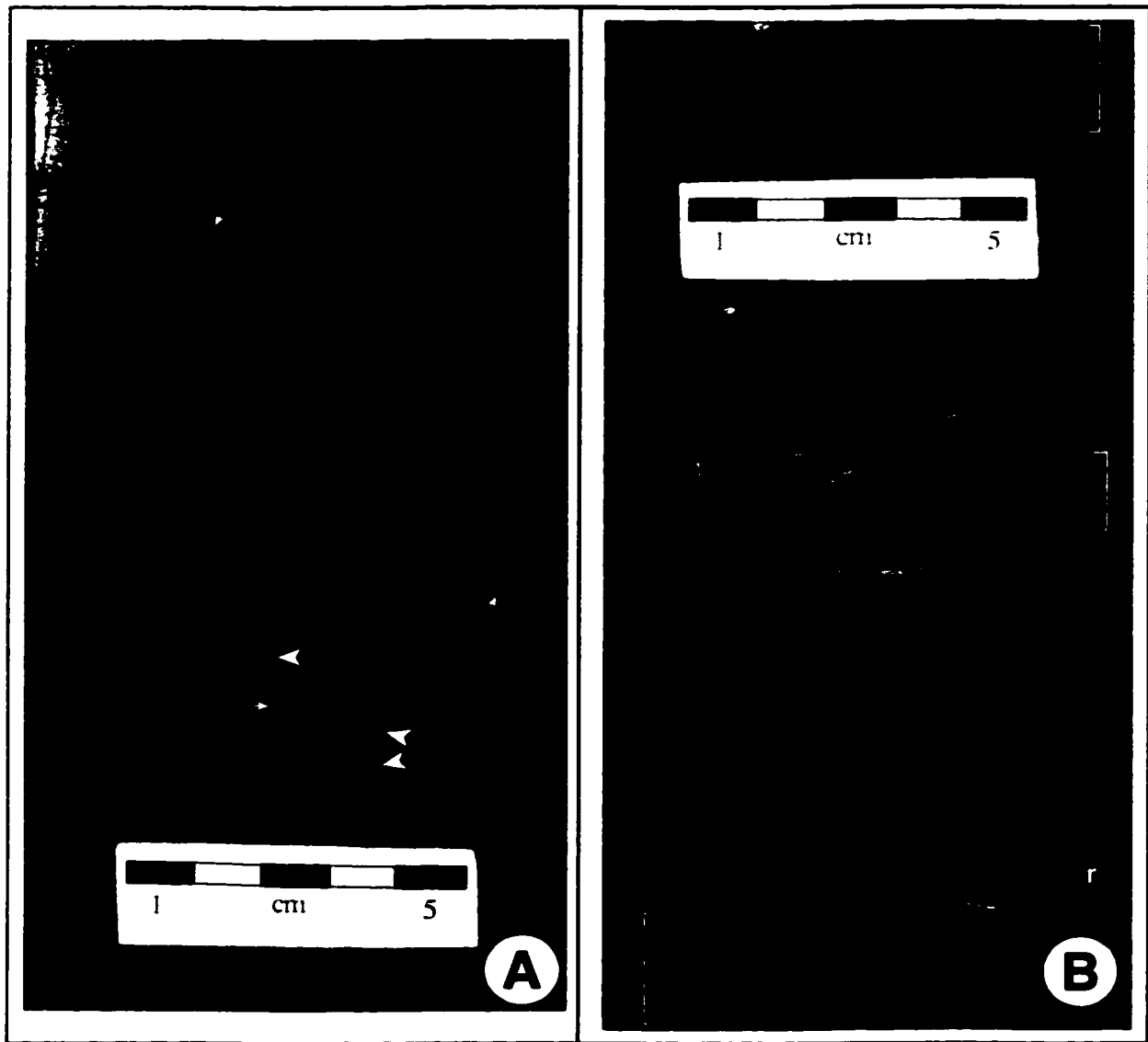
**Ichnological characteristics:** Bioturbate textures are essentially absent in this facies. However, isolated individual *Planolites* and *Palaeophycus* are developed locally throughout facies A (Figs. 3.1 (A), 3.3 (A)). Rare, possible *Chondrites* were observed to colonize single horizons (Fig. 3.3 (A)). Burrows fills of *Planolites* and the walls of *Palaeophycus* are commonly pyritized (Fig. 3.4).

**Interpretation and discussion:** the most prominent characteristic of facies A is lenticular deposition of the sand component. The apparent presence of texture- or



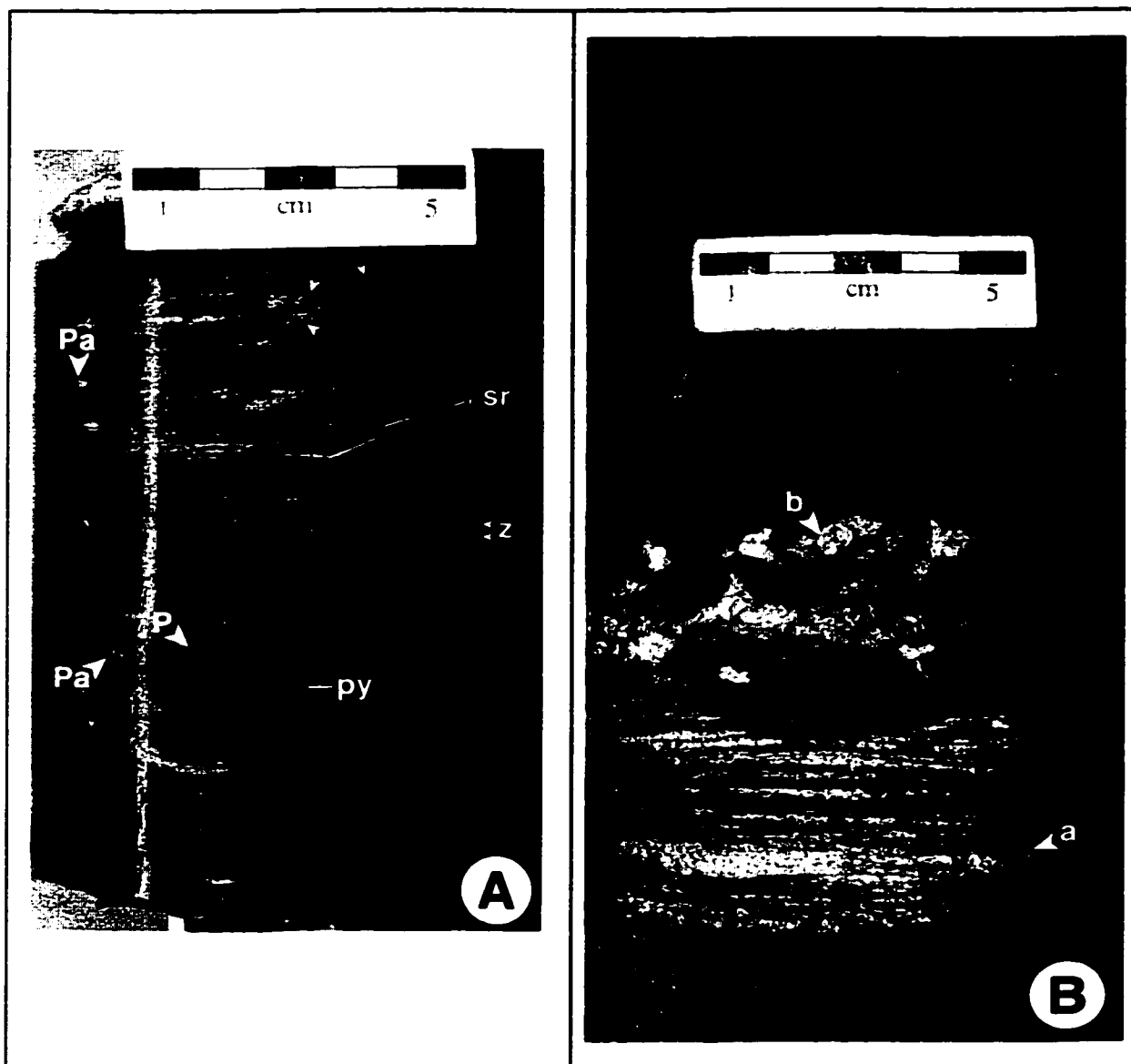
**Fig. 3.1 Facies A – bedding styles.**

(A) Typical facies A, with characteristically interlaminated lenticular sand layers (light gray) and wavy parallel silt layers (medium to dark gray). Note the general absence of bioturbation, except for a single, isolated *Planolites* [P]. The discordant-appearing structure at [c] is interpreted as a possible climbing ripple set. From 11-28-62-19w5 (6660'). (B) An example of facies A where both sand (light gray) and silt (medium gray) are predominantly wavy-parallel. Locally, laminae exhibit complete pyritization (dark masses, examples marked by [py]). Note the truncation of laminae at the surface [e]. Although rare, such truncating layers are encountered throughout facies A successions. From 14-33-64-18w5 (1777.75 m).



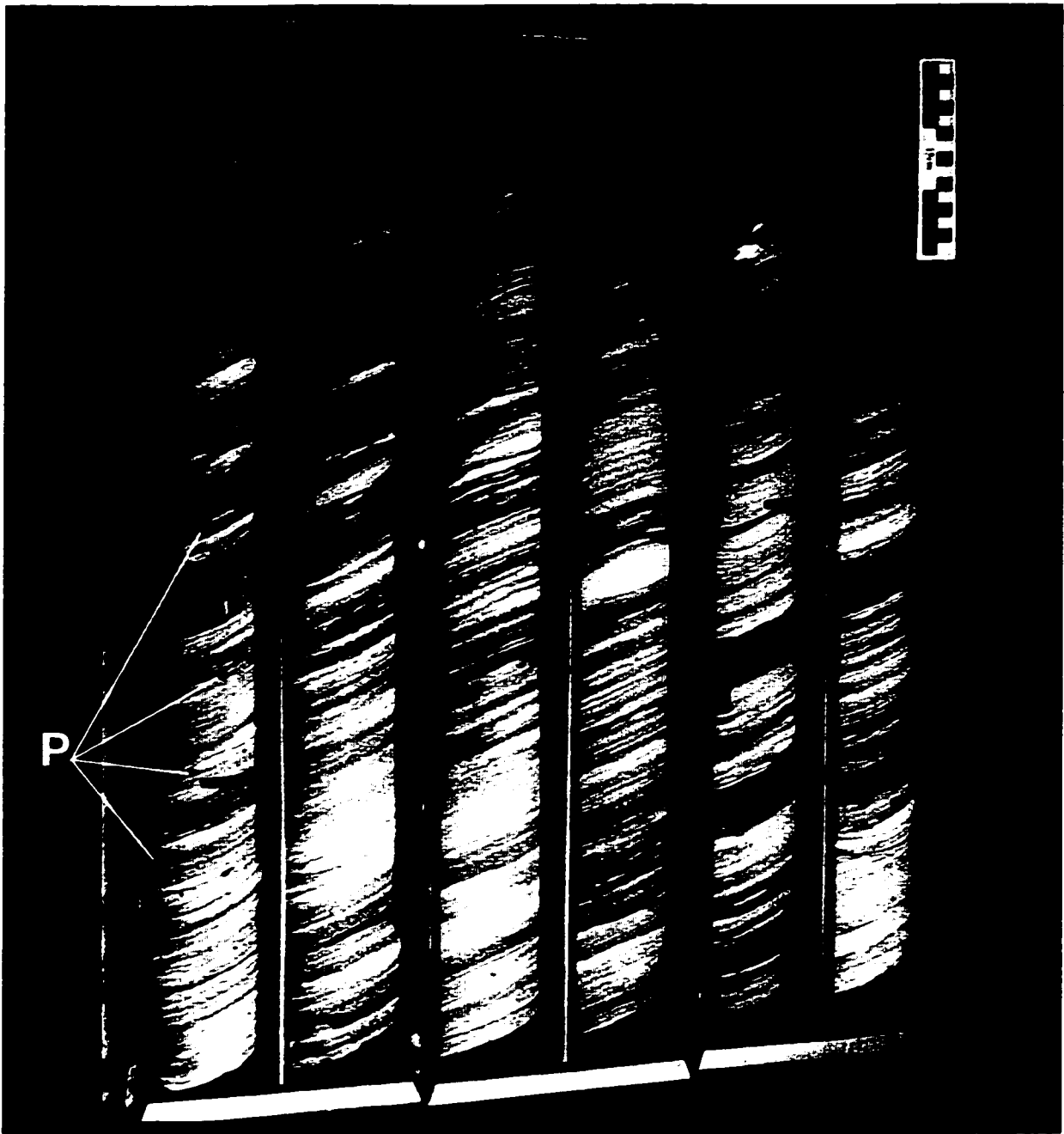
**Fig. 3.2 Facies A – sedimentary structures.**

(A) Thin-bedded facies A, showing distinct sand lenses (dark gray) enclosed within wavy parallel silt layers. Note that many of the silt layers are paired (e.g. large arrows). The disseminated, small dark bodies (e.g. small arrows) are pyrite crystals. From well 11-28-62-19w5, 6634' (2022 m). (B) Facies A, grading towards facies B. Note that sand content (dark gray) exceeds 50%, but retains lenticular lamination. The 'graded' pyrite zones [square brackets] which characterize facies A locally, interpreted as early-diagenetic Liesegang bands (see text), are well-developed in this example. [r] denotes a possible ripple, defined by the silt-suggested foreset lamination of a thicker sand lens. From well 11-28-62-19w5, 6645' (2025 m)



**Fig. 3.3 Facies A – ichnology and palaeontology.**

(A) a very silt-dominated (medium gray) example of facies A with minimal sand (light gray) content. The pyritization which characterizes facies A is evident in the completely mineralized horizon [py], and in the disseminated pyrite zone [z], which creates a lighter band within a dark, muddy silt layer. Ichnofossils in this unit include *Planolites* [P] and *Palaeophycus* [Pa]. The patch of irregular pellet-like bodies (e.g. small arrows) immediately below the scale, some of which appear to have a branching morphology, is interpreted as *Chondrites*. From well 15-29-64-18w5, 1773.8 m). (B) Unique occurrence of a terebratulid brachiopod coquina, at a contact between facies A (below) and facies B (above). This is an interesting feature as it is more comparable with faunal assemblages observed in the Middle Triassic (e.g. Zonneveld 1999, Zonneveld *et al.* 1997) than with any material observed elsewhere in this study. Note the well-preserved crinoid ossicle [b]. [a] denotes a sand lens with a suggestion of foreset laminae, possibly a ripple. From well (03)/10-34-64-19w5, 1778.5 m).



**Fig. 3.4 Facies A – box shot.**

Box shot showing the typical bedding styles in facies A at a larger scale. Sand is white to light gray, silts are medium gray. The dark bodies (e.g. [P]) in the first segment are pyritized *Planolites*. The bedding is at an apparent high-angle because this is a deviated well. Scale bar is in centimeters. From well 4-36-64-19w5 (1886-1889 m).



silt-defined foresets in some thicker sand lenses is interpreted to indicate deposition of the sand as starved ripples within a dominantly silt-depositional system. Deposition of silt appears to have been quiet settling from suspension, as low-angle parallel lamination is common. However, wavy-parallel laminations are also common in facies A silt layers. This is most probably due to minor reworking, presumably by the currents responsible for intermittent sand transport and deposition. Relatively rare episodes of quiescence deposited scattered, thin muddy silt layers. Sedimentation is interpreted to have been relatively continuous since significant discontinuities appear to be absent and truncation surfaces are rare. Identification of possible climbing ripples suggests there were also rare episodes of elevated sedimentation.

The prominence of pyritization in this facies is striking, and is interpreted to indicate dysaerobic conditions commonly prevailed during facies A deposition. This is also consistent with the extremely low-abundance, low-diversity ichnofossil assemblage of facies A, comprising only the cosmopolitan *Planolites* and *Palaeophycus*, and rare, dysaerobic-tolerant *Chondrites*.

The massive pyritization of mud or silt laminae, sand lenses, and burrows is presumed to have developed penecontemporaneously, within the sulphate reduction zone below the sediment-water interface. Locally, burrows are preferentially pyritized. This is most likely a consequence of organic molecules secreted by the trace makers that in turn catalyzed biological or chemical sulfate production.

The origin of the unusual, 'graded' pyrite deposits of facies A are attributed to very early diagenetic Liesegang-ring development. Liesegang bands are produced when solutions containing coprecipitates meet along a diffusing interface in porous media (e.g. Liesegang 1913, Sultan *et al.* 1990). Cyclic processes of supersaturation and depletion in such systems produce rhythmic distribution of precipitation horizons (Liesegang 1913, Sultan *et al.* 1990). Reducing pore waters enriched in sulphide, interacting with less reducing water comparatively enriched in ferrous ions at the redox boundary would have provided the necessary coprecipitates. The fine sand and silt of facies A provided the necessary porous medium. Thus a suitable geochemical setting was present.

The typical supersaturation-depletion Liesegang cycles would explain the even spacing of the pyritized zones. In some chemical systems, crystallization of the coprecipitates occurs in the form of discrete crystals, producing a disseminated appearance (Krug *et al.* 1993). Furthermore, Liesegang bands characterized by disseminated crystals can appear graded (*cf.* Krug *et al.* 1993, their Fig. 1.). Liesegang

banding can thus account for all characteristics of the facies A pyritized zones, in the context of a single process, and therefore it is considered the most likely origin of the graded pyritized zones.

Dysaerobic conditions are commonly associated with abundant deposition of organic material. This is not the case with facies A, in which organic matter is conspicuously absent. A second possibility is physical restriction of the environment. This seems unlikely at the local scale since the underlying Palaeozoic bedrock of the Kaybob/Kaybob South area displays minimal topography. There is no evidence for an autochthonous restriction such as a barrier-bar system. However, some evidence for local estuarine-like or channelized geometry exists (Chapter 4). At the regional scale, palaeotectonic reconstructions such as Golonka *et al.* (1994) show a substantial landmass – presumably island arcs later accreted to the continent – immediately off the west coast of North America, approximately in the same location as the modern mainland BC coastline. Such a landmass could have provided the necessary restriction of the lower Montney environment on a basinwide scale. Although there is a continuing lack of evidence for Lower Triassic sedimentation from the west (*e.g.* Gibson & Barclay 1989, Edwards *et al.* 1994), the presence of such an island arc system is becoming increasingly accepted (*e.g.* Wittenberg 1992, Zonneveld *et al.* 1997, Zonneveld 1999)

Alternatively, Wignall and Hallam (1993) have postulated that the latest Permian and earliest Triassic was characterized by a major global anoxic event that extended into relatively shallow waters. This most likely contributed significantly to dysaerobia in the facies A environment.

Facies A is interpreted to have been deposited in a relatively deep, possibly restricted, dysaerobic lower shoreface to offshore-transition, or prodelta to lower delta front equivalent. Subjection to minor currents that produced wavy silt and lenticular sand laminae suggests deposition above fairweather wave base. Evidence for even intermittent higher-energy or storm influence is absent and supports of a restricted setting interpretation.

### **Facies B: Upward fining interlaminated and interbedded very fine grained sand and silt**

**Sedimentological characteristics:** facies B consists of multiple, stacked fining-upward beds of interlaminated sand and silt. The sands are very fine-grained (<0.1 mm) and typically light to medium brown in colour. Silts are tan or light to medium

greenish-gray. Two major subfacies of B may be recognized (Fig. 3.10). Subfacies B1 beds are strongly ( $\geq 80\%$ ) silt-dominated and subfacies B2 beds are sand-dominated ( $\geq 60\%$ ). The following is a general description and discussion of facies B. Additional details specific to the two subfacies are discussed subsequently.

Each facies B bed normally contains a lower sand-dominated zone and an upper silty zone (Fig. 3.5). Bedding thickness is variable and ranges from ~1 cm up to ~80 cm. There is, however, a strong adherence to a median thickness of 2-6 cm in subfacies B1 and 4-10 cm in sandier beds. In most examples, the basal surface is sharp, commonly with small ( $< 1$  mm) sole marks. Less commonly, the contact is gradational with the underlying bed. The internal transition from the lower sandy zone to the upper silty zone is typically gradational. However, particularly in subfacies B1, it can be sharp.

The lower sandy zone exhibits two distinct characters. When thin ( $< 10$  mm) it typically appears structureless. Thicker accumulations, however, commonly incorporate wispy silt laminae and display a variety of sedimentary structures (Figs. 3.6, 3.12, 3.15-3.17). The most abundant are wavy parallel lamination, ripple cross-lamination, and paired silt drapes. Common structures include symmetrical and asymmetrical ripples, flaser lamination, and bidirectional cross-lamination. Rarely observed structures include tabular cross-lamination and climbing ripples. Not uncommonly, the lower sandy zones of sand-dominated successions appear mottled, with poorly preserved sedimentary structures, disrupted laminae, and prominent pelletization of any incorporated silt.

The upper silty zone varies considerably in appearance. When overall silt content is high ( $> 75\%$ ), the upper silty zone is distinct, commonly without any significant incorporation of sandy laminae. Silt laminae in such examples are typically wavy or low-angle parallel. Sand incorporated locally into the upper silty zone occurs as lenticular, or discontinuous wavy-parallel, laminae. In sand-dominated subfacies B2, the upper silty unit is commonly expressed only as a 'silt-enriched' zone, with 10-25% silt, over a basal sandy zone containing 2-5% silt or less. In such examples, the silty zone can exhibit the full suite of sedimentary structures described that normally characterize the lower sandy zone.

**Palaeontological characteristics:** Body fossils are very rare in facies B. However, in some core, rare bedding and lamination surfaces within facies B contain scattered, disarticulated valves of Lingulid brachiopods, most probably *Lingula*. In some exceptional cases, white, blue or purple coloration is visible, suggesting preservation

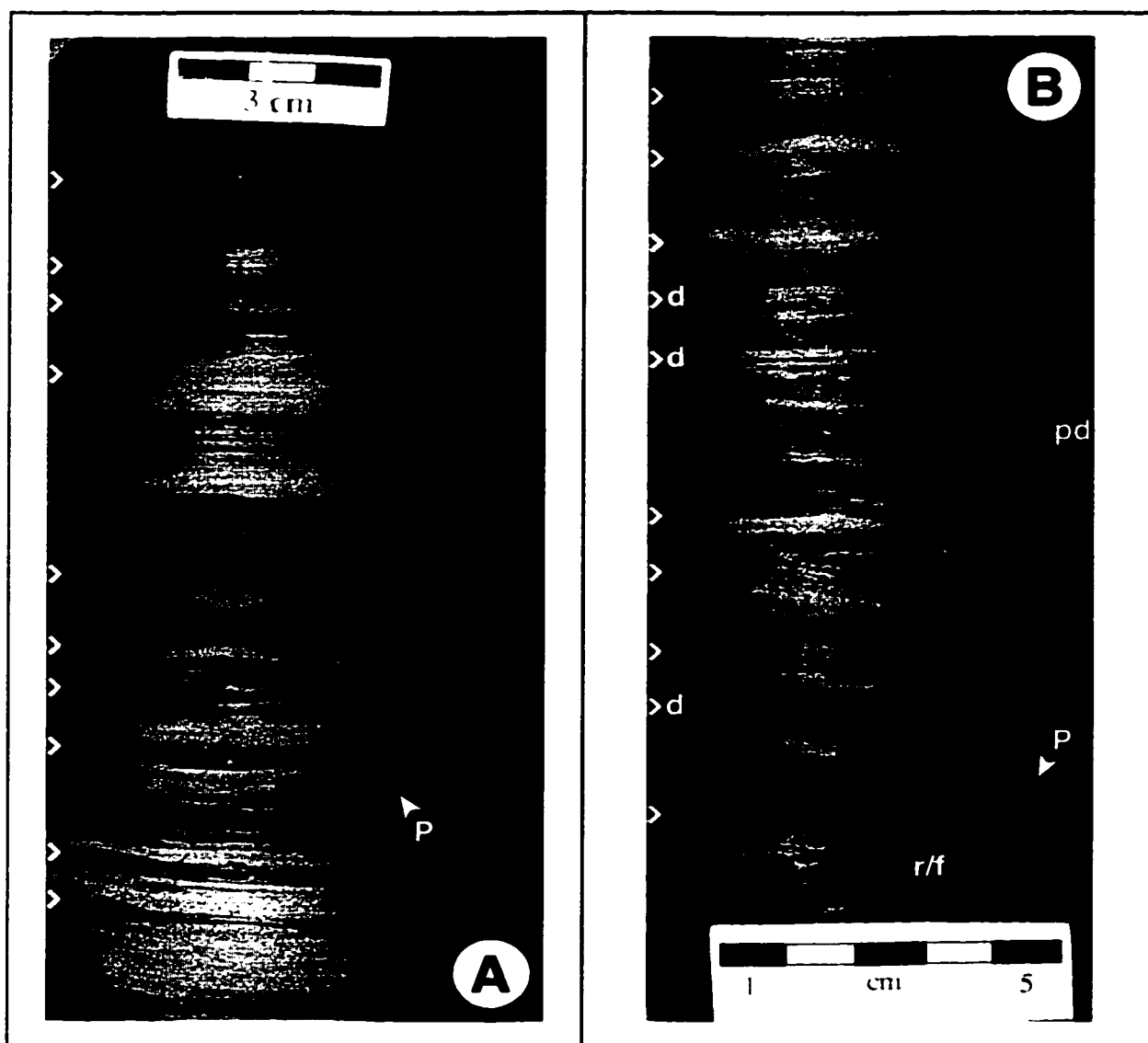
of the original, phosphatic shell material.

**Ichnological characteristics:** Bioturbation in this facies ranges from absent (Fig. 3.5) to abundant (Figs. 3.7 (B), 3.9 (B)). Facies B contains the most diverse ichnofossil assemblage of this study. It is characterized by abundant *Lingulichnus* (Fig. 3.7 (A), 3.9 (A)), common *Teichichnus*, *Thalassinoides*, *Palaeophycus*, and *Planolites*, uncommon *Diplocraterion* and *Skolithos*, and rare escape traces (Fugichnia). Accessory traces, observed as isolated specimens or from only one or two core, include ?*Arenicolites*, ?*Bergaueria*, *Chondrites*, and ?*Helminthopsis*. Overall, this assemblage is characteristic of an impoverished *Skolithos* ichnofacies (cf. Seilacher 1953, 1967, Pemberton *et al.* 1992a). Progressive vertical displacement (Fig. 3.8) is a common characteristic of *Lingulichnus*, which commonly occurs in dense monospecific communities stretching over several decimeters of core. Most *Lingulichnus* are also foreshortened, with an upper dwelling portion approximately the same length, or shorter, than the lower pedicle portion. *Lingulichnus* dwelling portions described in the literature and from modern environment are normally twice as long as the pedicle portions.

Compared with 'normal' populations described in the literature, most of the traces in this facies are conspicuously diminished in size. Most forms are restricted to facies B occurrences with ~50% or more sand content; where silt predominates, only *Lingulichnus*, *Planolites*, and *Palaeophycus* are observed.

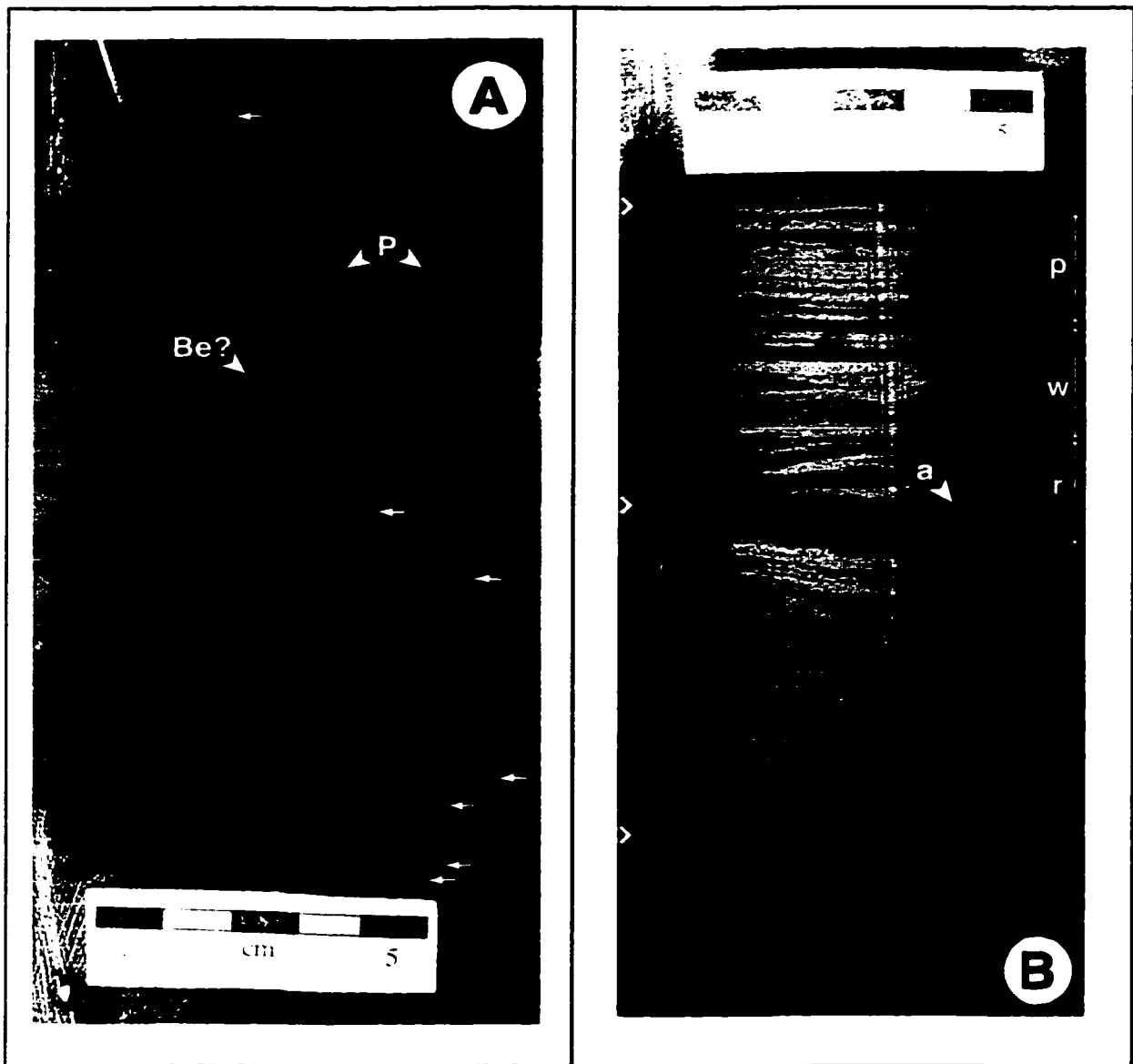
**Interpretation and discussion:** A substantial tidal influence on facies B sedimentation is interpreted from the prominence of such sedimentary structures as paired silt laminae, lenticular and flaser lamination, and bidirectional ('herringbone') cross-laminations. Locally, a series of multiple beds will resemble tidal rhythmites. It is important to emphasize that, individually, none of these are characteristic of tidal environments. However, where they occur collectively and in close association, a tidal interpretation is appropriate (Klein 1977, Reineck & Singh 1980). No evidence indicative of subaerial exposure was observed in facies B. Furthermore, paired silt drapes only occur in the context of two slack-water phases. Thus, facies B deposition is interpreted to have been entirely subtidal. A subtidal interpretation is also consistent with the observed ichnology: Emig (1986, 1997) unequivocally asserts that any post-Palaeozoic, near-monospecific assemblage of Lingulid brachiopods (the ascribed producer of *Lingulichnus*) is almost certainly of shallow subtidal origin.

The most conspicuous feature of facies B is deposition as multiple, stacked,



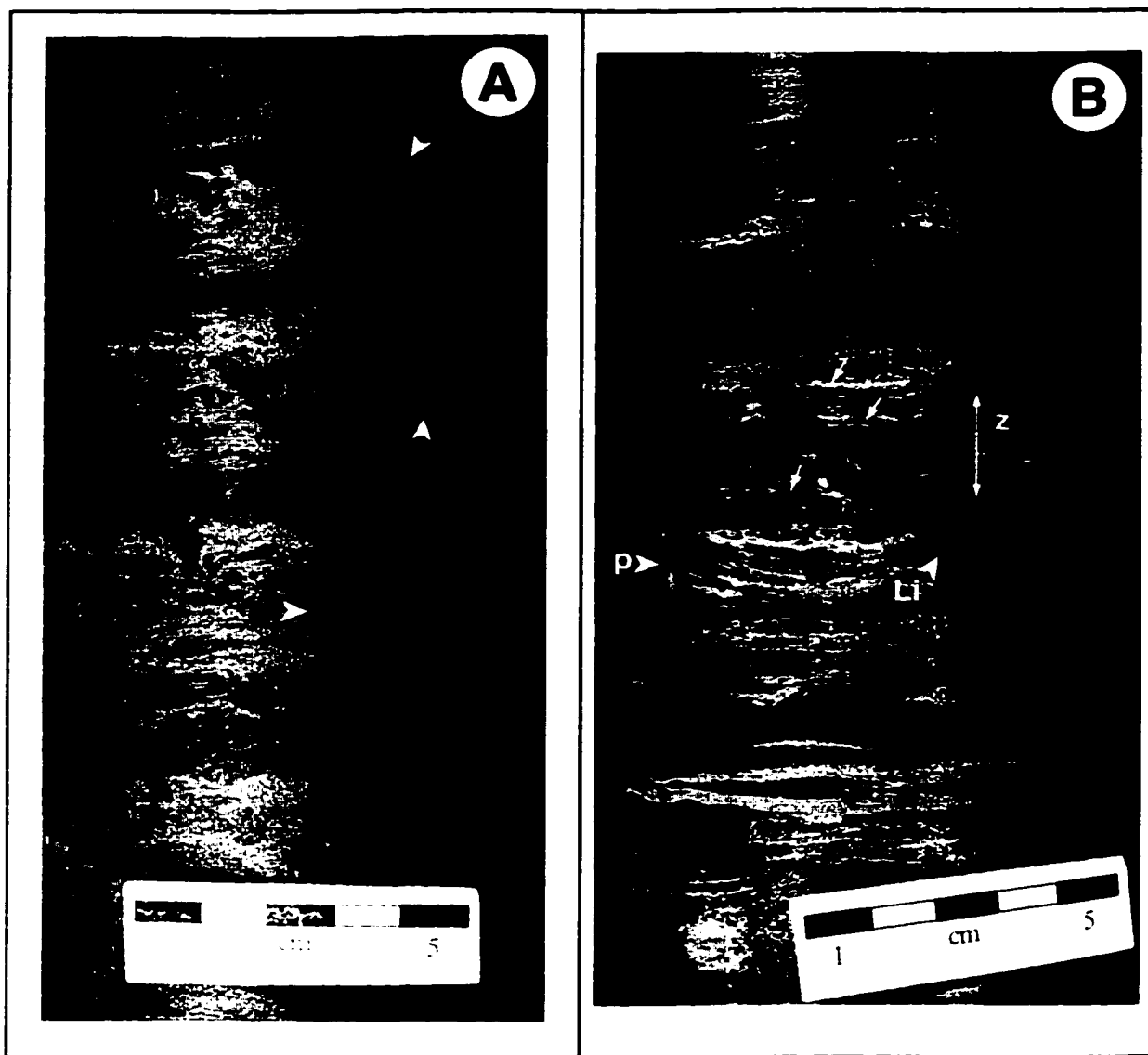
**Fig. 3.5 Facies B – bedding styles.**

(A) typical sand (dark) and silt (light) interlamination which characterizes facies B. This example is grading towards the silt-dominated subfacies B1. Flechettes (>) mark the top of each bed. Note the distinct segregation into a lower sandy unit (locally very thin) and upper silty unit. The large, round burrows [P] are *Planolites*. From well 10-11-62-19w5, 6902' (2104 m). (B) a second, more sand-dominated example. Flechettes mark the tops of beds. Lower sandy zones are the dominant component of each bed, and are characterized by ripply-to-flaser [r/f] laminations. Silty layers are typically wavy-parallel. Locally, the upper silty layer appears doubled [d], suggestive of a tidal rhythmite origin for this succession (cf. Boersma 1969, Visser 1980). However, the occurrence of paired drapes [pd] over structures within the lower sandy portions of some beds would seem to indicate multiple alternations of sand-silt sedimentation, and thus deposition of at least some beds over multiple tides. [P] is a possible *Planolites* burrow. From well 4-30-64-18w5, 1791.5 m).



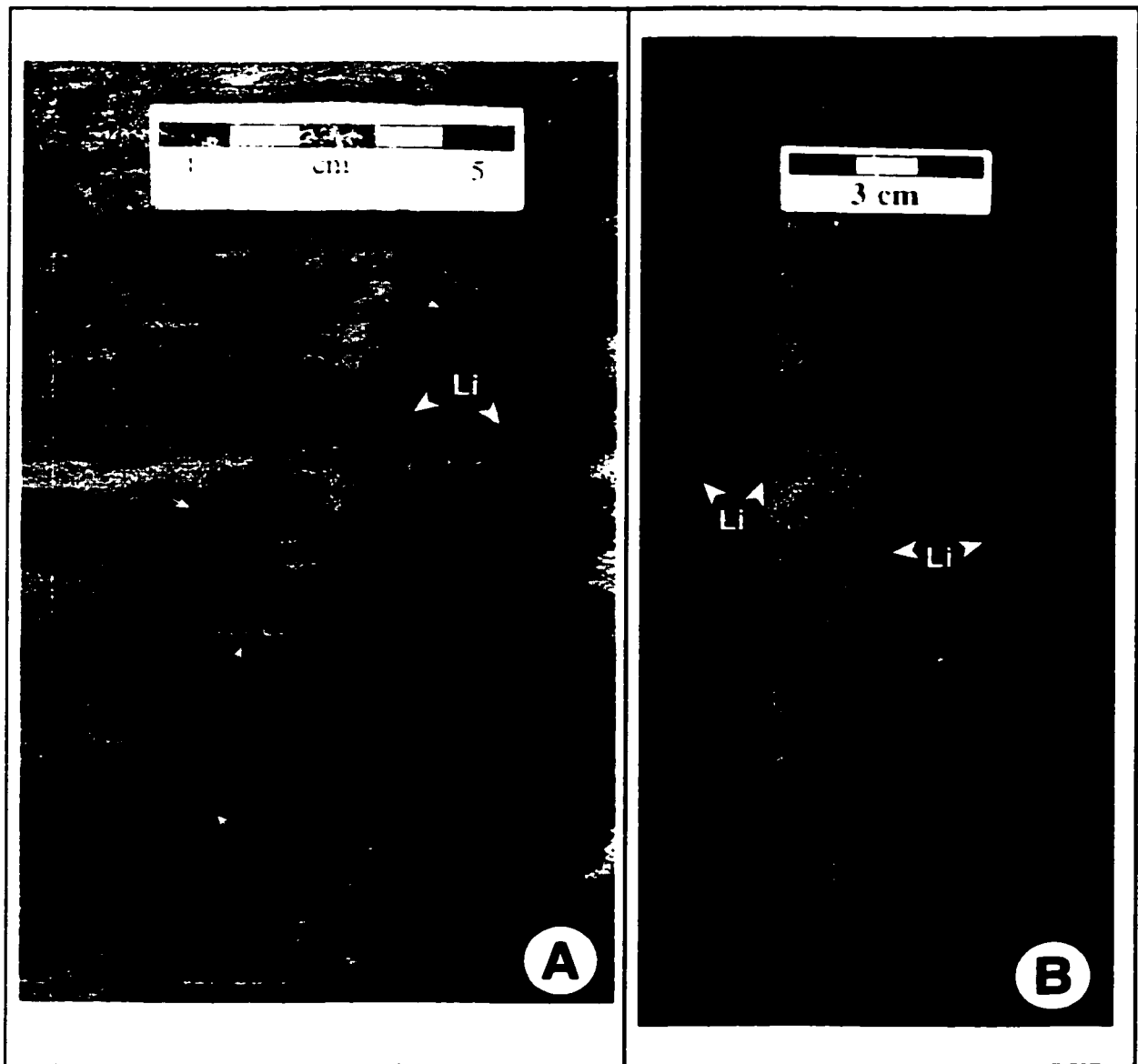
**Fig. 3.6 Facies B – sedimentary structures.**

(A) Abundant paired drapes (small arrows), with minor bioturbation by *Planolites* [P]. The relatively large depression with underlying deformed laminae is interpreted as *Bergaueria*. From well 8-32-61-20w5, 7098.5' (2164 m) (B) Large ripple [a] with silt-contrasted foresets. Flechettes mark the interpreted tops of beds, identified by a sharp surface overlying a concentration of silt laminae. Note the gradual transition of lamination styles in the top bed, ranging from ripply [r] through wavy [w] to approximately planar parallel [p]. From well 13-7-62-19w5, 7006' (2135 m).



**Fig. 3.7 Facies B – Bioturbation.**

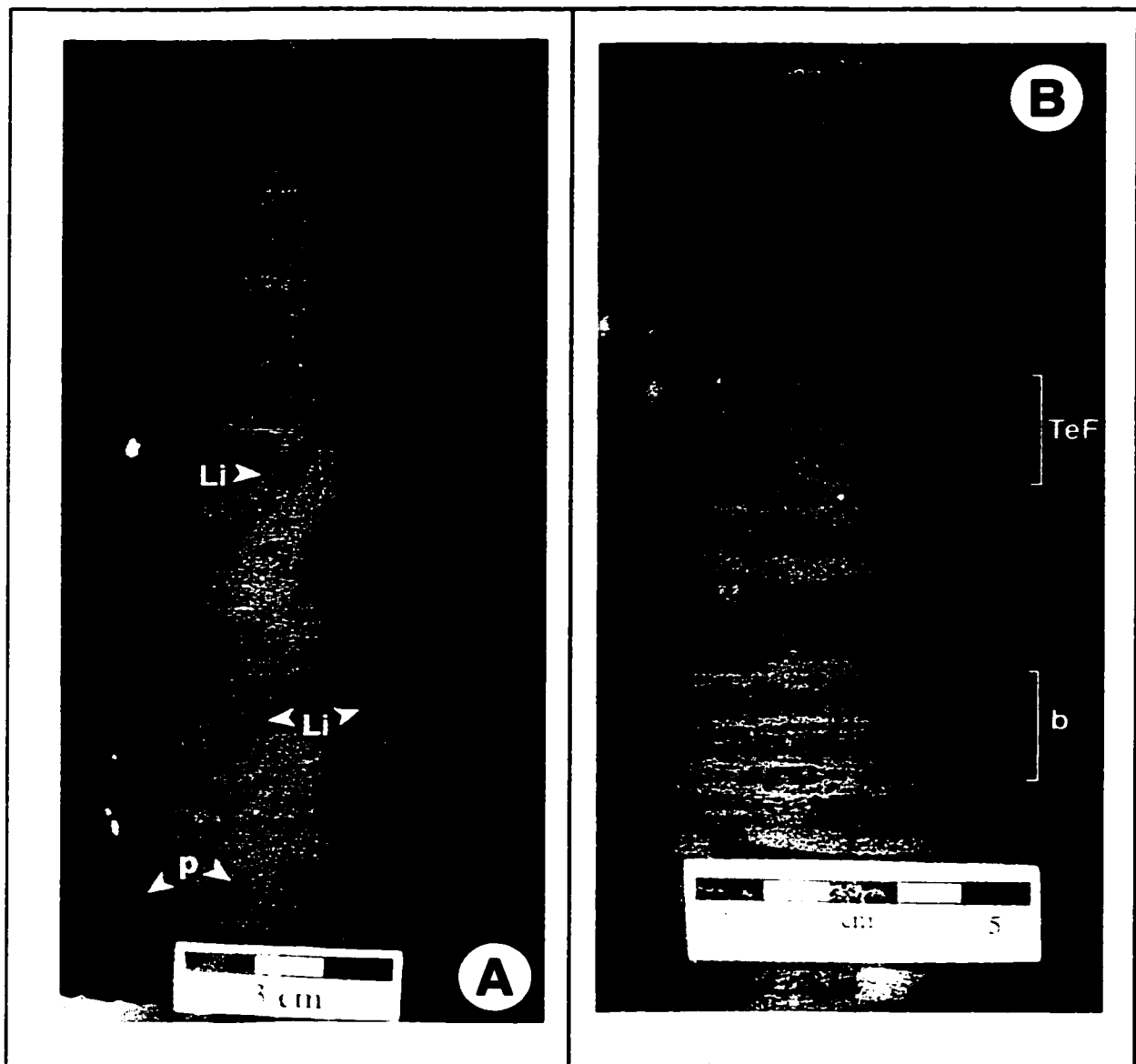
(A) bioturbate texture produced by abundant *Lingulichnus* (large arrows). The bedding-oblique, parallel alignment of burrows, a commonly observed characteristic, is equivocal in origin. It may represent a response to current direction. Alternatively, since this style of *Lingulichnus* burrowing is commonly associated with low-angle bedding (dipping to the left in this example), it may simply be a result of the non-horizontal bedding surface. A third possibility is that it represents a burrowing behaviour not observed in modern species. From well 5-7-62-19w5, 6929' (2112 m). (B) Locally abundant to pervasive bioturbation. In this example, a thin bed, characterized by pelletized material (near [z]) and disrupted laminae (small arrows) is interpreted to indicate an abundant bioturbate texture. [Li] is a *Lingulichnus*. [p] denotes a vertical structure, interpreted as the pedicle portion of *Lingulichnus*; which appears similar to *Skolithos*. From well 6-18-62-19w5, 2112.3 m.



**Fig. 3.8 Facies B – vertical migration of burrows.**

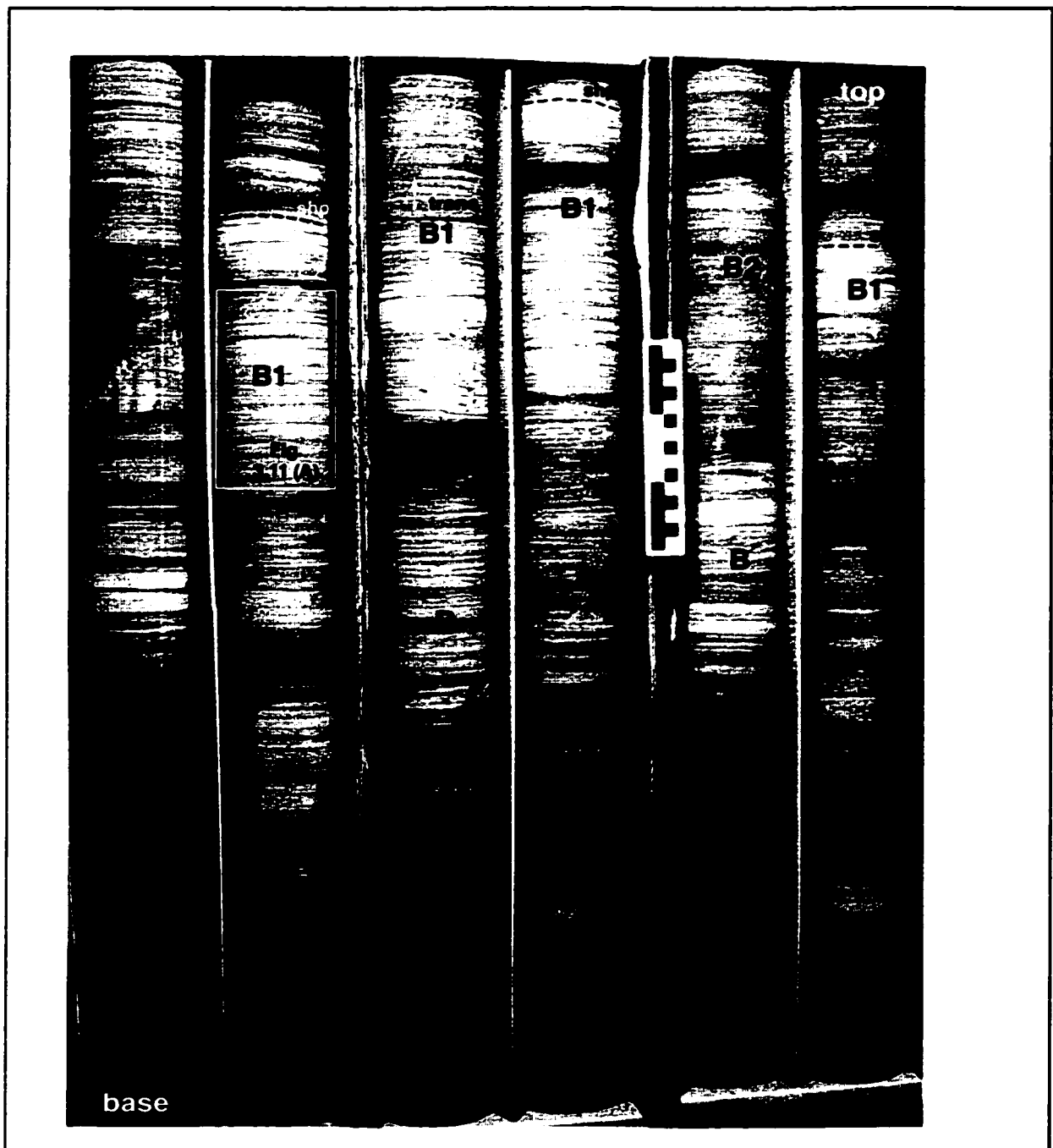
(A) from a somewhat anomalous occurrence of facies B, exhibiting substantial pyritization (disseminated black masses, e.g. small arrows) and light-colored sand. In this example, two *Lingulichnus* [Li] clearly migrated approximately 5 cm upwards (arrows are at top of burrows). Downwarped laminae and homogenized texture above the burrow openings may indicate the producing Lingulids migrated further upward. From well 1-11-65-21w5, 6120' (1865 m). (B) More vertically migrating *Lingulichnus* [Li], with better preservation. These examples clearly depict the funnel-shaped morphology of the upper (dwelling) portion of the burrow, with connected pedicle portions. Vertical shafts resembling *Skolithos*, developed locally in the burrow backfills, are overprinting pedicle portions from higher burrow positions. From well 4-2-62-20w5, 7055' (2150 m).





**Fig. 3.9 Facies B – additional ichnology.**

(A) A series of 2-4 sand dominated subfacies B2 beds within a subfacies B1 succession. Note the contrast between the apparent absence of burrows within the silt-dominated beds, and relatively large *Lingulichnus* within the sandy beds. The round bodies [p] in the lower silty bed are the pedicle shaft bases of the *Lingulichnus* [Li] which first appear at the base of the sandy succession. From well 4-2-62-20w5, 7061' (2152 m). (B) unusual bioturbate textures. The upper thoroughly bioturbated horizon [TeF] shows a distinctive fabric of concave-upward silt bodies interpreted as pervasive bioturbation by *Teichichnus*. The lower zone [b] is more typical of pervasive bioturbate textures in facies B, characterized by a pelletized silt component. In this example, distinct pelletization is visible in the top ~5 mm of the zone. From well 5-7-62-19w5, 6978' (2127 m).



**Fig. 3.10 Facies B – boxshot.**

A boxshot of facies B depicting some of the larger-scale relationships within facies B. Darker layers are sand, lighter layers are silt. Base and top are as indicated. In this example, several apparent fining up cycles predominate. Subfacies B2 (>60% sand) is located at the base of each cycle, grading through 'B' (60-20% sand) to B1 (<20% sand). A sharp surface [shp] or short transitional zone [trans] at the top of B1 forms the base of a succeeding cycle. Note the first B2 succession is considerably bioturbated with very indistinct internal structure, but that all overlying beds are apparently unbioturbated. There was clearly a shift in environmental parameters, although its nature is uncertain. Possible explanations include a shift to very rapid deposition, a significant ----->

(Fig. 3.10 cont.) shift in salinity, or an abruptly diminished food supply. Photographed from well 10-11-62-19w5, 6894 –6906' (2101-2105 m). Scale is in centimeters. The boxed in area is enlarged in Fig. 3.11 (A).

discrete fining-up beds. The appearance imparted is of a highly cyclic depositional mode characterized by normally abrupt initiation (sharp based beds, commonly with sole marks) and initially elevated energy levels (lower sandy zone) which then waned progressively (gradational transition to siltier deposition) until a subsequent episode. There are a number of depositional processes capable of producing a rhythmic or cyclic appearance. These include seasonal variation (*e.g.* glacial and lacustrine varves), tidal fluctuations of both small (*e.g.* semidiurnal couplets) and larger (*e.g.* neap-spring tidal bundles) timescales, and amalgamation of multiple, successive event deposits (*e.g.* turbidites, some tempestites).

Turbidites are common elsewhere in the Montney Formation (*e.g.* Edwards *et al.* 1994, Moslow and Davies 1994, 1997). Such an interpretation of facies B cyclicity is rejected based on the lack of any whole or partial Bouma sequences, the presence of a typically shallow-water, high-energy *Skolithos* ichnofacies, and a strong tidal influence on sedimentation. Furthermore, Lingulid brachiopods, recorded by abundant *Lingulichnus*, traditionally inhabit shallow (0-60 m) environments (Emig *et al.* 1978, Emig 1997). The absence of any bedding suggestive of HCS or SCS, prominence of silt deposition, and fine lamination of both silts and sands collectively discount periodic tempestites as the origin of facies B cyclicity.

Although an important influence, tidal processes do not seem to have controlled facies B cyclicity. Deposition as single tidal couplets is rejected on the basis of thickness and the presence of multiple paired drapes and multiple 'herringbone' sets within single facies B beds, indicating each was laid down over the course of several tides. Alternatively, Reineck & Singh (1980, p. 122) describe 'coarsely interlayered bedding', comparable in thickness to facies B beds. However, such deposits also seem to reflect single diurnal or semidiurnal sets, with the mud layer recording a single slack-water phase, again in contrast with the multiple tidal cycles in facies B-type beds. The lack of regularly thickening and thinning laminasets would seem to preclude origin of facies B cyclicity as neap-spring tidal bundling (*sensu* Boersma 1969, Visser 1980).

It is thus postulated that the apparent rhythmicity of facies B is seasonal in origin, most likely generated by a fluvial system with episodic flow. Such a system would have been consistent with the semi-arid to arid environment of the early Triassic in western Alberta, and also with the 'deltaic influence' on eastern Montney

deposition cited by most workers since Miall (1976) (see Chapter 2). Davies (1997a), however, flatly rejects any discernible fluvial influence on WCSB Triassic sediments. Furthermore, Davies (1997b) speculated that aeolian processes were the dominant mechanism of sediment transport during Montney time. This author agrees that aeolian processes were of significant importance, particularly in determining the narrow, very fine sand to coarse silt grain size fraction that constitutes almost the whole of Montney clastic deposits. However, it is not clear how aeolian transport could have resulted in the conspicuously regular internal grading of facies B beds and common adherence of most beds to a 4-10 cm median bed thickness. A fluvial system with a characteristic discharge range seems the most likely explanation for this regularity.

In the proposed model, each discharge episode would have been characterized by an initial rapid shift to sand deposition, preceded by a brief erosional phase. This produced the sharp base and foreshortened *Lingulichnus* of most facies B beds. Subsequent slow waning of the discharge episode resulted in progressively increasing silt deposition and internal gradation of the beds. Most discharge events lasted a few days, recorded by successive tidal structures in each bed. Tidal and/or wave reworking between discharge events may also have been important. Periods of fluctuating discharge brought on by closely spaced or extended onshore precipitation events would have produced the uncommon but persistent examples of gradationally superposed facies B beds.

The varying silt and sand content of facies B beds was controlled by proximity to the discharge point. Shallower proximal areas, more subject to both discharge and tidal currents, experienced higher sand deposition and increased tidal reworking, resulting in deposits of subfacies B2. Deeper, more distal areas were characterized by a dominance of silt deposition, most likely settling out of a hypopycnal flow, and produced deposits of subfacies B1.

The ichnology of facies B, with its impoverished, low-diversity but locally high-abundance *Skolithos* assemblage is indicative of a biologically stressed environment. Salinity and oxygenation are believed to have been the key controls on the facies B palaeocommunity.

Salinity conditions are interpreted to have fluctuated strongly, and not to have been consistently brackish, such as in many estuarine environments. On the surface, the observed low-diversity assemblage with dominantly diminutive forms is compatible with a brackish interpretation (*cf.* Beynon & Pemberton 1992, Pemberton & Wightman 1987, 1992). However, because there are numerous

organisms adapted to a *consistently* reduced salinity (my emphasis), brackish settings are normally characterized by considerably higher diversity (e.g. Alway & Moslow 1997, Buatois *et al.* 1997, Ranger & Pemberton 1992) than observed in facies B.

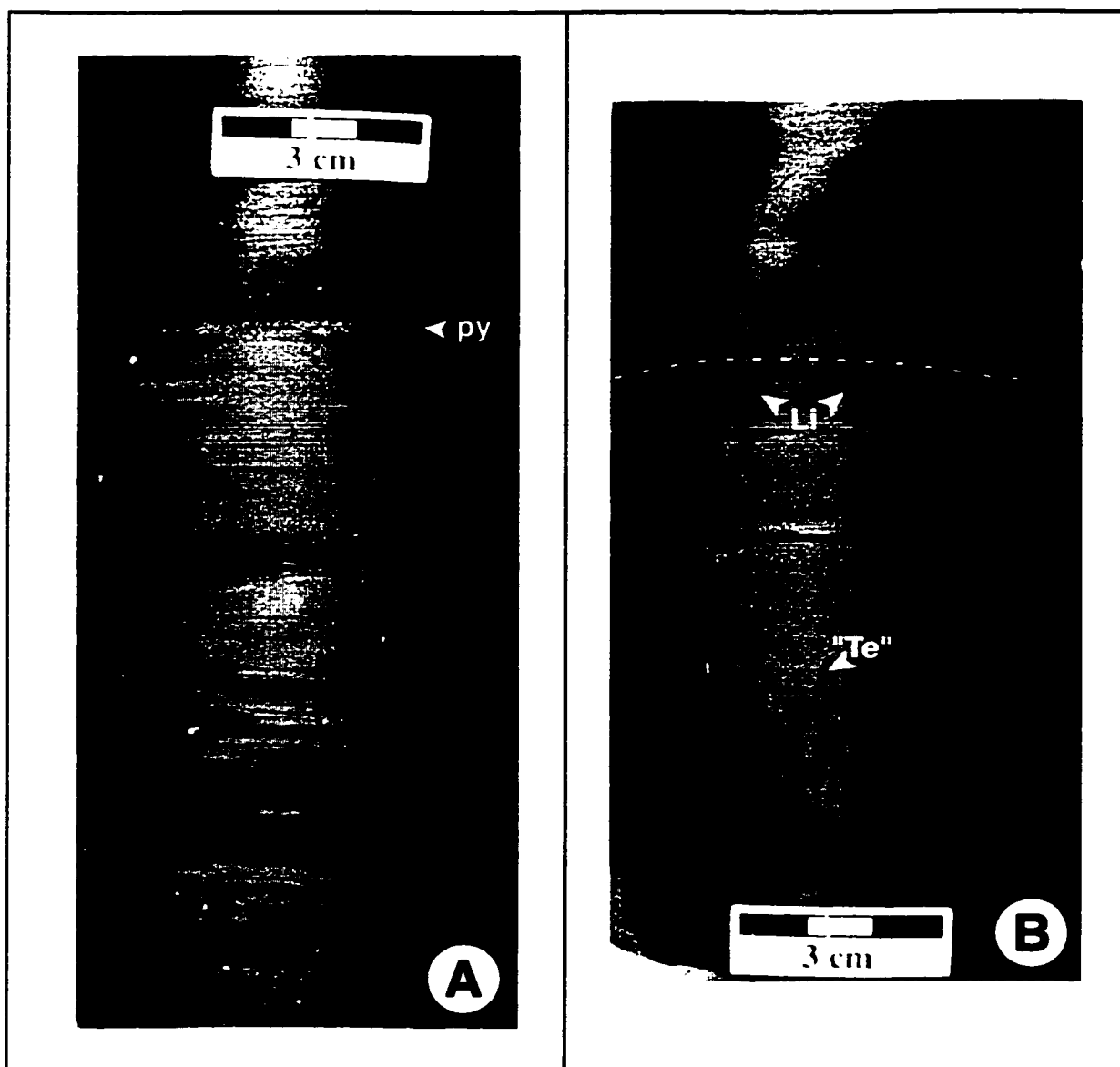
Conversely, conditions of extremely fluctuating salinity are intolerable to most organisms (Emig 1986, 1997). This could account for the exceptionally low ichnodiversity in facies B. In a revealing corollary, Lingulid brachiopods, the ascribed producers of the *Lingulichnus* that figure so prominently in facies B, are one of the few organisms able to withstand such an environment. Indeed, it constitutes their favoured habitat (Chapter 2), a point commensurate with the commonly observed non-diminutive size of *Lingulichnus* in subfacies B2. Finally, conditions of fluctuating salinity are consistent with the proposed fluvial-driven depositional model.

Salinity is interpreted to have been the primary stress in the shallower waters characterized by subfacies B2 deposits. Oxygenation stress is interpreted to have been responsible for the further reduced ichnodiversity, the switch to diminutive *Lingulichnus*, and elevated pyrite content which characterize the deeper and more distal subfacies B1. The most likely cause of oxygenation stress is intermittent lateral and upward expansion of the dysaerobic bottom waters that characterize facies A into the subfacies B1 environment. The conspicuous absence of organic material, terrigenous or otherwise, in any facies B sediments is inferred to indicate that a diminished food supply was probably a significant secondary stress.

Facies B is interpreted to have been deposited in a tidally dominated shoreface or, alternatively, the equivalent subaqueous deposits of a seasonal delta front. It is not clear whether such a delta would have been truly tidally dominated, or simply subject to significant tidal reworking during periods of low to zero discharge, when distributary channels would have effectively been narrow arms of the sea. Within a deltaic context, facies B is interpreted to have been deposited specifically on a distal bar, to the lower reaches of a distributary mouth bar.

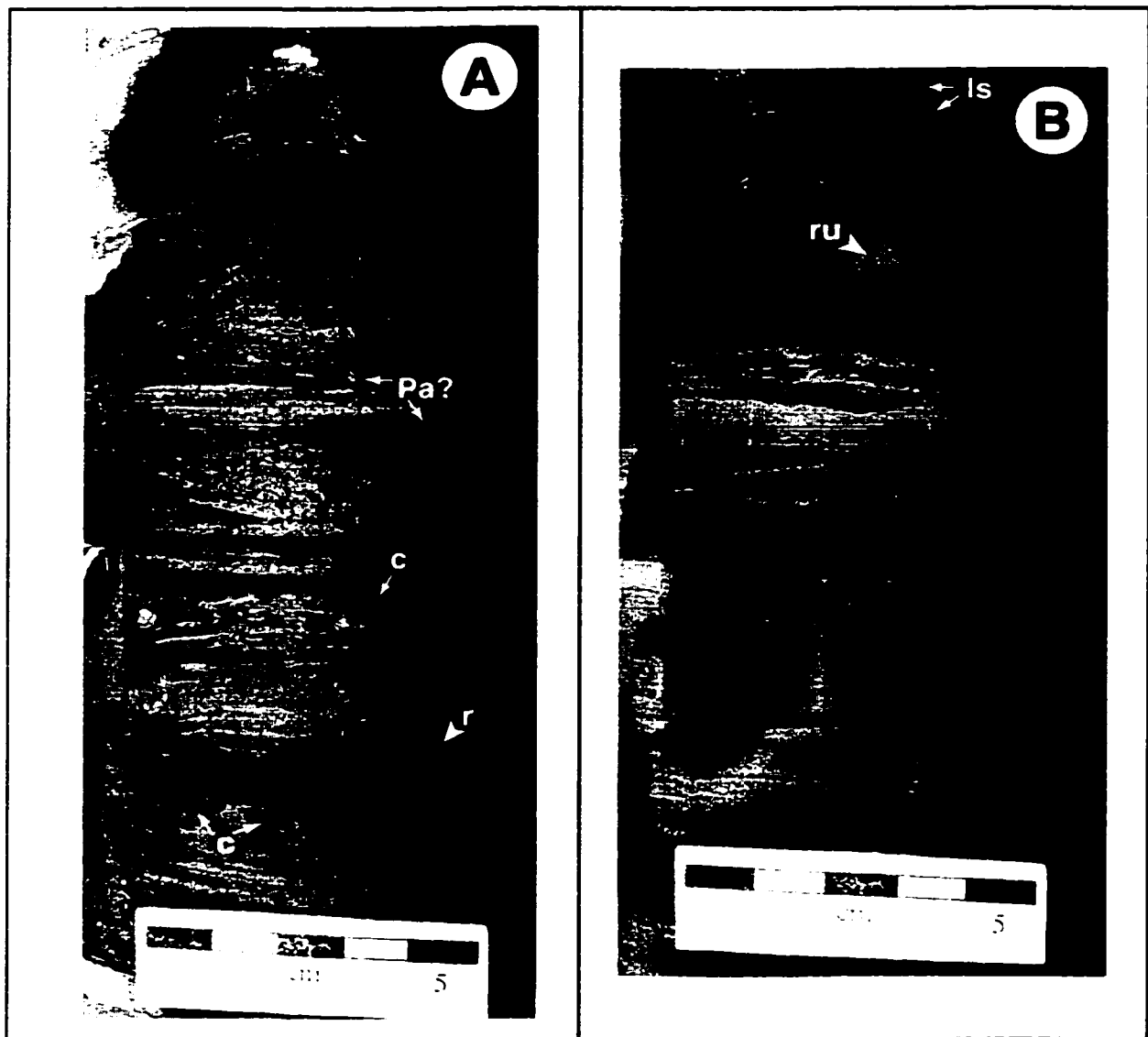
### **Subfacies B1: Silt-dominated facies B**

**Sedimentological characteristics:** subfacies B1 accumulations are characterized by a minimum 80% silt content (by volume), commonly ranging up to or exceeding 95% silt content (Fig 3.11 (A)). Beds are typically thinner, with a median 2-6 cm thickness. The lower sandy portion is typically <10 mm thick. It is commonly absent in one or more successive beds, or preserved only as burrow fill in the subjacent silt layer. This produces amalgamated silt layers up to several decimeters thick (Fig 3.11 (B)). Where the lower sandy zone is present, the overlying silty layer is more



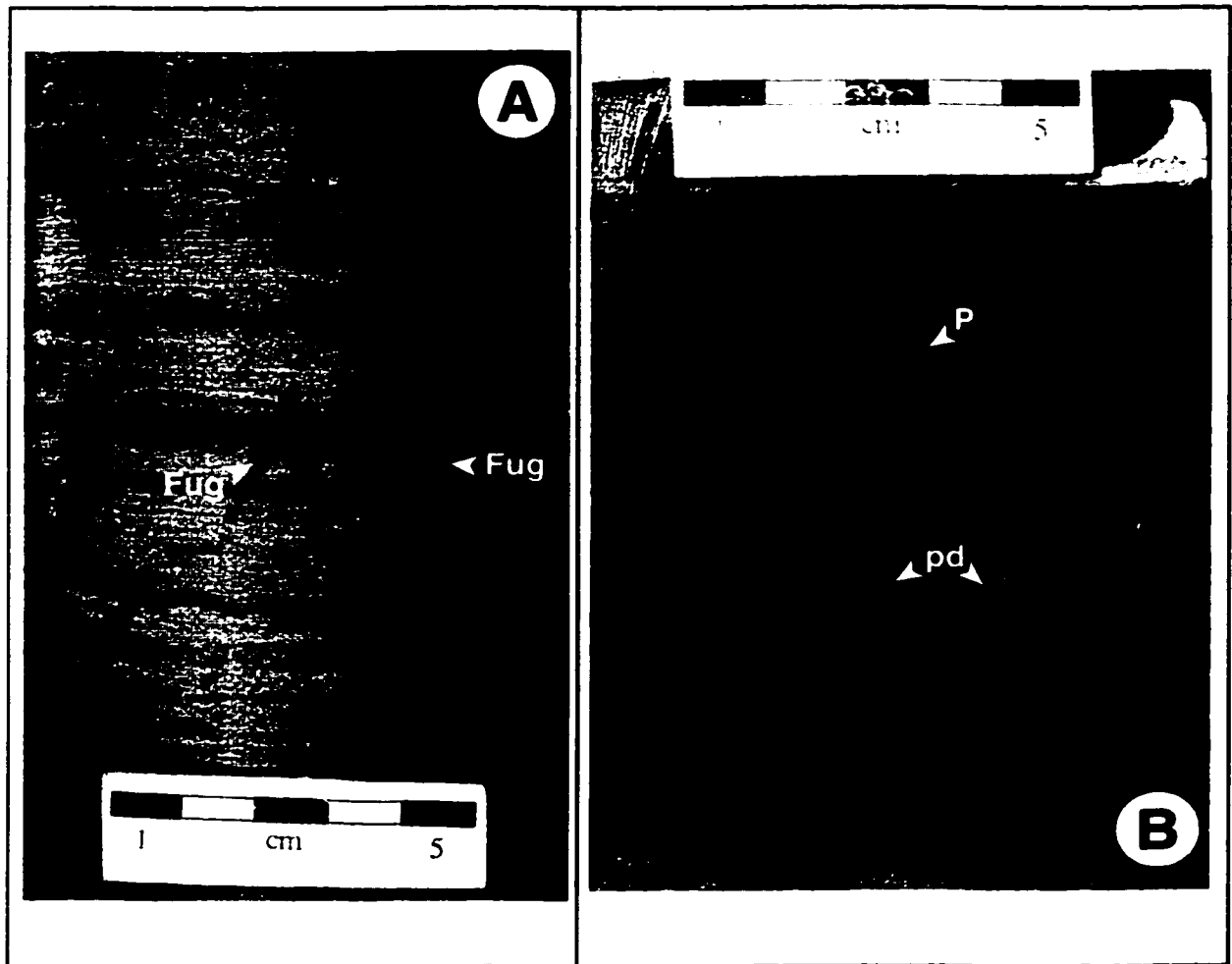
**Fig. 3.11 Subfacies B1 – bedding styles.**

(A) typical subfacies B1. Silt predominates heavily in this example, comprising ~90% of the core segment. Note the heavily pyritized sand layer [py]. From well 10-11-62-19w5, 6903' (2104 m). (B) Amalgamated silt beds in subfacies B1. The dotted line highlights a surface where a sand layer was removed, but the sand depositional event was recorded in the two *Lingulichnus* ichnofossils [Li]. The feature marked "Te" is either a genuine but indistinct *Teichichnus*, or the base of a *Lingulichnus* pedicle portion. In the latter case, the indistinct spreite would indicate vertical migration of the producing Lingulid. From well 4-2-62-20w5, 7071' (2155 m).



**Fig. 3.12 Subfacies B1 – sedimentary structures.**

(A) Somewhat unusual example of subfacies B1 in which many layers exhibit synsedimentary deformation. This is interpreted to indicate rapid deposition. [c] denotes load structures, where blebs of sand have intruded into an underlying silt layer. [r] exhibits distinct, silt-contrasted foresets and is interpreted as a current ripple. Bioturbate textures appear to be absent. However, locally developed bodies (e.g. [Pa?]) which appear lined are possibly *Palaeophycus*. From well 1-7-64-19w5, 1889.3 m. (B) Unbioturbated, very silty subfacies B1 which incorporates some sandy layers (dark, textured grey) and wispy sand lenses (white or light grey, e.g. [ls]). The origin of the large, laminated rip-up clast [ru] is perplexing. However, the subjacent thick sand layer was observed to exhibit small-scale faulting on the obverse side of this core segment, and it is probable the rip-up is related to this deformation. From well 15-29-64-18w5, 1771.1 m.



**Fig 3.13 Subfacies B1 – ichnofossils.**

(A) [Fug] denotes ichnofossils interpreted as probable escape structures (Fugichnia), or possibly as pedicle portions of *Lingulichnus*. They are clearly associated with the sand depositional episodes, with only the two larger examples in the middle of the photo crossing a silt layer. If these are indeed escape structures, they suggest the sand layers were deposited very rapidly. From well 11-22-62-21w5, 2195.1 m. (B) An excellent example of pedicle portion-only preservation of *Lingulichnus* [pd]. These are distinguished from *Skolithos* by the clear enlargement at the base of the burrows, which would have been occupied by the anchoring tip of Lingulid pedicles. [P] is a *Planolites* burrow. From well 13-7-62-19w5, 6996' (2132 m)



commonly sharp based than gradational. The upper silty zone of each bed is typically free of sandy laminae. However, a minor sand component occurring as lenticular bodies, or rarely thin wavy laminae, is incorporated locally.

Pyrite is an important accessory in subfacies B1, locally approaching concentrations comparable with facies A. It typically occurs as disseminated populations of small nodules and crystals. Near-complete pyritization of burrow fill is commonly associated with the pedicle portions of *Lingulichnus*.

**Ichnological characteristics:** silt-dominated subfacies B1 displays the impoverished *Lingulichnus-Planolites-Palaeophycus*—only assemblage described under facies B. In particular, the *Lingulichnus* of subfacies B1 is characterized by diminutive (typically 5 mm long, 2-3 mm diameter; up to 10 mm long and ~5 mm diameter), locally abundant populations, restricted to single horizons at the top of B1 beds. *Lingulichnus* in subfacies B1 do not exhibit the progressive vertical displacement observed in sandier facies B successions. In many cases, only the pedicle portion of *Lingulichnus* is preserved (Fig 3.13). Preferential pyritization of the pedicle portion is common and undoubtedly contributes to this phenomenon.

**Interpretation and discussion:** as previously indicated, subfacies B1 corresponds to the distal portion of the facies B depositional system. The distal character is interpreted primarily from the elevated (80%+) silt content of subfacies B1 beds and the dominance of low-angle parallel lamination. Supporting evidence includes a diminished tidal influence on sedimentation (only paired drapes are common) and elevated pyrite content, both interpreted to indicate relative depth. The fine, dominantly low-angle lamination of the silts is also indicative of minimized wave processes.

Silts are interpreted to have reached B1 subenvironments as hypopycnal flows originating at a fluvial point source. They settled quietly out of suspension, with minor reworking by weak currents. This produced the mix of low-angle and wavy parallel lamination. The basal sandy portion of some B1 beds was deposited during the initial phase of larger discharge events. Lenticular beds of sand within the silty layers are interpreted as starved ripples that migrated into B1 environments, entrained by bottom currents. In many cases, these are not accompanied by any suggestion of erosion in underlying laminae. This is understood to indicate sand migration commonly took place between discharge episodes, after the silt deposits had become somewhat cohesive. The presence of truncated burrows with a sandy

fill, but no superjacent sand layer, is indicative of intermittent stronger erosive events.

The B1 environment could be described as 'hyperstressed', as it is highly impoverished compared even to subfacies B2. The additional reduction in diversity, as discussed under facies B above, is attributed to diminished oxygenation. The dense populations of diminutive *Lingulichnus* indicate that Lingulid brachiopods, tolerant of considerable oxygen depletion (Chapter 2), were able to sporadically colonize the B1 subenvironment.

The restriction of B1 *Lingulichnus* to the topmost horizons is attributed to substrate consistency. Lingulids are able to establish burrows in unconsolidated silt but not maintain them (Chapter 2). Successful colonization is thus interpreted to have been attendant upon post-depositional consolidation of B1 silty substrates as discussed above. This limited colonization to the tops of beds. However, this also limited colonization until after discharge episodes, and thus after periods of optimum terrigenous organic influx. Such a constraint, further magnified by the distal setting of B1, would have exacerbated the food supply stress interpreted for facies B. This is interpreted to have dictated the diminutive size of B1 *Lingulichnus* populations, by either limiting growth, or more likely by starving the juvenile populations soon after colonization.

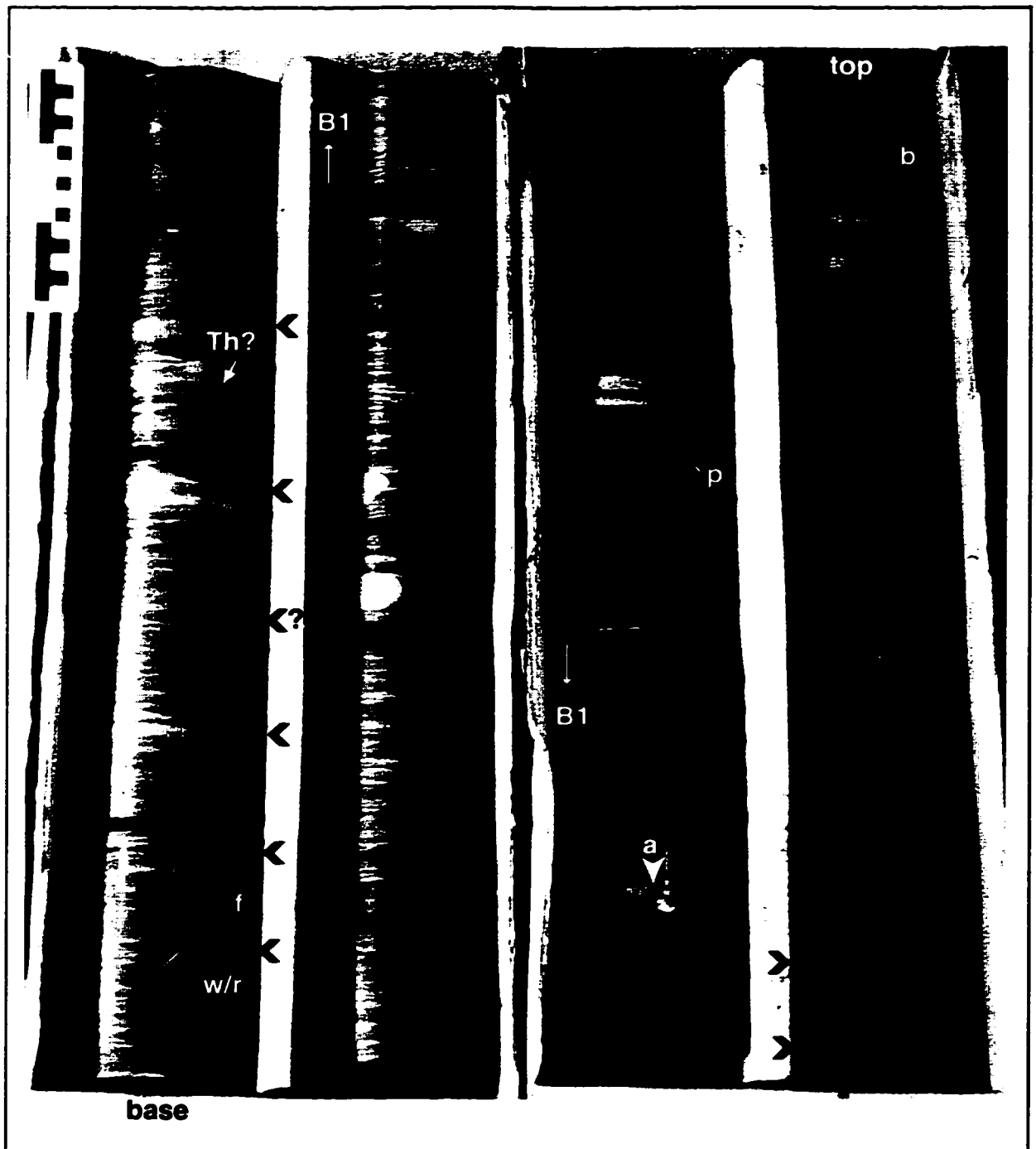
Facies B1 is interpreted to have been deposited in a tidally influenced lower shoreface, or a tidally influenced, deltaic distal bar

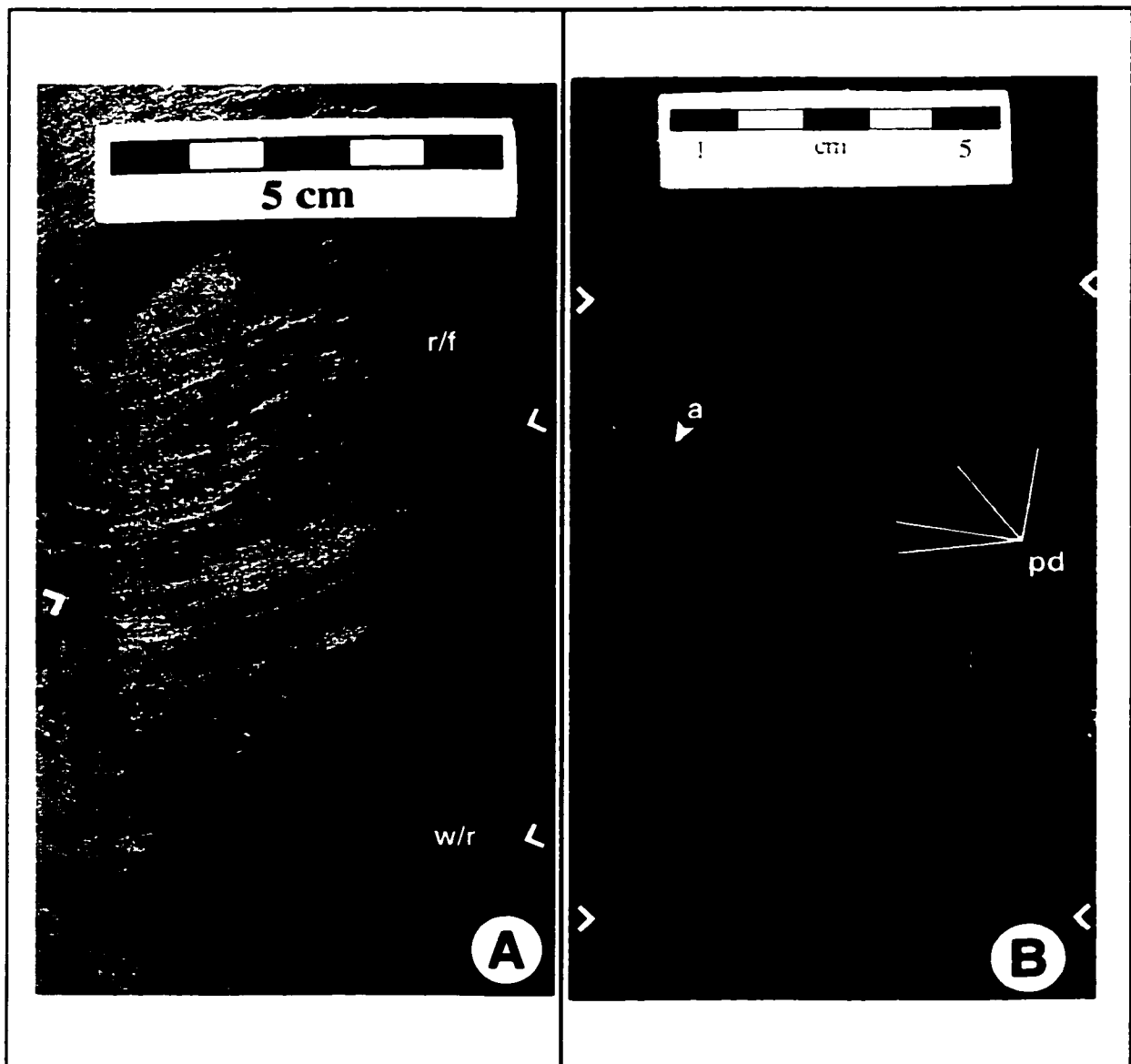
### **Subfacies B2: Sand-dominated facies B**

**Sedimentological characteristics:** subfacies B2 comprises those occurrences of facies B with a sand content exceeding 60% by volume, commonly ranging to over 90%. Median bed thickness is typically 4-10 cm (Fig. 3.14). The upper silty zone of B2 beds is commonly not silt-dominated, but 'silt-enriched' to 20-40% by volume (Figs. 3.14, 3.15(A)). Mottling of both the sandy and silty portions, associated with pelletized silt and disrupted laminae, is common (Figs. 3.17 (A), 3.18 (A), 3.22). Typically, the lower sandy zone comprises 75% or more of bed thickness, and incorporates a silt component as wispy laminae (up to ~10% of the lower zone by volume). The lower sandy portions of subfacies B2 beds are host to most of the sedimentary structures described as characteristic of facies B. Preservation of sedimentary structures is of particularly high quality to the northeast (TWP 64-65, RGE 18-19w5) of the study area, within very sandy B2 beds characterized by a distinctive low-gamma, high-porosity geophysical response.

**Fig. 3.14 Subfacies B2 – Box shot.**

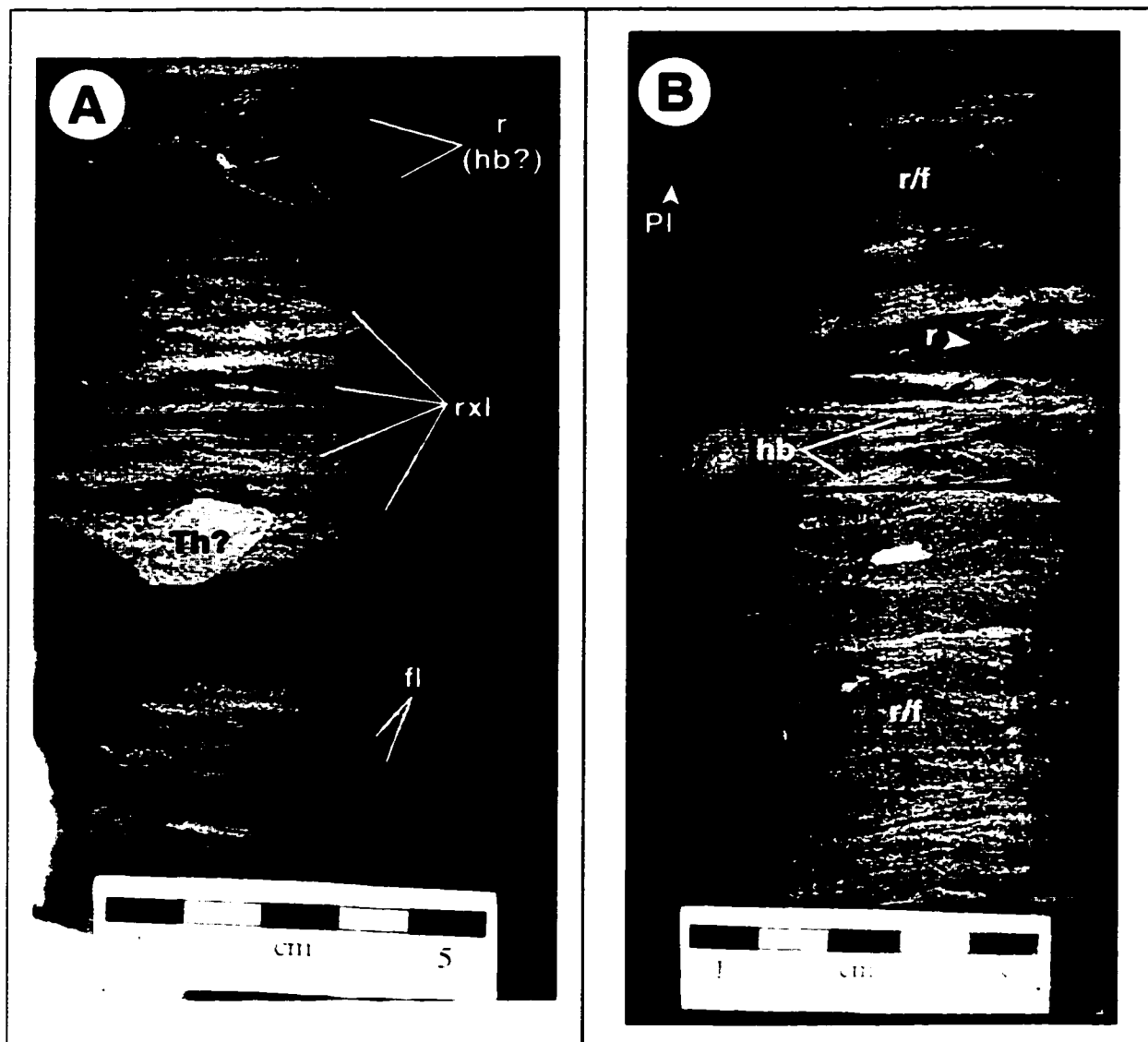
Sand-dominated (85%+) B2 with a subfacies B1 interbed (dotted lines, [B1]). The large, rounded blotches on the core of the second box are acid stains left by a previous worker. Each bed is dominated by the sandy lower portion. The upper portion is silt-enriched but dominantly sandy. Silt laminae progressively increase in thickness and numbers upwards. The tops of beds are defined by an abrupt shift from silt-enriched to very sandy deposition. Tops of several successive beds in the first box are marked with flechettes ( > ). Note the common adherence to a median thickness of ~5 cm. Most beds contain wavy parallel to ripply laminae [e.g. [w/r)]. Locally, flaser lamination [f] is developed. The large, rounded discordant feature [Th?] is a probable *Thalssinoides* burrow. A thin deformed bed [cf. Facies D] with convolute lamination may be observed at [a]. Locally, beds are mottled and exhibit indistinct internal structure (e.g. [b]), interpreted to indicate abundant or pervasive bioturbation. Most silt laminae in these beds are paired and regularly spaced, evidence of a significant tidal influence on sedimentation. From well 2-2-63-20w5, 6683-6690' (2037-2039 m). Scale is in centimeters.





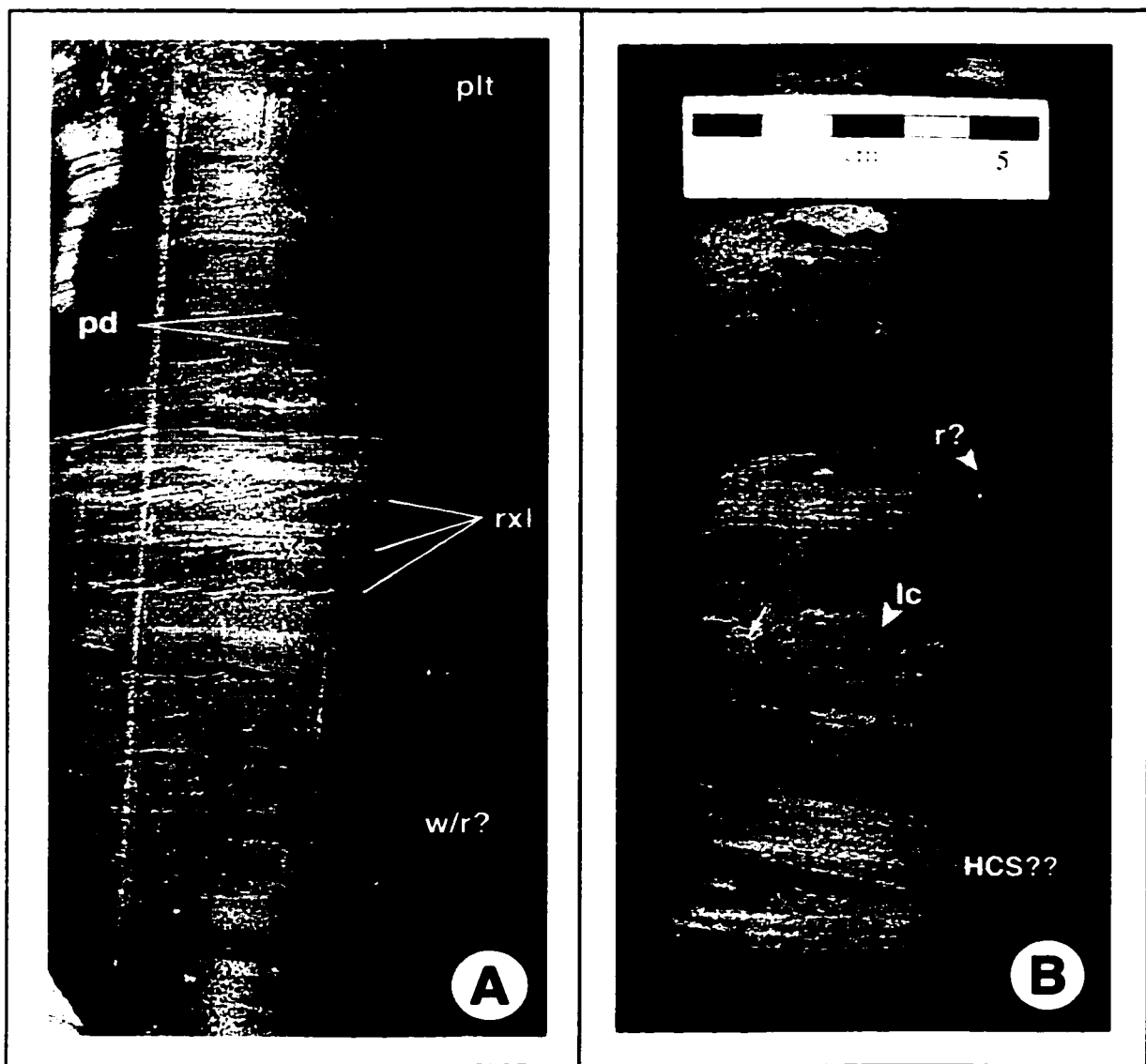
**Fig 3.15 Subfacies B2 – bedding styles.**

(A) a core segment from a deviated well showing typical bedding. The tops of beds are marked by flechettes (>). The complete bed in the bottom half of the photo is ~5 cm thick, which is typical of most subfacies B2 accumulations. The bed is sand dominated (~90%), with the silty upper portion defined only as a 'silt-enriched' zone of thicker silt laminasets. Note the wavy-parallel to ripply lamination [w/r] in the sandy portion of the lower bed and the ripply- to flaser-laminated [r/f] developed in the sandy portion of the overlying bed. From well 4-36-64-19w5, 1860 m. (B) A slightly siltier example of subfacies B2, with a comparatively thick 'silt-enriched' zone. Two complete beds are present (tops: >), with the upper one being somewhat thinner than typical (~2 cm vs. ~5-6 cm). The lower sandy portion of each bed contains wispy, discontinuous silt laminae. These become progressively more continuous, more numerous, and thicker upwards, producing a gradational transition from the lower sandy portion to the upper silt-enriched portion. Note the prominent pairing of silt drapes [pd]. [a] denotes a burrow, interpreted as either a large *Planolites*, or poorly defined *Lingulichnus*. From well 11-28-62-19w5, 6600' (2012 m).



**Fig. 3.16 Subfacies B2 – sedimentary structures I.**

(A) an example of the excellently preserved sedimentary structures found in the northeast of the study area (see text). Note the abundance of silt flasers (e.g. [fl]) and ripple cross laminations [rxl] with well-defined foresets. This particular occurrence is interpreted as small-ripple bedding (cf. Reineck & Singh 1980). The cross laminated horizon at the top of the photo [r] contains foresets with opposing dips, and may represent 'herringbone' cross lamination (hence [hb?]) or intersecting small-scale trough cross lamination. [Th?] denotes a large, mud-filled burrow interpreted as a probable *Thalassinoides*. From well 4-30-64-18w5, 1792.4 m. (B) a segment from slightly higher (@ 1792.2 m) in the same well, exhibiting well-defined bidirectional ('herringbone', [hb]) cross-sets. The small black arrows indicate foreset directions in successive horizons. Note also the prominence of ripple to flaser lamination [r/f] over most of the photo. [r] denotes a large ripple with well-defined, silt contrasted foresets. [Pl] is a small *Planolites* burrow.



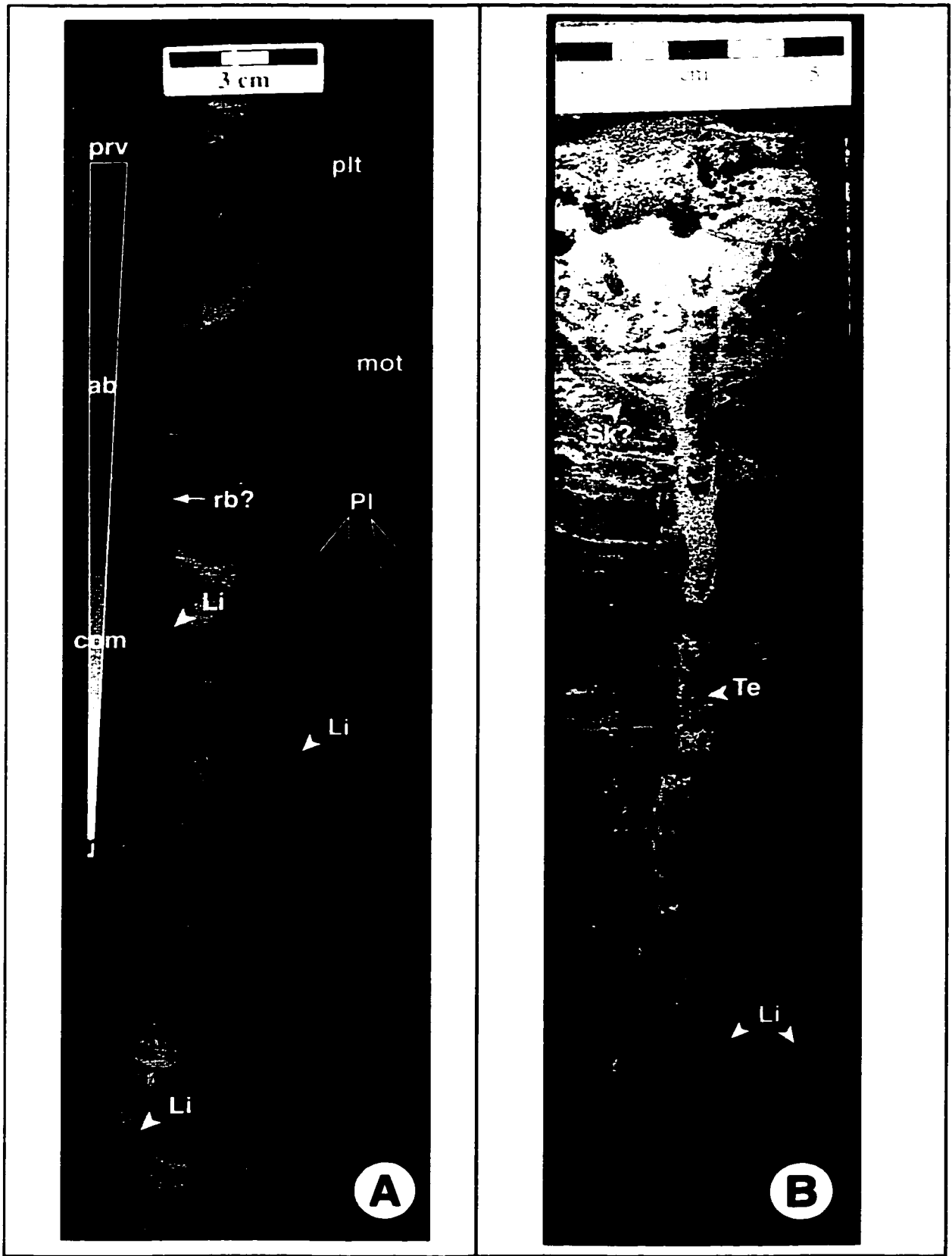
**Fig. 3.17. Subfacies B2 – sedimentary structures II.**

(A) exhibiting well-defined wavy-parallel to rippled lamination [w/r] and well-developed ripple cross lamination [rxl]. The latter is expressed within the silty upper portion of the bed. Note the prominent paired silt laminae (e.g. [pd]) in the upper half of the photo. At the very top is a pelletized horizon [plt] comprised of irregular silt pellets within a sand matrix, interpreted as a pervasive bioturbate texture (see text). Pelletized beds occur locally in most B2 successions. From well 4-30-64-18w5, 1789.9 m. (B) a less typical, somewhat siltier occurrence of B2 that displays well formed load casts [lc] where a sandy bed plastically intruded upon an underlying silt layer. The small arrow highlights an incipient flame-structure. Note the foreset laminae at [r?], suggestive of a relatively large ripple. The concavo-convex lamination at the base of the photo is interesting. Although resembling HCS bedding (hence [HCS??]), it is dominated by silt and not sand. It is somewhat perplexing why the high-energy conditions necessary to produce HCS transported mostly silt, within a sand-dominated depositional regime. It is possible that the concavo-convex layering is a weakly expressed or incipient slump fold. From well 15-29-64-18w5, 1767 m.

**Fig. 3.18 Subfacies B2 – Vertical migration and sedimentation rates.**

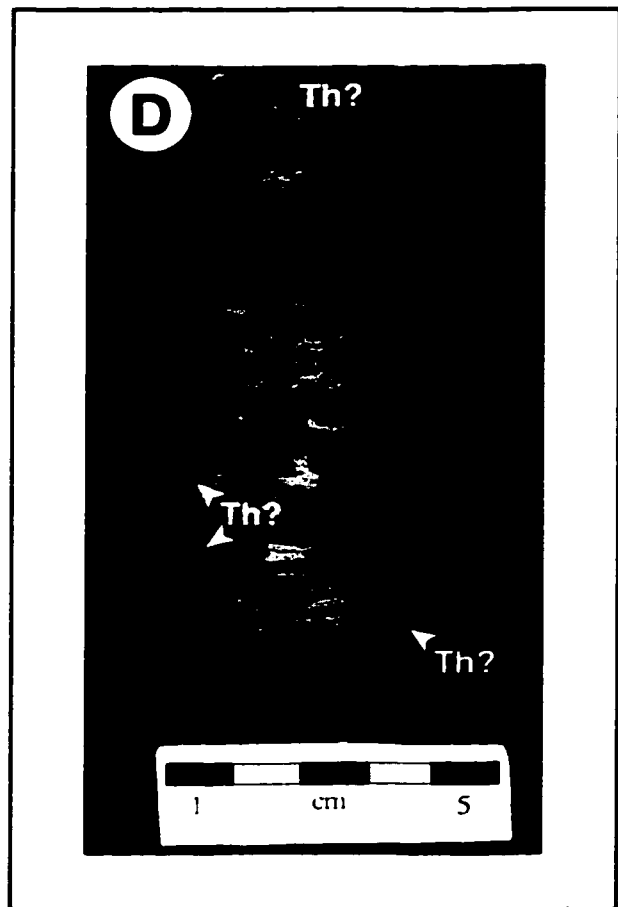
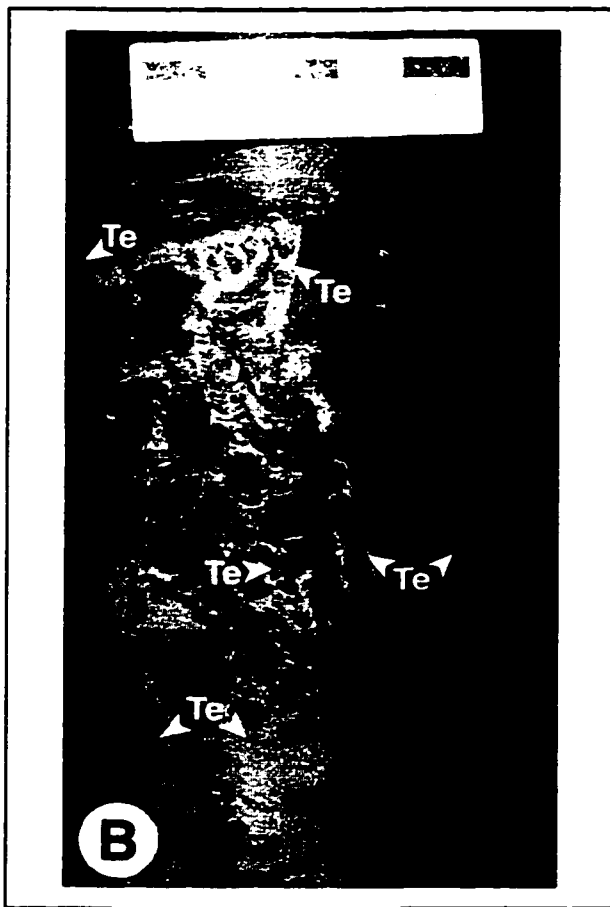
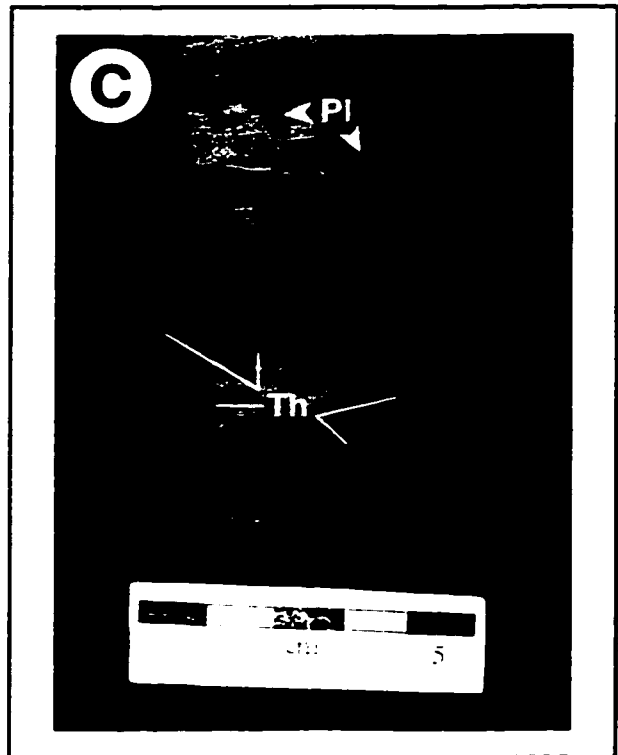
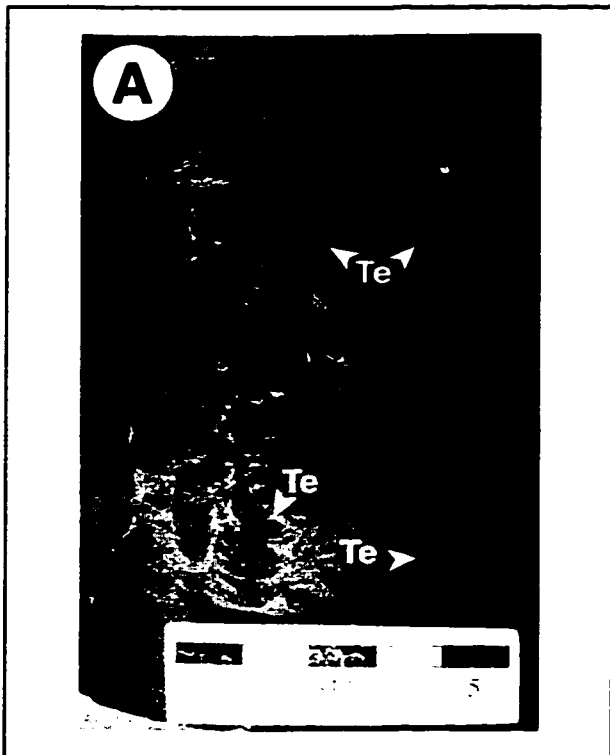
(A) Vertically migrating *Lingulichnus* [Li]. Note the minimal change in width of the burrow on the left, from bottom to top. Based on Lingulid growth rates, this suggests a minimum sedimentation rate of ~15 cm/8 years (see text). A second interesting feature in this photo is a distinct biological gradient (graph, left side), from moderate bioturbation near the base to pervasive at the top. [mot] indicates a horizon of abundant bioturbation characterized by a few relict laminations. [plt] indicates a zone of pervasive bioturbation with no relict primary structures and a pelletized silt content. [PI] denotes several clustered burrows interpreted as *Planolites*. From well 4-2-62-20w5, 7048-7049' (~2148.5 m). (B) A 'super'-*Teichichnus* [Te] stretching over more than 21 cm of core. For a burrow of this diameter (~0.5 cm) this is impressive, and interpreted to be a consequence of relatively rapid and continuous deposition. Note the mottled, abundantly bioturbated horizon [bt] at the top, dominated by silt, which suggests an abrupt decrease in sedimentation rates. Other burrows in this image: [Li] *Lingulichnus*, and a large oblique burrow [Sk?] interpreted as a *Skolithos*. From well 8-32-61-20w5, 7060-7061' (~2152 m).





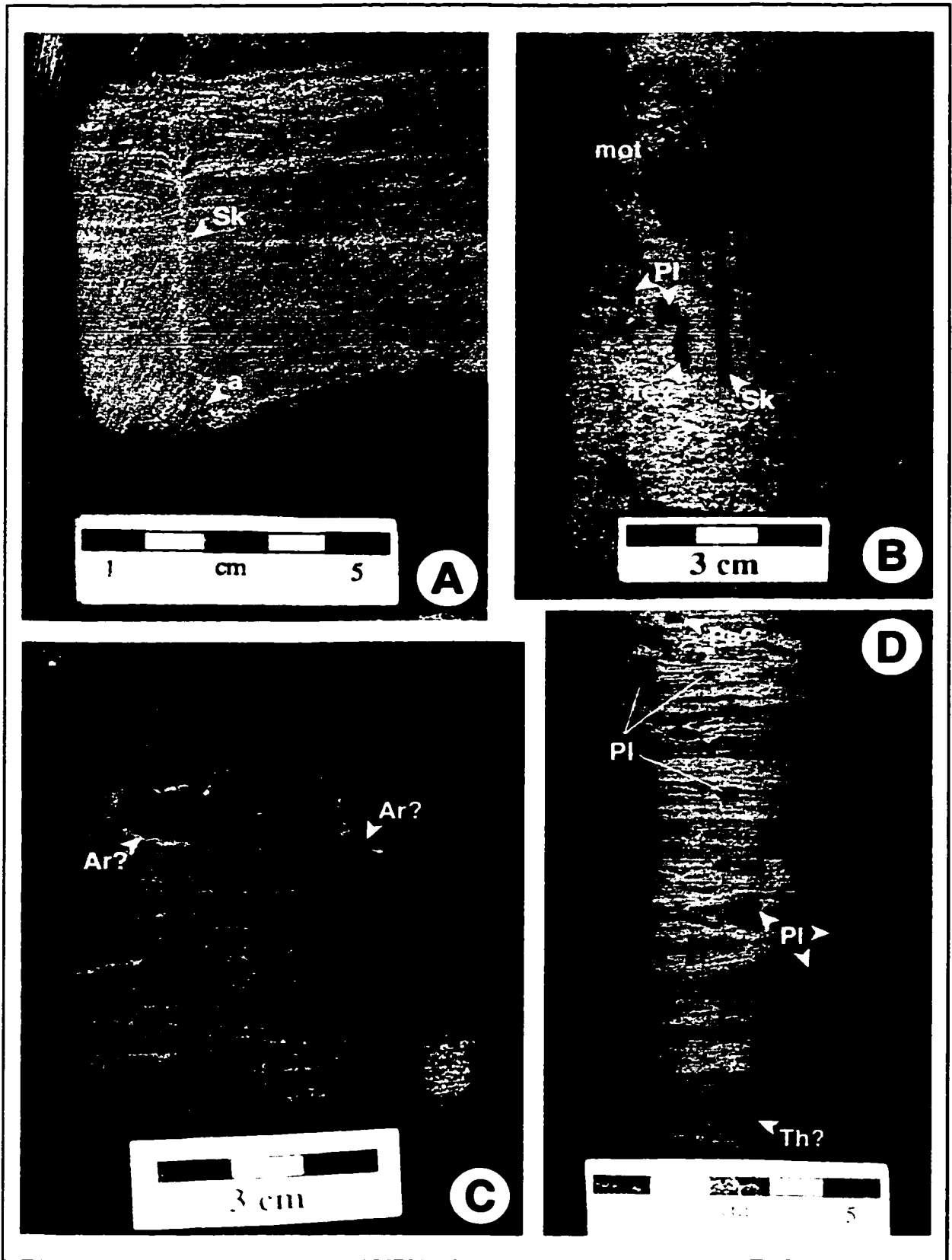
**Fig. 3.19 Subfacies B2 – Ichnofossils I.**

(A) A horizon densely colonized by *Teichichnus* [Te]. From well 5-7-62-19w5, 6938' (2115 m). (B) Excellently preserved *Teichichnus* [Te] from well 12-33-61-20w5, 7112' (2168 m). Excluding *Planolites* and *Palaeophycus*, *Teichichnus* is the second most abundant (*Lingulichnus* being the first, at ~90%+) ichnofossil found in sediments of this study, comprising perhaps 2-3% of all observed burrows. (C) Large clustered horizontal burrows interpreted as *Thalassinoides* [Th]. The indicated subjacent sand 'bed', which appears to be discordant (note the silt body at the extreme right) may be a longitudinal burrow section. Smaller horizontal burrows [Pl] are *Planolites*. From well 8-32-61-20w5, 7079' (2158 m). (D) Possible *Thalassinoides* [Th?]. These examples are perhaps small enough to be considered a robust form of *Planolites*, hence the questionable identification. The large body marked [Th?] at the top of the photo is pyritized, and also interpreted as a possible *Thalassinoides*. From well 6-18-62-19w5, 2112.4 m.



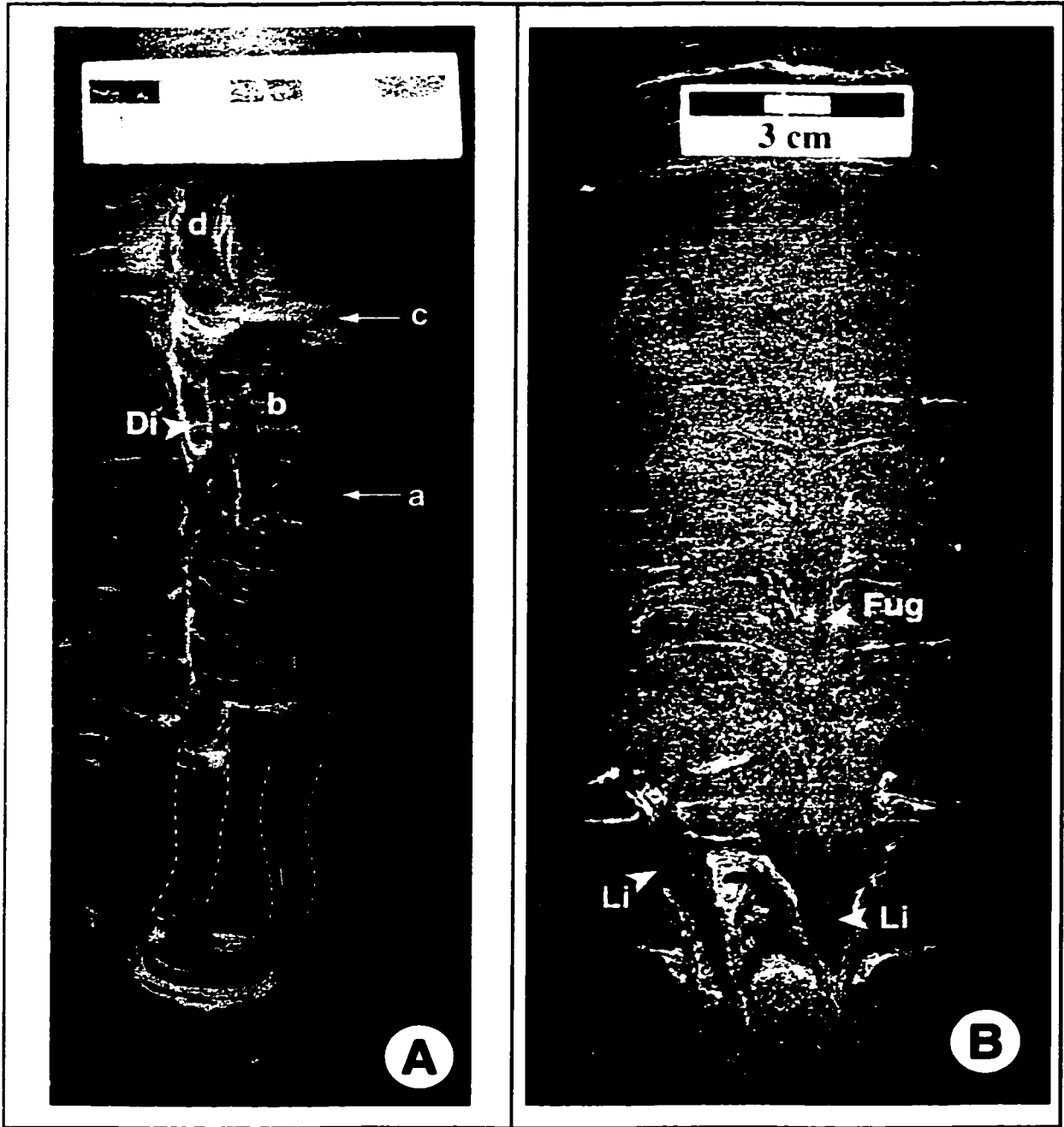
**Fig. 3.20 Subfacies B2 – Ichnofossils II.**

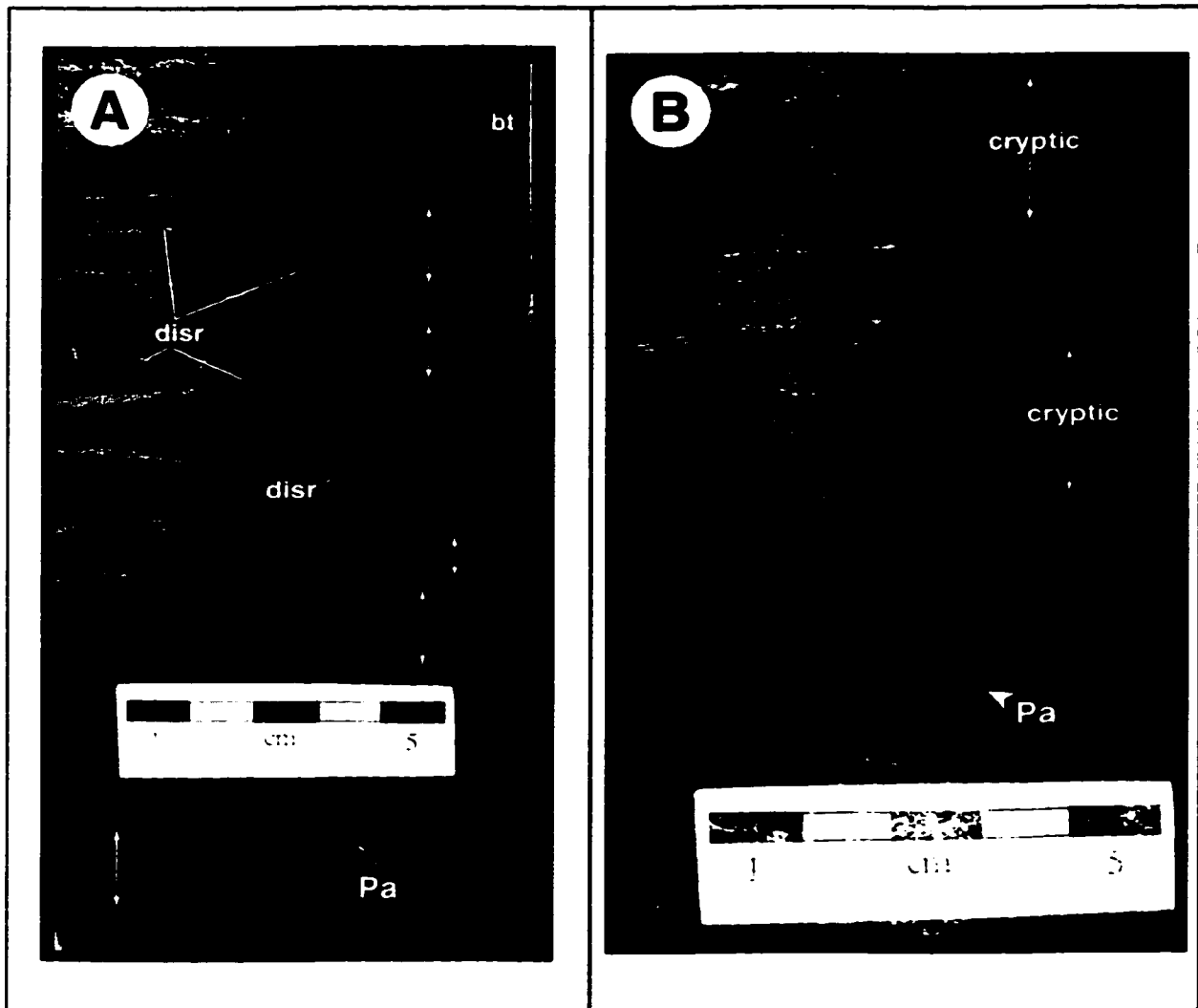
(A) Indistinct, vertical shaft interpreted as a *Skolithos* [Sk]. Note the disturbance of the coquinal grains at the base of the shaft [a]. This is suggestive that the shift from coquinal to clastic sedimentation was accomplished without any significant hiatus or lithification, since the tracemaker appears to have reworked the bioclasts. From well 13-7-62-19w5, 6994' (2132 m). (B) prominent vertical shaft, interpreted as *Skolithos* [Sk] within mottled [mot] silt and sand. This is part of a short clastic succession within a thick bioclastic accumulation. Other identifiable burrows: a possible *Teichichnus* [Te?] and *Planolites* (e.g. [Pl]). From well 12-6-62-20w5, 6974' (2126 m). (C) Very sandy subfacies B2 containing possible *Arenicolites* [Ar?]. From well 8-32-61-20w5, 7076' (2157 m). (D) Abundant *Planolites* (e.g. [Pl]) and *Palaeophycus* [Pa]. The large burrows at the base are interpreted as *Thalassinoides* [Th?] although, similarly to Fig. 3.19 (D), these are perhaps small enough to be robust *Planolites*. From a non-subfacies B2 interbed in a B2 succession of well 8-32-61-20w5, 7092' (2162 m).



**Fig. 3.21 Subfacies B2 – Ichnofossils III.**

(A) An excellently preserved *Diplocraterion* [Di]. The spreite in this example appears to be retrusive; note how topmost 'U' of the burrow (at [d]) appears empty of backfill. The undisrupted primary lamination visible around [b] suggests a somewhat interesting behavioural history. It appears that the producer migrated rapidly from [a] to [c], without leaving a spreite. After tunneling up quickly to a new level, the normal 'U'-burrow morphology was reestablished. From well 12-33-61-20w5, 7135' (2175 m). (B) Two *Lingulichnus* [Li], and an associated escape structure (Fugichnia) [Fug]. The Lingulid that produced the burrow on the right appears to have been forced to migrate rapidly upward through the overlying sandy bed. This would suggest very rapid deposition of the transected bed. Although not apparent in this photo, the transected layer had a color gradation reminiscent of facies F, which is interpreted as a storm- or sediment-gravity flow deposit (see Facies F). From well 8-32-61-20w5, 7065' (2153 m).





**Fig. 3.22 Subfacies B2 – indiscrete bioturbate textures.**

(A) pelletized bedding. A common characteristic of subfacies B2 is pelletization of silt and disruption of laminae over short intervals within beds. This example shows several pelletized horizons (double-headed arrows), exhibiting the characteristic, randomly distributed, irregular-shaped silt bodies which characterize these pelletized zones. Numerous disrupted laminae (e.g. [disr]) are also evident. Together, these features are interpreted as evidence for locally pervasive bioturbation (see text). From well 11-28-62-19w5, 6575' (2004 m). (B) cryptically bioturbated horizons. Cryptically bioturbated deposits are characterized by thorough disruption of sediments that nonetheless does not destroy primary sedimentary structures (marked [cryptic] in the figure). It is normally attributed to complete reworking by meiofaunal sediment ingesters and grazers. [Pa] denotes a possible *Palaeophycus* burrow. From well 1-11-65-21w5, 6095' (1858 m).



**Ichnological characteristics:** subfacies B2 beds are the primary host for all facies B ichnofossils and consequently display the complete facies B suite (Figs. 3.18-3.21). *Lingulichnus* populations comprise over 90% of individual burrow specimens. The burrows are typically 1-2 cm in diameter and 4-5 cm long; some are considerably larger. This size is almost an order of magnitude greater than *Lingulichnus* of subfacies B1. Near-monospecific *Lingulichnus* communities, with abundant vertical displacement structures and rare Fugichnia are commonly developed and may extend across several decimeters of core.

*Teichichnus* and clusters of large (~10 mm), horizontal burrows interpreted as *Thalassinoides* are common, and were observed to densely colonize single horizons. *Planolites* and *Palaeophycus* range from common to uncommon. *Skolithos* and *Diplocraterion* are rare, but locally exhibit excellent preservation. The four other ichnogenera that characterize facies B are represented by single or questionable specimens, with the exception of possible diminutive *Arenicolites* found to be abundant in one core (6-18-62-19w5).

**Interpretation and discussion:** as previously indicated, subfacies B2 corresponds to shallower, proximal environments of the facies B depositional system. Relatively shallow depth is inferred from the abundant evidence for tidally influenced deposition and the dominance of simple dwelling structures produced by infaunal suspension feeders (*Skolithos* ichnofacies, indicative of generally high-energy conditions). Most of the interpretation of facies B is based on the characteristics of subfacies B2 since sediments of the latter contain most of facies B ichnofossils and sedimentary structures. The general discussion of facies B thus addresses most observed characteristics of subfacies B2 and is not repeated here.

The mottled and pelletized appearance commonly observed in B2 beds is interpreted as an abundant to pervasive bioturbate texture. This is based on the irregular to rarely branched shape of the silt pellets, and the scattered presence in many examples of partially preserved laminae with abundant burrows. An alternative explanation of the mottling, by fluidization and dewatering, is rejected for two main reasons. Firstly, individual sandy beds commonly display pelletization of a few laminae, between undisrupted sedimentary structures or laminae. Secondly, no other structures consistent with dewatering, such as dish-and-pillar structures, homogenization, or sand volcanoes have been observed.

Abundant, progressive vertical displacement of *Lingulichnus* burrows is interpreted as slow vertical migration in response to an elevated sedimentation

rate. An important characteristic of these structures is their relatively consistent width. Examination of experimental Lingulid growth curves (Fig. 2.6 (B)) reveals rapid growth to an optimum size in the first 4-5 years, followed by minimal growth until death. Based on a typical Lingulid life span of 8-12 years (Chapter 2), the unchanging thickness of some migrating B2 burrows (e.g. Fig. 3.18 (A)) thus indicate minimum sedimentation rates of as much as ~30 cm/8 years. Escape structures (Fugichnia) found in close association with *Lingulichnus* indicate sedimentation was at times very much more rapid, with some examples (e.g. Fig 3.21 (B)) suggesting rates of ~5-10 cm in a few hours.

Subfacies B2 is interpreted to have been deposited in a tidally-dominated upper shoreface, or as the upper distal bar, to lower distributary mouth bar, of a tidally influenced delta.

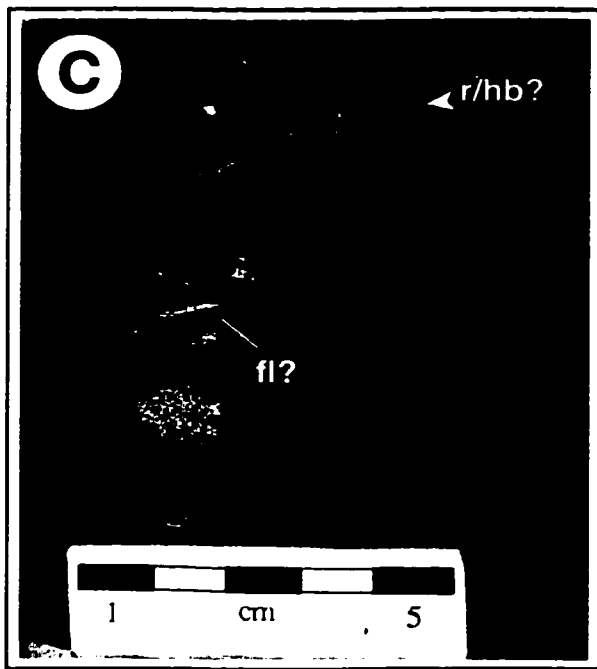
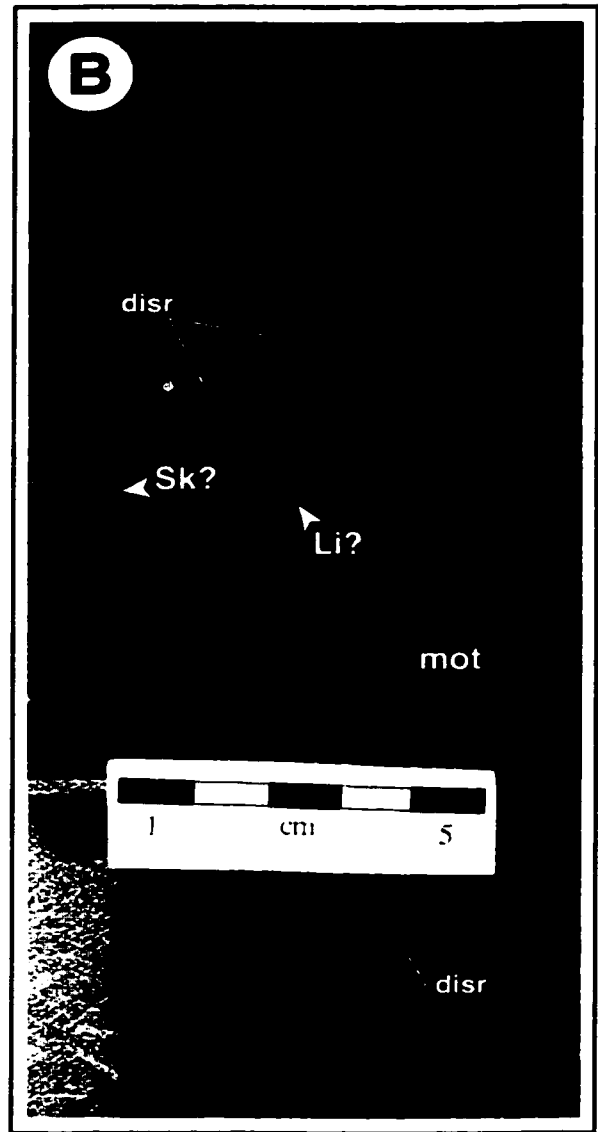
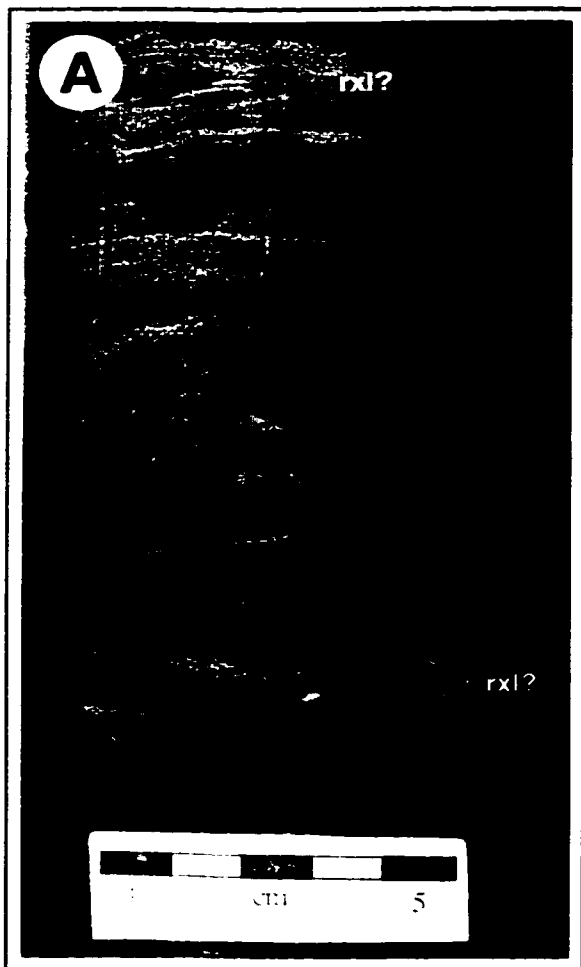
### **Facies C: Upward coarsening, interlaminated sand and minor silt**

**Sedimentological characteristics:** facies C (Fig. 3.23) comprises relatively thick beds of very fine grained (>0.1 mm), medium brown to reddish or purple sand with minor intercalated tan-colored silt. The upward coarsening character of facies C is defined by a basal silt content of 20-50% which quickly diminishes to 2-5% over most of the bed. This characteristic and relatively thick bedding, commonly 40-50 cm ranging to several meters, are all that distinguish facies C from the lithologically and sedimentologically very similar subfacies B2.

The basal silty zone (typically <15% of the accumulated bed) commonly exhibits wavy parallel lamination of silt layers and wavy parallel or ripple lamination of sandy layers.

Sedimentary structures are rare in the sands which characterize the bulk of a facies B bed, but show considerable variety and include low-angle parallel and ripple lamination, tabular and ripple cross-lamination, bidirectional cross-lamination, asymmetrical ripples, and paired silt drapes. However, most of facies C exhibits only thoroughly disrupted laminae and a pelletized silt component.

**Ichnological characteristics:** discernible ichnofossils are rare in this facies. Scattered individuals in less disrupted zones include *Lingulichnus*, *Planolites*, *?Thalassinoides* and possible escape traces. Burrows were not observed in the basal silty zone of any facies C beds.



**Fig. 3.23 Facies C.**

(A) typical facies C, with significantly depleted silt content compared to subfacies B2 and isolated, silt-contrasted sedimentary structures within texturally undistinguished sands. [rxl] denotes possible ripple cross-laminated zones. From well 15-29-64-18w5, 1762.5 m. (B) abundant bioturbation in facies C. Primary physical structures in this example have been thoroughly destroyed, with abundant pelletization of silt ([mot] zone) and disrupted laminae (e.g. [disr]). Two burrows are identifiable: *Lingulichnus* [Li] and a probable *Skolithos* [Sk]. From well 11-28-62-19w5, 6571.5' (2003 m). ----->

(Fig. 3.23 cont.) (C) possible tidal structures in facies C. [fl?] denotes a possible silt flaser, [r/hb?] denotes a ripple with a possible reactivation surface. A suggestion of opposite dipping foreset laminae over the ripple suggests herringbone cross-lamination (hence [hb?]). From well 15-29-64-18w5, 1762 m.

**Interpretation and discussion:** the paucity of preserved sedimentary structures or ichnofossils in facies C make interpretation difficult. This problem is further exacerbated by the fact the few preserved individual structures are isolated, commonly 'floating' in unremarkable sediments, leaving no context from which to draw relationships between structures.

Collectively the variety and type of preserved structures is comparable with facies B, and are interpreted to indicate a similar tidally influenced setting. The abundance of sand in this facies, and its normal stratigraphic position overlying facies B beds, is interpreted to indicate deposition in a high-energy, very shallow setting. Circumstantial evidence for intermittent subaerial exposure or deposition is present in the reddish or purple tint of some layers.

The abundance of disrupted or diffuse lamination and abundant pelletization of silt content, commonly in association with rare poorly preserved ichnofossils, is interpreted to indicate a pervasive bioturbate texture.

Facies C is interpreted as the shallowest and most source-proximal portion of the depositional system proposed for facies B, and consequently represents the uppermost portion of a tidally-dominated shoreface (subaqueous portion of tidal sandflat?), or the upper distributary mouth bar to lower subaqueous levee deposits of a tidally-influenced delta.

## CLASTIC FACIES ASSOCIATION TWO

Clastic Association Two (CA2) comprises 5 facies (D, E, F, G, and H). As previously noted, minor beds of facies D and G are also commonly encountered in the context of CA1. However, D and G accumulations are thicker and more abundantly encountered in close association with facies E, F and H and thus are included within CA2.

Intercalation of the five CA2 facies is commonly quite complex; however a general succession may be described. Typically, there is a basal occurrence of homogenized or partially homogenized silt and sand (facies G) and/or convolute to chaotically bedded silt and sand (facies D). These are overlain either by massive, apparently structureless sands (facies E) or texturally graded sand (facies F). These

are in turn locally overlain by massive sand with pelletized silt (facies H). Within any given accumulation of CA2 sediments, this succession may be repeated more than once. Furthermore, any part in a given single succession may be absent. Common variations on the general CA2 succession include the presence of facies H at the base of as well as the top of facies E, interchange of facies D with facies G, and facies F overlying facies E.

The grain size parameters of CA2 are the same as for CA1, comprising a narrow very fine sand (0.1-0.06 mm) to coarse silt (0.06-0.03 mm) grade. In an important exception, facies E commonly incorporates or (rarely) is entirely composed of fine sand (0.1-0.25 mm). Bioturbate textures in CA2 are typically rare to absent. However, facies D and G, interpreted as penecontemporaneous alterations of preexisting deposits, locally contain an ichnofossil assemblage comparable to immediately subjacent or superjacent CA1 beds.

#### **Facies D: Convolute and chaotically laminated sand and silt.**

**Sedimentological characteristics:** facies D (Figs. 3.24-3.26) is defined by convolute to chaotic laminations, mesoscale slump folding, microfaulting and, commonly, apparent partial or complete homogenization of preexisting material. Consequently, the lithology of unhomogenized examples of this facies closely resembles that of adjacent facies. Where homogenization is substantial, facies D comprises mostly undifferentiated, light grey silty sand. Most facies D beds are 5-50 cm thick. However, in some examples (*e.g.* well 10-32-62-21w5; Fig. 3.24) facies D may extend continuously across several meters of core.

In addition to convolute and chaotic laminations, a wide variety of sedimentary structures are commonly observed. These include flame structures (up to ~5 cm high), diapirs extending up to ~30 cm into superjacent beds, ball-and-pillow structures, rollovers, decollement-type folds, full and partial rip-ups of subjacent beds, and synthetic microfaults with drag deformation of laminae along fault surfaces.

**Ichnological characteristics:** bioturbate textures are not observed in this facies, unless deformation and homogenization of the facies D precursor sediments is mild. In such cases, any observed ichnofossils clearly predated the deformational episode and are thus associated with the precursor beds and not with facies D *per se*.

Pyrite is a common component of moderately to significantly homogenized

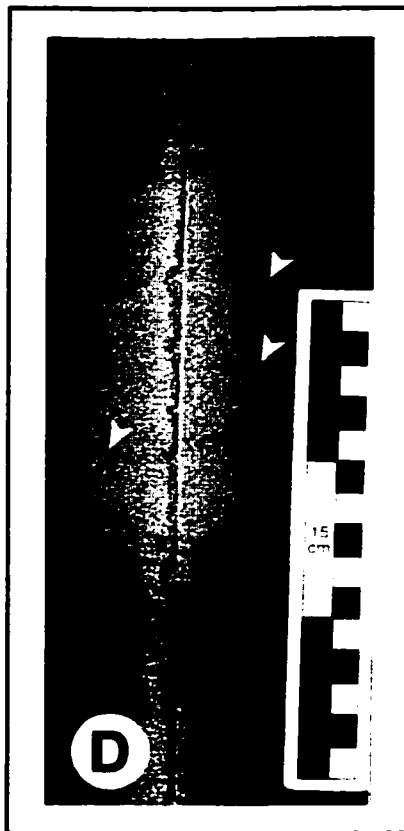
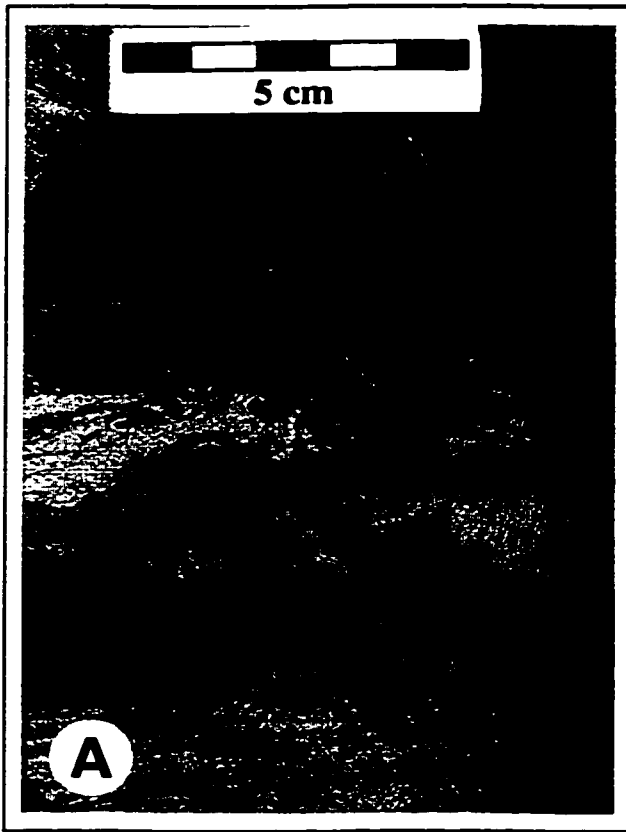


**Fig. 3.24 Facies D – box shot.**

Example of a relatively thick facies D succession, showing a variety of typical facies D sedimentary structures. Well developed convolute lamination is visible around [cv], and associated with the large rollovers marked by the small black arrows. Chaotic lamination may be observed at the base of the first box (at [ch]). In this example, facies D is gradationally overlain by homogenized, unremarkable sediments of facies G. Close association of facies D and G is common. This sequence is interpreted as a large scale slump: the chaotic lamination at the base and immediately overlying high angle layers are interpreted as sheared sediments at the base of the slump. The actual slumped material comprises the series of convolute and rolled-over beds. The gradationally overlying facies G beds reflect post-slump dewatering (*cf.* Facies G, below). From well 10-32-63-21w5, 7115-7128' (2169-2173 m).

**Fig. 3.25 Facies D – sedimentary structures I.**

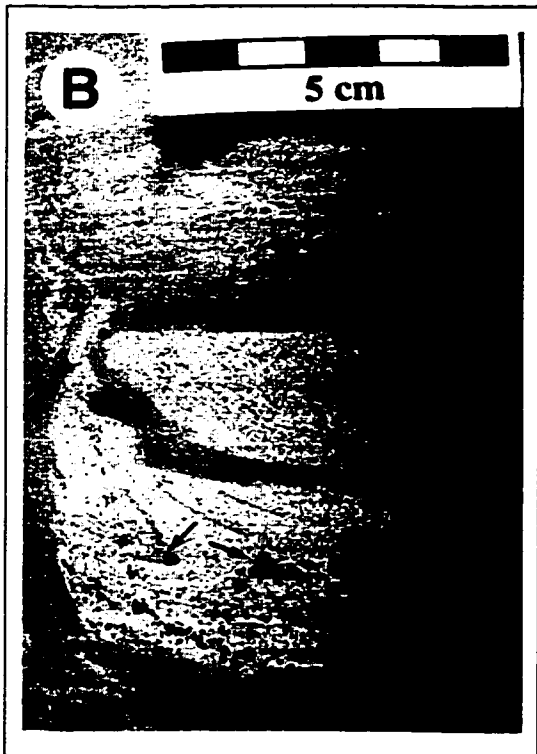
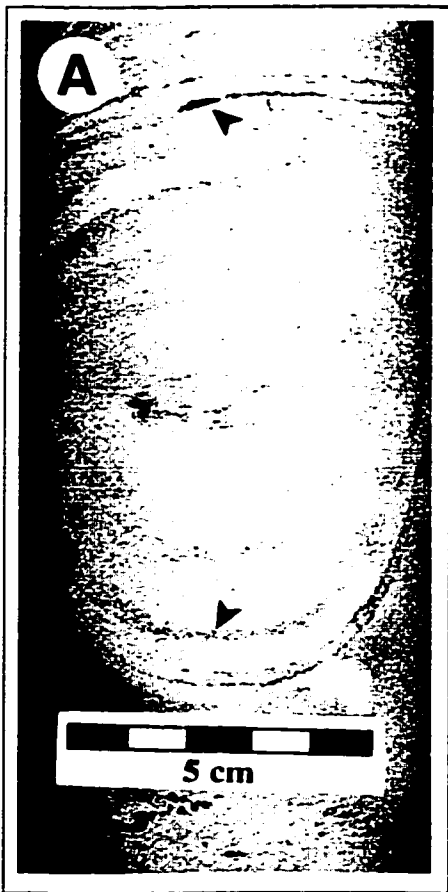
(A) thin bed of convolute laminae immediately overlying less well-defined convolutions and flame structures. Many occurrences of facies D are similarly encountered as thin (2-5 cm) beds within sediments of CA1 (e.g. Fig. 3.14). From well 6-8-65-21w5, 6338.5' (1932 m). (B) Chaotic laminations. From well 11-22-62-21w5, 2200.75 m. (C) Slump folded sand-silt interlaminations. The overlying dark rock is the Jurassic Nordegg Formation. Note the underlying high angle lamination. In this particular example, laminae were observed to progressively shift from horizontal to the ~15° slope visible here over ~1 m of core. It seems likely the slump fold at the top was intimately related to this progressive oversteepening. From well 4-30-64-18w5, 1785.1 m. (D) Large rollover that has been homogenized internally. Note the distinctly discordant graded pyrite zones which transect the rollover horizontally (arrows). Similar to facies A and G, these are interpreted as Liesegang bands; the discordance clearly indicates some form of post-depositional (*i.e.* diagenetic) origin for these graded horizons. From well 10-16-62-21w5, 7154' (2181 m).





**Fig. 3.26 Facies D – sedimentary structures II.**

(A) Large rollover. The darker layers (black arrows) are pyritized. From well 10-32-63-21w5, 7125' (2172 m). (B) Textbook sand pillow (*cf.* Reineck & Singh 1980, p. 88). The dark-colored material that highlights internal structure (*e.g.* arrows) is all pyrite. From well 6-8-65-21w5, 6317.5' (1925.5 m). (C) Synthetically microfaulted subfacies B2. Note the distinctly curved basal fault surface and successive, overlying horizontal faults, clearly indicative that this is a rotational slump block. White arrows denote displacement directions on some faults. From well 10-16-62-21w5, 7114.5' (2168 m). (D) an unusual tear and injection structure in homogenized sandy silt (facies G). The infilling and overlying material is a facies E massive sand. It is believed this feature formed because the underlying silty bed had become cohesive. It was thus subject to friction-induced tearing-up. The tearing may have taken place when the facies E bed was emplaced, or may have been related to the slump-faulting event pictured in (C) located ~50 cm above this photo. From well 10-16-62-21w5, 7116' (2169 m).



facies D. Graded pyrite zones similar to those of facies G are common, as are partially or completely mineralized laminae and burrows. The zones of graded, disseminated pyrite are typically concordant with the convolute laminations. However, discordant pyrite zones that horizontally or subhorizontally cut across convolute sediments are common in many examples.

**Interpretation and discussion:** as implied in the foregoing descriptions, facies D is interpreted as syndepositional to penecontemporaneous soft-sediment deformation. In most examples, partially homogenized examples of facies D exhibit diffuse or relict structures, lamination, and ichnofossils commensurate with facies B. Furthermore, most examples of facies D occur as a transitional body of sediments between unmodified sediments of CA1 affinity (mainly facies B, rarely facies A) and various facies of CA2, most prominently E or G. Clearly, deposits of facies B were the main precursor of facies D deformation.

The common homogenization of facies B lithologies is attributed to dewatering processes that accompanied deformation. Direct evidence for dewatering processes, such as distinct dewatering structures, is absent. However, two anecdotal lines of reasoning exist. Firstly, facies D beds are characterized by silty sand, even when formed within silt-dominated successions, indicating some post-depositional removal of fines. Secondly, there is no observed evidence for pervasive bioturbation, the only other major cause of homogenization in sediments (*e.g.* Reineck & Singh 1980)

Thin transitional beds of this facies are dominated by convolute laminations, small pillows, flame structures, and in one example, prominent diapiring into the overlying bed. These typically occur between discrete beds or successions of CA1, or between CA1 and CA2. They are interpreted to represent simple sediment loading and consequent deformation, a common characteristic of many environments (summarized in Reineck & Singh 1980).

However, very thick successions of this facies extending several meters characterize some wells (*e.g.* 10-32-63-21w5, 7105-7128'(2165-2172.5 m)). These typically contain chaotic laminations, thoroughly homogenized layers, and relatively large (10-30 cm diameter) rollovers. These exceptionally thick deformed units are interpreted as large-scale slump deposits. Locally preserved synthetic microfaults, with curved fault surfaces at their base, are interpreted as gravity faults. These are interpreted to indicate rotational slumping at smaller scales.

Rotational slides and large scale slumping are generally associated with

elevated gradients and rapid sedimentation or subjection to seismic shock (Reineck & Singh 1980). In shallow-water settings, they are most commonly associated with deltaic environments (*e.g.* Coleman 1981, Bhattacharya & Walker 1992, Reading & Collinson 1996).

### **Facies E: Massive, apparently structureless to diffusely laminated sand**

**Sedimentological characteristics:** facies E consists of apparently structureless to (rarely) diffusely laminated, light to medium brown very fine (<0.1 mm) sand. Not uncommonly, these beds incorporate a distinct fine sand (0.1-0.25 mm) component. In rare examples, fine sand is dominant (>50% volumetrically). Facies E beds are typically ~20 cm to ~1 m in thickness.

These beds commonly appear structureless. However, some examples display diffuse low angle laminations, locally. These may be parallel or non-parallel. Importantly, one occurrence of facies E (well 3-24-62-21w5, 6906'; Fig. 3.27 (A)) exhibits distinct HCS lamination. Rarely, the bases of facies E beds exhibit convolute lamination when facies D is the immediately subjacent unit. Dolomitization or silicification of this facies is common, further obliterating internal structure.

The basal contact of this facies is typically sharp and commonly truncates underlying laminae. However, rare examples were observed to have apparently gradational contacts with facies G, H, or subfacies B2. When sharp, the basal portion of the bed commonly incorporates a lag of rip-up clasts or shell fragments (Fig 3.27 (D)). The upper contact of facies E beds is typically gradational.

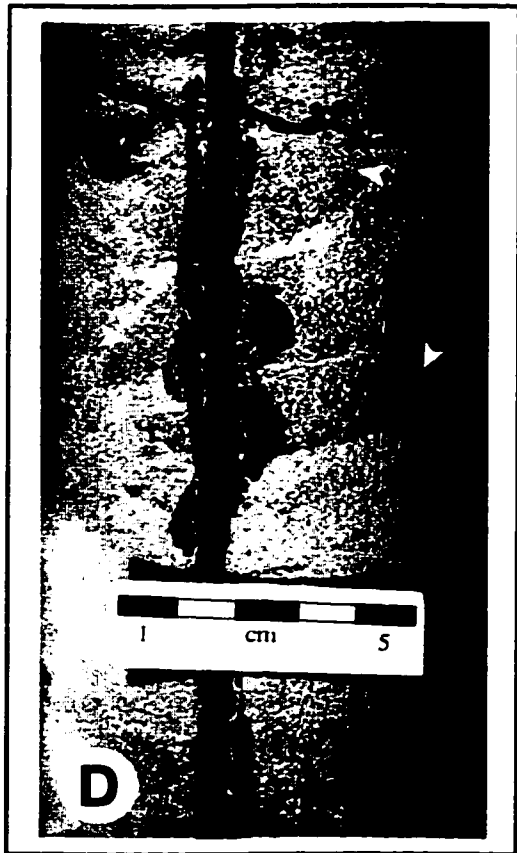
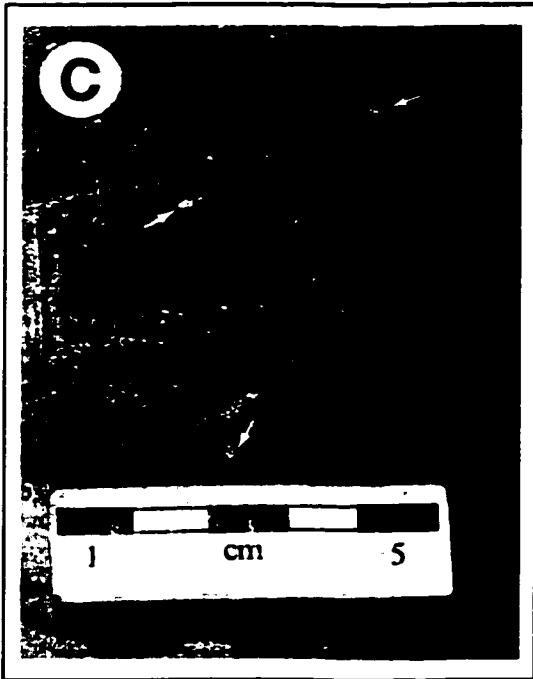
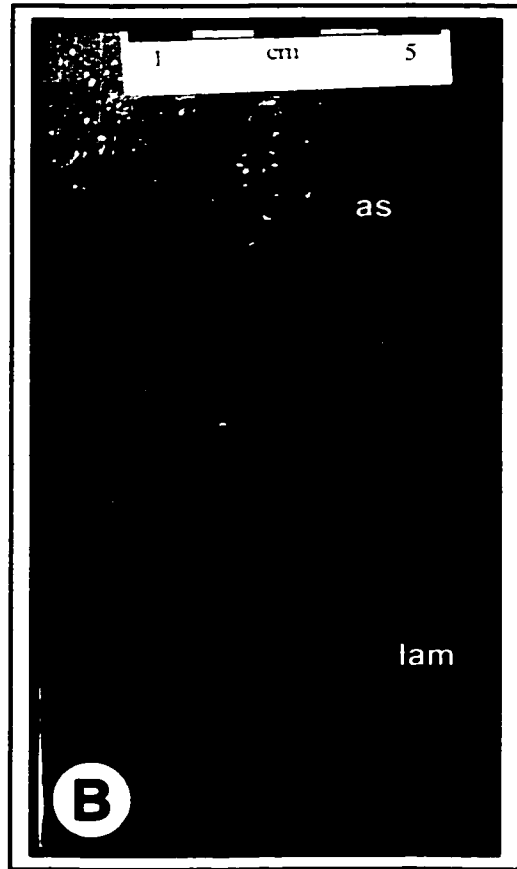
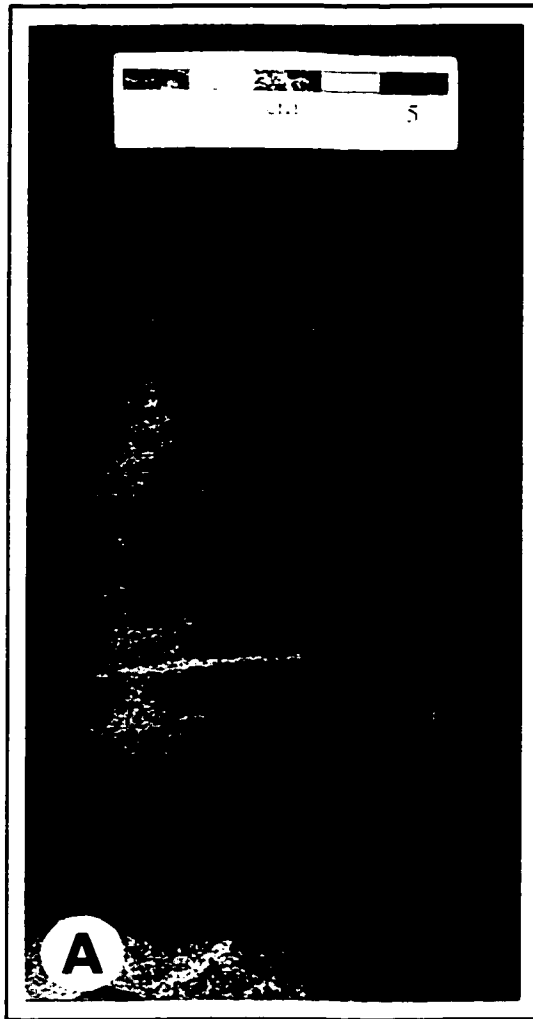
In one well (1-11-65-21w5, ~6081'; Fig. 3.27 (C)), facies E was observed to incorporate grains up to 1 mm in size (lower very coarse sand), at a stratigraphic horizon laterally consistent with the coquinal facies association.

**Palaeontological characteristics:** the shell fragments observed in this facies were unfortunately too poorly preserved for identification. However, they were generally calcitic and relatively robust, and thus are interpreted as comminuted valves of pelecypods or articulate brachiopods.

**Ichnological characteristics:** ichnofossils are absent in facies E, with the exception of very rare examples where burrows were observed at the top of E-type beds immediately overlain by facies B beds. In such cases, the ichnofossil assemblage was identical to that described for facies B. They are thus considered to have been

**Fig. 3.27 Facies E.**

(A) Sandstone exhibiting convex-upward lamination interpreted as hummocky cross-stratification. Note the visibly coarser material that comprises the bed. Incorporation of fine grained (0.25-0.5 mm grain size) sand is a distinctive characteristic of facies E. From well 3-24-62-20w5, 6906' (2105 m). (B) Example of facies E showing both planar-parallel lamination [lam] and apparently structureless bedding [as]. Both are common within facies E, but rarely found together. The white speckling in the upper structureless layer is disseminated dolomite crystallization, interpreted to have been formed after deposition. From well 15-29-64-18w5, 1765.3 m. (C) An example of facies E from the anomalous, coarse grained occurrences of the northwest (see text), that are laterally equivalent to coquina deposits. Although the bed is predominantly fine-grained, typical of facies E, it incorporates medium to coarse sand grains (>0.5 mm) (*e.g.* arrows). From well 1-11-65-21w5, 6-81' (1854 m). (D) Facies E is commonly dolomitized or, as in this example, silicified. Note the incorporation of large rip-up clasts (arrows), a characteristic of the basal portion of many facies E beds. From well 10-16-62-21w5, 7143.5' (2177 m).



associated with the later facies B deposition.

**Interpretation and discussion:** Most beds of facies E can be interpreted in a relatively straightforward manner as episodic storm-derived beds. This interpretation is supported by a variety of characteristics, including a common association with deformed and dewatered beds (facies D and G), a commonly erosive base, the common incorporation of a shelly or coarse-clastic lag, and a predominantly structureless appearance with locally developed, diffuse plane-parallel or curved lamination. The curved laminae are considered to represent poorly preserved HCS or SCS lamination. More circumstantial evidence includes the one clearly HCS-laminated facies E bed, and the common preferential dolomitization or silicification of the facies. This latter characteristic is interpreted to indicate deposition as a clean, well-sorted, high-porosity unit and thus predisposition to such remineralization.

Locally, structureless beds of facies E that gradationally overlie subfacies B2 may represent thoroughly bioturbated beds of facies C with a negligible silt content.

#### **Facies F: Texturally graded, well-sorted sand**

**Sedimentological characteristics:** facies F comprises well-sorted beds of very fine-grained (<0.1 mm) medium to dark brown sands. Beds are typically 5-20 cm thick. They are characterized by a basal zone of clean, very well sorted sand, grading upward into moderately well sorted, siltier sand. This textural gradation is commonly accentuated by a distinct color variation, dark brown basally, becoming progressively lighter brown upwards. Some examples (*e.g.* well 4-30-64-18w5, ~1793 m; Fig. 3.28 (B)) are characterized by an uppermost zone that is comparable to beds in subfacies B2, with wispy silt laminae and a comparable suite of sedimentary structures.

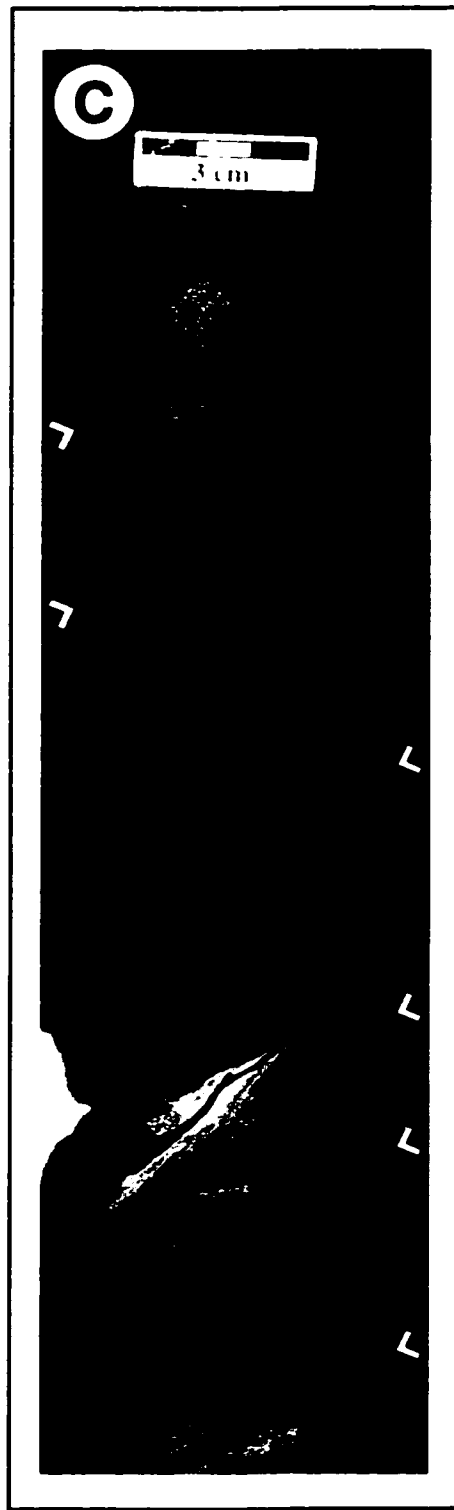
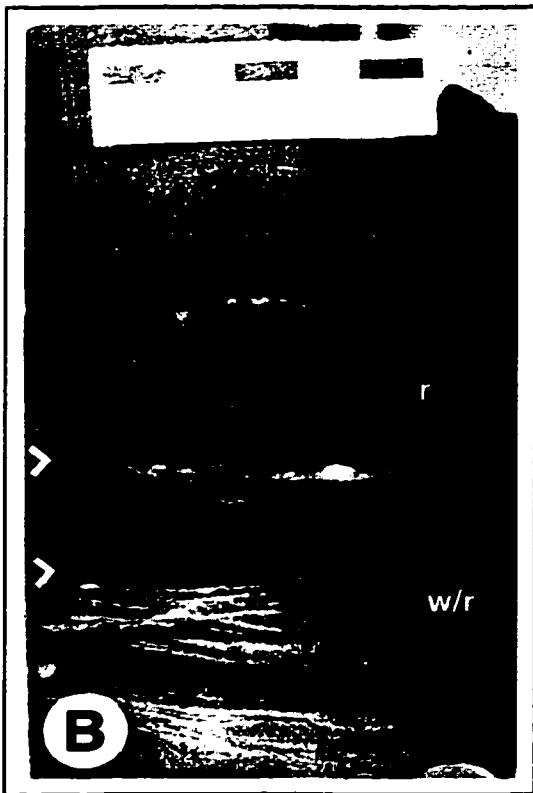
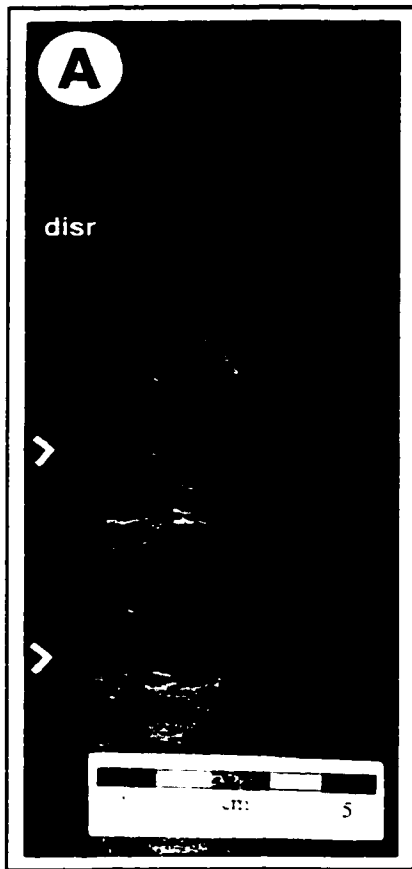
Amalgamation is a common characteristic of facies F beds (Fig. 3.28 (C)), with accumulated thicknesses commonly approaching one meter. The basal contact of F-type beds is predominantly erosive, and commonly truncates underlying beds. Where F-type beds overlie silt-rich facies such as A, B1, or G, the contact is commonly characterized by flame structures and loading features.

**Ichnological characteristics:** bioturbate textures are predominantly absent in facies F. No ichnofossils have been observed in the gradationally textured beds or portions of F-type beds. However, in the rare examples of facies F where the uppermost

**Fig. 3.28 Facies F.**

(A) Typical facies F, showing distinct colour gradation basally and a return to tidally influenced or reworked sedimentation, similar to facies B, at the top. Flechettes (>) demarcate the base of successive facies F beds. From well 1-7-64-19w5, 1880 m. (B) Thin beds of facies F (bases: >) overlying subfacies B2. The inclusion of silt and preservation of sedimentary structures lessens progressively upwards, lending a nearly gradational appearance to this B2-to-F transition. This suggests that the periodic perturbations which produce facies F may have been somewhat inherent in the local environment of CA1, rather than completely independent (*i.e.* solely storm-derived, for example). From well 4-30-64-18w5, 1793.2 m. (C) sharp transition from subfacies B2 (light-colored sediments at base) through partially amalgamated facies F, to fully amalgamated beds. This amalgamated facies F succession is a producing reservoir. The well is deviated, producing the apparently high-angle bedding. From well 4-36-64-19w5, 1870 m.





portion is comparable to subfacies B2 in appearance, distinct *Lingulichnus* and questionable *Planolites* or *Palaeophycus* have been observed.

**Interpretation and discussion:** the only distinguishing characteristics of facies F are an erosive base and a vague internal gradation. Graded beds are most commonly associated with turbidity currents (Reineck & Singh 1980, Boggs 1995) or storm deposits (e.g. Johnson & Baldwin 1991). Davies *et al.* (1997), in a regional review of the Montney Formation, described this facies and interpreted it as the deposits of a density (*i.e.* turbidity) or gravity (*i.e.* debris) flow. This interpretation is reasonable and followed here. The local presence of various, facies B-like sedimentary structures, and rare ichnofossils, in the upper portions of facies F beds is attributed to tidal reworking of the upper portions of F-type beds after deposition.

**Facies G: Homogenized to partially homogenized, pyritiferous silty sand.**

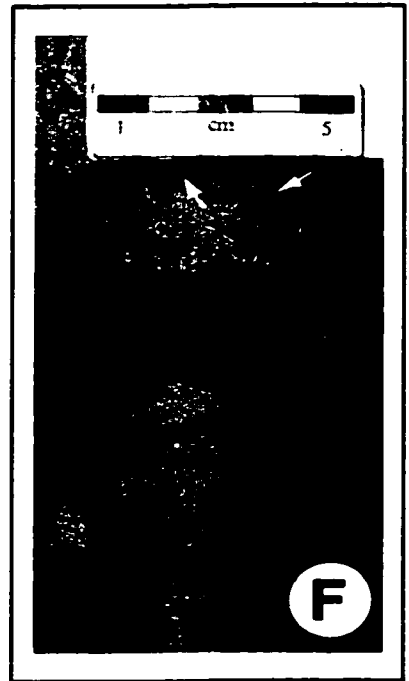
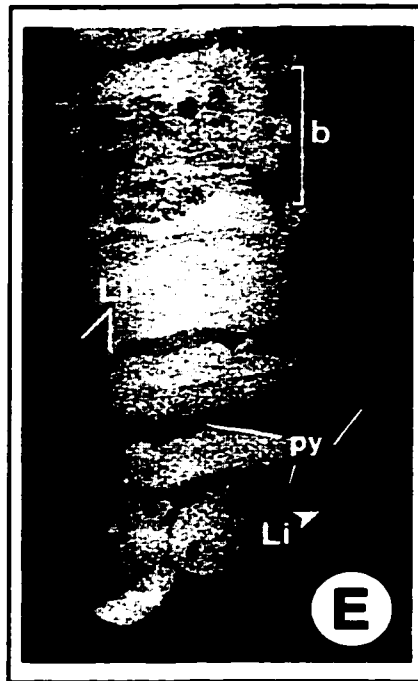
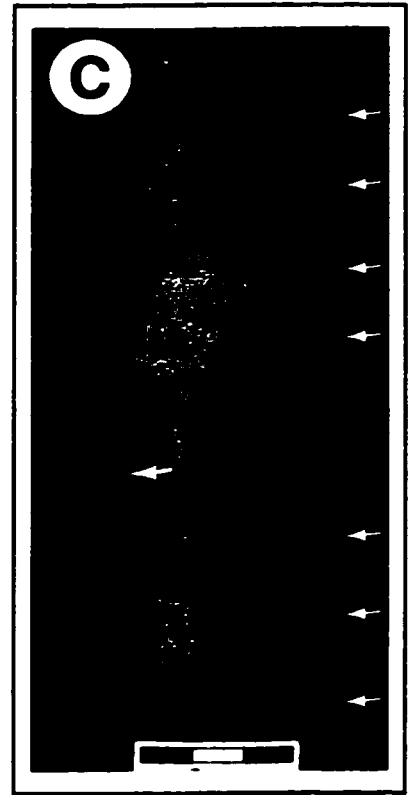
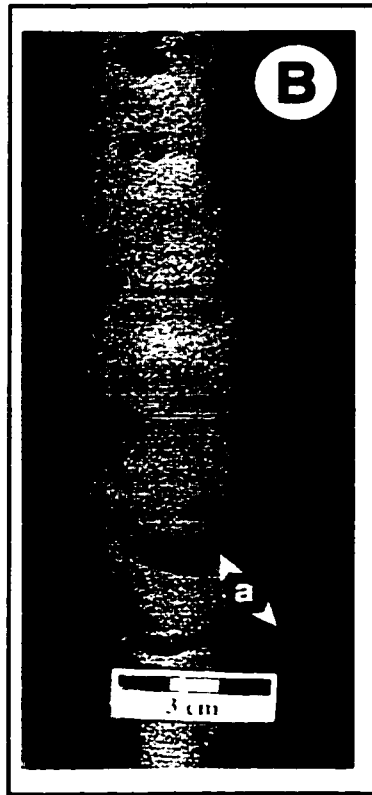
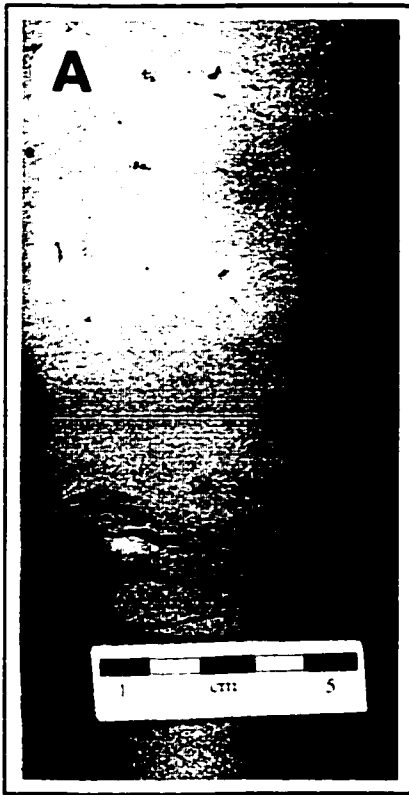
**Sedimentological characteristics:** facies G (Fig 3.29) consists of diffusely laminated to apparently structureless, light gray silty sand and medium gray sandy silt. Beds of this facies range in thickness from ~5 cm up to several meters, with a median of 10-40 cm. Pyrite is an important accessory component of this facies, commonly comprising ~3-5% of the total bed volume (e.g. Figs 3.29 (B), (D), (E)).

Thoroughly homogenized beds of facies G typically do not display any internal structure, with the rare exception of local, very diffuse lamination. Partially homogenized examples typically display diffuse laminations and sedimentary structures that are highly reminiscent of facies B and its subfacies. The basal contact of facies G is typically gradational with underlying lithologies. The upper contact is variably gradational (typically with facies A, B, or D and rarely with facies H) or sharp (typically with facies E or F). Facies G is unique in that it is also a common component of the coquinal facies association: it is a defining element of coquinal facies L and M (see below).

Pyrite mineralization is an important attribute of facies G. Complete pyritization of individual laminae or burrows, particularly the pedicle portions of *Lingulichnus* (Fig 3.29 (B)), is common in both partially and fully homogenized examples. Pyritization of entire horizons (*i.e.* several adjacent laminae and all associated burrows; Fig. 3.29 (E)) is also common, locally prominent over several discrete but closely (1-2 cm) spaced multiple horizons. Pyrite in facies G also occurs as discrete nodular masses ~5-20 mm in diameter.

**Fig. 3.29 Facies G.**

(A) typical facies G, completely homogenized and exhibiting no internal structure. The concentric fracturing immediately above the scale is of unclear origin, but most likely represents expansion of the core following extraction and loss of confining pressure. The black blebs at the top of the photo are pyrite masses. From well 10-16-62-21w5, 7151' (2180 m). (B) Facies G showing substantial pyritization (dark masses). [a] highlights concentric 'graded' pyrite horizons. The concentric organization is considered an important argument in favour of a diagenetic, Liesegang-band origin for the graded pyrite beds found in this and other facies (see text). From well 3-24-62-20w5, 6814.5' (2077 m). (C) Thoroughly homogenized facies G with a succession of graded pyrite bands (white arrows). From well 10-32-63-21w5, 7116' (2169 m). (D) Partially homogenized G, exhibiting relict and diffuse laminations. Prominent in this example are pyritized pedicle portions [pd] of *Lingulichnus*, a feature developed locally in numerous facies G occurrences. A complete, pyritized *Lingulichnus* is visible in the top-right corner at [Li]. From well 11-18-61-21w5, 8019' (2444.5 m). (E) Partially homogenized facies G showing a distinct resemblance to facies B, which is interpreted as the precursor of most facies G beds (see text). [Li] denotes clearly preserved *Lingulichnus*. The large burrow [b] is also a probable *Lingulichnus*. The very dark, irregular horizons near the base of the photo [py] are completely pyritized. From well 11-28-61-21w5, 8018' (2444 m). (F) Another example of partially homogenized G that resembles facies B. The curved features immediately below the scale (e.g. arrows) are calcitic shell fragments and sand-filled moulds of shells. From well 10-32-63-21w5, 7089' (2161 m).



The most common mode of pyritization in facies G is as evenly spaced zones of graded pyrite (Figs. 3.29 (B), (C)). These are typically ~5-10 mm thick and appear to fine upward; more rarely, they appear to coarsen upward. The graded pyrite zones are typically discordant, cutting across visible clastic laminations at a low angle. Rarely (*e.g.* Fig. 3.29 (B)), they occur as concentrically nested arcs.

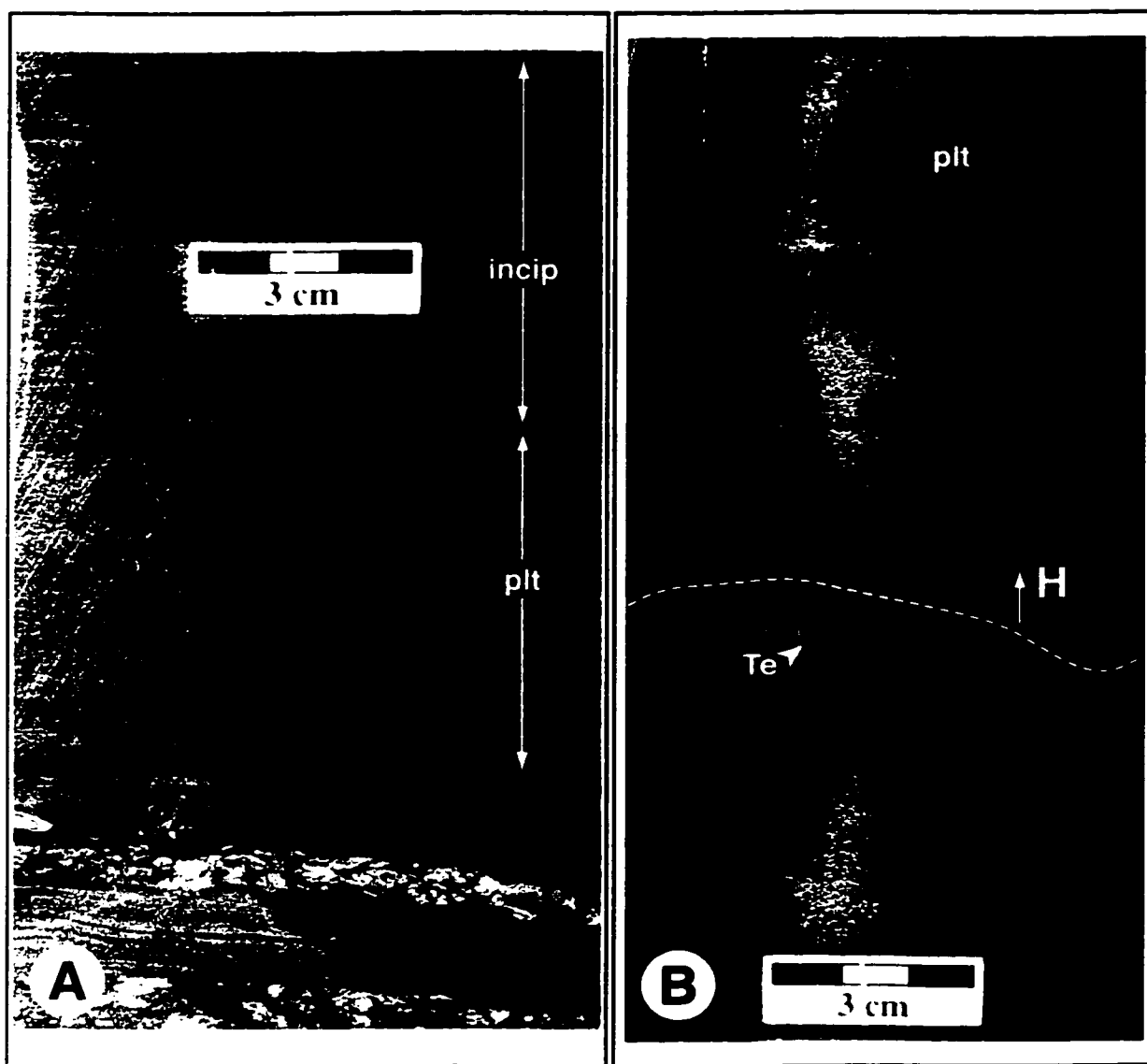
**Ichnological characteristics:** in thoroughly homogenized examples of facies G, burrows are typically obliterated along with all other preexisting sedimentary structures. Locally, however, pyritized *Lingulichnus* pedicle portions are preserved. Partially homogenized examples of facies G commonly exhibit a diffuse ichnofossil assemblage commensurate with that of facies B.

**Interpretation and discussion:** facies G is interpreted as dewatered sediments. Similar to facies D, there is no direct evidence for dewatering, such as distinct dewatering structures (*e.g.* dish-and-pillar structures, sand volcanoes). Several lines of anecdotal evidence exist, however. These include a close association with rapid, storm/event deposited facies E and F, a common association with deformed layers (facies D), an absence of any evidence for biogenic homogenization (mottling, ichnofossils), and a distinct silty sand composition even where facies G is incorporated into silt dominated layers. This last characteristic is interpreted to indicate some form of post-depositional removal of fines. Also similar to facies D, partially homogenized beds of G typically exhibit relict or diffuse sedimentary structures and ichnofossils comparable with facies B and its subfacies, suggesting that facies B was the primary precursor of facies G.

The evenly spaced, generally 'fining-up' zones of graded pyrite that characterize many facies G beds are interpreted as Liesegang bands. The rationale is the same as for similar deposits described under facies A. The local occurrence of concentrically nested pyrite bands in facies G is considered an important support for the Liesegang band interpretation, as they clearly suggest some form of radially propitiated alteration.

#### **Facies H: Very fine sand and pelletized silt**

**Sedimentological characteristics:** volumetrically minor but persistent facies H consists of discrete, medium brown sandstone beds with a moderate (~5-15% by volume, locally more) component of pelletized, tan to light gray silt (Fig. 3.30). The



**Fig. 3.30 Facies H.**

(A) Facies H overlying interbedded silty sand and coquina (facies L). Thorough pelletization [plt] is apparent in the middle portion of the photo. Close examination reveals a randomized orientation of pellets and subrounded to irregular shapes which appear to interlock. In this particular example, the silt pellets comprise the bulk of the unit. More commonly a sandy matrix predominates. [incip] denotes an overlying zone of incipient pelletization. From a distance it appears to have retained considerable lamination, but close examination shows that the lighter-colored component is mostly broken up into diffuse, rounded bodies. From well 4-27-61-21w5, 2333.5 m. (B) Facies H overlying heavily bioturbated subsfacies B2. Note the single identifiable *Teichichnus* in the B2 unit. The facies H bed is thoroughly pelletized [plt] with a few discontinuous, disrupted laminae. Distribution of pellets is random, but many appear to be aligned subvertically; this may indicate pelletization in this bed was produced by dewatering (with the silt pellets analogous to pillars in a dish-and-pillar structure) rather than by bioturbation. From well 7-14-63-21w5, 6778' (2066 m).

silt pellets are typically small (max. 1-2 mm long) and subrounded, or rarely branched, in shape. These are distributed randomly, but more or less evenly, within a matrix of well-sorted very fine-grained (<0.1 mm) sand. Typical facies H beds are relatively thick (~15-50 cm) and exhibit a conspicuous lack of any internal lamination or sedimentary structures. Preferential alignment of silt pellets occurs rarely. Concentration at distinct horizons was not observed.

Facies H is distinguished from pelletized beds of subfacies B2 by relative thickness of bedding (B2 beds are typically 4-10 cm thick) and the common absence of any laminations, disrupted or otherwise. Facies H is similarly distinguished from the commonly thick-bedded and pelletized facies C by the absence of any lamination or sedimentary structures, and by the close association of H-type beds with facies E, F and G.

**Ichnological characteristics:** no ichnofossils or discrete bioturbate textures are observed in facies H.

**Interpretation and discussion:** Pelletization in facies H is of a somewhat enigmatic origin. *In situ* formation of pellets in all examples is interpreted from their thoroughly randomized distribution and orientation (*i.e.* no discernible concentration into horizons, or grain alignment). In most examples, the pelletization is suggestive of pervasive bioturbation, based on common irregular to branched pellets and a structureless appearance of the hosting sands. This interpretation is perhaps appropriate where facies H gradationally overlies facies E (interpreted as storm beds). Opportunistic organisms commonly colonize the tops of storm deposits (*e.g.* Moslow & Pemberton 1988, Pemberton *et al.* 1992b)) and could produce a pervasive bioturbate texture.

Locally, however, facies H occurs at the base of, and grades into, facies E storm beds. In such cases, it typically also grades into an underlying unit of facies G. Abundant bioturbation in the basal portion of a storm bed seems unlikely, and hence an alternative explanation is required. It is proposed that during dewatering of the facies G precursor (presumably a direct result of sediment loading by the overlying storm deposit), the displaced pore waters and any transported fines mixed with the newly deposited storm sand. This produced the mottled appearance and pelletized silt component that characterizes these occurrences.

It is possible that some or all facies H occurrences at the top of facies E may similarly be due to dewatering and sediment mixing, not pervasive bioturbation.

## BIOCLASTIC FACIES ASSOCIATION

The bioclastic association (BFA; also coquinal association) comprises 5 facies (I, J, K, L, and M). Facies I is by far the dominant member. Thick accumulations of I function as a host for the other BFA facies. Facies K, L, and M are essentially accumulations of facies I with an intercalated siliciclastic component. In contrast with the fine-grained clastic facies associations, the BFA is composed of coarse skeletal grains. These bioclasts are dominantly whole and comminuted valves of pelecypods, with a minor brachiopod component and accessory gastropods. The size of BFA grains ranges from ~0.5-1.0 mm (coarse sand size) to as much as ~30 mm (coarse gravel). The median grain size comprises the granule (2-4 mm) and lower fine gravel (4-8 mm) grades.

No well-defined vertical succession for the components of the bioclastic association exists. 'Fine'-matrix coquina (facies I) is dominant, but punctuated in no particular order by individual beds or short successions of coarse-matrix coquina (facies J), interbedded sand and coquina (facies K), and interbedded silt and coquina (facies L). Any or all of the latter three may be absent in a given core. Only fractured and 'brecciating' sandy silt and coquina (facies M) showed a distinct position in the bioclastic association, commonly occurring at the base of the coquinal succession in a core, or more rarely, immediately overlying significant internal erosive surfaces of the coquinal succession.

Facies I, J, K, and M were all limited to the thick coquinal accumulations that correlate with the Coquinal Middle Dolomite Member of Davies *et al.* (1997). Facies L accumulations were also thickest and most common in this context. However, discrete beds of facies L, isolated from any other coquinal context, were not uncommonly incorporated into the two clastic associations. Such cases were predominantly noted from CA2.

The bioclastic facies association has a distinctly discordant morphology, cutting down into sediments of CA1 and CA2. It is further characterized by an erosive base, and clearly truncates preexisting units.



## **Facies I: 'Fine'-matrix coquina**

**Sedimentological characteristics:** facies I (Figs. 3.31 (A), (B)) consists of light gray, dolomitic coquina. The 'fine' grain size is defined by the predominance of skeletal grains in the 1-2 mm (coarse sand) and 2-4 mm (granule) size fractions. Comminuted valves of the 1-2 mm category typically comprise 40-80% of the bed volume. A minor (<5%) very coarse (4-10 mm) fraction, consisting of whole and partial valves is commonly present. The remainder of facies I beds comprises whole and partial valves or moulds in the 2-4 mm size grade.

Beds of facies I are typically structureless in appearance. Alignment of coarser grains is locally suggestive of low-angle parallel, or rarely convolute, laminations. Bedding thickness in this facies varies considerably, from ~10 cm up to several meters. Stylolitized horizons are common but widely spaced. Contacts with adjacent beds are typically gradational. They are sharp, stylolitized, or erosive, locally.

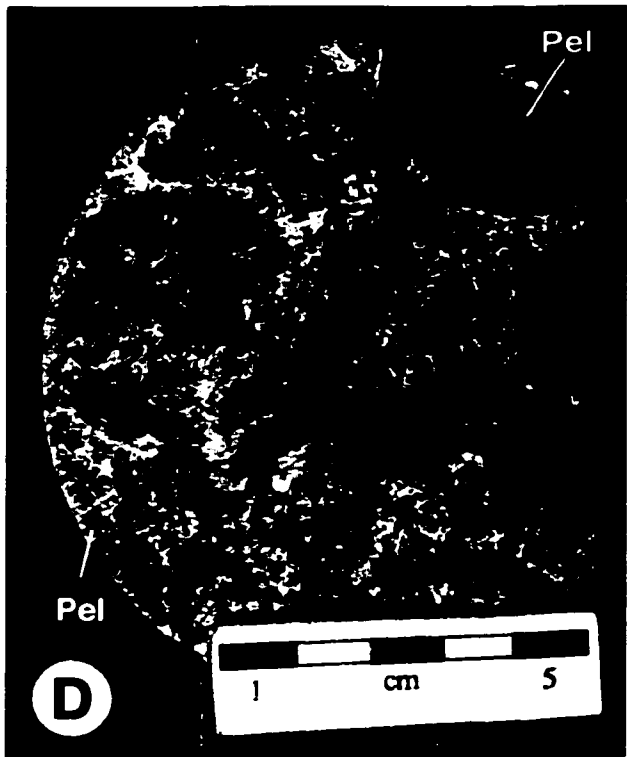
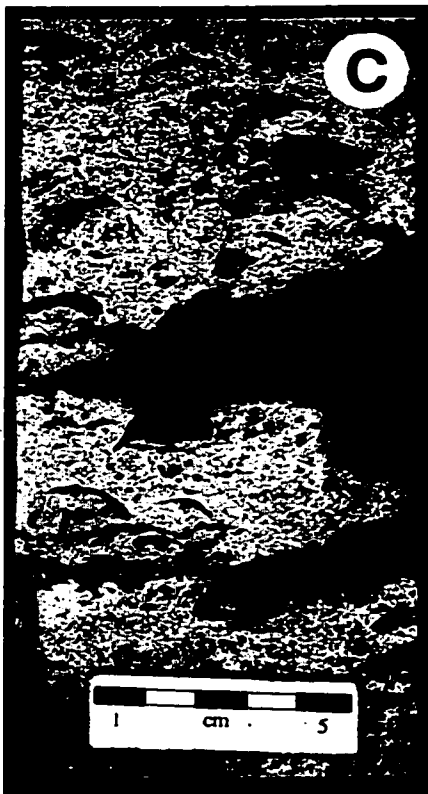
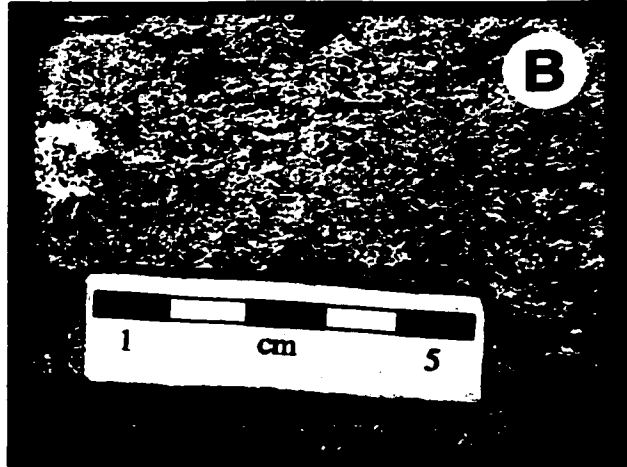
In apparently structureless beds, grains (or moulds) that retain significant curvature are oriented somewhat randomly. Approximately half are observed to be in a hydrodynamically stable convex-up orientation. However, one quarter to one half are typically oriented concave-up, with the remainder in any orientation, including vertical. Matrix grains are commonly packed between and around larger bioclasts in a random fashion.

Void space is very common in facies I, dominated by intergranular, shelter and mouldic porosity. In thin-section, voids are commonly lined with epitaxial dolomite. Replacement of shells by dolomite is pervasive, and many grains are preserved only as 'ghosts'. Hydrocarbon staining commonly imparts a brown or purplish tint to facies I deposits, and solid bitumen is commonly observed to partially fill pore spaces. An uncommon but persistently observed variant of I, characterized by incorporation of fines (grains <0.5 mm) and occlusion of pore-space, is termed 'tight' I in lithologs.

**Palaeontological characteristics:** the strong dolomitization of facies I impedes identification of body fossils. However, there is a clear, near-monospecific predominance of thin shelled 'paper-pecten' morphology pelecypods identified as *Claraia stachei*. Less commonly observed fossils included a large, strongly ribbed scallop-like pelecypod (Fig. 3.29 (D)) and moulds of a robust, unornamented pelecypod (Fig. 3.29 (E)). Rare fossils included phosphatic shell fragments interpreted as comminuted *Lingula* and fragmented valves of articulate brachiopods.

**Fig. 3.31 Facies I and Facies J.**

(A) Facies I with an altered or weathered appearance, from immediately below the sub-Jurassic unconformity. Thorough dolomitization is evident in this photo, with most shells and fragments appearing as relict 'ghosts' (e.g. small arrows). From well 13-7-62-19w5, 6903' (2104 m). (B) Close up shot of typical facies I, exhibiting considerable porosity. Note the size of most fragments and voids, ranging from 1-5 mm. From well 13-7-62-19w5, 6999' (2133 m). (C) Typical facies J, comprising a matrix of 2-5 mm fragments with numerous whole valves up to ~30 mm across. Note the articulated individual [a]. From well 13-7-62-19w5, 6905' (2105 m). (D) Top of a core segment showing several fossilized individuals [pel] of a Pecten-like species with strongly ribbed shells (e.g. the well-contrasted individual in the lower left). From facies J, in well 13-7-62-19w5, 6973' (2125 m). (E) Top and bottom of two core segments from Fig. 3.31 (C). Note the robust, unornamented pelecypod shell mould filled with solid bitumen (arrows). From facies J, well 13-7-62-19w5 6905' (2105 m).



Microscopic gastropod shells were very rarely observed in thin section.

**Ichnological characteristics:** no macroscale ichnofossils or unequivocal bioturbate textures were observed in this facies. The random orientation of many valves at the macroscale is possibly indicative of an abundant bioturbate texture.

In thin sections, clusters of concentrically aligned grains and concentrically aligned void spaces are very common, suggesting pervasive microscale bioturbation (*cf.* Keswani 1999).

**Interpretation and discussion:** facies I is essentially a bioclastic hash. The dominance of disarticulated and fragmented shells, the variable orientation of grains, and locally preserved low angle laminations of this facies indicate considerable transport and probable post-depositional reworking of the constituent bioclasts. A predominance of rapid deposition is interpreted from the apparently structureless appearance of most accumulations. However, locally abundant microscale bioturbation, and possibly macroscale bioturbation at all levels, regular interfingering of other coquinal facies, and common intercalation of laminated I with structureless I, all indicate that deposition was most likely episodic, with only relatively thin beds (5-50 cm) deposited at any given time.

Facies I is interpreted as channel fill deposits, based on the above internal characteristics as well as the overall (downcutting and erosive) morphology of the BFA succession. For a number of reasons, elucidated in the interpretation of other coquinal facies, as well as lateral stratigraphic relationships discussed in Chapter 4, these are interpreted to have been subtidal channels, possibly with some incorporation of storm-derived layers.

#### **Facies J: Coarse-matrix coquina.**

**Sedimentological characteristics:** facies J (Fig. 3.31 (C)) consists of light gray, dolomitic coquina and is in most respects comparable to facies I. It is distinguished by the predominance of granule-sized (2-4 mm) skeletal grains, which typically comprise 60-80% of bed volume. A minor (5-10%) fine (1-2 mm) size fraction is commonly incorporated. The remainder comprises coarse grains, typically of a fine gravel (4-10 mm) grade, but with individual bioclasts up to ~35 mm in size.

Beds of facies J are typically structureless in appearance with a highly randomized orientation of the smaller component grains. Larger (>10 mm) grains

are dominantly in a hydrodynamically stable, concave-down position. Whole valves are common, with rare articulated shells (Fig. 3.31 (C)). Facies J accumulations are typically 10-30 cm thick. Upper and lower contacts are commonly gradational with facies I. Rarely, beds range up to ~2.0 m in thickness. In such examples one or both contacts are typically sharp. Examples of facies J grading towards facies K contain suggestions of low-angle parallel lamination, locally.

**Palaeontological characteristics:** body fossils in facies J are identical to those described for facies I, distinguished only by increased numbers of whole valves and larger specimens.

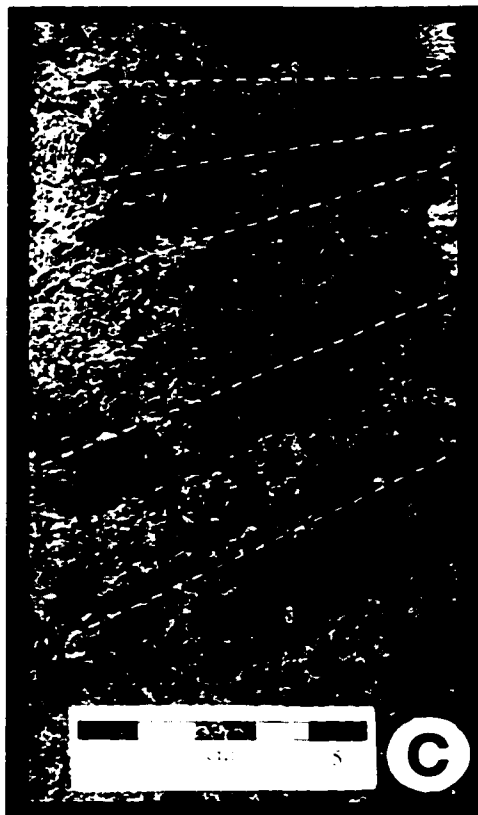
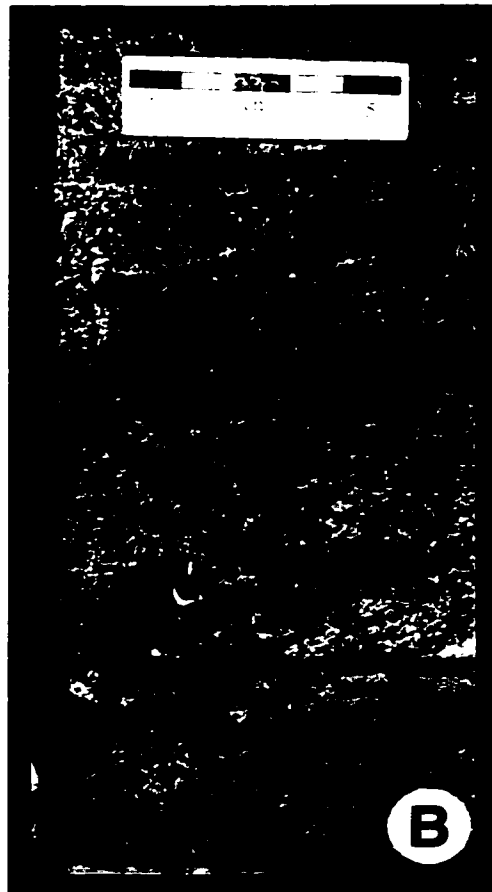
**Ichnological characteristics:** no suggestions of ichnofossils or bioturbate textures are observed at any scale in facies J.

**Interpretation and discussion:** the larger grain size and increased occurrence of unfragmented shells in this facies are interpreted to indicate the component grains were transported a shorter distance than shells of facies I. Alternatively, the coarser grade may indicate deposition in deeper or more restricted settings, less subject to regular smashing by waves. One possible explanation is that facies J represents lag deposits, winnowed more or less *in situ* from the walls or base of a facies I channel. Shells at the base of the channel would perhaps already have been deep enough, and shells excavated from the walls could have settled into deeper areas, thus avoiding the pounding by waves and attendant comminution that characterized shallower areas.

**Facies K: Interbedded very fine sand and coquina.**

**Sedimentological characteristics:** facies K (Fig. 3.32) consists of finely interbedded tan-colored silty sand and light gray coquina. The coquinal layers are comparable in all respects with facies I, rarely with facies J. The silty sand layers are distinctly siliclastic, and occur as irregular, patchy bodies or as distinct layers which are continuous across core.

Accumulations of this facies are typically 20-50 cm thick but extend to a few meters locally. The incorporated sand layers are typically 0.5-2 cm thick, ranging to about 5 cm. These are dispersed relatively evenly within a dominantly coquinal succession; bioclastic layers are typically 5-20 cm thick ranging up to 50 cm in thicker



**Fig 3.32 Facies K.**

(A) photo depicting the basic characteristics of facies K. The featureless, irregular bodies are sandy interbeds within a coquinal succession, which in this example grades towards facies J in composition. Note the ragged, irregular perimeter of the sandy beds, interpreted to indicate a measure of post-depositional winnowing. In this example, the intercalated coquinal layers exhibit a somewhat randomized orientation of constituent grains. (B) Facies K with few discrete sand beds (featureless patches) but a distinct alignment of bioclasts into relatively high angle beds. Much of the sand in this example is interstitial, forming the matrix of the darker-colored bands within the coquinal layers. (C) Lithologically typical facies K, with irregular sandy beds and high-angle parallel aligned bioclasts. This example also exhibits the progressive decrease in angle of the bedsets (dashed lines) that is developed locally in many facies K beds. This is interpreted as mesoscale channel-fill cross bedding (*cf.* Reineck & Singh 1980, p. 106). All photos from - - - - ->

(Fig. 3.32 cont.) well 13-7-62-19w5. Depths: (A) 6990' (2131 m); (B) 6976' (2126 m); (C) 6998' (2133 m).

facies K accumulations. Contacts between the sandy and shelly layers are gradational locally; expressed as a sandy matrix within the shelly layers that disperses away from the sand bed. Commonly, the sand-coquina contact is sharp; such examples typically display an irregular or ragged appearance.

Internal structure beyond this coarse interlayering is not abundant. The bioclastic layers exhibit grain alignments suggestive of subparallel low-angle laminations, locally. The sand layers are typically homogenized in appearance, with rare examples showing diffuse low-angle parallel lamination. However, a common macroscale characteristic of the interbedded sands and coquinas is a progressive vertical decrease in angle of dip (Fig. 3.32 (C)).

**Palaeontological characteristics:** coquinal layers of facies K display a fossil assemblage commensurate with facies I. No body fossils were observed within the sandy layers.

**Ichnological characteristics:** no ichnofossils or bioturbate textures were observed in facies K.

**Interpretation and discussion:** the alternating deposition of very fine sand and comparatively coarse coquina in this facies is clearly indicative of fluctuating energy levels. Typically even spacing of the intercalated sand layers further suggests fairly regular fluctuations. The ragged, patchy appearance of some sand layers may be indicative of post-depositional winnowing of fines, which suggests intermittent current strengths able to move very fine sand but not coarse bioclasts.

The commonly inclined bedding of this facies, defined by relatively high angles of dip in sandy layers and in the alignment of bioclasts of shelly layers, is interpreted to indicate deposition under the influence of unidirectional currents, perhaps as bars. This is supported by the local tendency of the inclined sand-coquina interbeds to decrease in dip from top to bottom, interpreted as possible mesoscale channel-fill cross bedding (*cf.* Reineck & Singh 1980).

A facies K setting characterized by regularly fluctuating energy conditions, dominantly unidirectional currents, mesoscale channels, combined with the overall downcutting morphology of the Bioclastic Association, suggests this facies was deposited in a tidal channel to tidal-delta setting.

## **Facies L: Interbedded silty sand and coquina**

**Sedimentological characteristics:** facies L (Fig. 3.33) consists of interbedded light gray dolomitized coquina, and light to medium gray silty sand. The bioclastic layers are comparable to facies I. These typically incorporate substantial interstitial silt or very fine sand and thus resemble the 'tight' variant of I. The siliclastic interbeds closely resemble facies G of Clastic Association 2, locally including a comparable amount of pyrite.

Accumulations of facies L are typically 0.5-2.0 m thick, ranging to ~4.0 m locally. Relative proportions of the siliclastic and coquinal components are variable, ranging from 20-80% coquina. Thickness of individual beds varies between occurrences of facies L, ranging from 5-80 mm for both the siliclastic and bioclastic layers. Within individual occurrences, however, relative thicknesses of beds tend to be consistent. Contacts of facies L with adjacent units are typically sharp or erosive. However, contacts with the lithologically very similar facies M are commonly gradational or indistinct.

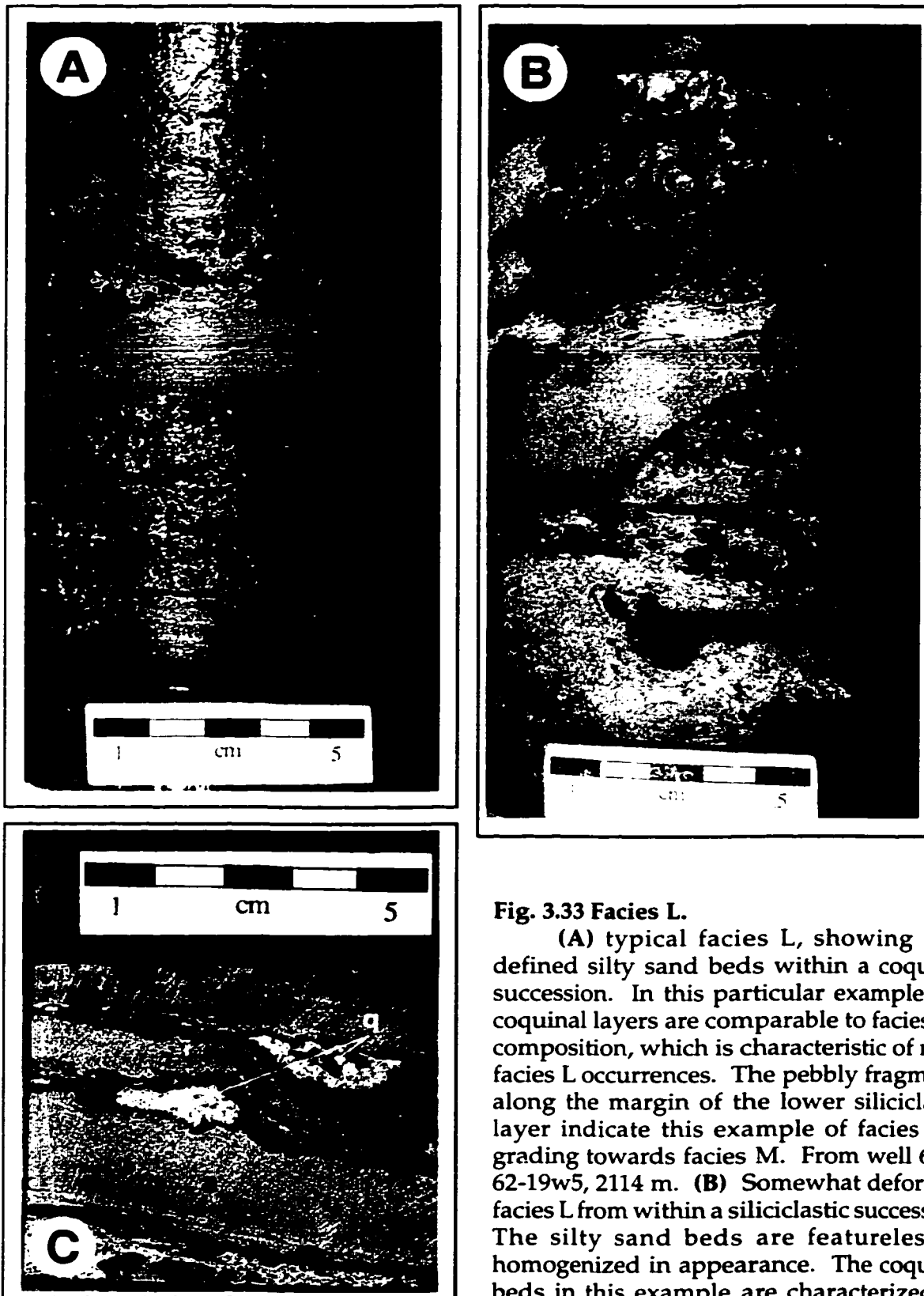
Facies L interbeds are low-angle parallel or wavy, locally irregular, with sharp contacts. Rarely, the contact is gradational, expressed as a progressive change in interstitial clastic content of the relevant coquinal layer. Internal structures are uncommon in the coquinal beds, which typically comprise only randomly oriented bioclasts. Very rarely, grain alignment is suggestive of low-angle subparallel lamination. The siliclastic beds are typically homogenized in appearance, rarely exhibiting diffuse internal wavy or low-angle parallel lamination. Laminae and bedding surfaces of the siliclastic beds exhibit pyritization, locally.

Uniquely, facies L is commonly found outside the Bioclastic Association context. It is locally incorporated as thin (2-20 cm) beds within both siliclastic associations, although more commonly in CA2.

**Palaeontological characteristics:** the coquinal layers of facies L exhibit fossils commensurate with facies I.

**Ichnological characteristics:** ichnofossils or bioturbate textures are absent in this facies. In some very rare examples, pyritized or very diffuse structures suggestive of *Lingulichnus* and *Planolites* were observed within siliclastic layers of facies L.





**Fig. 3.33 Facies L.**

(A) typical facies L, showing well defined silty sand beds within a coquinal succession. In this particular example, the coquinal layers are comparable to facies I in composition, which is characteristic of most facies L occurrences. The pebbly fragments along the margin of the lower siliciclastic layer indicate this example of facies L is grading towards facies M. From well 6-18-62-19w5, 2114 m. (B) Somewhat deformed facies L from within a siliciclastic succession. The silty sand beds are featureless to homogenized in appearance. The coquinal beds in this example are characterized by calcite lined vugs. From well - - - ->

(Fig. 3.33 cont.) (03)/10-34-64-19w5, 1778.3 m. (C) Interesting facies L occurrence in which two silty layers ([a] and [b]) enclose a slump-folded coquinal layer. Note that neither silty sand bed exhibits any internal deformation, with wispy bedding-parallel laminations clearly visible. This is interpreted to indicate both silty sand beds had become cohesive before the slumping episode. It seems the coquinal layer was less competent and deformed, carrying the superjacent silt bed, and any other overlying material, along as a raft as it slipped downslope. It seems that fluid or some other supporting medium was involved, as the coquinal bed was not flattened after deforming. This left void spaces, later infilled by quartz [q]. From well 13-7-62-19w5, 6999' (2133 m).

**Interpretation and discussion:** facies L is in most respects very similar to facies K. It is distinguished from the latter mainly by incorporation of silty sand or sandy silt rather than just sand, and by a distinct lack of inclined layering. Alternation of relatively coarse coquina with fine sand and silt beds is indicative of strongly fluctuating energy conditions. Preservation of lamination within the siliciclastic layers, locally, and common homogenization of the siliciclastic sediments elsewhere are interpreted to indicate quiet suspension settling of siliciclastics, alternating with rapid deposition of bioclastic layers that commonly induced dewatering. Decollement and slump folding of a coquinal layer (well 13-7-62-19w5, ~6999'; Fig. 3.33 (C)) suggests that the sandy silt beds commonly reached a cohesive state, remaining undeformed while providing a slip surface for overlying layers.

The incorporation of facies L into otherwise clastic associations suggests that conditions necessary for its deposition were not intimately tied to the processes that produced the bulk of the Bioclastic Association. The alternation of beds seems to be episodic, varying from quiet deposition of fines to rapid deposition of coquina. This extreme variation is attributed to episodic storms rather than tides, and thus facies L is interpreted as a bioclastic tempestite. Incorporation of facies L into the BFA is thus coincidental and not tied directly to autocyclic variations in the BFA setting. However, its deposition in this setting was without doubt facilitated by an abundant source of bioclastic material, hence the thicker accumulations of L within the coquinal association.

### **Facies M: Coquina with interbedded fractured and 'brecciating' silty sand**

**Sedimentological characteristics:** facies M consists of light grey dolomitized coquina interbedded with light grey silty sand. It is distinguished from the lithologically identical facies L by the common development of blocky fracturing and partially to

fully disconnected blocky clasts (hence 'brecciating') at the tops of siliclastic interbeds (Figs. 3.34 (A), (B)). The coquinal component is similar to facies I, but locally incorporates finer (down to 0.25 mm) bioclastic grains.

Accumulations of facies M are highly variable, ranging from single siliclastic-bioclastic couplets ~10 cm thick, to thick successions of several meters which commonly include numerous facies L beds. Bedding within facies M ranges up to ~50 cm in thickness. The character of the internal bedding contacts is defined by the siliclastic beds, which are gradational with coquina basally and sharply 'brecciating' at the top. Transitions between facies M and adjacent units are typically sharp to erosive. However, contacts with facies L are gradational or indistinct, locally.

Sedimentary structures are typically absent in siliclastic beds, which appear thoroughly homogenized. Coquinal beds exhibit randomized grain alignments, but typically contain a distinct size gradation. They are very fine-grained at their base, coarsening upwards to size parameters typical of facies I. Commonly the finest grains are packed into fractures of the underlying, 'brecciating' siliclastic bed. Upper portions of the coquinal layers locally exhibit a reversed gradation incorporating increasing amounts of interstitial clastics as a superjacent siliclastic bed is approached. Commonly, the basal portion of a coquinal layer incorporates clasts of the subjacent brecciating siliclastic bed. These are typically angular and in-situ, clearly fractured off of adjacent siliclastics (Fig. 3.34 (C)). However, subangular to subrounded and (rarely) deformed rip-up clasts are also present, locally.

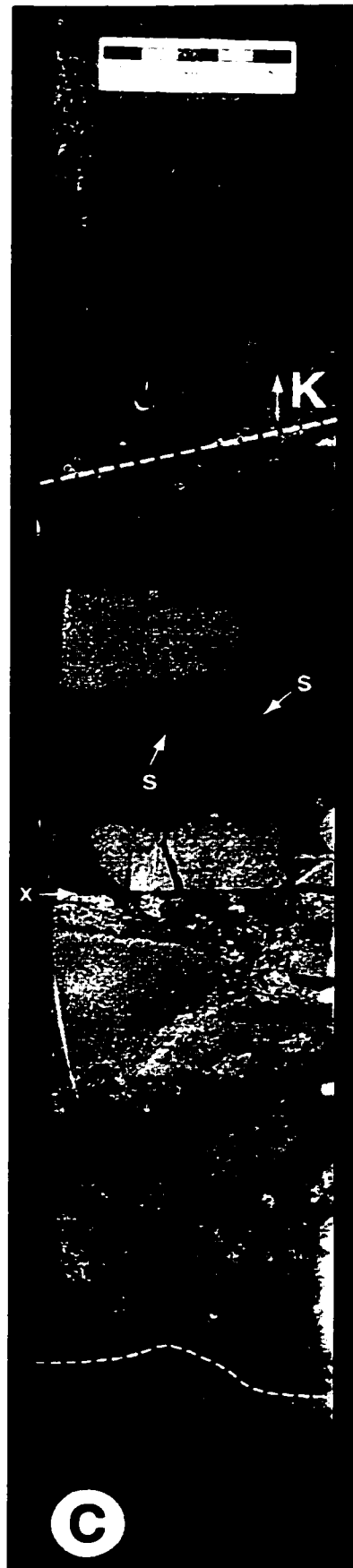
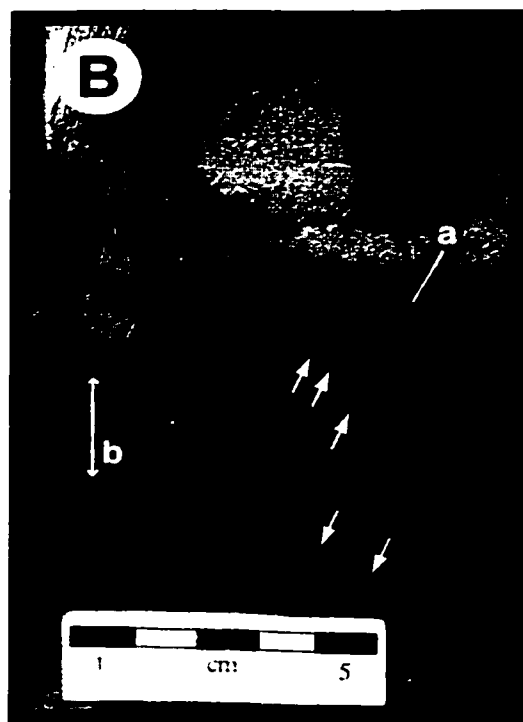
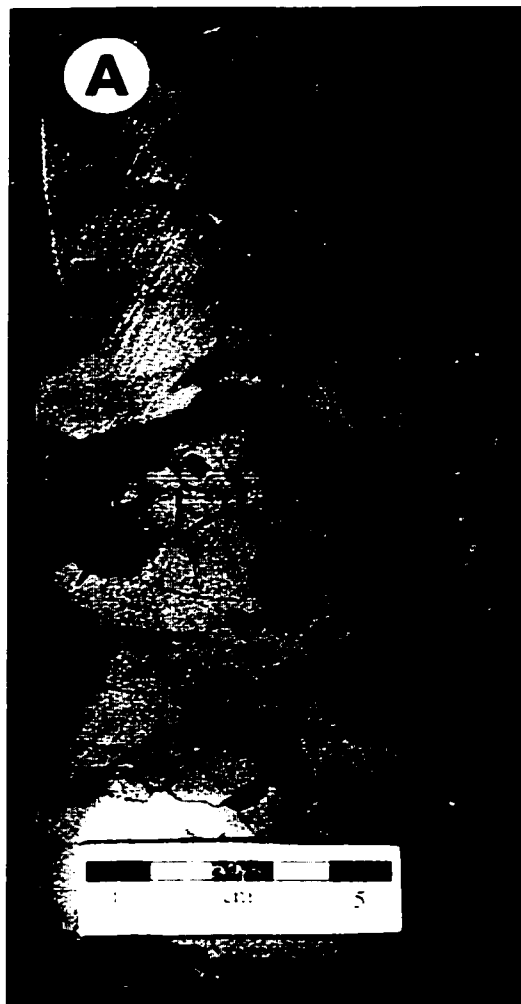
**Palaeontological characteristics:** coarser zones of facies M coquinal layers exhibit fossils commensurate with facies I.

**Ichnological characteristics:** no ichnofossils or bioturbate textures were observed in facies M.

**Interpretation and discussion:** facies M is lithologically very similar to facies L, and is typically interbedded with the latter at a relatively small scale (e.g. Fig 3.33 (A)). Clearly, however, facies M has undergone substantial alteration compared to L. This is indicated by induration or even early lithification of the silt layers in facies M, permitting the development of blocky fracturing and detached angular clasts. Lithification, followed by fracturing and erosion, suggests a substantial hiatus in deposition and subaerial exposure. Apparent leaching or weathering indicated

**Fig. 3.34 Facies M.**

(A) Typical facies M, showing the blocky fracturing and incipient clasts of a sandy silt bed, erosively overlain by relatively fine-grained coquina. (B) Example of facies M exhibiting clear evidence of weathering or leaching in the form of dark bands (arrows) running parallel to the brecciation surface. Multiple intersecting fractures have produced a number of incipient clasts through the zone marked [b]. Note the particularly interesting clast [a] that has clearly detached but remains almost *in-situ*. (C) A much thicker occurrence of facies M, extending 30+ cm. The thin dashed line marks the top of the unbrecciated siliciclastic bed. This is overlain by ~20 cm of closely packed, large rip-ups which grades up into coquina. The coquinal layer continues to grade into the sand-coquina interbeds of facies K (an enlarged close up of this facies K unit is found in Fig. 3.32 (B)). Note that, amongst the jumbled rip-ups, shell fragments are relatively small and indistinct but become coarser further up, with some distinct, whole valves (e.g. [s]). [x] denotes a missing core segment. All these examples are from well 13-7-62-19w5. Depths: (A) 6980' (2127.5 m); (B) 6984.5' (2129 m); (C) 6976-6978' (2126-2127 m).



by banding parallel to fracture surfaces in some facies M siliciclastic layers (e.g. Fig 3.34 (C)), supports this interpretation.

Deposition of facies M appears to have been intimately tied to deposition of facies L. The lithological similarity of M and L, and the thin interlayering of the two, impels the interpretation that facies L beds were the precursors subjected to facies M alteration and erosion. It seems desirable to avoid invoking rapid sea-level fluctuations as the primary cause of the depositional-'hiatal' cycles exhibited in facies L/M interbeds.

Although speculative, the following model is thus proposed. The facies M environment was normally very shallow to subaerial. Storms accompanied by initial erosion would intermittently deposit coquinal layers. The initial erosive phase entrained the rip-ups that are commonly observed in the coquinal layers of M. Presumably, the coquinal storm bed either had somewhat undulatory upper surfaces that impounded water or were regularly submerged, perhaps in an intertidal zone. This permitted accumulation of mostly windborne silty sand deposits over the coquina. Downward sifting of these siliciclastics, perhaps assisted by vertical pore water migration during tides, produced the gradational concentration of interstitial material at the top of some coquina beds. Desiccation and early carbonate cementation under relatively hypersaline conditions in the shallow to impounded water bodies, induced quick lithification of the siliciclastics. These were then subject to weathering, fracturing, and eventually erosion by the next storm event.

Facies M is considered to have most likely developed on bars or banks that normally protruded above the fair weather high-water mark. These could have been berms, short-lived barriers, or channel levees. A second possibility is that they represent brief hiatal surfaces produced at the top of an ongoing channel filling exercise during short, local scale regressions.

Alternatively, as discussed by Davies (1994, 1997a), and Davies *et al.* (1997), the coquinal association may represent a major (3<sup>rd</sup> order regression) lowstand. In such a case, the typical location of facies M at the base of the cycle is highly relevant, as M might then represent the lowstand lag or an initial stage of transgressive fill. The model discussed above would still be applicable, with the restricted evaporative setting perhaps constrained by channel walls.

## ANOMALOUS OR UNCOMMON FACIES

Two facies were observed to have very limited distribution in core from this study area. They are notable either because they are representative of a distinct geophysical response in well logs with poor core control (Facies O), or because they have been noted by other workers to be common outside the study area (Facies N).

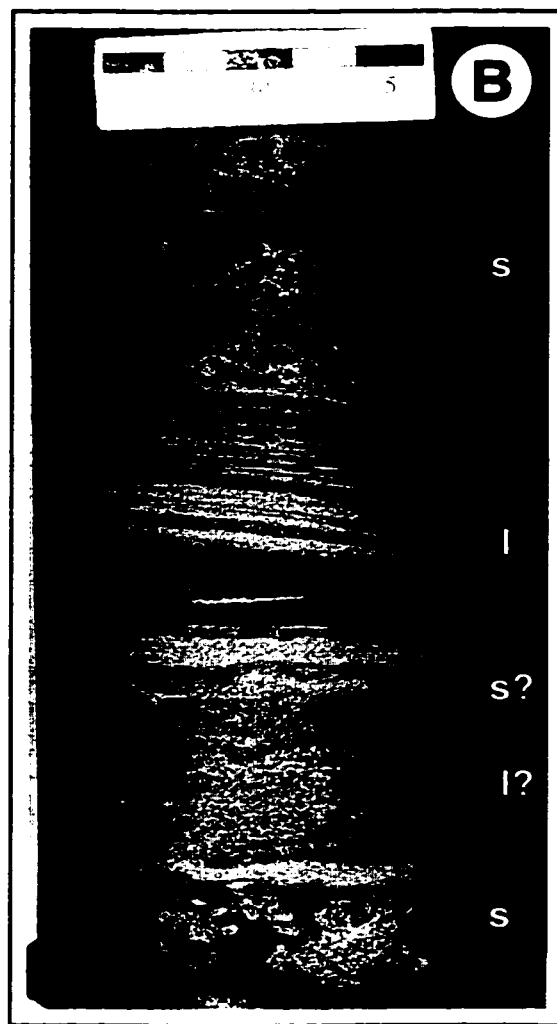
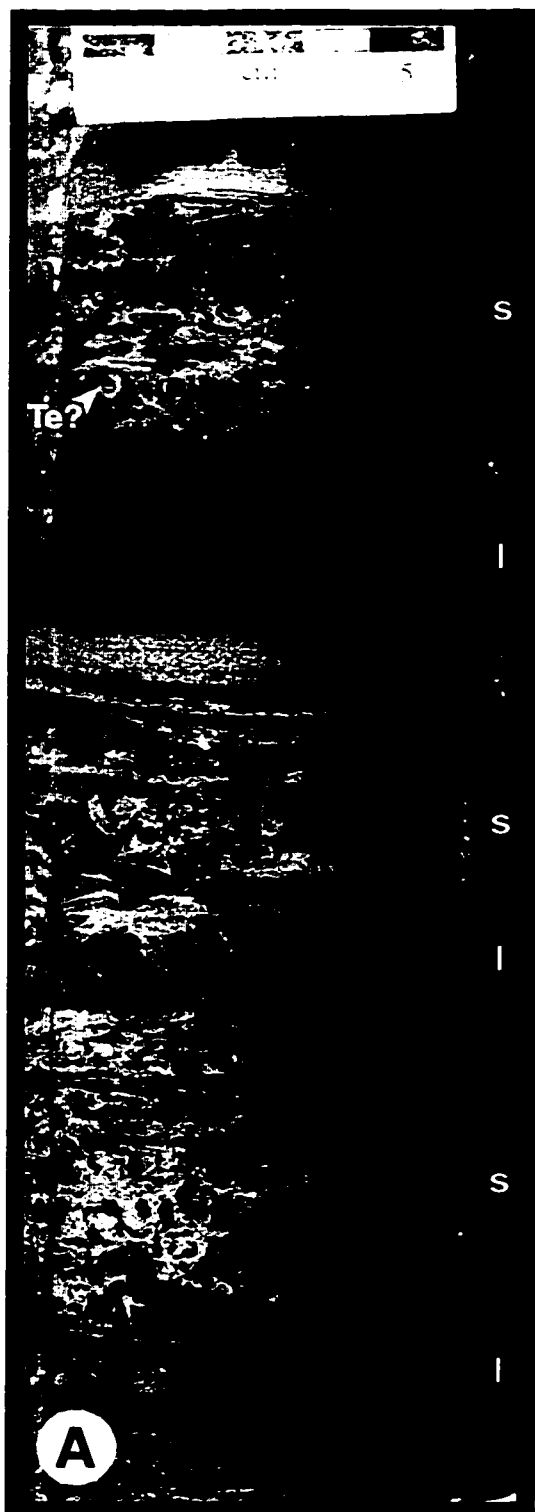
### **Facies N: 'Lam-scram' sand or sand and silt**

**Sedimentological characteristics:** facies N (Fig. 3.35) consists of medium brown very fine to fine grained sand (<0.25 mm), locally incorporating up to 40% light brown or tan silt. It is characterized by a distinct alternation of finely laminated to scrambled layers ('lam-scram' bedding). Accumulations of facies N range up to approximately three meters.

Individual beds of this facies are typically 5-20 cm thick. Laminated layers are sandy and exhibit well-developed low angle to plane parallel lamination. These are slightly curved, locally. Scrambled layers, which commonly incorporate silt, are mottled and do not contain identifiable laminations or sedimentary structures. Laminated layers typically exhibit a sharp to erosive base. Scrambled layers typically exhibit a sharp, irregular base when silt content is elevated. Where silt content is minimal, the base of scrambled layers is somewhat diffuse.

**Ichnological characteristics:** laminated layers do not exhibit any ichnofossils or bioturbate textures. Scrambled layers are characterized by an abundant to pervasive bioturbate texture and contain few discernible traces. However, individual *Lingulichnus*, *Planolites*, *?Palaeophycus*, *Skolithos* and possible *Teichichnus* were identified, locally.

**Interpretation and discussion:** Laminated-to-scrambled bedding requires alternating conditions of rapid, high-energy sedimentation and relatively stable lower-energy sedimentation. Each bed is initially deposited as a laminated body of sediment, commonly with curved laminae that are suggestive of HCS or SCS bedding. After deposition, the upper portion of the bed is thoroughly reworked by colonizing, opportunistic organisms, typically producing an abundant to pervasive bioturbate texture. Most occurrences of 'lam-scram' bedding are associated with tempestites (e.g. Bromley 1990, Pemberton *et al.* 1992b, MacEachern 1994).



**Fig. 3.35 Facies N.**

(A) Several successions of laminated [l] and 'scrambled' [s] layers. Each couplet of a lower laminated unit and upper scrambled unit comprises a single 'lam-scram' bed. Note that the transition from a scrambled layer to an overlying laminated bed is invariably sharp, abrupt, and commonly truncates underlying structures. Identifiable burrows within the 'scrambled' sediments are very rare; one possible *Teichichnus* [Te?] is distinguishable. From well 1-11-65-21w5, ~6088' (~1856 m). (B) A second example from well 3-24-62-20w5 (6900' (2103 m)), a short distance above the HCS bed in Fig. 3.27 (A). The laminated unit in the middle of this photograph, with curved laminae that thin upwards, may also be ----->



(Fig. 3.35 cont.) HCS-bedded. Few distinct burrows are visible in the scrambled unit at the top, but appears to have been predominantly by horizontal burrowers; this is in contrast with the predominantly vertical burrows that characterize most of the ichnofossil occurrences in this study.

Facies N exhibits clear 'lam-scram' style layering, and planar to curved lamination in the lower portion of each bed. Hence, Facies N is interpreted as an accumulation of intermittent storm-deposited beds.

#### **Facies O: Upward-fining, interlaminated and interbedded silt and fg-mg sand**

**Sedimentological characteristics:** facies O consists of multiple, stacked interbeds of interlaminated, medium brown sand and light brown to tan-colored silt. Sands are fine (0.1-0.25 mm) to medium (0.25-0.5 mm) grained and commonly incorporate a minor (1-5%) coarser-grained (<0.5 mm) fraction. Individual beds are typically 5-20 cm thick, with a median of 6-10 cm. Upward fining is defined by thicker and more numerous silt laminae in the upper portion of beds. The basal, sandy portion of beds is typically structureless. Laminations in the upper silt-enriched portion are wavy-parallel to ripply. Facies O is associated with the anomalously coarse grained examples of facies E described previously.

The coarse grade of this facies is reflected in geophysical well logs by a strong leftward deflection of gamma ray logs, and a moderate leftward deflection of sonic and porosity logs. Within the study area, this facies and corresponding response are only observed in the extreme northwest (TWP 64-65, RNG 21w5), immediately subjacent to the sub-Jurassic unconformity. This geophysical response and stratigraphic level is very similar to, and could be mistaken for, that of the Bioclastic Facies Association. It has been mapped as part of the Coquinal Middle Dolomite Member (e.g. Davies *et al.* 1997, p. 247: their Fig. 1).

**Ichnological characteristics:** Ichnofossils observed in facies O include *Lingulichnus*, *Planolites*, *Palaeophycus*, *Skolithos* and ?*Teichichnus*. Bioturbate textures are common to abundant in the silty upper portion of facies O beds, but absent in the sandy lower portions.

**Interpretation and discussion:** the interpretation of facies O is identical in all respects to that of subfacies B2. The only distinguishing characteristic is the considerable incorporation of coarser sediment grades.

The importance of facies O is its stratigraphic lateral equivalence to the coquinal association, discussed in more detail in Chapter 4. It is relevant primarily because it supports the interpretation that the ambient depositional environment of the Lower Montney persisted into the time of the coquinal deposition despite a substantial elevation of ambient energy (and hence coarser sedimentation).

## CHAPTER 4: STRATIGRAPHIC RELATIONSHIPS AND PALAEOENVIRONMENT

### Part 1. Internal stratigraphic relationships

The establishment of a detailed stratigraphic model for the Montney Formation in the Kaybob/Kaybob South Area was not a primary goal of this study. The internal stratigraphy of the Montney is notoriously difficult to decipher using the primary tool of subsurface correlation, geophysical well logs. Most geologists simply schematize the internal stratigraphy in a general way (*e.g.* Gibson & Barclay 1989, their Figure 10.16a; Edwards *et al.* 1994, their Figures 16-7, 16-8). Although occasional sections are published that attempt to depict some internal features (*e.g.* Edwards *et al.* 1994, their Figure 16-4a), these are invariably tentative.

At the regional scale, application of sequence stratigraphic principles (*e.g.* Davies 1992, Davies *et al.* 1997, Edwards *et al.* 1994) has suggested the presence of 3 to 4 informal stratigraphic subdivisions in the Montney. A few wells in the deepest parts (RNG 21w5, TWPs 61-65) of the Kaybob/Kaybob South area suggest a similar stratigraphic pattern, but this quickly disintegrates when one tries to extend the interpreted surfaces into areas of thinner, laterally heterogeneous lithologies to the east.

Three lithological characteristics of the eastern Montney are responsible for these problems. Firstly, there is a lack of vertical lithological heterogeneity because of the very narrow, coarse silt to fine sand grain size fraction of most Montney sediments. This lack of contrasting lithologies reduces the resolution of gamma, resistivity, and spontaneous potential logs. The fine-scale interlamination of the sands and silts further degrades the resolution of these logs. A second problem is abundant pyritization of several Montney lithofacies. This alters rock density, degrading the usefulness of density-dependent porosity and sonic logs. Pyrite can also distort gamma ray responses because of incorporated elemental impurities. The third problem, more important in subcrop-edge proximal areas than elsewhere in the Montney, is an abundance of lateral and vertical facies changes, many of which are gradational. Three sample wells from this study area, depicting some of the problems with identification of surfaces, are illustrated in Figs. 4.1 to 4.3.

The main consequence of these characteristics is a considerably reduced degree of certainty in correlations. It is possible to construct short cross sections through closely spaced wells with good core control, particularly where bioclastic

**Fig. 4.1. Problems in Montney correlation: well 11-28-62-19w5.**

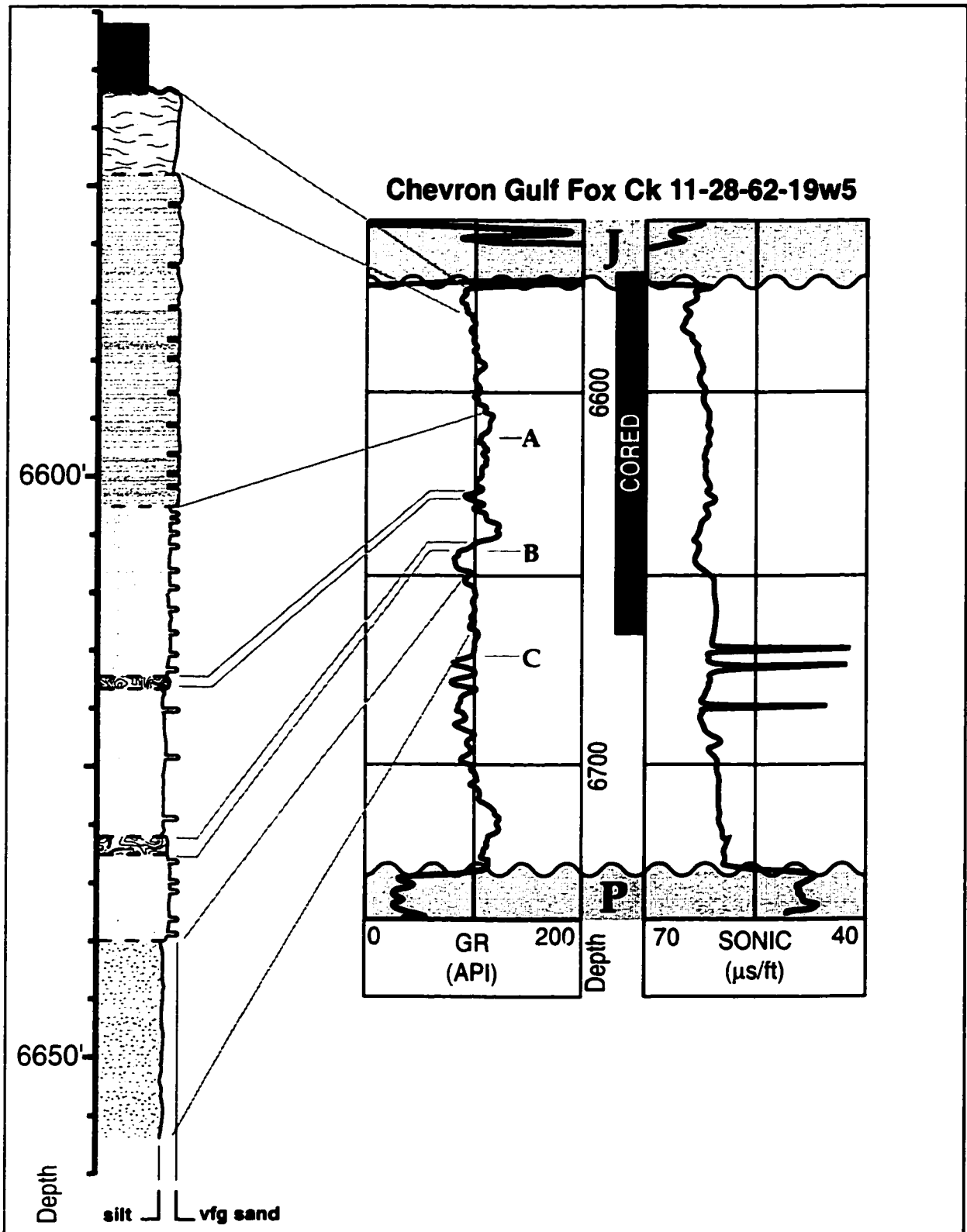
Well 11-28-62-19w5 represents a typical well from the thinner accumulations of the Montney in the east of the study area. It depicts two prominent features of the CA1 assemblage: the full succession of facies A to C is developed and the contacts between facies are all gradational. In this particular well, even the two deformed (facies D) beds exhibit gradational contacts with both overlying and underlying lithofacies. Note also the overall coarsening up trend, from facies A at the base, through several intercalations of facies B/subfacies B1, up into subfacies B2 and finally capped by facies C.

Some of the correlation problems within the Montney are also expressed in this well. Two relative gamma highs occur at points A and B. The gamma spike is particularly strong at B, and reinforced by an abrupt change in the sonic log at the same horizon. Both appear to form the base of log responses which flare upward, consistent with a coarsening-upward lithology

Without reference to the actual core, both of these points would commonly be interpreted as sequence stratigraphic surfaces, most likely the base of parasequences. However, examination of the core clearly shows that the major response at B is no more than a rapid transition from facies B towards its silt-dominated subfacies B1. The supposed surface at A has even less expression in the core, occurring within a uniform and uninterrupted facies B unit.

C denotes a possible true base of this succession, but this cannot be assured since there is no equivalent core.


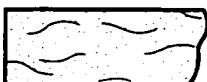


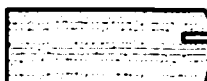

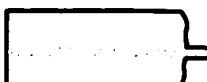
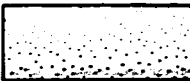



See Fig. 4.2. caption for a key to the lithological strip log

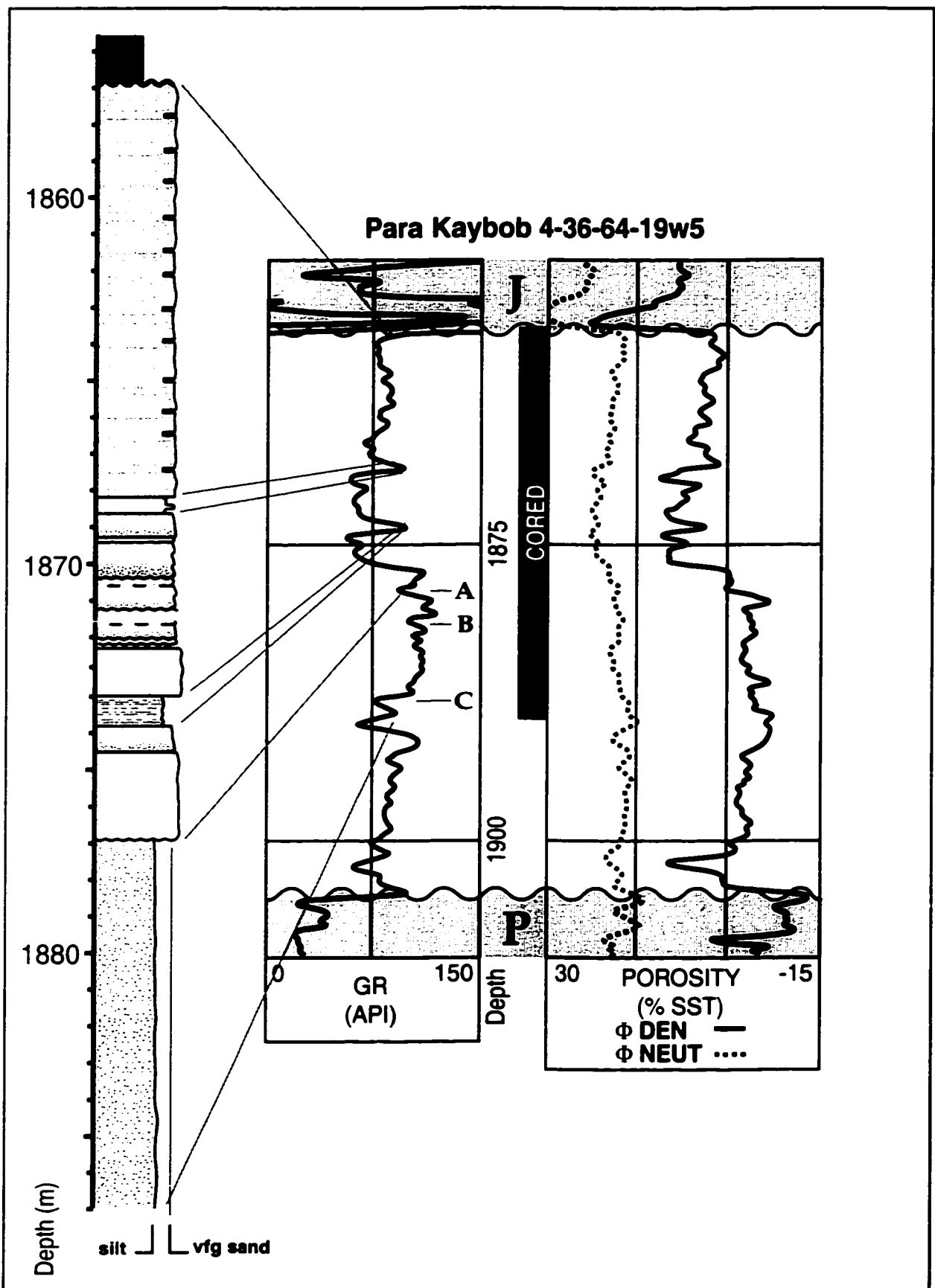


**Fig. 4.2. Problems in Montney correlation: well 4-36-64-19w5**

This well penetrates the high-porosity, low-gamma sand unit mapped in the northeast portion of this study area. Note how the sand body comprises mostly facies E and F, and that subfacies B2 predominates in the tapering gamma response above 1870 m. Three apparently prominent surfaces in the well, at A, B and C do not show at all within the core. The horizons marked by these 'surfaces' occur within the bottom succession of facies A. Within these sediments, no corresponding hiatus or even erosive truncation of laminae is observed. Pyrite was relatively abundant within facies A around the level of the letter C. and may have contributed to the sharp deflection of the gamma curve over this interval.

Key for lithological strip logs in Figs 4.1 to 4.3

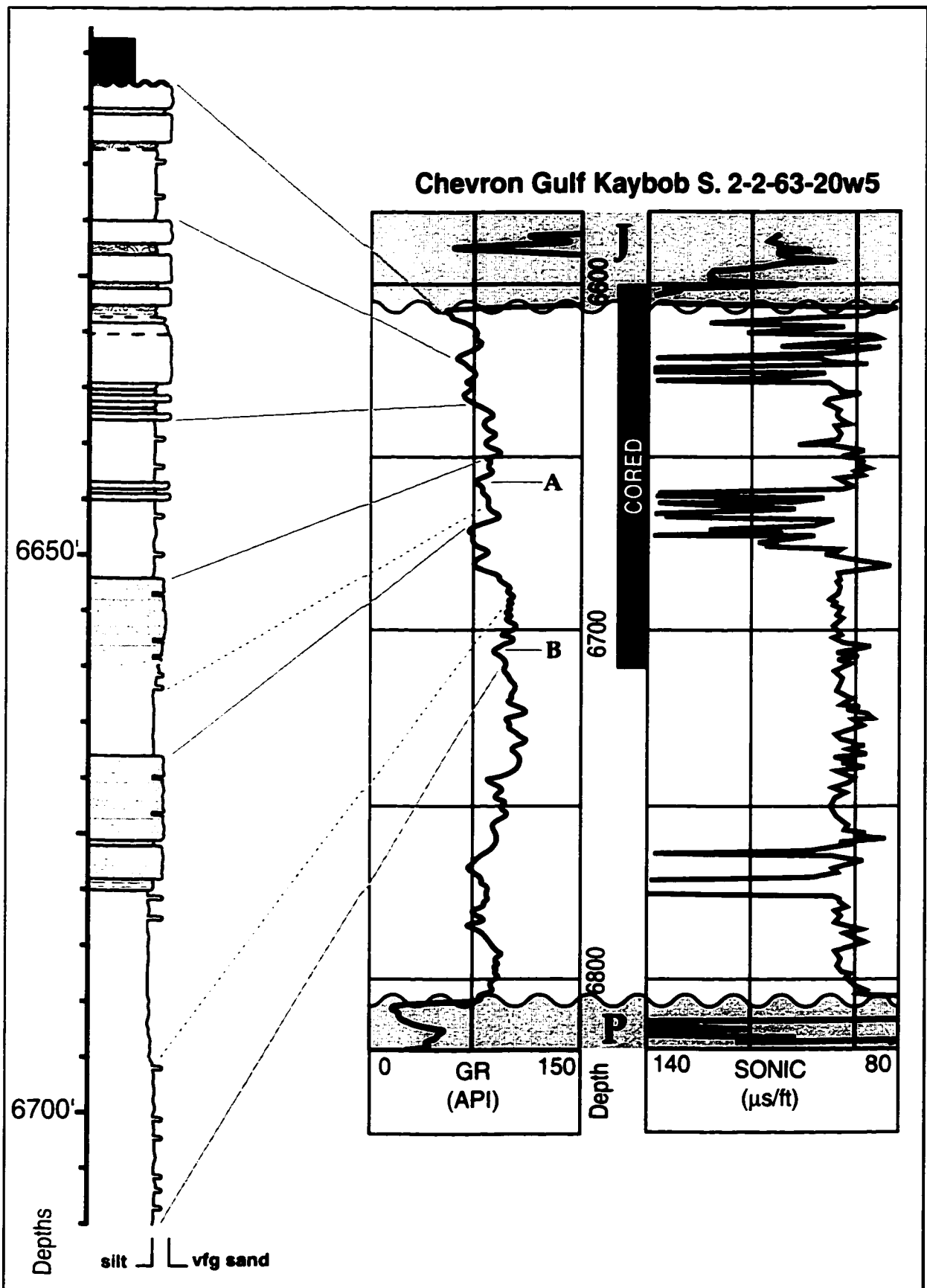
LITHOLOGY		CONTACTS
<b>CA 2</b>	<b>CA 1</b>	
 Facies D	 Facies C	 erosive
 Facies G	 Subfacies B2	sharp
 Facies E	 Subfacies B1/ non-B2 Facies B	gradational
 Facies F	 Facies A	
 Organic Shale (Jurassic)		 unconformity



**Fig. 4.3 Problems in Montney correlation: well 2-2-63-20w5**

This final example shows some of the acute problems encountered in sonic logs as well as gamma ray logs. Note the fairly abrupt gamma deflection at A, and then examine the corresponding sonic response. The sonic log suggests a zone of exceptional porosity, which is simply not the case. The elevated porosity zone is actually an accumulation of silt-dominated subfacies B1. Point B on the gamma curve shows yet another example of a supposed surface with poor core analogues. In this particular case however, it occurs approximately at the location where a facies B deposit undergoes a transition to silt-dominated B1. No surface or hiatus is evident.





lithologies provide a distinctive geophysical response that contrasts with adjacent siliciclastics (*e.g.* Figs. 4.5, 4.6). However, attempts to extend these sections laterally generally fail, becoming lost in areas of low lithological contrast.

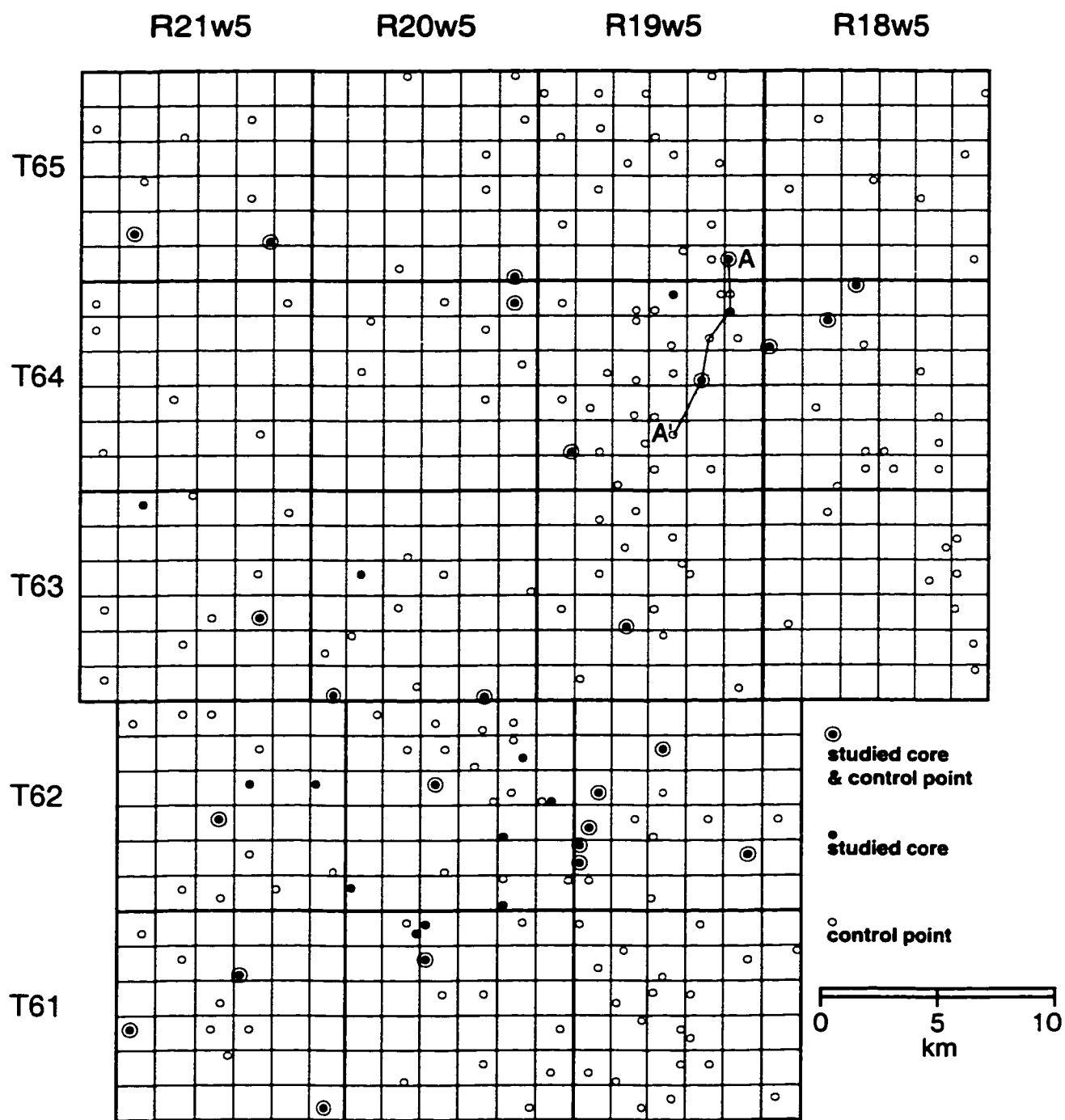
Despite these problems, two units of importance to the palaeoenvironmental interpretation in this area are readily mappable. Both of these units are laterally restricted and cut erosively across preexisting lithologies. The first of these mappable units is the accumulated Bioclastic Association (Figs. 4.5 and 4.6). This unit in particular tends to exhibit elongate and apparently sinuous thickness trends in the southwest (TWP 61-62, RGE 20-21). The second mappable unit (Figs. 4.7 and 4.8) is the low-gamma, high-porosity, sandy succession found in the northwest (TWP 64-65, RGE 18-19w5). The porous sandy unit exhibits a distinct, upward-tapering log response (Fig. 4.7) consistent with a fining-upward succession. Both of these units, based on their internal features and overall morphology, are interpreted as channel-constrained deposits.

## **Part 2. Lateral relationship of CA2 lithologies and the Bioclastic Association.**

### **Evidence for lateral equivalence**

An unexpected development of this localized study was an apparently lateral and gradational facies transition from the Bioclastic Association to more basinward clastic deposits. This was unexpected because the coquinal units have commonly been described in recent literature as hiatal deposits, emplaced subsequent to, and independently of, the underlying siliciclastics (*e.g.* Podruski *et al.* 1988, Gibson & Barclay 1989, Edwards *et al.* 1994, Davies *et al.* 1997). In the east, particularly where the Bioclastic Association is thickest in the southwest corner of TWP 62-19w5 (map, Fig. 4.4), the base of the BFA is indeed sharp and apparently erosive. To the west, however, the sharply defined base disappears. In core, apparently 'coquinal' successions of well logs may contain, or be predominated by, significant amounts of siliciclastics that are indistinguishable from CA2.

This feature is developed most obviously in wells of TWP 64-65, RGE 21w5. In this area, a 10-30 foot (3-9 m) zone of low-gamma and locally high porosity characterizes well-log responses immediately below the sub-Jurassic unconformity. This horizon is laterally equivalent to the main bioclastic accumulation in the south of the study area, and commonly mapped as part of the 'Coquinal Middle Dolomite' (*e.g.* Davies *et al.* 1997, their Fig. 1). Two cores from this horizon observed during



**Fig. 4.4 Core location map.**

This map indicates the distribution of well-control in this study. 'Studied core' are wells which included a core examined and logged by this author. 'Control point' indicates a well whose geophysical logs were studied, in order to map the Permian surface and the two mappable units in the text. Numerous attempts to correlate between these and cored wells failed for the reasons described in the text. The section marked at A-A' is depicted in Fig. 4.7.

**Fig. 4.5 Isopach map of the Bioclastic Association**

This map includes data from wells where siliciclastics were clearly adjacent to or interclated with bioclastic accumulations. The contour interval is 10 ft. (~3 m) This non - metric measure was more practical because most wells in the study area are older, with units in feet. Note the coloration scheme for the contour intervals.

The most prominent characteristics of this map are the NW-SE trending depositional axis of the BFA, and the distinctive, somewhat sinuous E-W or NE-SW trending isopach thicks in the south. Note also that the thickest coquinal mass, in 61-19w5 is somewhat lobate or crescentic in shape. These are interpreted as potential evidence for a contemporaneous barrier-bar system, with tidal inlet channels and tidal deltas.

B-B' is the section in figure 4.6.

R22W5

R21W5

R20W5

R19W5

R18W5



T65

T64

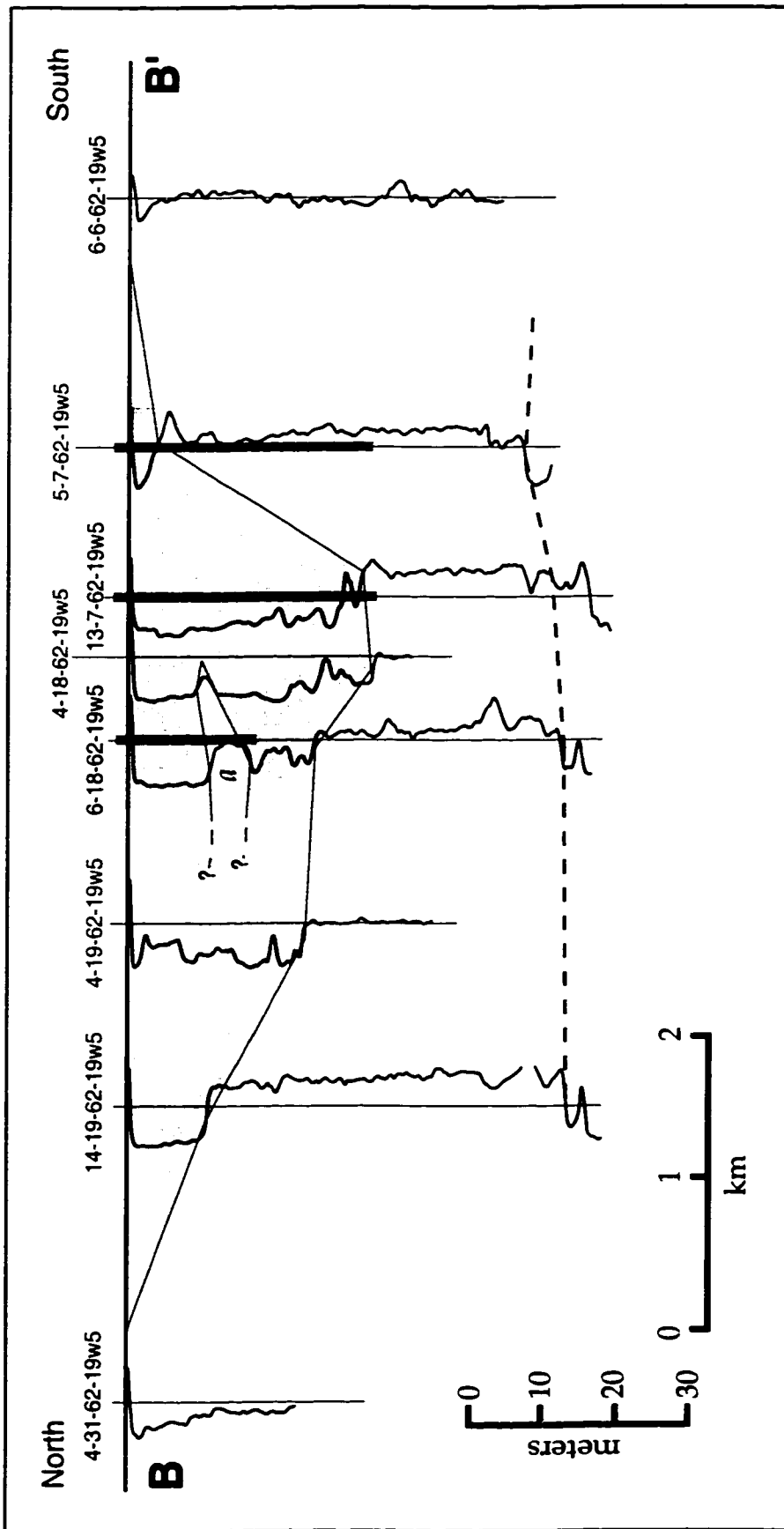
T63

T62

T61

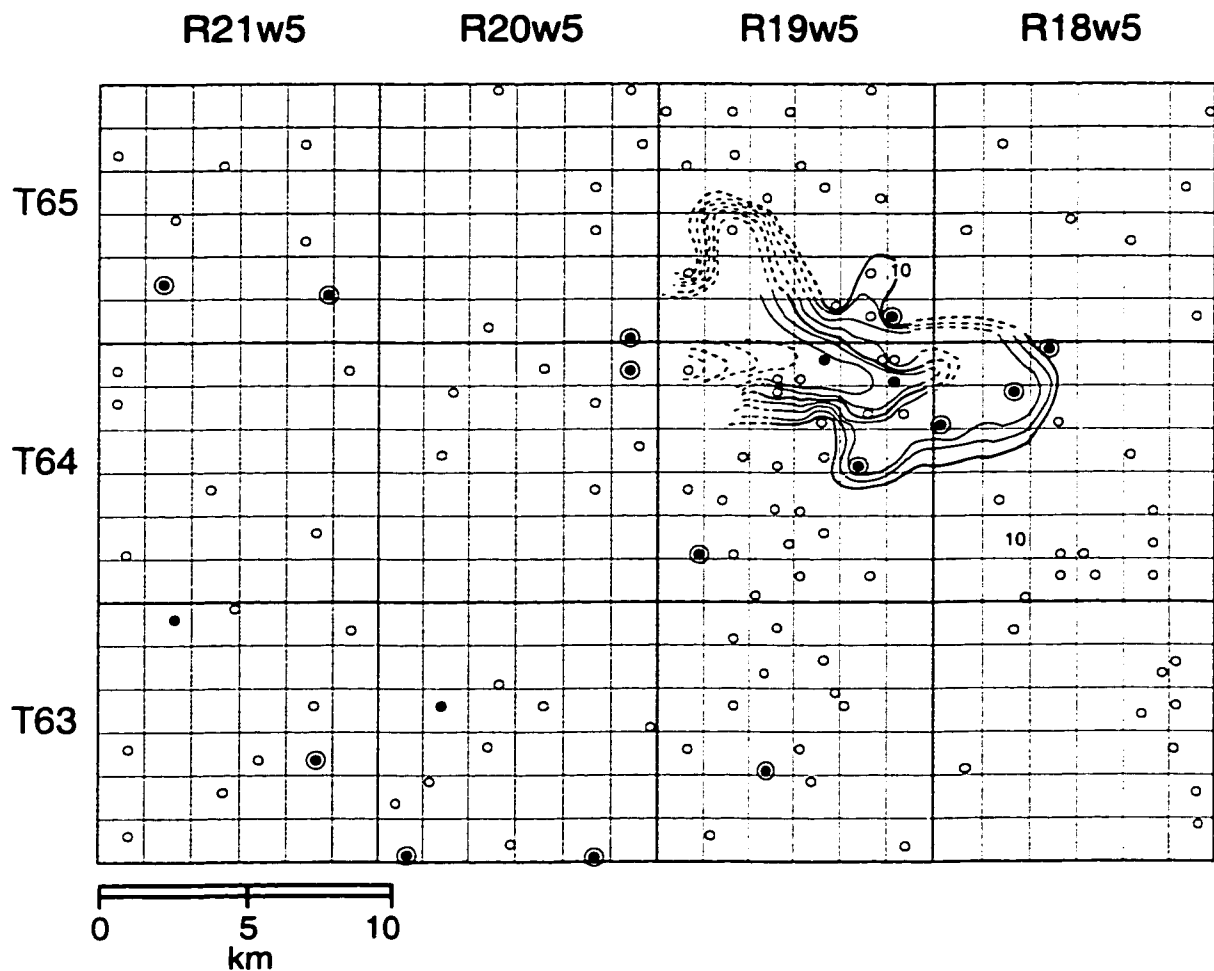
5 km

<b>LEGEND:</b>	<b>SHADED CONTOUR INTERVALS:</b>	
	0-10' (0-3 m)	30-50' (10.5-15 m)
o = control point	10-30' (3-10.5 m)	50'+ (15 m+)



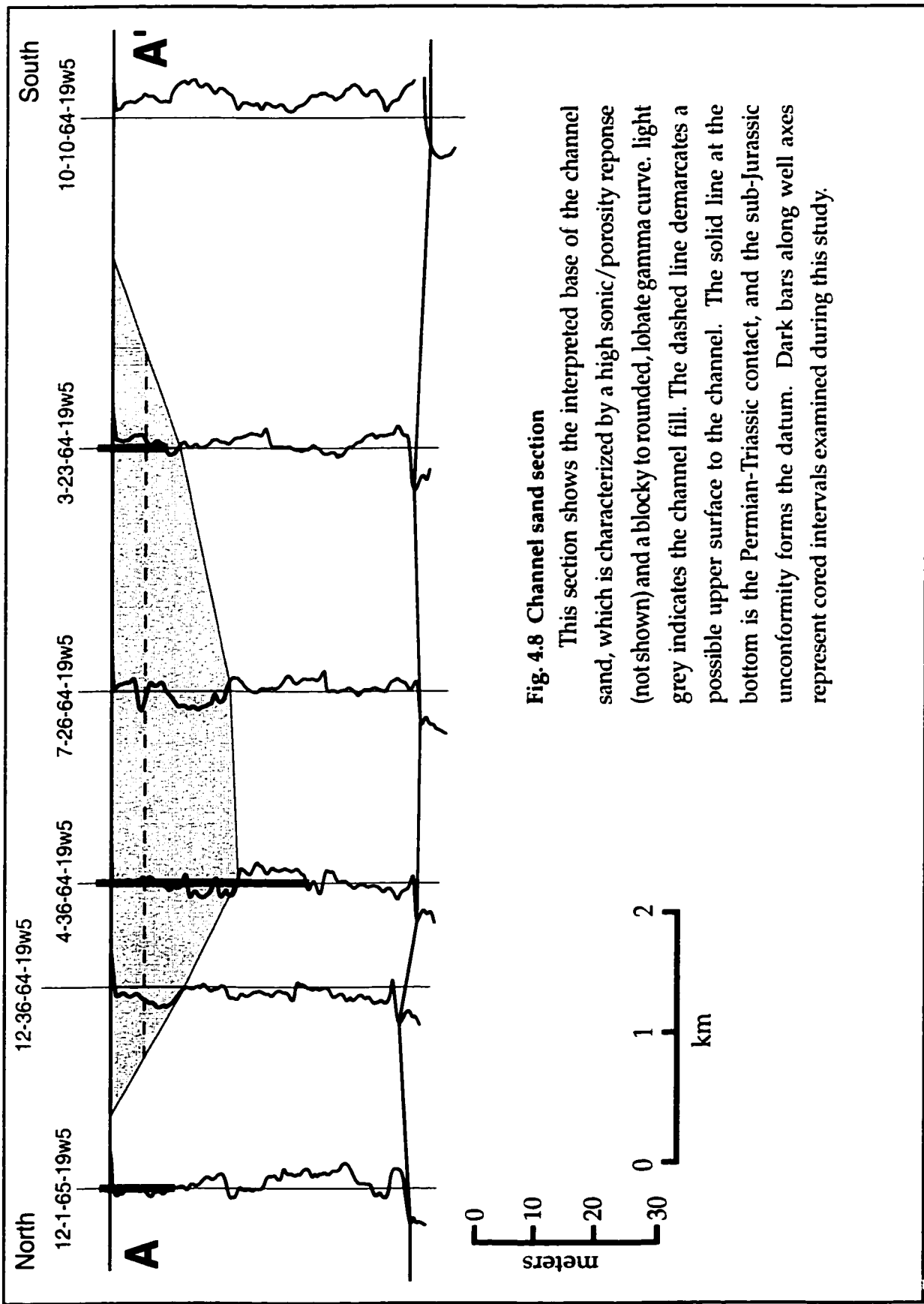
**Fig. 4.6 Coquina cross section**

This cross-section depicts the rationale used in mapping the base of the bioclastic association. Light grey areas are bioclastic. The thick dashed line at the base of the section is the Permian-Triassic unconformity. The sub-Jurassic unconformity forms the datum. The bioclastic association in this area is normally described by abrupt decrease in gamma curves as depicted. Note that the thicknesses in 4-18-62-19 and 13-7-62-19 are exceptional; these occur in the thickest part of the coquina assemblage. Dark bars along well axes represent cored intervals examined during this study. [a] is a siliciclastic accumulation within the coquina.



**Fig. 4.7 Depth to base of the sand unit.**

This map depicts the base of the mappable sand unit. Although less distinct than for the BFA in Fig. 3.5, this deposit is also elongate along a shoreline-perpendicular axis and laterally restricted. It is interpreted as a channel deposit, possibly a subaqueous tidal channel or a distributary. Sedimentary structures in this unit showed excellent preservation, particularly for subfacies B2. Contour interval is 10 feet here as well, for the same reason as Fig. 3.5. An anomalous sand body occurs deep within well 7-31-64-19w5, significantly below the horizon of the channels deposits in well 4-36-64-19w5 (Fig. 3.2). It is not clear if the unit in 7-31 represents an earlier channel or correlates to this one, hence the dotted lines indicating a tentative interpretation.



**Fig. 4.8 Channel sand section**

This section shows the interpreted base of the channel sand, which is characterized by a high sonic/porosity response (not shown) and a blocky to rounded, lobate gamma curve. light grey indicates the channel fill. The dashed line demarcates a possible upper surface to the channel. The solid line at the bottom is the Permian-Triassic contact, and the sub-Jurassic unconformity forms the datum. Dark bars along well axes represent cored intervals examined during this study.



the course of this study, however, were entirely siliciclastic in composition (1-11-65-21w5, 6077-6127' [1852-1868 m], and 6-8-65-21w5, 6267-6344' [1910-1934 m]), containing facies G, a coarse-grained variant of facies E, and facies N and O. Conversely, in a neighboring well (6-35-64-21w5) this horizon is characterized by porous coquina (*cf.* Davies *et al.* 1997, their Fig. 20(C)). Nothing distinguishes these units on well logs. Except for facies N, the siliciclastics in these wells are similar to facies of the Lower Montney. They are, however, characterized by elevated energy levels, expressed in the increased grain size of facies O with respect to facies B, and in the tempestite origin of facies E and N (Chapter 3). These energy levels, however, would be consistent with the conditions necessary for deposition of the coarse Bioclastic Association.

To the southwest (TWP 61-62, RNG 19-21w5), in the main coquinal depocentre of the study area, the relationship between the BFA and adjacent siliciclastics is expressed more subtly. In these areas, there is a progressive increase in apparent intercalation of siliciclastic and bioclastic facies west of the 19w5 range line. These intercalated siliciclastic horizons are most commonly characterized by facies of CA2. Locally, facies interpreted to have originated in higher-energy CA1 settings (*i.e.* facies C and subfacies B2) are also incorporated.

### **Part 3. Palaeoenvironmental interpretation of the Kaybob/Kaybob South area**

#### **Clastic Association One: review and comments**

The fine lamination and gradational interrelationship of CA1 facies, indicative of relatively quiet deposition, and volumetric predominance of CA1 within the preserved succession of this study area, suggest that this facies assemblage represents the ambient, 'normal' mode of Lower Montney deposition.

The gradational interrelationship and close genetic affinity of CA1 facies is clearly expressed in well 11-28-62-19w5 (Fig. 4.1). In this example, almost 90 feet (27.5 m) of core, comprising over half the total preserved Montney in the well, represent one continuous gradational succession from A to C. The only interruptions are two thin convolute beds of facies D at 6623' (2019 m) and 6636' (2023 m) enclosing a package of subfacies B1 sediments, and even these exhibit gradational contacts with adjacent units.

Based on sedimentology and ichnology (Chapter 3), the depositional setting of the constituent CA1 facies may be narrowed down to two possibilities. In the

first case, CA1 represents the offshore transition through shoreface of a (dysaerobic) clastic tidal shoreline. In the second case, CA1 represents the prodelta to upper delta front of a tidally influenced delta.

The following key sedimentological characteristics of CA1 may be extrapolated from its facies. Firstly, sedimentation was episodic to seasonal, producing the rhythmic appearance of facies B. Within this episodic context, deposition was nonetheless relatively quiet, resulting in fine interlamination of silt and sand in all CA1 facies. A tidal influence on sedimentation was significant, indicated by abundant tidal-associated sedimentary structures in facies B and C. The setting was highly salinity- and oxygen-stressed, expressed by a low-diversity assemblage of mostly diminutive ichnofossils and an abundance of pyrite. Sedimentation rates were relatively high locally, indicated by vertical adjustment of burrows, and common intercalation of thin, loaded and deformed (facies D) or dewatered (facies G) beds.

#### **Clastic Association Two: review and comments**

The key lithologic elements of CA2 are event deposited beds (facies E, storm beds, and facies F, sediment gravity flow deposits) and related alterations of preexisting material such as deformation (facies D) and dewatering (facies G and some facies H). This assemblage is developed in two differing depositional contexts. In the first case, it occurs as single or repeated, relatively short (decimeter scale) successions within CA1. The second context is as relatively thick (scale of several meters) successions with minor intercalated beds of CA1 affiliation. This latter expression of CA2 is typical of siliciclastic successions that are stratigraphically equivalent to, and probably coeval with, the Bioclastic Association (Part 2, above).

In the first case, CA2 represents short-term perturbations of the CA1 environment, induced by storms and/or autocyclic variations within the CA1 depositional regime. In the latter case, where CA2 predominates, it seems likely that conditions favouring CA2 sedimentation became dominant, representing a shift to (open sea?) storm-dominated deposition from earlier, restricted CA1 environments.

#### **Bioclastic Association: review and comments**

As indicated in Chapter 3 and Part 1 of this chapter, the Bioclastic Association represents a laterally restricted, locally discordant body of sediments, interpreted as channel-fill deposits. Most of the components of a marginal marine channel system

seem to be present. Facies J, with its coarser bioclasts and rarely articulated individuals, represents minimally transported channel lag deposits. Facies K, characterized by intercalated sand and mesoscale 'channel fill' cross bedding represents tidal deltas or washover fans. Characteristically regular alternation of fine sand and coarse bioclasts in facies K favours a tidal delta interpretation. Facies L represents beds produced by alternation of storm and quiescent deposition. Facies M represents subaerially exposed and eroded beds of facies L. Deposits of facies I are also episodic in nature, characterized by a mix of apparently structureless and low-angle laminated beds. Furthermore, facies I represents the primary mode of bioclastic deposition, serving as the background for intercalation of other bioclastic facies.

### **Ambient (CA1) palaeoenvironment: discussion**

The fundamental issue regarding the Lower Montney Formation sediments in this area is whether they were deposited in a tide-dominated shoreface or deltaic-tidal context. The evidence for both interpretations is present, but not quite sufficient for an unequivocal interpretation. However, after prolonged consideration, this author favours a deltaic or deltaic-proximal setting.

Firstly, the importance of facies B cannot be understated. This facies represents the bulk of CA1 sedimentation in the study area. As was discussed earlier in the interpretation of this facies, a seasonal effect is the only explanation for facies B rhythmicity that is consistent with the sedimentological and ichnological data. The only medium through which this seasonal rhythmicity could have been effected, considering the arid continental setting of the time, seems to have been fluvial. This, in and of itself, would strongly suggest a deltaic setting, but is by no means conclusive. It can be argued that the fluvial influence on the Kaybob/Kaybob South area was spatially remote, and was expressed locally only through its control of sediment available for transport by longshore currents or tidal circulation. Hence, other lines of reasoning must be invoked in favour of a genuinely deltaic setting.

One of the strongest arguments is the clear physical and environmental gradient expressed throughout the whole of the CA1 assemblage. Physically, there is a distinct but gradual shift in depth, average grain size, and energy levels from facies A through to facies C. Environmentally, there are the interpreted robust gradients in oxygenation, salinity, and food supply that produced the distinctive ichnological characteristics of these facies. For these gradients to be so strongly expressed, it seems unlikely that their source was at a significant distance.

A second line of reasoning is the distinctive and exceptional predominance of *Lingulichnus*. The Lingulid brachiopods that produce *Lingulichnus*, as discussed in Chapter 2 and in the interpretation of facies B, are known to favour shallow subtidal settings. They are particularly well adapted to such settings that are further characterized by strong and regular freshwater influx. The ability of Lingulids to tolerate extreme salinity fluctuation is key to their success in such habitats, because most of their more advanced and specialized competitors are unable to deal with such conditions. The abundance of *Lingulichnus* in CA1 sediments is thus supportive of a proximity to a substantial, episodic source of fresh water.

A third, somewhat anecdotal, line of evidence is apparent restriction of the Lower Montney CA1 environment. Firstly, there is the abundance of pyrite in CA1 facies. Although this is in part attributed to the global anoxic event that characterized this time, this cannot fully explain the locally significant presence of pyrite in subfacies B2 and facies C; some geographic restriction of the environment must also be invoked. Secondly, there is the distinctly minimized presence of (CA2) storm or other high-energy deposits within most CA1 successions, which suggests some measure of sheltering from the open shelf and sea.

As discussed in Chapter 2, there is a lack of relief on the Permian rocks that regionally underlie the Montney and thus bedrock topography cannot explain the restricted setting of CA1. This requires some form of autochthonous restriction. In the absence of evidence for a seaward barrier island system, this leaves an estuary, or deltaic embayment or distributary, as the most likely cause of any restriction. Evidence for channelization (Figs. 4.6 and 4.7) and a lack of evidence for brackish conditions, tend to favour a distributary/embayment setting over an estuarine interpretation.

A fourth line of evidence is provided by the very thick accumulations of deformed, slumped, and synsedimentary-faulted facies D deposits which occur locally within CA1 successions and independent of other CA2 facies (except G). As discussed in the interpretation of facies D, such successions are most commonly related to elevated sedimentation rates and gradients. In shallow water settings, this is most typical of a delta front.

Thus, deposition of CA1 in the more distal, subaqueous portion of a tidally influenced delta is interpreted for the CA1 succession. In this context, the deltaic interpretations of CA1 facies apply (Chapter 3). Facies A therefore represents prodelta deposits. Facies B was deposited on the lower delta front; subfacies B1 represents a distal bar setting and subfacies B2 was deposited on the distal portions

of distributary mouth bars. Facies C is interpreted as upper mouth bar to subaqueous levee deposits. The occasional subaerial exposure of these settings in modern deltas (e.g. Reineck & Singh 1980, Reading & Collinson 1996) would be consistent with the localized redbed appearance of facies C.

The absence of classical 'tide-dominated delta' morphology, characterized by longitudinal bars, tidal sand ridges, and a distinctive 'funnel-shape' is not critical. It may simply indicate that the scale of the tide-dominated delta is far beyond that of the study area. However, it is more likely due to the interpreted seasonal-episodic nature of the delta. A partial modern analogue, the MacArthur River delta of northern Australia (described by Woodroffe & Chappell 1993) is a seasonal delta with flow varying from zero to more than  $3200 \text{ m}^3\text{s}^{-1}$ . Between discharge episodes, it is subject to significant tidal reworking, but does not adopt any of the classical, tide-dominated deltaic morphologies. Rather, it is an elongate crescent-shaped body. Abandoned distributaries on this delta effectively become elongate tidal channels, which are infilled by sediments exhibiting well-preserved 'tidal' structures, such as herringbone cross-lamination and flasers (Woodroffe & Chappell op. cit.). This is perhaps an analogue for the porous, channelized sand in the northwest of the Kaybob/Kaybob South area (Figs. 4.6. and 4.7) which also contained the best-preserved examples of subfacies B2.

### **CA2 and the Bioclastic Association: interpretation**

As discussed above, the sediments of CA2 and the BFA are considered integral parts of the Lower Montney depositional system. Thin intercalations of CA2 facies in the CA1 setting are most likely due to occasional storm events that were able to overcome the normal sheltering of the CA1 environment. The thickest CA2 incorporations into CA1 occur in the channelized sand of the northwest. Thus, they may also represent episodic, high-energy autocyclic changes (e.g. distributary avulsions, crevasse splays) that had an effect similar to that of storms (erosion, rapid deposition, and overloading of earlier sediments) in subaqueous areas.

However, the thicker CA2 assemblages and potentially related coquinas require a different explanation. The coquinal isopach in Fig. 4.4 suggests an overall northwest-southeast axis for the Bioclastic Association and related siliciclastics. This is in fact parallel to the presumed Montney palaeoshoreline. Furthermore, the isopach thicks in these units trend east-west, or northeast-southwest, perpendicular to the overall depositional axis and to the palaeoshoreline. Combined with the fact that these deposits are composed primarily of hashed bioclastics and storm-derived

siliciclastics, it seems reasonable to interpret these units as a (mostly subaqueous) barrier-bar complex. The shoreline-perpendicular isopach thicks would thus represent major, semi-permanent tidal inlet channels; these served as the primary depocentre for the bioclastic lithologies. Thinner accumulations of coquina within dominantly CA2 successions would represent shorter-lived tidal inlets. Finally, the bulk of CA2 deposits at this stratigraphic level would represent the body of the barrier bars and adjacent, subaqueous storm beds.

The source of bioclastic material is problematic. A comparable suite of body fossils has not, as far as this author has been able to determine, been described from basinward portions of the Montney. This suggests that the bioclasts were derived from landward areas, perhaps winnowed from preexisting, more shore-proximal bioclastic deposits.

The high-energy, open shoreface setting needed to produce a barrier-bar-channel complex may have been coeval with the delta setting of CA1, but developed elsewhere in the Montney basin. Alternatively, it is possible that the shift to a high-energy shoreface was intimately tied to basin-wide changes accompanying the sea-level fall and lowstand generally interpreted for the time of coquinal deposition. It is unfortunately not clear which of these rationales best applies to the transformation of depositional regimes between the time of CA1-dominated deposition and CA2/BFA-dominated deposition.

### **Summary and depositional history: Kaybob/Kaybob South area**

A tidally influenced, deltaic setting, defined by Clastic Association One, has been interpreted for the lower portion of the Lower Montney sediments in this study area. This deltaic environment was characterized by highly seasonal or episodic deposition that produced the near-rhythmic appearance of most CA1 beds. A minimized presence of high-energy (CA2 or BFA) sediments in this succession is interpreted to indicate deposition under relatively sheltered conditions, away from the open shelf.

After an unknown amount of time, a less sheltered setting developed, characterized by a shift to the highest-energy CA1 facies (B2 and C) and dominated by storm-influenced sediments of CA2 and the Bioclastic Association, and locally characterized by a probable barrier-bar complex. It is not clear whether this shift was accomplished as a natural succession of laterally coexistent environments, or represents a fundamental change in basin parameters that accompanied the 3<sup>rd</sup> order sea level lowstand associated with coquinal deposition in the literature.

## CHAPTER 5: SUMMARY AND CONCLUSIONS

### Introductory remarks

This study focused on the sedimentology and ichnology in a small, but economically significant area of the Montney Formation around the Kaybob and Kaybob South hydrocarbon pools. The primary goal of this effort was a detailed and accurate analysis of the Montney palaeoenvironment at a local scale, intended to complement and build upon recently published regional interpretations and discussions (*e.g.* Barclay & Gibson 1989, Gibson 1993, Edwards *et al.* 1994). It is also hoped this study will provide a foundation for further detailed examinations of this complex and enigmatic unit of the Western Canada Sedimentary Basin. The major observations and results of this study are summarized below.

### Sedimentology and Ichnology

In the Kaybob/Kaybob South area, three major facies associations characterize the Lower Montney Formation. Two (CA1 and CA2) are siliciclastic while the third is bioclastic (the BFA).

CA1 constitutes the bulk of the preserved Montney within the study area. This association comprises three facies (A, B, and C), characterized by thin interlamination of very fine sand and varying amounts of silt. Sedimentary structures in this association are indicative of relatively quiet deposition within an overall fluvial- and tidal-influenced setting, expressed most strongly in facies B. The ichnology of CA1 describes an impoverished *Skolithos* ichnofacies, characterized by a low diversity, locally high-abundance assemblage of simple dwelling traces. *Lingulichnus*, a burrow attributed to the inarticulate brachiopod *Lingula*, is particularly prominent.

CA2 occurs as discrete accumulations within CA1. Locally, CA2 predominates in the top 25-30% of the preserved Montney. CA2 comprises a heterogeneous association of five very different, but closely associated facies (D, E, F, G, and H). Two of these, facies E and F represent abruptly deposited sediments. Facies D, G, and H are penecontemporaneous alterations of preexisting lithologies that locally accompany emplacement of facies E and F but are also developed as independent accumulations.

The Bioclastic Association occurs as an accumulation of varying thickness at the topmost horizons of the preserved Montney in the south and west of the study area. The thickest accumulations of this association occur along its eastern margin,

where they locally exceed 100 feet (27 m) in thickness and are characterized by an erosive base and downcutting morphology. To the west, this association becomes less distinctive and intermingles with CA2-dominated successions. The BFA comprises 5 facies dominated by coarse sand to fine gravel sized bioclasts and interbedded siliciclastic material. Where present, sedimentary structures indicate deposition as channel fill and tidal delta sediments within a storm-influenced system.

Two additional clastic facies were described but not assigned to a facies association. Both are compositionally similar to CA1. Facies N comprises 'lam-scam' sediments of a tempestite origin. Facies O is comparable in most respects to subfacies B2, distinguished by incorporation of medium to coarse-grained sand. Both were observed from siliciclastic accumulations laterally equivalent to the BFA.

### **Internal Stratigraphy**

Internal stratigraphic relationships of the Montney Formation are not easily deciphered. Geophysical responses within the Montney are typically subdued or distorted, resulting in poor resolution and a low degree of certainty for correlations. Two locally mappable units are present, a high-porosity sand body in the northeast, and the BFA in the west and southwest. Both are laterally restricted and exhibit downcutting morphology, indicating deposition within channels.

The Bioclastic Association in the Kaybob/Kaybob South area appears to have a well-developed lateral association with accumulations of siliciclastic CA2, and anomalous facies N and O. This relationship is best expressed in the northwest of the study area. In this vicinity, facies E, N, and O exhibit a geophysical response indistinguishable from adjacent bioclastic deposits, and have commonly been mapped as such. In the south, thicker accumulations of CA2 appear to be interdigitated with BFA deposits at the same stratigraphic horizon.

### **Palaeoenvironmental framework**

Interpretations of individual facies are summarized in Table 3.1 and do not require repetition here.

The sediments of CA1 were deposited in one of two settings: a seasonally fluvial-influenced tidal clastic coastline, or a tidally influenced seasonal delta. Evidence that rules out one or the other absolutely is absent. However, the strong gradient in physical and biological parameters and the presence of abundant *Lingulichnus*, supported by evidence for channelization, autocyclic sheltering and restriction, and extensive slumping, are interpreted to favour a deltaic setting.



Expression of CA2 as thin accumulations within dominantly CA1 successions is interpreted as minor, storm or flood induced perturbations of the CA1 environment.

The BFA and laterally equivalent thicker expressions of CA2 were deposited in a storm-dominated setting, and represent elements of a barrier-bar system. Evidence favouring this interpretation includes: a palaeoshoreline-parallel depositional axis locally transected by shoreline-perpendicular isopach thicks, a channel or inlet depositional setting for most bioclastic facies, and the episodic deposition of several facies in both the BFA and CA2.

## CONCLUSIONS

1. The Lower Montney Formation in the Kaybob/Kaybob South area is mainly characterized by a tidally influenced seasonal deltaic setting.
2. The upper reaches of the Lower Montney in this area were characterized by a barrier-bar system comprising both bioclastic and siliciclastic components.
3. The Bioclastic Association exhibits a probable lateral equivalence to siliciclastic accumulations and was thus not deposited independently of the siliciclastics in subcrop-edge areas.
4. The ichnology of the Lower Montney Formation in the Kaybob/Kaybob South area is essential to successful interpretation of the palaeoenvironmental setting. In particular, the ichnofossil *Lingulichnus* provided an invaluable tool in the diagnosis of Lower Montney environmental parameters and gradients.

## REFERENCES

- Alway, R. H. S., and Moslow, T. F. 1997. *Sequence stratigraphy and depositional facies of an incised-valley fill, Lower Cretaceous Bluesky Formation, Aitken Creek Field, British Columbia*. IN: Pemberton, S. G., and James, D. P. (eds.) *Petroleum geology of the Cretaceous Mannville Group, Western Canada*, pp. 56-75.
- Armitage, J. H. 1962. *Triassic oil and gas occurrences in northeastern British Columbia, Canada*. *Journal of the Alberta Association of Petroleum Geologists* 10(2): 35-56.
- Barss, D. L., Best, D. W., and Meyers, N. 1964. *Chapter 9: Triassic*. IN: McCrossan, R. G., and Glaister, R. P. (eds.) *Geological history of western Canada*. Calgary, Alberta Association of Petroleum Geologists, pp. 113-136.
- Best, E. W. 1958. *The Triassic of the North Saskatchewan-Athabasca Rivers area*. IN: Hemphill, C. R. and Jennings, E. W. (eds.) *Nordegg*. Alberta Society of Petroleum Geologists (with Edmonton Geological Society) *Guidebook*, 5th annual field conference. pp. 39-49.
- Beynon, B. M., and Pemberton, S. G. 1992. *Ichnological signature of a brackish water deposit: an example from the Lower Cretaceous Grand Rapids Formation, Cold Lake Oil Sands area, Alberta*. IN: Pemberton, S. G. (ed.) *Applications of ichnology to petroleum exploration: a core workshop*. SEPM, Calgary, pp. 199-221.
- Bhattacharya, J. P., and Walker, R. G. 1992. *Deltas*. IN: Walker, R. G., and James, N. P. (eds.) *Facies Models*. Geological Association of Canada. pp. 157-177.
- Boersma, J. R. 1969. *Internal structure of some tidal mega-ripples on a shoal in the Westerschelde estuary, the Netherlands*. Report of a preliminary investigation. *Geologie en Mijnbouw* 48: 409-414.
- Boggs, S., Jr. 1995. *Principles of sedimentology and stratigraphy, 2<sup>nd</sup> Edition*. Prentice-Hall, Englewood, NJ. 774 pages.

- Bromley, R. G. 1990. *Trace fossils: biology and taphonomy*. Unwin-Hyman, London, 280 pages.
- Buatois, L. A., Mangano, G. M., and Maples, C. G. 1997. *The paradox of nonmarine ichnofauna in tidal rhythmites: integrating sedimentologic and ichnologic data from the Late Cretaceous of eastern Kansas, USA*. *Palaios* 12(5): 467-481.
- Coleman, J. M. 1981. *Deltas: processes and models of deposition for exploration*. Burgess, CEPCO Division, Minneapolis. 124 pages.
- Davies, G. R. 1994. Lower Triassic (Montney) stratigraphic framework, WCSB. IN: Moslow, T. F. and Davies, G. R. (eds.) *Turbidite facies field seminar: Triassic, Jurassic and Precambrian exposures, Front and Main Ranges and Foothills of the Banff and Jasper area*. Graham Davies Geological Consultants Ltd., Calgary, Alta., pp. 5•1 - 5•4.
- Davies, G. R. 1997a. *The Triassic of the Western Canada Sedimentary Basin: tectonic and stratigraphic framework, paleogeography, paleoclimate and biota*. *Bulletin of Canadian Petroleum Geology* 45(4): 434-460.
- Davies, G. R. 1997b. *Aeolian sedimentation and bypass, Triassic of western Canada*. *Bulletin of Canadian Petroleum Geology* 45(4): 624-642.
- Davies, G. R., Moslow, T. F., and Sherwin, M. D. 1997. *The Lower Triassic Montney Formation, west-central Alberta*. *Bulletin of Canadian Petroleum Geology* 45(4): 474-505.
- Dawson, G. M. 1881. *Report on an Exploration from Port Simpson on the Pacific Coast to Edmonton on the Saskatchewan, embracing a portion of the northern part of British Columbia and the Peace River Country*. Geological and Natural History Survey, Canada, Report of Progress, 1879-80, part B. 177 pages.
- Dawson, G. M. 1888. *Report on an Exploration in Yukon District, Northwest Territory, and adjacent portion of British Columbia*. Geological Survey of Canada Annual Report III(B): 183 pages.

- Dowling, D. B. 1907. *Report on the Cascade Coal Basin, Alberta*. Geological Survey of Canada, Sessional Paper 26b. 37 pages.
- Edwards, D. E., Barclay, J. E., Gibson, D. W., Kvill, G. E., and Halton, E. 1994. *Triassic strata of the Western Canada Sedimentary Basin*. IN: Mossop, G. D., and Shetsen, I. (comps.) Geological Atlas of the Western Canada Sedimentary Basin. Calgary, Canadian Society of Petroleum Geologists and Alberta Research Council, pp. 259-276.
- Emig, C. C. 1981. *Implications des données récentes sur les Lingules actuelles dans les interprétations paléoécologiques*. Lethaia 14(2): 151-156.
- Emig, C. C. 1982. *Terrier et position des Lingules (brachiopodes, inarticulés)*. Bulletin de la Société Géologique de France 107(2): 185-194.
- Emig, C. C. 1983. *Comportement expérimental de Lingula anatina (brachiopodes, inarticulés) dans divers substrats meubles (Baie de Mutsu, Japon)*. Marine Biology 75(2/3): 207-213.
- Emig, C. C. 1986. *Conditions de fossilisation du genre Lingula (Brachiopoda) et implications paléoécologiques*. Palaeogeography, Palaeoclimatology, Palaeoecology 53: 245-253.
- Emig, C. C. 1990. *Examples of post-mortality alteration in recent brachiopod shells and (paleo)ecological consequences*. Marine Biology 104: 233-238.
- Emig, C. C. 1997. *Ecology of inarticulated brachiopods*. IN: Kaesler, R. L. (ed.) Treatise on invertebrate paleontology, Part H, Brachiopoda (revised). Geological Society of America and University of Kansas, Boulder, Colorado and Lawrence, Kansas. pp. 473-496.
- Emig, C. C., Gall, J.-C., Pajaud, D., and Plaziat, J. C. 1978. *Réflexions critiques sur l'écologie et la systématique des Lingules actuelles et fossiles*. Geobios 11(5): 573-609.

- Ferguson, L. 1963. *The paleoecology of Lingula squamiformis Phillips during a Scottish Mississippian marine transgression*. *Journal of Paleontology* 37(3): 669-681.
- Frey, R. W., and Pemberton, S. G. 1985. *Biogenic structures in outcrops and cores. I. Approaches to ichnology*. *Bulletin of Canadian Petroleum Geology* 33: 72-115.
- Gibson, D. W. 1965. *Triassic stratigraphy near the northern boundary of Jasper National Park, Alberta*. Geological Survey of Canada Paper 64-9. 144 pages.
- Gibson, D. W. 1968. *Triassic stratigraphy between the Athabasca and Smoky Rivers of Alberta*. Geological Survey of Canada Paper 67-65. 114 pages.
- Gibson, D. W. 1971a. *Triassic stratigraphy of the Sikanni Chief River – Pine Pass region, Rocky Mountain Foothills, northeastern British Columbia*. Geological Survey of Canada Paper 70-31. 105 pages.
- Gibson, D. W. 1971b. *Triassic petrology of Athabasca-Smoky River region, Alberta*. Geological Survey of Canada Bulletin 194. 59 pages.
- Gibson, D. W. 1974. *Triassic rocks of the southern Canadian Rocky Mountains*. Geological Survey of Canada Bulletin 230. 65 pages.
- Gibson, D. W. 1975. *Triassic rocks of the Rocky Mountain Foothills and Front Ranges, northeastern British Columbia and west-central Alberta*. Geological Survey of Canada Bulletin 247. 61 pages.
- Gibson, D. W. 1993. *Triassic*. IN: Stott, D. L., and Aitken, J. D. (eds.) *Sedimentary cover of the craton in Canada*. Geological Survey of Canada, Ottawa, pp. 294-320.
- Gibson, D. W., and Barclay, J. E. 1989. *Middle Absaroka Sequence: the Triassic stable craton*. IN: Ricketts, B. D. (ed.), *Western Canada Sedimentary Basin, a case history*. CSPG, Calgary, AB, Canada, pp. 219-232.
- Gibson, D. W., and Edwards, D. E. 1990. *An overview of Triassic stratigraphy and depositional environments in the Rocky Mountain Foothills and Western Interior*

*Plains, Peace River Arch area, northeastern British Columbia. Bulletin of Canadian Petroleum Geology 38A: 146-158.*

Golonka, J., Ross, M. I., and Scotese, C. R. 1994. *Phanerozoic paleogeographic and paleoclimatic modeling maps*. IN: Embry, A. F., Beauchamp, B., and Glass, D. J. (eds.) *Pangea: Global environments and resources*, CSPG Memoir 17. CSPG, Calgary, AB, Canada. pp. 1-47

Hammen, C. S., Hanlon, D. P., and Lum, S. C. 1962. *Oxidative metabolism of Lingula. Comparative biochemistry and physiology 5: 185-192.*

Hammond, L. S. 1983. *Experimental studies of salinity tolerance, burrowing behaviour and pedicle regeneration in Lingula anatina (Brachiopoda, Inarticulata)*. *Journal of Paleontology 57: 1311-1316.*

Henderson, C. M. 1997. *Uppermost Permian conodonts and the Permian-Triassic boundary in the Western Canada Sedimentary Basin. Bulletin of Canadian Petroleum Geology 45(4): 693-707.*

Hunt, A. D., and Ratcliffe, J. D. 1959. *Triassic stratigraphy, Peace River area, Alberta and British Columbia, Canada. American Association of Petroleum Geologists, Bulletin 43(3): 563-589.*

Irish, E. J. W. 1951. *Pierre Greys Lakes map-area, Rocky Mountains of Alberta and British Columbia. Geological Survey of Canada Memoir 258. 66 pages.*

Irish, E. J. W. 1965. *Geology of the Rocky Mountain Foothills, Alberta (between latitudes 53°15' and 54°15')*. Geological Survey of Canada Memoir 334.

Johnson, H. D., and Baldwin, C. T. 1996. *Shallow clastic seas*. IN: Reading, H. G. (ed.) *Sedimentary environments: processes, facies and stratigraphy*. Blackwell Science Limited, Oxford. pp. 232-280.

Keswani, A. D. 1999. *An integrated ichnological perspective for carbonate diagenesis*. Unpublished M.Sc. thesis, University of Alberta. 125 pages.

Kindle, E. D. 1944. *Geological reconnaissance along Fort Nelson, Liard, and Beaver Rivers, northeastern British Columbia and southeastern Yukon*. Geological Survey of Canada Paper 44-16.

Kindle, E. D. 1946. *Appendix I. The Middle Triassic of Liard River, British Columbia*. IN: McLearn, F. H. 1946. *A Middle Triassic (Anisian) fauna in Halfway, Sikanni-Chief, and Tetsa valleys, northeastern British Columbia*. Geological Survey of Canada Paper 46-1. 23 pages.

Kindle, E. M. 1924. *Standard Palaeozoic section of Rocky Mountains near Banff, Alberta*. *Pan-American Geologist* 42(2): 113-124.

Klein, G. deV. 1977. *Clastic Tidal Facies*. Champaign, Illinois, Continuing Education Publication Company. 149 pages.

Krug, H. J., Brandstädter, H., and Jacob, K. H. 1993. *Morphological instabilities in pattern formation by precipitation and crystallization processes*. *Geologische Rundschau* 85(1): 19-28.

Lambe, L. M. 1916. *Ganoid fishes from near Banff, Alberta*. *Transactions, Royal Society of Canada, Series 3*. 10(IV): 35-44.

Liesegang, R. E. 1913. *Geologische Diffusionen*. Steinkopf, Dresden and Leipzig. 180 pages.

MacEachern, J. A. 199\_. TITLE. Unpublished Doctoral thesis, University of Alberta. NNN pages.

Manko, E. M. 1960. *The Triassic of the Rock Lake area*. Edmonton Geological Society Guidebook, 2<sup>nd</sup> annual field conference. pp. 25-42.

McConnell, R. G. 1887. *Report on the geological structure of the Rocky Mountains*. Geological Survey of Canada, Annual Report 1886, part D. 40 pages.

McConnell, R. G. 1891. *Report on an Exploration in the Yukon and MacKenzie Basins*,

- Northwest Territory*. Geological Survey of Canada, Annual Report IV(D): 163 pages.
- McLearn, F. H. 1939. *Some Neo-Triassic ammonoid faunas of the Peace River Foothills, B. C.* Canadian Field-Naturalist 53: 70-71.
- McLearn, F. H. 1945. *The Lower Triassic of the Liard River, British Columbia*. Geological Survey of Canada Paper 45-28. 6 pages.
- McLearn, F. H. 1946. *A Middle Triassic (Anisian) fauna in Halfway, Sikanni-Chief, and Tetsa valleys, northeastern British Columbia*. Geological Survey of Canada Paper 46-1. 23 pages.
- McLearn, F. H., and Kindle, E. D. 1950. *Geology of northeastern British Columbia*. Geological Survey of Canada, Memoir 259. 236 pages.
- Mederos, S. M. 1995. *Sedimentology and sequence stratigraphy of the Montney Formation in the Sturgeon Lake A and B pool*. Unpublished M.Sc. thesis, University of Alberta. 229 pages.
- Mederos, S. M., and Moslow, T. F. 1996. *Sedimentology and sequence stratigraphy of the Sturgeon Lake Field, Alberta*. AAPG Abstract, American Association of Petroleum Geologists, Bulletin 80(8): 1313-1314.
- Metherell, R. G. 1966. *Kaybob South Field*. IN: Century, J. R. (ed.) Oil Fields of Alberta Supplement. ASPG, Calgary, AB, Canada. pp. 58-59.
- Meyer, R. C. 1960. *Sturg. Lake South Field*. IN: White, R. J. (ed.) Oil Fields of Alberta. ASPG, Calgary, AB, Canada. pp. 196-197.
- Miall, A. D. 1976. *The Triassic sediments of Sturgeon Lake South and surrounding areas*. IN: Lerand, M. (ed.) The sedimentology of selected clastic oil and gas reservoirs in Alberta. Calgary, Canadian Association of Petroleum Geologists, pp. 25-43.
- Moslow, T. F., and Davies, G. R. 1994. Turbidite facies from the Montney Formation:



subsurface of west-central Alberta. IN: Moslow, T. F. and Davies, G. R. (eds.) *Turbidite facies field seminar: Triassic, Jurassic and Precambrian exposures, Front and Main Ranges and Foothills of the Banff and Jasper area*. Graham Davies Geological Consultants Ltd., Calgary, Alta, pp. 6•1 - 6•5.

Moslow, T. F., and Davies, G. R. 1997. *Turbidite reservoir facies in the Lower Triassic Montney Formation, west-central Alberta*. Bulletin of Canadian Petroleum Geology 45(4): 507-536.

Moslow, T. F., and Pemberton, S. G. 1988. *An integrated approach to the sedimentological analysis of some Lower Cretaceous shoreface and delta front sandstone sequences*. IN: James, D. P., and Leckie, D. A. (eds.) *Sequences, stratigraphy, sedimentology: surface and subsurface*, CSPG Memoir 15. CSPG, Calgary, pp. 373-386.

Mountjoy, E. W. 1962. *Mount Robson (southeast) map area, Rocky Mountains of Alberta and British Columbia (83E SE)*. Geological Survey of Canada Paper 61-31. 114 pages.

Orhard, M. J., and Tozer, E. T. 1997. *Triassic conodont biochronology, its calibration with the ammonoid standard, and a biostratigraphic summary for the Western Canada Sedimentary Basin*. Bulletin of Canadian Petroleum Geology 45(4): 675-692.

Paine, R. T. 1970. *The sediment occupied by some recent lingulid brachiopods and some palaeoecological implications*. Palaeogeography, Palaeoclimatology, Palaeoecology 7: 21-31.

Paull, R. K., Paull, R. A., and Laudon, T. S. 1997. *Conodont biostratigraphy of the Lower Triassic MacKenzie Dolomite Lentil, Sulphur Mountain Formation in the Cadomin area, Alberta*. Bulletin of Canadian Petroleum Geology 45(4): 708-714.

Pelletier, B. R. 1960. *Triassic stratigraphy, Rocky Mountain Foothills, northeastern British Columbia 94J and 94K*. Geological Survey of Canada Paper 60-2. 33 pages.

- Pelletier, B. R. 1961. *Triassic stratigraphy of the Rocky Mountain Foothills, northeastern British Columbia 94K and 94N (parts of)*. Geological Survey of Canada Paper 61-8. 32 pages.
- Pelletier, B. R. 1963. *Triassic stratigraphy of the Rocky Mountain Foothills, Peace River District, British Columbia*. Geological Survey of Canada Paper 62-26.
- Pemberton, S. G., MacEachern, J. A., and Frey, R. W. 1992a. *Trace fossil facies models: environmental and allostratigraphic significance*. IN: Walker, R. G., and James, N. P. (eds.) *Facies Models*. Geological Association of Canada. pp. 157-177.
- Pemberton, S. G., MacEachern, J. A., and Ranger, M. J. 1992b. *Ichnology and event stratigraphy: the use of trace fossils in recognizing tempestites*. IN: Pemberton, S. G. (ed.) *Applications of ichnology to petroleum exploration: a core workshop*. SEPM, Calgary, pp. 85-118.
- Pemberton, S. G., and Wightman, D. M. 1987. *Brackish water trace fossil suites: examples from the Lower Cretaceous Mannville Group*. IN: Currie, P. J., and Koster, E. H. (eds.) *Mesozoic terrestrial ecosystems*. Tyrell Museum of Palaeontology, Drumheller, pp. 183-190.
- Pemberton, S. G., and Wightman, D. M. 1992. *Ichnological characteristics of brackish water deposits*. IN: Pemberton, S. G. (ed.) *Applications of ichnology to petroleum exploration: a core workshop*. SEPM, Calgary, pp. 141-168.
- Plaziat, J.-C., Pajaud, D., Emig, C. C. and Gall, J.-C. 1978. *Environnements et distribution bathymétrique des Lingules actuelles; conséquences pour les interprétations paléogéographiques*. *Bulletin du Société Géologique de France* 20(3): 309-314.
- Podruski, J. A., Barclay, J. E., Hamblin, A. P., Lee, P. J., Osadetz, K. G., Procter, R. M., and Taylor, G. C. 1988. *Conventional Oil Resources of Western Canada (light and medium), Part I: Resource Endowment*. Geological Survey of Canada Paper 87-26, pp. 1-125.

- Ranger, M. J., and Pemberton, S. G. 1992. *The sedimentology and ichnology of estuarine point bars in the McMurray Formation of the Athabasca Oil Sands deposit, northeastern Alberta, Canada*. IN: Pemberton, S. G. (ed.) *Applications of ichnology to petroleum exploration: a core workshop*. SEPM, Calgary, pp. 401-422.
- Reading, H. G. and Collinson, J. D. 1996. *Clastic coasts*. IN: Reading, H. G. (ed.) *Sedimentary environments: processes, facies and stratigraphy*. Blackwell Science Limited, Oxford. pp. 154-231.
- Reineck, H.-E., and Singh, I. B. 1980. *Depositional Sedimentary Environments, second edition*. Springer-Verlag, New York, USA. 549 pages.
- Rowell, A. J., and Grant, R. E. 1987. *Phylum Brachiopoda*. IN: Boardman, R. S. (ed.) *Fossil Invertebrates*. Blackwell Scientific Publications, pp. 445-496.
- Savazzi, E. 1991. *Burrowing in the inarticulate brachiopod Lingula anatina*. *Palaeogeography, Palaeoclimatology, Palaeoecology* 85: 101-106.
- Seilacher, A. 1953. *Studien zur Palichnologie. I. Über die Methoden der Palichnologie*. *Neues Jahrbuch für Geologie und Paläontologie, Abhandlungen* 96(3): 421-452.
- Seilacher, A. 1967. *Bathymetry of trace fossils*. *Marine Geology* 5: 413-428.
- Selwyn, A. R. C. 1877. *Report on exploration in British Columbia in 1875*. Geological Survey of Canada, Report of Progress 1875-76.
- Shimer, H. W. 1911. *Lake Minnewanka section [Alberta]*. Geological Survey of Canada, Summary Report, 1910. pp. 145-149.
- Smith, A. G., Smith, D. G., and Funnell, B. M. 1994. *Atlas of Mesozoic and Cenozoic coastlines*. Cambridge University Press, Cambridge, UK. 99 pages.
- Sultan, R., Ortoleva, P., DePasquale, F., and Tartaglia, P. 1990. *Bifurcation of the*

- Ostwald-Liesegang supersaturation-nucleation-depletion cycle.* Earth-Science Reviews 29: 163-173.
- Thayer, C. W., and Steele-Petrovic, H. M. 1975. *Burrowing of the Lingulid brachiopod Glottidia pyramidata: its ecologic and paleoecologic significance.* Lethaia 8: 209-221.
- Tozer, E. T. 1967. *A standard for Triassic time.* Geological Survey of Canada, Bulletin 156. 103 pages.
- Tozer, E. T. 1994. *Canadian Triassic ammonoid faunas.* Geological Survey of Canada Bulletin 467. 663 pages.
- Twitchett, R. J., and Wignall, P. B. 1996. *Trace fossils and the aftermath of the Permian-Triassic mass extinction; evidence from northern Italy.* Palaeogeography, Palaeoclimatology, Palaeoecology 124(1-2): 137-151.
- Visser, M. J. 1980. *Neap-spring cycles reflected in Holocene subtidal large-scale bedform deposits: a preliminary note.* Geology 8: 543-546.
- Warren, P. S. 1945. *Triassic faunas in the Canadian Rockies.* American Journal of Science 243(9): 480-491.
- Wignall, P. B., and Hallam, A. 1992. *Anoxia as a cause of the Permian/Triassic mass-extinction: facies evidence from northern Italy and the western United States.*
- Wignall, P. B., and Hallam, A. 1993. *Griesbachian (earliest Triassic) palaeoenvironment changes in the Salt Range, Pakistan and Southeast China and their bearing on the Permian-Triassic mass extinction.* Palaeogeography, Palaeoclimatology, Palaeoecology 102(3-4): 215-237.
- Wittenberg, J. 1992. *Origin and stratigraphic significance of anomalously thick sandstone trends in the Middle Triassic Doig Formation of west-central Alberta.* Unpublished M.Sc. thesis, University of Alberta, Edmonton. 600 pages.

- Woodroffe, C. D., and Chappell, J. 1993. *Holocene emergence and evolution of the McArthur River Delta, southwestern Gulf of Carpentaria, Australia*. *Sedimentary Geology* 83(3-4): 303-317.
- Yatsu, N. 1902. *On the habits of the Japanese Lingula*. *Annotationes Zoologicae Japonensis* 4(2): 61-67.
- Zonneveld, J.-P. 1999. *Sedimentology and sequence biostratigraphic framework of a mixed siliciclastic-carbonate depositional system, Middle Triassic, northeastern British Columbia*. Unpublished Ph.D. thesis, University of Alberta, Edmonton. 287 pages.
- Zonneveld, J.-P., Moslow, T. F., and Henderson, C. M. 1997. *Lithofacies associations and depositional environments in a mixed siliciclastic-carbonate coastal depositional system, upper Liard Formation, Triassic, northeastern British Columbia*. *Bulletin of Canadian Petroleum Geology* 45(4): 553-575.